Synthesis and Complexes of Heterocyclic Ligands

A thesis submitted in partial fulfilment of
the requirements for the degree of
Doctor of Philosophy in Chemistry
at the
University of Canterbury.

Christopher Richardson

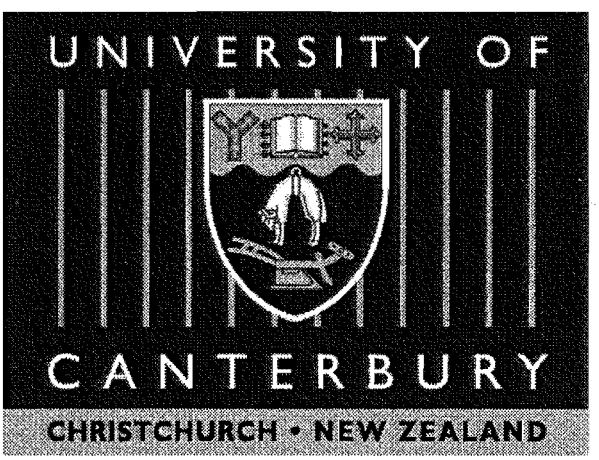

University of Canterbury
Christchurch
New Zealand

1999

Contents

Acknowledgments

I first wish to thank Associate Professor Peter J. Steel for his help, guidance and supervision throughout the duration of this work. I also wish to acknowledge all those who have passed through Lab. 655 during the past three and a half years, I have enjoyed your company very much. My thanks also go out to all the helpful technical staff of the Dept. of Chemistry, and in particular to Mr. Bruce Clark for the running of many mass spectrometric samples.

To my friends, family and my partner Belinda, I thank you for all the support I have received.

Abbreviations

a.m.u.	atomic mass unit
bpy	2,2'-bipyridine
dmb	4,4'-dimethyl-2,2'-bipyridine
CIS	coordination induced shift
DMF	N,N'-dimethylformamide
DMSO	dimethyl sulfoxide
EI	electron impact
equiv.	molar equivalent
FABMS	fast atom bombardment mass spectrometry
GHMBC	gradient heteronuclear multiple bond correlation
GHSQC	gradient heteronuclear single-quantum correlation
IR	infrared
M	molar
MC	metal-centred
MLCT	metal-to-ligand charge-transfer
NMR	nuclear magnetic resonance
nOe	nuclear Overhauser effect
PMD	photochemical molecular device
PPA	polyphosphoric acid

PTC	phase-transfer catalysed
RORC	ring-opening ring-closing
SCE	saturated calomel electrode
TOCSY	total correlation spectroscopy
TPY	2,2':6',2''-terpyridine

Abstract

The coordination chemistry of twenty chelating heterocyclic ligands, seven of which are new, is described. These ligands all contain heterocyclic ring systems that have previously received little attention in the literature. The specific ring systems involved are benzoxazoles, benzisoxazoles, benzothiazoles, benzotriazoles, 1,2,4- and 1,2,5-heterodiazoles, and the 1,4,2,5-dioxadiazene systems.

Many of the complexes synthesised are of ruthenium(II). These include monoruthenium complexes of the type $[Ru(bpy)_2(L)]^{2+}$, homodinuclear complexes $\{[(bpy)_2Ru(\mu\text{-}BL)Ru(bpy)_2]^{4+}$ with μ-BL representing a doubly bidentate bridging ligand} as well as heterodinuclear ruthenium/palladium and ruthenium/platinum $\{[(bpy)_2Ru(\mu\text{-}BL)MCl_2]^{2+}$ with M = Pd/Pt} complexes.

Also investigated are the coordination and supramolecular chemistry of many of the ligands with palladium(II), silver(I) and copper(II) metal ions. The X-ray crystal structures of five ligands and twenty complexes are described. An unexpected, previously unreported, heterocyclic transformation mediated by the $Ru(bpy)_2^{2+}$ cation is also reported.

A combination of multinuclear NMR, UV-visible spectroscopy, cyclic voltammetry and X-ray crystallography has been used to study the nature of the metal-ligand and metal-metal interactions in the complexes produced.

Chapter 1

Introduction

Since the preparation of 2,2'-bipyridine (bpy) over 110 years ago,[1] this versatile bidentate chelating ligand has been of great value in coordination, organometallic, analytical and, more recently, in metallosupramolecular chemistry. This is because of the stable metal complexes it forms with nearly all of the metallic elements of the periodic table.[2]

In 1936 Burstall first synthesised the tris(2,2'-bipyridine)ruthenium dication [$Ru(bpy)_3^{2+}$].[3] However, it was not until 1959 that the important properties of $Ru(bpy)_3^{2+}$ were realised, with the spectroscopic investigation carried out by Paris and Brandt.[4] Since then $Ru(bpy)_3^{2+}$ has arguably become the most studied and used coordination complex. A unique combination of chemical stability, redox properties, excited state properties and luminescence emission have made $Ru(bpy)_3^{2+}$ suitable for a wide range of investigations, and there has been a tremendous amount of work on the compilation of data on $Ru(bpy)_3^{2+}$ and its derivatives.[5,6] Ruthenium(II) is a d^6 metal ion and has a ground electronic configuration of $(t_2g)^6$, and in the one-electron oxidised form, [Ru(III)], has the configuration $(t_2g)^5$. In these oxidation states ruthenium is inert to ligand substitution. Upon excitation by light $Ru(bpy)_3^{2+}$ has a relatively long-lived excited state and combined with its photo-stability is an ideal photocatalyst. There has been particular interest in the use of $Ru(bpy)_3^{2+}$ in the photo-catalytic process of splitting water to oxygen and hydrogen.[5]

In the search for better photocatalysts, the differing properties of heterocyclic ligands have provided a mechanism for 'tuning' the physical properties of the complex. That is, by changing the donor/acceptor properties of the ligands the properties of the resultant complex are altered. The heterocycles most investigated have continued to be π-deficient six-membered aromatic heterocycles, the azines. The introduction of substituents into the pyridine rings of bpy can alter the physical and chemical properties, but more dramatic effects can result from changing the heterocycles themselves.[7] The isomeric diazines, pyridazine, pyrimidine and pyrazine have been incorporated into chelating ligands, as have ligands containing a benzo-fused azine, eg quinoline and isoquinoline.[6,7] Ligands containing a π-excessive azole have received less attention. The N-heterocyclic pyrazole,[7,8] imidazole,[7] 1,2,4-triazole[10] and tetrazole[9] systems have been incorporated into ligands, although these have not been studied in as much detail as the azine ligands. Importantly, the azole-

containing ligands have imparted significantly different properties to complexes, because of their very different electronic properties compared to the azines.

Little effort has been expended in studying other more exotic heterocyclic systems, and yet these systems may offer exciting new properties. The aim of this thesis is to determine the properties of some previously unexplored N-heterocyclic systems, thereby assessing their suitability for use in coordination chemistry, as well as learning about the heterocycles themselves. We aimed to do this by incorporating the chosen heterocycles into chelating ligands, and examining these ligands in $Ru(bpy)_2^{2+}$ complexes. Also, where appropriate, their metallosupramolecular chemistry will also be investigated by preparing complexes with other metal ions. The heterocyclic systems chosen for investigation in this study are shown in Fig. 1.1.

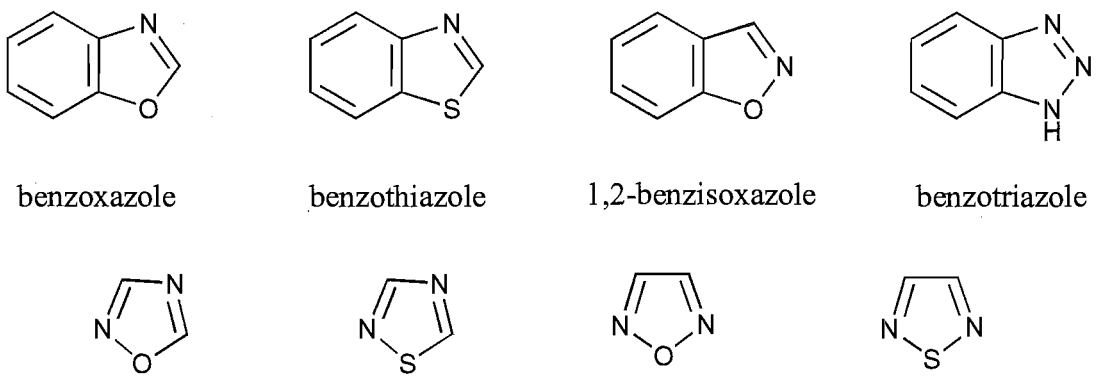

Fig. 1.1

A theme throughout this work is the synthesis of N-heterocyclic ligands that also contain oxygen or sulfur atoms in the ring. Furthermore, we intend to study some isomers, the 1,2,4- and 1,2,5-heterodiazoles, where only the order of the atoms in the rings is changed. In Chapters 2 and 3 the benzo-fused systems benzoxazole, benzothiazole, 1,2-benzisoxazole and benzotriazole are investigated, while Chapters 4 and 5 deal with the 1,2,4-heterodiazoles and the 1,2,5-heterodiazoles, respectively.

In recent years there has been a tremendous upsurge in the area of supramolecular chemistry. A supramolecular species may be defined as a complex assembly consisting of molecular components. The 'supermolecule' has definite properties attributable to the components, and new properties arising from the incorporation of the components into the assembly.[10] The construction of metallosupramolecular species is based upon the interactions of metal ions with organic ligands, and so far the use of nitrogen donor ligands has dominated this field. The range of metal geometries exceeds those of strictly organic components and so offers greater diversity in the geometry of the assembly. By the judicious choice of components it is possible to assemble metallosupramolecular complexes with desired

properties, thus 'tailor making' molecules, and there have been many impressive examples of the construction of metallosupramolecular architectures such as molecular squares,[11] grids,[12-14] helicates,[15-17] cylinders,[18] a cube,[19] interpenetrating networks,[20] and various other topology's.

Upon moving from mononuclear to polynuclear ligand-bridged transition metal complexes there is, in addition to metal-ligand interactions, the possibility of metal-metal interactions in the form of energy- and electron transfer, magnetic interactions and intervalence transfer.[21] These interactions are generally mediated by the bridging aromatic heterocycle *via* the π-system of the ligand. Perhaps the most important of these processes are those activated by light, as the conversion of solar energy into other useful forms is very desirable. By performing useful work functions, these complexes behave as molecular machines and have been termed Photochemical Molecular Devices (PMDs). Many of the useful processes involve multi-electron catalysis. Therefore the design of multinuclear complexes to cope with this requirement is essential.

From the extensive photochemical investigations of mononuclear ruthenium polypyridyl complexes, this unit was a logical choice to use in constructing potential PMDs. The design of specific systems offers many possibilities for chemists to explore, and both antenna and chain-like systems have been constructed using ligand-bridged ruthenium polypyridyl units. Metallodendrimers are also a notable example of such a design motif. The construction of these types of metallosupramolecular complex has been based upon convergent and divergent syntheses, using the 'complexes as ligands' strategy.[22-26] In divergent syntheses, each extension is a new generation to the metallodendrimer, and by such a methodology a 22-nuclear complex has been successfully synthesised.[27]

Currently receiving attention are ligand-bridged dinuclear systems of the form $(N\text{-}N)_2M\text{-}(L\text{-}S\text{-}L)\text{-}M(N\text{-}N)_2^{n+}$, where M = Ru, (N-N) is a terminal ligand such as bpy and L-S-L is a doubly bidentate ligand separated by a spacer S. With the advent of high-yielding metal-catalysed coupling procedures, the synthesis of oligopyridines and ligands containing extended alkynyl- or phenyl-type spacers have become easily accessible. The bridging ligand determines the distance between the metals, and the electronic structure of the ligand plays a role in determining the electronic interaction between the metal-based units. In later chapters some effort was made to synthesise dinuclear complexes and look at the metal-metal interaction.

A result of bidentate ligand coordination to octahedrally coordinated metal ions is the formation of stereoisomers. This aspect 'the stereochemical problem' has been the subject of an excellent recent review.[28] In octahedral metals, coordination from symmetrical bidentate ligands, such as bpy, gives rise to two enantiomeric forms, Λ and Δ. As the number of metal-based units containing three bidentate ligands increases so to does the number of

stereoisomers. In dinuclear complexes, two stereogenic centres gives rise to a pair of diastereoisomers, ΔΔ/ΛΛ (racemic) and ΔΛ/ΛΔ (meso). In contrast to the stereoisomers formed with bidentate ligands, octahedral metals with two terdentate ligands, such as 2,2':6',2"-terpyridine (tpy), give achiral complexes. Thus terdentate ligands have been proposed to offer significant advantages over bidentate ligands, especially for the construction of rod-like complexes, where linking two tpy ligands in the 4'-positions with a rigid linear spacer allows the metals to be in a direct line. However, some authors[191] have argued "that the successful construction of advanced materials for use as molecular devices will require assemblies in more than one dimension and a more subtle selection of molecular building blocks. Further, we contend that this diversity can be provided through the diastereo- and enantio-isomerism of octahedral complexes derived from bidentate chelating ligands."

If chirality is to be controlled, a synthesis starting with an enantiomerically pure material of known chirality must be used, the alternative being separation of isomers after formation. Keene has covered the subject of chromatographic separation in a recent review.[29] Researchers have further addressed the issue of chirality by trying to predetermine the chirality of the complex by introducing chiral ligands. The chiragen family of ligands, which incorporate a β-pinene group, are perhaps the best-known examples of such chiral ligands.[30-35] Other researchers have incorporated different chiral moieties such as camphor[36-38] into ligands.

The ligands used in this work are designed to chelate. However, they are also capable of acting as bridges between different metal ions. It is this mode that leads to the construction of supramolecular assemblies, drawing upon the information encoded into the components of the system to determine the resulting structure. A principle of the method of synthesis of these types of metallosupramolecular complexes is based upon the lability of the coordinate bond. Whereas in the work with ruthenium the nitrogen-ruthenium bond is inert to ligand substitution, the construction of metallosupramolecular complexes with some metals relies on the lability of the coordinate bond as well as other factors of solubility, enthalpy and entropy.[39-41] With labile metal ions, such as copper(I) and silver(I), the metallosupramolecular assembly may be able to assemble and disassemble allowing exploration of various geometries and binding arrangements, exploring the potential energy surface, until the final structure is arrived at.

The three metals chosen for this purpose in the present work are silver(I), copper(II) and palladium(II). This selection is based upon their differing geometrical preferences. Silver(I) has a wide range of bonding geometries, although shows a preference to be two-coordinate (bent or linear) or three-coordinate (T-shaped or trigonal). The use of silver(I) in the construction of supramolecular architectures has been discussed in a recent review.[42] Copper(II) also demonstrates flexibility in its coordination modes, ranging from four-coordinate (square planar) and five-coordinate (square-pyramidal or trigonal bipyramidal) to

six-coordinate (tetragonal).[241] On the other hand, palladium(II) demonstrates little flexibility in its bonding geometry, preferring to be four-coordinate square planar. However, this fact is utilised in the construction of systems requiring two *cis* coordination sites, leading to squares or rectangles, or those requiring linear *trans* coordination, giving chain-like structures.

The technique of X-ray crystallography is the method of choice for the characterisation of metallosupramolecular complexes involving labile metal ions, as it provides structural detail that other techniques cannot. Indeed, solution techniques such as NMR spectroscopy and mass spectrometry often provide little useful information of complexes of labile metal ions. This is in contrast to the solution stability of chelating ruthenium complexes, which are well behaved in mass spectrometers giving reliable information about nuclearity. Ruthenium complexes can also be fully characterised by NMR spectroscopy.

In summary, this thesis describes the synthesis of a number of chelating heterocyclic ligands containing unusual heterocycles and the preparation of their ruthenium complexes. Cyclic voltammetry, NMR spectroscopy and UV-visible spectroscopy are then used to study these complexes providing information about the metal-ligand and metal-metal interactions. Coordination and supramolecular complexes with selected other metals will also be described.

Chapter 2

Benzoxazoles, benzisoxazoles and benzothiazoles

2.1 Introduction

In this chapter a study of the benzo-fused analogues of oxazole, isoxazole and thiazole is presented. These are aromatic heterocycles with a five membered ring containing two heteroatoms fused to a benzene ring. The heterocyclic ring systems and ring numbering are shown in Fig. 2.1.

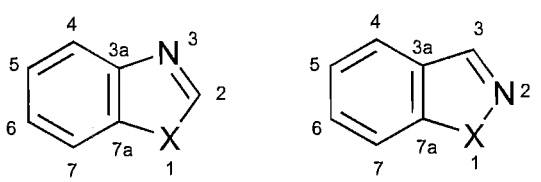

X = O, S

Fig. 2.1

The ligands specifically are 2,2'-bibenzoxazole, (**1**), 2,2'-bibenzothiazole, (**2**), 2,2'-methylenebisbenzoxazole, (**3**), 2,2'-methylenebisbenzothiazole, (**4**), 3,3'-bi-1,2-benzisoxazole, (**5**), and 3-(2-pyridyl)-1,2-benzisoxazole, (**6**) (Fig. 2.2).

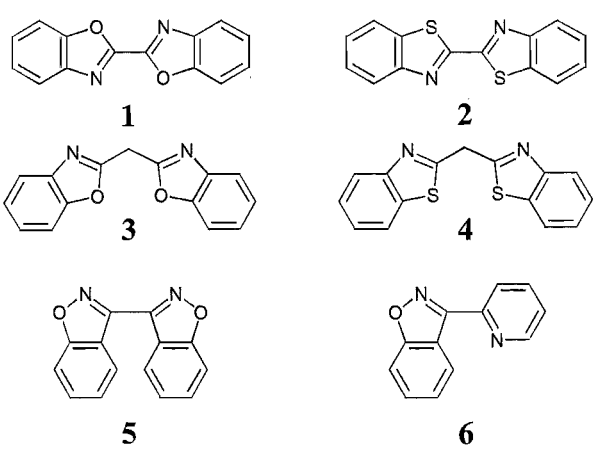

Fig. 2.2

Firstly, a brief description of the syntheses of the known ligands **1**, **2**, **3**, and **4**, from literature procedures, is given. Descriptions of attempted syntheses of the ligand 3,3'-bibenzisoxazole (**5**) and the successful synthesis of 3-(2-pyridyl)-1,2-benzisoxazole (**6**), are then discussed.

Although ligand **1** has been known for over a century,[43] and ligand **2** for more than seventy years,[44] the preparation and study of ruthenium complexes with these simple ligands has not been reported. However, ruthenium complexes of other ligands containing benzothiazoles have been studied and reported.[45-47] Ligands **1** and **2** are fluorescent and their properties have been examined.[48,49] Ligands **3** and **4** have been particularly well studied by a group of Italian chemists, who have systematically examined the properties of the heterocycles together with the acidity of the methylene bridge.[50a-e] However, relatively little of their work, other than X-ray crystallographic studies, has been concerned with the properties of complexes with these ligands. We felt a study of the parent biheterocycles and the methylene-bridged bisheterocycles would provide further information about the electronic nature of these heterocyclic systems.

Further interest was in a comparison of the benzisoxazole ring *vs* the benzoxazole ring. Up to 1991, no literature reports concerning the coordination chemistry of benzisoxazole-containing ligands had been published.[51] This chapter also describes some coordination chemistry of ligand **6**, as well as some aspects of coordination chemistry, with metal ions other than ruthenium, for some of the other ligands.

2.2 Syntheses of Ligands

As stated in the introduction to this chapter, **1**, **2**, **3**, and **4** are known compounds. These ligands were synthesised according to literature procedures involving cyclocondensations of 2-amino(thio)phenol with the diethyl esters of oxalic or malonic acid (n = 0,1) in polyphosphoric acid (PPA), as shown in Scheme 2.1.

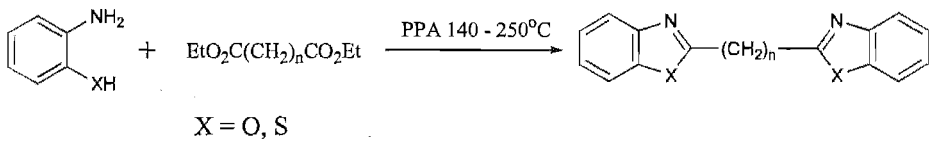

Scheme 2.1

By this method **1**, **2**,[52] **3**[53] and **4**[52] were prepared in yields of 60%, 8%, 54% and 17%, respectively. The lower than reported yields for ligands **2** and **4** were subsequently attributed to the impure nature of the starting 2-aminothiophenol. The yield of ligand **3** was close to the stated literature yield of 52%.

The X-ray crystal structures of **1** and **2** were carried out in order to determine the conformation of the biheterocycles in the solid state. The structures of **1** and **2** are shown in Fig. 2.3 and Fig. 2.4, respectively. The asymmetric unit of each contains one half-molecule and, by virtue of the centre of inversion within the inter-ring bond, the conformations of the biheterocycles are planar and *trans*. This conformation has been reported for other biheterocycles such as 2,2'-bipyridine (bpy).[54] Since the completion of this study, Hahn *et al.*[55] have published the X-ray crystal structure of **1**.

Ligand **1** crystallises in the monoclinic space group $P2_1/c$, while ligand **2** crystallises in the monoclinic space group $P2_1/n$. The change in space group is simply a change of axis for the glide plane. The obvious difference between the two ligands is the large distortion of the five-membered ring of the benzothiazole. The reason for this distortion is that the larger sulfur atom has considerably longer bonds to the C2 and C7A carbons [S1-C2 1.741(2), S1-C7A 1.730(2)] than does the oxygen of the benzoxazole ring [O1-C2 1.352(3), O1-C7A 1.388(2)].

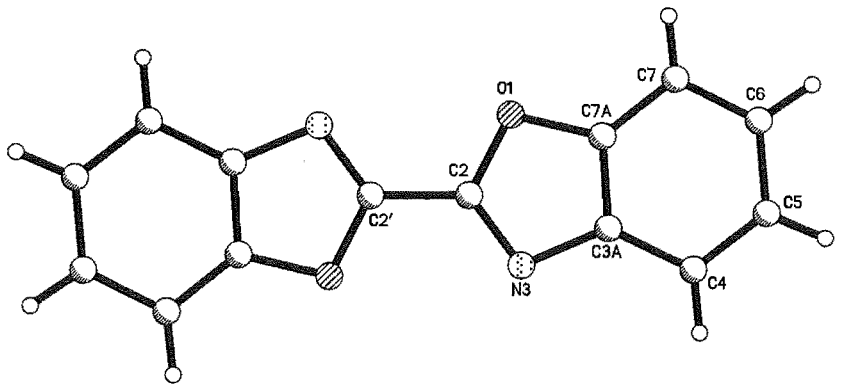

Fig. 2.3 Perspective view, with atom labelling, of **1**. Selected bond lengths (Å) and angles (°): O1-C7A 1.388(2), C2-N3 1.301(2), N3-C3A 1.396(3), C3A-C7A 1.378(3), C5-C6 1.391(3), C7A-C7 1.373(3), O1-C2 1.352(3), C2-C2′ 1.449(4), C3A-C4 1.399(3), C4-C5 1.378(3), C6-C7 1.391(3), C7A-O1-C2 103.4(2), N3-C2-O1 116.7(2), C2-N3-C3A 103.0(2), C3A-C7A-O1 107.3(2).

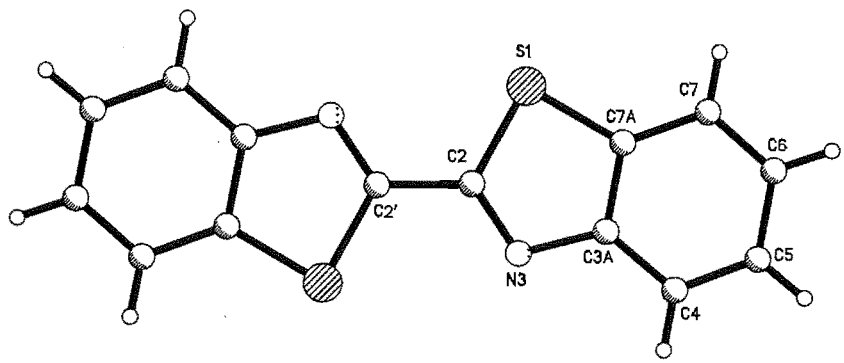

Fig 2.4 Perspective view, with atom labelling, of **2**. Selected bond lengths (Å) and angles (°): S1-C7A 1.730(2), C2-N3 1.299(3), N3-C3A 1.390(2), C3A-C7A 1.408(3), C5-C6 1.401(3), C7-C7A 1.400(3), S1-C2 1.741(2), C2-C2' 1.459(4), C3A-C4 1.397(3), C4-C5 1.375(3), C6-C7 1.378(3), C7A-S1-C2 88.12(9), N3-C2-S1 117.6(2), C2-N3-C3A 109.2(2), C3A-C7A-S1 110.00(14).

The conformations of these aromatic biheterocycles are subject to forces that govern the crystal structure. In the solid state, crystal packing forces such as π-π stacking are maximised when the aromatic biheterocycles are planar. In the structure of ligand **2**, the planar aromatic ligands are stacked at a distance of 3.62(5)Å. Also, for reasons of conjugation, the aromatic rings prefer to be coplanar. Another crystal packing force in the structures of ligands **1** and **2** is an edge to face interaction, which leads to a herringbone array (Fig. 2.4b). The closest intermolecular distance for this interaction in the crystal structure of ligand **2** is from H6 of one ligand to C5 of another at 2.928(3)Å. In these crystal structures, the biheterocycles have adopted the *trans* coplanar conformation. One might expect that the lone pairs on the sulfur (or oxygen) and nitrogen atoms would repel each other, and the aromatic rings would lie at an angle to each other to minimise this electrostatic interaction. With a planar system there are two possible conformations about the inter-ring bond with

respect to the heteroatoms, *viz* 1) where the same heteroatom is on the same side of the inter-ring bond (*cis*) or 2) where the same heteroatoms are on different sides of the inter-ring bond (*trans*). Crystal packing forces are, of course, non-existent when the molecules are in solution, and for this reason their conformation may be different in solution.

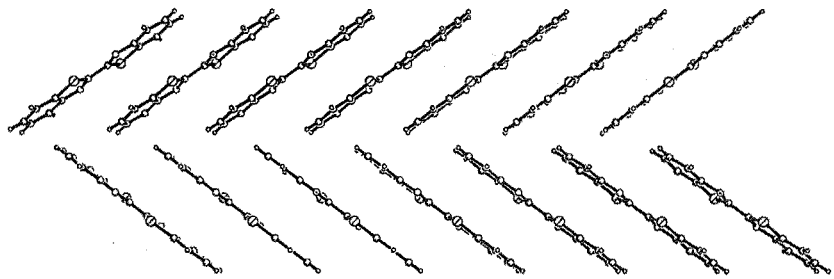

Fig. 2.4b Perspective view of the herringbone array in the crystal structure of **2**.

One possible route to the biheterocycle **5** is through a $Ni^{(0)}$-catalysed coupling of a suitably halo-substituted benzisoxazole. 3-Chloro-1,2-benzisoxazole is known,[56] and was synthesised according to the reported procedure, starting from the commercially available salicylhydroxamic acid, as shown in Scheme 2.2.

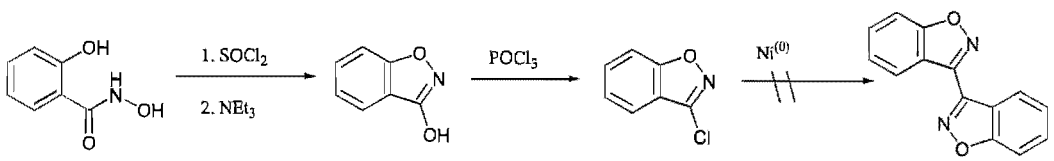

5

Scheme 2.2

The coupling procedure used was based on that described by Iyoda *et al.*,[57] which had previously been found to be the best procedure by other workers in this group.[58] However, the $Ni^{(0)}$ coupling reaction was unsuccessful, with no biheterocycle isolated. Possibly this is due, at least in part, to the sensitive nature of the benzisoxazole ring.

A method that has been used for the preparation of benzisoxazole itself, is the reaction of hydroxylamine-O-sulfonic acid with 2-hydroxybenzaldehyde.[59] We thought it might be possible to extend this method to a double cyclisation of the appropriate 2,2'-dihydroxybenzil, as shown in Scheme 2.3. This substrate was prepared *via* a benzoin condensation of 2-methoxybenzaldehyde, oxidation of the benzoin with copper(II) and deprotection of the methoxy groups with boron tribromide. However, an attempted ring closure reaction did not give any product that could be positively identified as **5**.

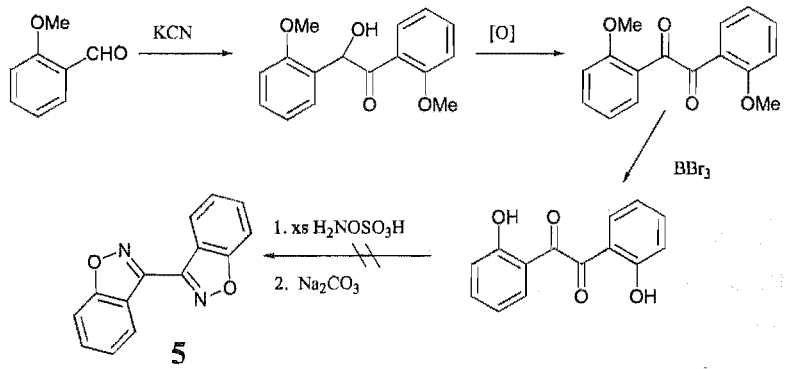

Scheme 2.3

With both these attempts at synthesising the biheterocycle **5** proving unsuccessful, a study of the benzisoxazole ring system with a ligand containing only one benzisoxazole ring was investigated. The benzisoxazole ring linked to a 2-substituted pyridine ring, *viz* **6**, was chosen as the synthetic target. The method used to synthesise **6** is shown in Scheme 2.4.

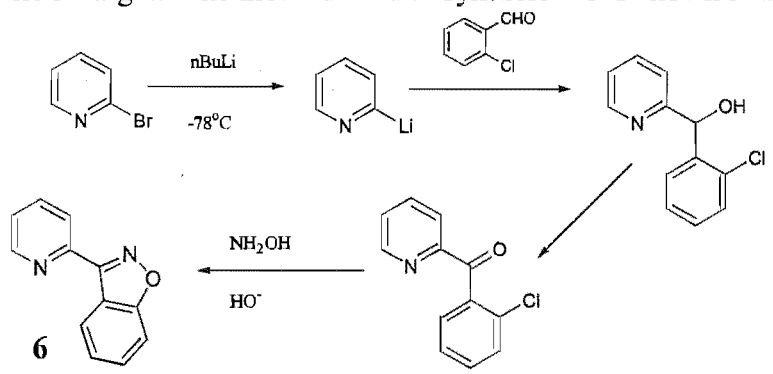

Scheme 2.4

2-Bromopyridine was converted to its 2-lithio derivative by reaction with n-butyllithium in THF at -78°C. 2-Chlorobenzaldehyde was added and, after work-up, the corresponding alcohol was obtained as an oil. This was oxidised to the ketone by Jones reagent. Conversion of the ketone to the benzisoxazole was effected by treatment with hydroxylamine in concentrated base, as described for the phenyl analogue.[60] The overall yield for this 5-step sequence was 19%. Characterisation of this new ligand by ^{1}H and ^{13}C NMR spectroscopy, EI mass spectrometry and elemental analysis confirmed its structure.

2.3 Synthesis and Characterisation of Complexes

One of the methods of characterisation used in this work is NMR spectroscopy, in particular ^{1}H NMR spectroscopy. When a ligand forms a coordination complex, differences in the NMR spectra of the ligand and the complex are observed. These changes are described as coordination induced shifts (CIS = $\delta_{complex}$ - δ_{ligand}). A number of factors have previously been identified which contribute to the magnitude and sign of ^{1}H NMR CIS values in $[Ru(bpy)_2L]^{2+}$ complexes. These include ligand-to-metal σ donation, metal-to-ligand π back donation, chelation imposed conformational changes and inter-ligand through-space ring-current anisotropy effects.[61-63] By the calculation and interpretation of CIS values for the introduced ligand, and by assignment of the other spectral signals, much information about the structure and the nature of bonding in the $[Ru(bpy)_2L]^{2+}$ complex can be gleaned. This necessitates correct ^{1}H NMR assignment.

When individual signals for the different protons are well separated, assignments are generally straightforward and unambiguous, but, in cases where the spectral signals are overlapped, the assignment may be difficult, even for two-dimensional techniques such as ^{1}H-^{1}H correlation spectroscopy (COSY). This difficulty can be resolved by one-dimensional total correlation spectroscopy (1-D TOCSY). The 1-D TOCSY experiment can selectively irradiate a separated single proton resonance and allow the transfer of magnetisation to the other protons in the same spin system.[64-66]

An example of 1-D TOCSY is shown in Fig. 2.5. The experiment begins with the irradiation of a selected resonance, in this case, a H6 proton of a pyridine ring at 8.71 ppm (Trace I). With increased mixing times the magnetisation is transferred to other protons in the spin system which increase in intensity. In Trace II, the magnetisation has been transferred from the H6 proton to the other protons of the ring, and ultimately, in Trace III, the H3 proton has received the magnetisation and is the most intense signal. Therefore, each subsequent spectrum, with longer mixing times, gives an unambiguous assignment and an accurate measure of the chemical shift of the other protons in the spin system.

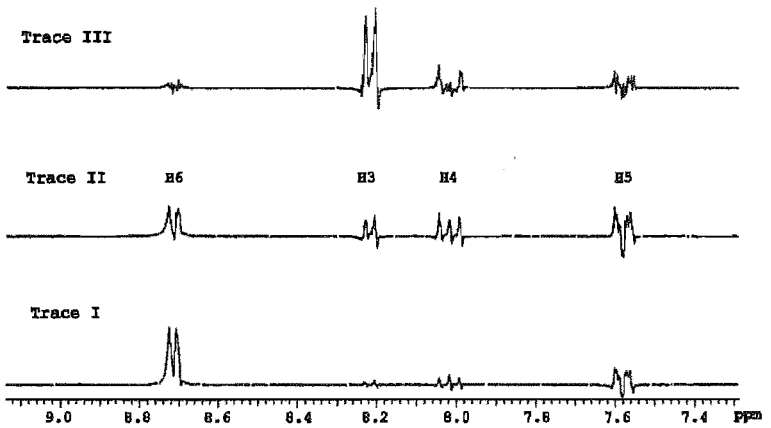

Fig. 2.5

2.3.1 Ruthenium Complexes

Reaction of ligand **1** with bis(2,2'-bipyridine)dichlororuthenium, $[Ru(bpy)_2Cl_2]$, in 3:1 ethanol/water required, due to the low solubility of **1**, a long reflux time. Furthermore, a ^1H NMR spectrum of the material isolated after work-up showed a much more complicated spectrum than expected, suggesting a mixture of products. The desired $[Ru(bpy)_2(\mathbf{1})]^{2+}$ complex, (**7**), contains a two-fold rotational axis of symmetry. Hence, the 24 aromatic protons, 16 from the bipyridine ligands and 8 from **1**, should give rise to only 12 signals. One chemical shift that is diagnostic in ruthenium complexes such as these is the H6 proton of a pyridyl ring that is proximate to a coordinated chloride ion. This proton is heavily deshielded by the chlorine and is shifted downfield. The geometric relationship is demonstrated in Fig. 2.6.

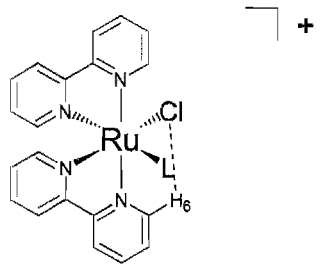

Fig. 2.6

This deshielded proton was evident in the spectrum, and since the chloro-product and **7** are cations of different charge, chromatography on alumina allowed the separation of the two complexes. The ^1H NMR of the first fraction contained 24 aromatic proton resonances, which corresponds to six inequivalent ring systems. 1-D TOCSY spectra identified 4 different pyridyl rings and two different rings for the ligand **1**. Accordingly, the complex was formulated as $[Ru(bpy)_2Cl(\mathbf{1})](PF_6)$, (**8**). The chemical shifts and CIS from **1** and **8** are shown in Table 2.1.

The proton that has the chemical shift of 5.95 ppm easily distinguishes the coordinated ring. This proton is heavily shielded by ring-current anisotropy of the pyridine ring it is nearest to, and so is shifted upfield giving a very large CIS of -2.04 ppm. This is assigned as proton H4 of the coordinated ring. Irradiation of this proton in a 1-D TOCSY experiment gave the chemical shifts of the rest of the coordinated ring protons.

Although all signals for the uncoordinated ring were found by 1-D TOCSY, definitive assignment of the signals to H4'-H7', which would have required a GHSQC experiment, was not achieved. This was in part due to ligand dissociation from the complex. Assignment was also not possible through coupling constant information as two of the signals were considerably broadened, presumably due to slow rotation about the inter-ring bond. The chemical shifts of the H4'-H7' protons are interesting, as all signals are far upfield of the corresponding signals in the free ligand. This is presumably due to the position that the non-coordinated ring occupies when the ligand is bound in a monodentate fashion (Fig. 2.7). With the coordinated ring aligned with H4 pointing towards the adjacent pyridine ring, the uncoordinated ring must point towards another pyridine ring and experiences the effect of ring-current anisotropy.

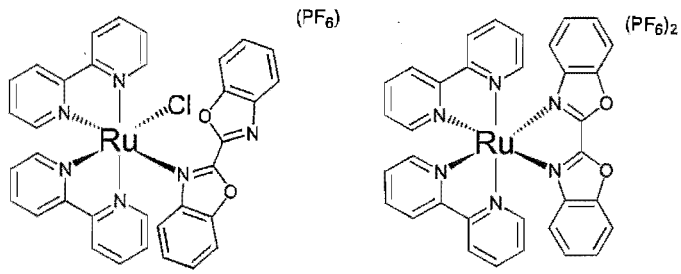

8 **7**

Fig. 2.7

Table 2.1 ^{1}H NMR Chemical Shifts[a] and Coordination Induced Shifts[b] of the coordinated benzoxazole ring of **8** and chemical shifts of **1**.

	H4	H5	H6	H7
8	5.95	7.25	7.55	7.87
1	7.99	7.59	7.66	7.89
CIS	-2.04	-0.34	-0.11	-0.02

[a] For deuterated acetonitrile solutions. [b] CIS = ($\delta_{complex}$ - δ_{ligand}).

The second fraction showed the expected 12 proton resonances for complex **7**. The ^{1}H NMR spectrum of **7** is shown in Figure 2.8, and selected NMR data are given in Table 2.2. Assignment of the three individual ring systems was made by 1-D TOCSY. This, however, does not distinguish which pyridine ring is *cis* and which *trans* to the benzoxazole ligand. A ^{1}H nOe experiment, irradiating H4 of the benzoxazole ring, showed enhancement in both H6

protons of the bipyridines. Because of this result, complete ^{1}H NMR assignment was not possible.

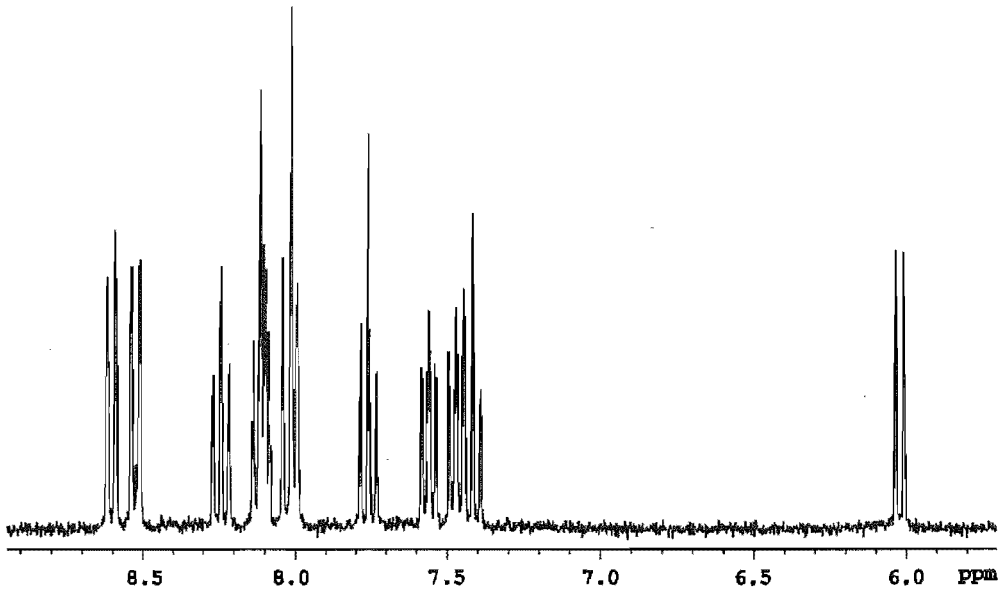

Fig. 2.8 ^{1}H NMR spectrum of $[Ru(bpy)_2(1)](PF_6)_2$ (**7**).

Table 2.2 ^{1}H NMR Chemical Shifts[a] and Coordination Induced Shifts[b] of **7** and **1**.

	H4	H5	H6	H7
7	6.03	7.43	7.75	8.01
1	7.99	7.59	7.66	7.89
CIS	-1.96	-0.16	+0.09	+0.11

[a] For deuterated acetonitrile solutions. [b] CIS = ($\delta_{complex}$ - δ_{ligand}).

Again the H4 protons show a very large upfield shift, although, interestingly, this shift is not quite as large as the CIS of the coordinated ring of the complex **8**. This may be explained by the angle of coordination. When the ligand is coordinated by only one atom, the H4 proton is placed slightly closer to the shielding pyridine ring, resulting in a slightly larger CIS. This is also true for the H5 protons that are similarly affected.

A second method of preparation of ruthenium complexes employed in this work involves the use of a silver salt with a non-coordinating anion such as $AgBF_4$ or $AgClO_4$. The silver salt is used to remove chloride from the $Ru(bpy)_2Cl_2$ reactant and hence prevent it acting as a ligand. The resulting anion was then usually exchanged for hexafluorophosphate by metathesis. By this method, complex **7** was produced, selectively, in 64% yield.

Small crystals of complex **7** were grown by slow evaporation of a dichloromethane solution, one of which was used for X-ray diffraction analysis. Complex **7** crystallises in the triclinic space group P-1, with the cationic metal complex, two hexafluorophosphate counterions and a dichloromethane solvate molecule in the asymmetric unit. A perspective

view of the cation is shown in Fig. 2.9, with the counterions and solvate molecule omitted for clarity.

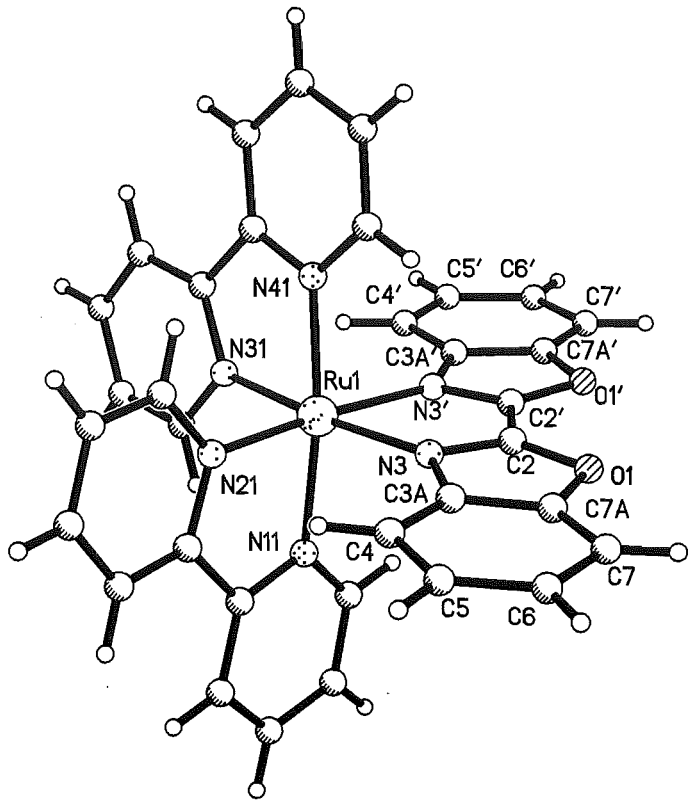

Fig. 2.9 Perspective view, with partial atom labelling, of **7**. Selected bond lengths (Å) and angles (°): Ru1-N3 2.112(5), Ru1-N3' 2.102(5), Ru1-N11 2.088(5), Ru1-N21 2.029(5), Ru1-N31 2.048(5), Ru1-N41 2.069(5), N3-Ru1-N3' 77.6(2), N11-Ru1-N21 78.6(2), N31-Ru1-N41 78.2(2), C2-N3 1.322(8), O1-C2 1.350(7), O1-C7A 1.395(8), N3-C2-O1 115.2(6), C2-N3-C3A 104.2(5), C3A-C7A-O1 107.3(6), C2'-N3' 1.314(8), O1'-C2' 1.351(7), O1'-C7A' 1.395(8), N3'-C2'-O1' 115.7(6), C2'-N3'-C3A' 104.9(6), C3A'-C7A'-O1' 109.4(6)

The crystal structure of complex **7** proved that the ligand was chelating in a N,N'-manner. Among the other notable features of this crystal structure is the conformational change that the ligand has undergone. In the crystal structure of ligand **1** (Fig. 2.3), the orientation of the nitrogens about the inter-ring bond was *trans*. Upon chelation to the $Ru(bpy)_2^{2+}$ unit the nitrogens are *cis*. The bond lengths of the coordinating nitrogens of the benzoxazole ligand [2.102(5)Å and 2.112(5)Å] are slightly longer than those of the auxiliary bpy ligands [2.029(5)Å to 2.088(5)Å], probably due to its greater steric demand. Each of the chelating ligands is planar, with very little twisting of the rings, although the benzoxazole ligand is slightly bowed. The general features of this $Ru(bpy)_2L^{2+}$ complex have been noted previously for other related complexes.[67-70]

Another quantitative measure that this crystal structure allowed was the distance from H4 to the centre of the pyridine ring of the bpy ligand into which it points. The distance of

H4 to the bpy ring is 2.848(5)Å. This is closer than the distance from the H6 of one bpy to the centre of the pyridine ring into which it points [3.188(5)Å] and therefore explains the large negative CIS value.

The reaction of ligand **2** with $Ru(bpy)_2Cl_2$ in 3:1 ethanol/water gave the complex $[Ru(bpy)_2(\mathbf{2})]^{2+}$ (**9**), which was isolated as the hexafluorophosphate salt. Again, due to the very low solubility of the ligand, a long reflux time (3 days) was needed in order to obtain a reasonable yield of complex (*ca.* 66%). Because of the insolubility of **2**, no ^1H NMR spectrum could be recorded in deuterated acetonitrile. For this reason, the CIS from **2** and **9** could not be calculated. In the ^1H NMR spectrum of complex **9**, one proton (at 6.28 ppm) was considerably upfield of the others, as a result of the ring-current anisotropy. 1-D TOCSY was used to identify the other protons in this system and the two different spin systems of the bpy ligands.

In this symmetrical complex, it is not immediately obvious which of the protons of the benzothiazole rings (H4 or H7) is the upfield signal at 6.28 ppm, as N,N'- or S,S'-chelation is possible. In order to unambiguously assign the ^1H NMR spectrum of **9** this signal had to be assigned to either H4 or H7. To accomplish this the use of heteronuclear correlation was necessary.

A ^{13}C NMR spectrum of this complex was obtained with 16 of the possible 17 carbons found by a ^{13}C NMR experiment. Comparison with the spectra of related complexes, and with benzothiazole,[71] did not allow a complete assignment. The comparison did allow for the ready assignment of many signals to the bpy ligands, and the assignment of the C3A (151.87ppm) and C7A (135.87 ppm) carbons of the benzothiazole ligand based upon chemical shift, as well as the realisation that the unrecorded carbon was C2 of the bibenzothiazole. However, it did not allow for the distinction of C4 from C7, which was needed to confirm the mode of bonding. A GHSQC experiment, which might resolve the ambiguities, was performed and is shown in Fig 2.10. Importantly, the proton at 6.28 ppm correlated to the most upfield carbon at 120.45 ppm. However, this carbon is at a different position than is usual for both C4 and C7 carbons of benzothiazole rings and therefore distinction could not be made on this basis. The GHSQC spectrum was useful as it did allow definite assignment of some carbons to the already differentiated bpy spin-systems, although, in the case of the C3's of the bpy ligands, the resolution is not good enough for assignment to a specific spin system. Since the upfield proton must be either H4 or H7, a GHMBC experiment should be able to correlate it to one of the already identified C3A or C7A carbons. In the GHMBC experiment the ^1H-^{13}C coupling was set for 3-bond coupling. Therefore H4 should correlate to C7A and C6, and H7 to C3A and C5 (Fig. 2.11). Indeed, the GHMBC spectrum (Fig. 2.10) does give the correlations that enable confirmation of the mode of bonding. The upfield proton at 6.28 ppm correlates to C7A at 135.87 ppm and to what must be C6 at 129.26 ppm. Conversely, the other doublet of the benzothiazole ligand, at 8.32 ppm,

correlates with C3A at 151.87 ppm and C5 at 129.55 ppm. This determined that the ligand was chelating through the nitrogen atoms. The GHMBC spectrum also allowed the assignment of the quaternary bpy carbons to their respective spin systems.

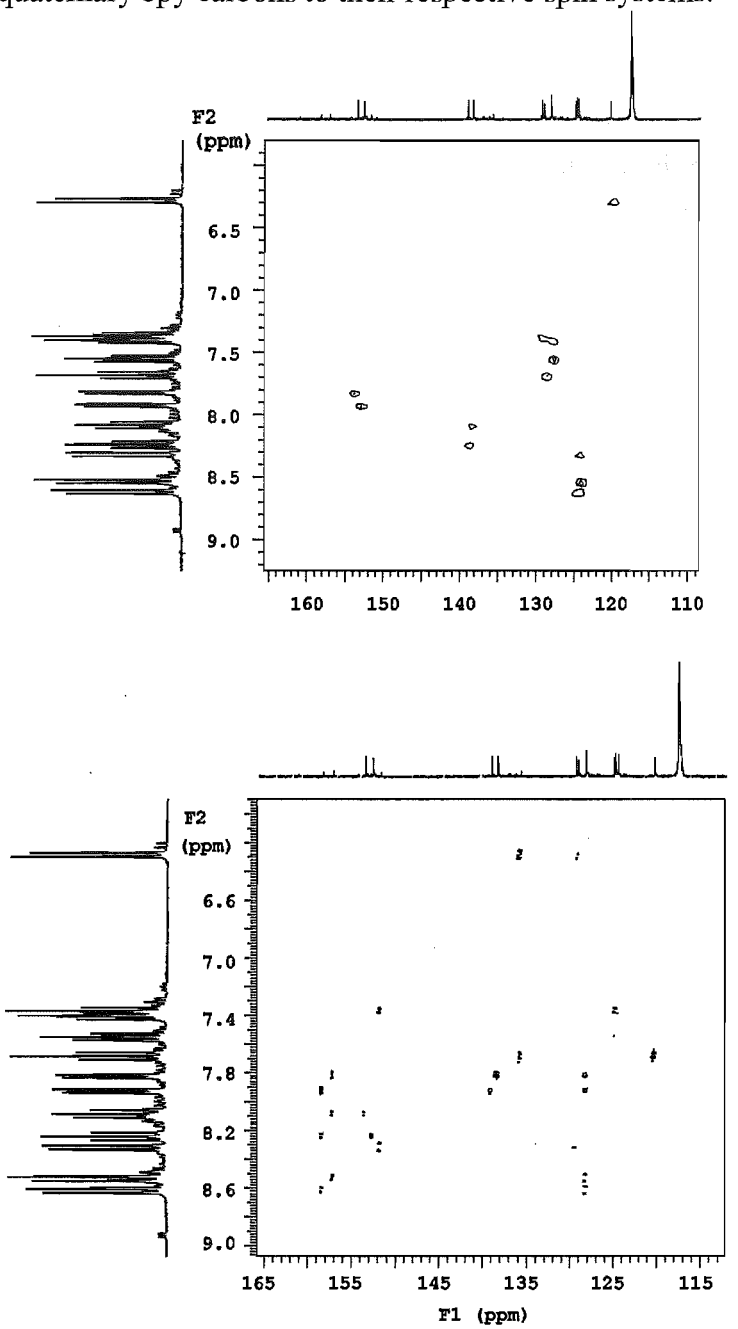

Fig. 2.10 GHSQC (top) and GHMBC spectra (bottom) of $[Ru(bpy)_2(\mathbf{2})](PF_6)_2$ (**9**).

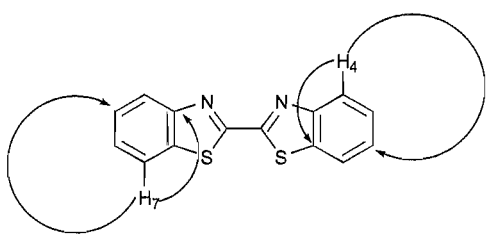

Fig. 2.11

It has been demonstrated that the metal-to-ligand charge-transfer (MLCT) energy of $[Ru(bpy)_2L]^{2+}$ complexes is an indicator of the HOMO-LUMO energy gap in such complexes.[6] The UV-visible spectra of complexes **7** and **9** are shown in Fig. 2.12.

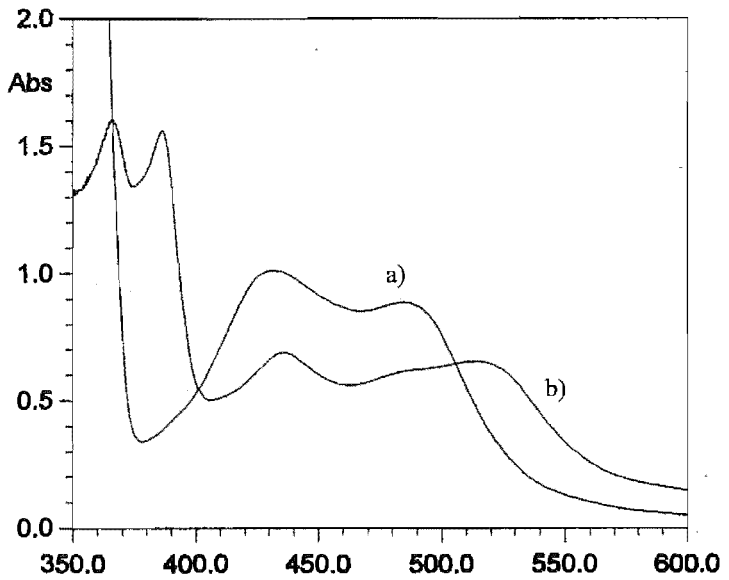

Fig. 2.12 UV-visible spectra of a) $[Ru(bpy)_2(\mathbf{1})](PF_6)_2$, (**7**), and b) $[Ru(bpy)_2(\mathbf{2})](PF_6)_2$, (**9**).

The UV-visible spectrum for complex **7** shows that the lowest energy MLCT is at 485 nm and this transition is assigned as (M)d—(L)π^*. This transition is at longer wavelength than that in $Ru(bpy)_3^{2+}$ (452 nm), and indicates that the HOMO-LUMO gap is smaller in **7** than it is in $Ru(bpy)_3^{2+}$. The spectrum contains other transitions which are at higher energy; the transition at 436 nm can be assigned to (M)d—(bpy)π^*, whereas the transition at 357 nm is ligand centred (LC). The UV-visible spectrum for complex **9** shows that the lowest energy MLCT is at 516 nm, indicating that the energy gap for **9** is smaller than in **7** and in $Ru(bpy)_3^{2+}$. The transition at 431 nm can also be assigned, in a similar manner to **7**, as (M)d—(bpy)π^* and the transitions at 386 and 366 to LC transitions.

A method that gives a direct measure of the orbital energies in ruthenium complexes is cyclic voltammetry. The cyclic voltammograms of complexes **7** and **9** are shown in Fig. 2.13, and Table 2.3 gives the absorption maxima and redox potentials for **7** and **9** compared to those of $Ru(bpy)_3^{2+}$.

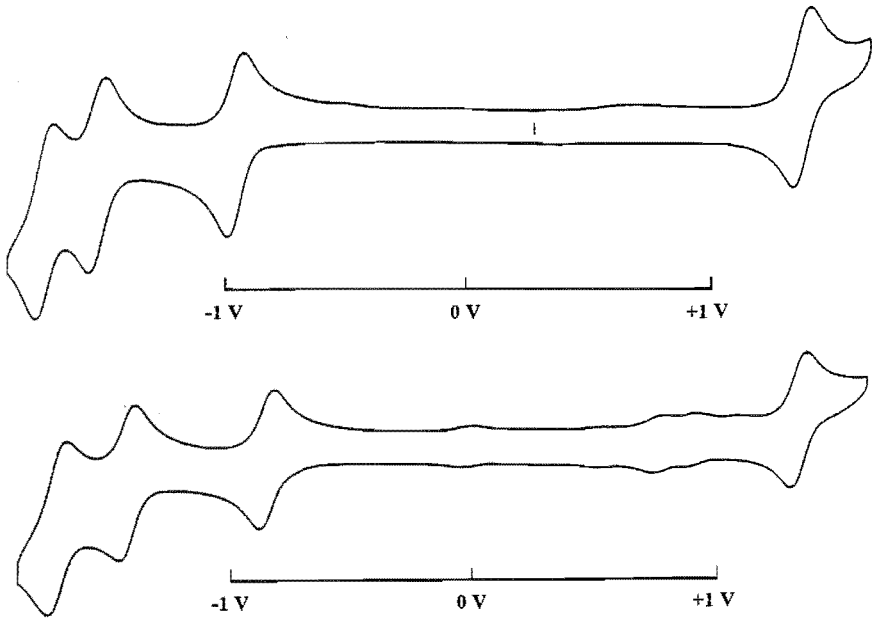

Fig. 2.13 Cyclic voltammograms for $[Ru(bpy)_2(\mathbf{1})](PF_6)_2$ (**7**) (top) and $[Ru(bpy)_2(\mathbf{2})](PF_6)_2$ (**9**).

Table 2.3 Absorption Maxima[a] with Molar Absorption Coefficients[b] and Redox Potentials[c] of complexes **7** and **9**.

	λ_{max} (ε)	E_{ox}	E_{red1}	E_{red2}	E_{red3}	$\Delta E_{ox\text{-}red1}$
$Ru(bpy)_3^{2+}$	452 (13 600)	1.26	-1.33	-1.51	-1.75	2.59
7	485 (7 300)	1.36	-0.97	-1.55	-1.77	2.33
9	516 (8 500)	1.32	-0.86	-1.46	-1.73	2.18

[a] In nanometers. [b] $M^{-1}cm^{-1}$. [c] In volts *vs* SCE in acetonitrile.

Complexes **7** and **9** are both slightly harder to oxidise than $Ru(bpy)_3^{2+}$. Since oxidations of such complexes are well known to be metal centred, this suggests that the ruthenium atom in these complexes is less electron rich than in $Ru(bpy)_3^{2+}$. Reductions in $[Ru(bpy)_2L]^{2+}$ complexes have been shown to be ligand localised.[6] The first reductions of **7** and **9** are ligand based, and **9** is easier to reduce than **7** by 110 mV. The second and third reductions are in excellent agreement with the corresponding reductions in $Ru(bpy)_3^{2+}$ and can, on this basis, be ascribed to the auxiliary bpy ligands. The $\Delta E_{ox\text{-}red1}$ value for the complexes are in agreement with the data from the UV spectra, for which the same orbitals are involved [(M)d—(L)π^*]. The HOMO-LUMO [(M)d—(L)π^*] energy gap in the complexes is considerably reduced by substitution of a bpy ligand with ligand **1**, and further reduced by substitution with ligand **2**, as evidenced by the $\Delta E_{ox\text{-}red1}$ values. This suggests that, in the complexes **7** and **9**, the π^* orbitals are lower-lying than those in $Ru(bpy)_3^{2+}$.

The effect of benzo-fusion to heterocyclic rings is to lower the energy of the π^* orbitals. For example, the π^* orbitals of 2,2'-biquinoline (**10**) are lower in energy than those

of 2,2'-bipyridine (bpy). As a consequence, the ruthenium complexes of **10** have different properties to those of $Ru(bpy)_3^{2+}$.[72] Ligand **2** is the benzo-fused analogue of the well-studied ligand 2,2'-bithiazole (btz).[63,73] Although electrochemical and spectroscopic data for the analogous $[Ru(bpy)_2btz]^{2+}$ complex are not available, the homoleptic complex $Ru(btz)_3^{2+}$ has been examined electrochemically.[74] This allows for a semi-quantitative comparison between these two complexes. The oxidation potential for $Ru(btz)_3^{2+}$ is 1.33 V, and the authors observed that for the substitution of pyridine rings with thiazoles there existed an increase in oxidation potential of *ca.* 0.01 V per thiazole. The oxidation potential for $[Ru(bpy)_2(\mathbf{2})]^{2+}$ is 1.32 V, which is very similar, and suggests that the effect of benzo-fusion of the ligand is small in relation to oxidation of the metal. The reduction potentials are related to the lowest lying π^* orbitals of individual ligands. This fact allows for comparison of the first reduction potentials of $Ru(btz)_3^{2+}$ (-1.08 V) and $[Ru(bpy)_2(\mathbf{2})]^{2+}$ (-0.86 V). Although there exists a difference in the other ligands in the complexes, the effect of benzo-fusion is clearly to lower the energy of the π^* orbital. This type of comparison cannot be made for complex **7**, as 2,2'-bioxazole is unknown.[75]

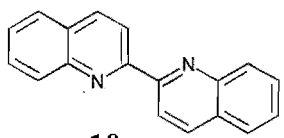

10

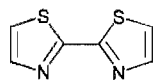

btz

The only identifiable product, after chromatography on alumina, from the reaction of ligand **3** with $Ru(bpy)_2Cl_2$ in 3:1 ethanol/water was the complex $[Ru(bpy)_2(\mathbf{3}\text{-H})](PF_6)$, (**11**). The ^1H NMR spectrum of the complex gave the expected 12 aromatic signals, and these were able to be assigned to individual rings by means of a ^1H-^1H COSY spectrum (Fig. 2.14), but the signal for the bridge only integrated for one proton. An attached-proton test (APT) ^{13}C NMR experiment, shown in Fig. 2.14, and a high-resolution FAB mass spectrum confirmed that the bridge had become deprotonated in the reaction, or when chromatographed on the alumina column, and that the complex exists as the mono-cation **11**.

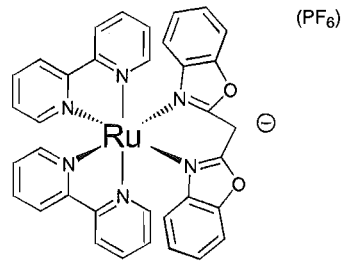

11

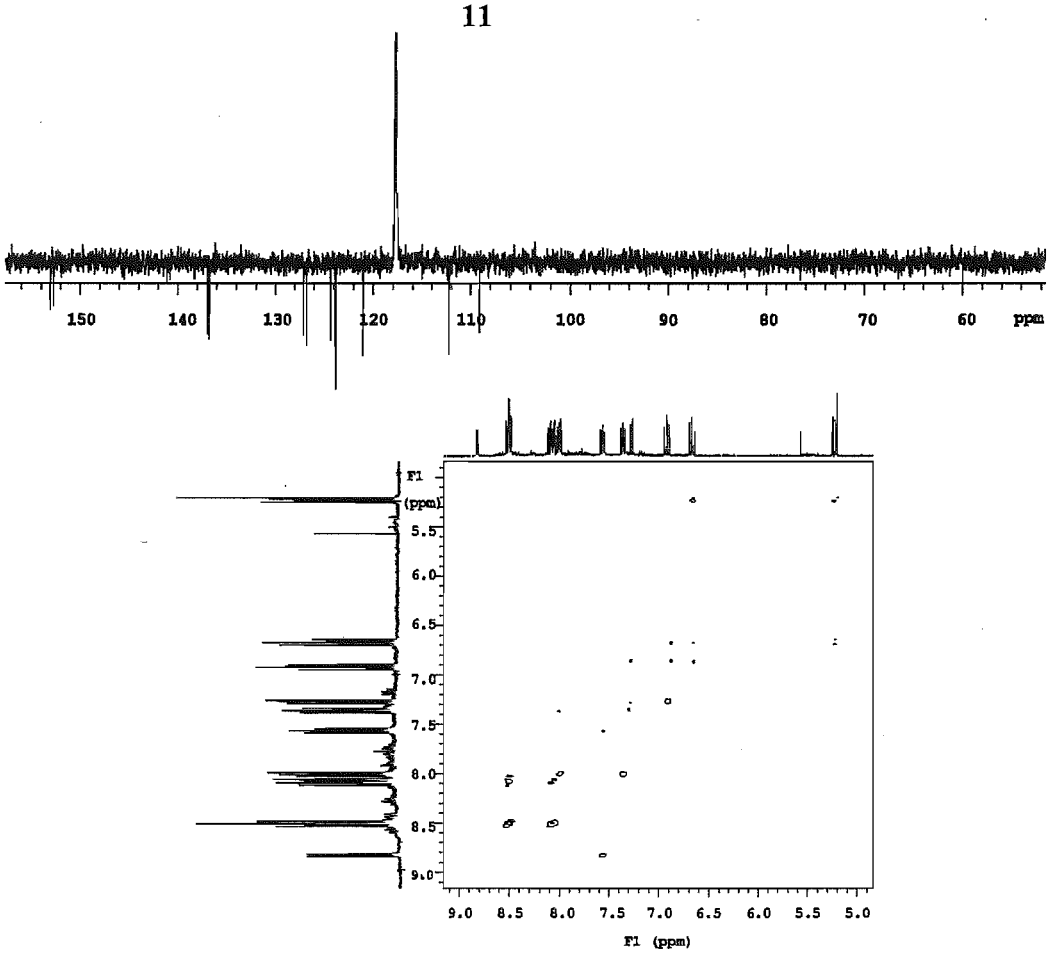

Fig. 2.14 ^{13}C APT and COSY spectra of $[Ru(bpy)_2(\mathbf{3}^-)](PF_6)$ (**11**).

When this reaction was repeated using the silver salt method, FABMS of the crude product suggested that the same complex, **11**, was formed in the reaction. The material was purified by chromatography on alumina, and one dark green fraction (**11**) was isolated in a significantly better yield of 50%. This type of coordination has been observed before for ligand **3**.[50b] The chemical shift of 59.99 ppm (CD_3CN) for the methine carbon in **11** is in good agreement with the value for the methine carbon in the complex $Rh(CO)_2$(**3**-H) at 61.37 ppm ($CDCl_3$).

Table 2.4 gives the ^1H NMR data for complex **11**. The upfield shift of H4 is very large and indicates a close proximity to the shielding pyridine rings. This can be explained by the fact that this ligand forms a six-membered chelate ring, which places H4 closer to the

adjacent pyridine ring than was so in the complex 7, which has a five-membered chelate ring. The methine bridge proton has a CIS of +0.47 ppm, which shows it has moved downfield upon bridge deprotonation. One H6 proton of the bpy ligands in **11** is at 8.83 ppm, and is assigned to the pyridine ring *cis* to the benzoxazole ligand. This proton generally reflects the aromaticity of the ring over which it sits, and in these complexes, it is typically shielded by ring-current anisotropy. Clearly it is not shielded in this case but deshielded. It has been shown that deprotonation of the bridge in ligand **4** leads to an increase in π-electron density on the nitrogen atom,[50c] and this may explain the deshielded position of this proton.

Table 2.4 ^{1}H NMR Chemical Shifts[a] and Coordination Induced Shifts[b] of **3** and **11**.

	H4	H5	H6	H7	CH^-/CH_2
11	5.20	6.65	6.95	7.28	5.20
3	7.65	7.42	7.45	7.75	4.73
CIS	-2.45	-0.77	-0.50	-0.47	+0.47
	bpy H3	bpy H4	bpy H5	bpy H6	
	8.52	8.09	7.57	8.83	
	8.49	8.05	7.36	8.00	

[a] For deuterated acetonitrile solutions. [b] CIS = ($\delta_{complex}$ - δ_{ligand}).

The UV-visible spectrum for complex **11** shows a shoulder at 482 nm and an intense absorption at 405 nm (ε 17 600 $M^{-1}cm^{-1}$) (Fig. 2.15). As has been postulated,[50c] the electron of the deprotonated bridge is presumably delocalised around the chelate ring of the benzoxazole ligand. To promote an electron from a metal d orbital to this already electron rich environment (MLCT) may be an unfavourable process.

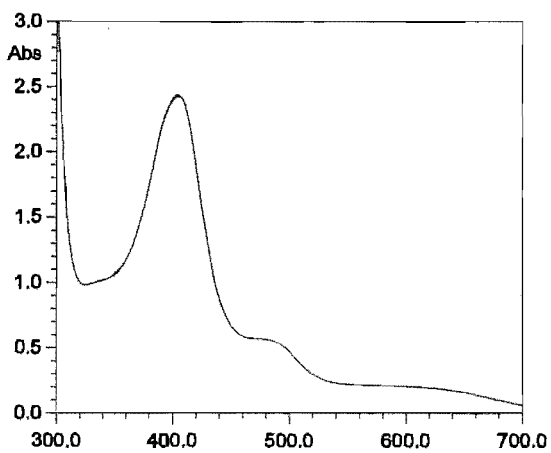

Fig. 2.15 UV-visible spectrum of $[Ru(bpy)_2(3^-)](PF_6)$ (**11**).

Electrochemically, complex **11** exhibits a reversible one-electron oxidation at +1.39 V and a one-electron irreversible reduction at -1.04 V, giving $\Delta E_{ox\text{-}red1}$ = 2.45 V. The oxidation potential of complex **11** suggests that the ruthenium atom is less electron rich, relative to

$Ru(bpy)_3^{2+}$, as the oxidation potential is 130 mV higher. The reduction process is obviously that of the benzoxazole ligand, based upon its potential, and, interestingly, it is irreversible. The $\Delta E_{ox\text{-}red1}$ value is consistent with the (M)d-(L)π^* transition being the shoulder at 482 nm in the UV-visible spectrum of complex **11**, leaving the intense transition at 405 nm as the (M)d-(bpy)π^* transition (Fig. 2.15).

Ligand **4** proved difficult to coordinate to the $Ru(bpy)_2^{2+}$ unit in a bidentate chelating manner. Reaction of **4** with $Ru(bpy)_2Cl_2$ under the standard conditions gave, on first inspection of the ^1H NMR spectrum (Fig. 2.16a), a complex with a coordinated chlorine anion and presumably the ligand bound in a monodentate fashion $[(bpy)_2RuCl(4)](PF_6)$, **12**, (Fig. 2.17). This was based upon the characteristic downfield H6 proton (10.18 ppm), and the presence of an upfield signal at 6.28 ppm. In the usual fashion, further ^1H NMR assignment of this complex was attempted. By the irradiation of the above signals and others in 1-D TOCSY experiments, five spin systems were identified, including two for the benzothiazole ligand. The chemical shifts and assignments for these signals are listed in Table 2.5.

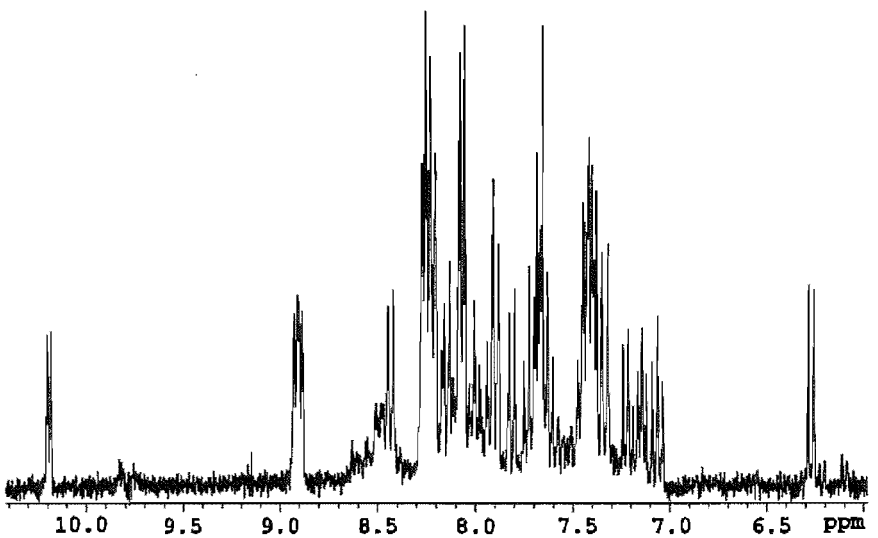

Fig. 2.16a

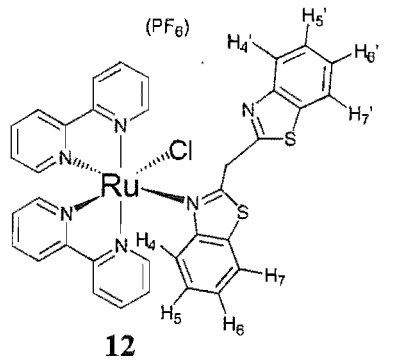

12

Fig. 2.17

Table 2.5 ^{1}H NMR Chemical shifts[a] of the benzothiazole ligand and identified bpy ligands.

H4	H5	H6	H7	H4'	H5'	H6'	H7'
6.28	7.06	7.38	7.90	7.33	7.22	7.42	7.81

bpy H3	bpy H4	bpy H5	bpy H6
8.43	8.00	7.40	10.18
8.91	8.18	7.42	8.26
8.90	8.23	7.14	8.06

[a] For deuterated acetonitrile solutions.

Having identified these rings, further assignment was attempted using ^{1}H nOe experiments by irradiating the already identified bpy H3 protons. This would hopefully allow the identification of the pyridyl partners that make up the bpy ligands. These experiments gave unexpected results. Each spectrum showed the presence of large negative nOe's (Fig. 2.16b). This type of enhancement is evident in molecules undergoing a fluxional process that involves chemical exchange. By the selective irradiation of either side of the multiplet at *ca.* 8.9 ppm, and using the intensity of the negative nOe obtained, the exchanging partner could be ascertained. The assignment was confirmed in one case by the back-irradiation of the other isolated H3 at 8.43 ppm. To see if this fluxional process involved the ligand, the upfield H4 proton was irradiated in a ^{1}H nOe experiment, and the resulting spectrum is shown in Fig. 2.16c.

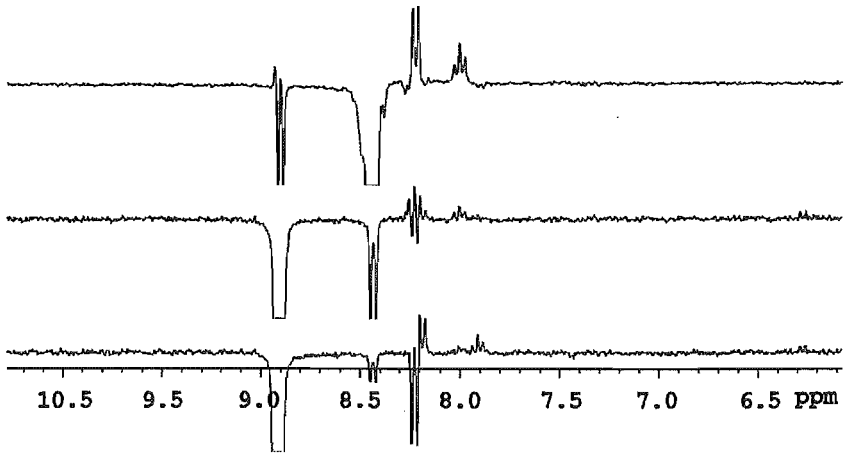

Fig. 2.16b

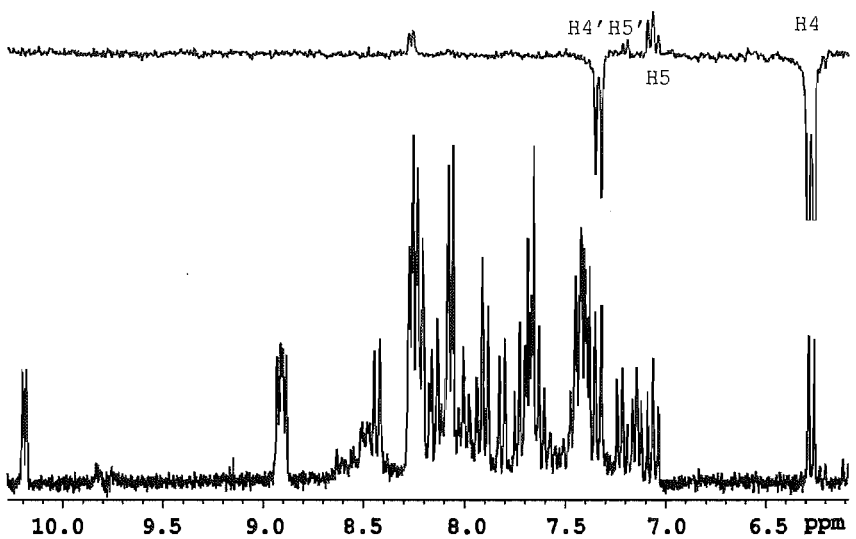

Fig. 2.16c

The expected positive nOe from H4 to H5 on the coordinated ring is seen in the signal at 7.06 ppm. Of more interest is the large negative nOe to a doublet at 7.33 ppm, which is the signal for H4' in the uncoordinated ring, thereby confirming that the two rings of the ligand are interchanging. The exchanging H4' shows a small positive nOe to the H5' proton at 7.22 ppm. The remaining signal to be assigned is the positive enhancement at 8.26 ppm. This signal shows a correlation to a H6 proton of a pyridyl ring identified by the previous 1-D TOCSY experiments (Table 2.5). Examination of the coupling constant of this signal in the ^{1}H nOe spectrum confirmed it was a H6 proton. This enhancement is to the pyridyl ring adjacent to the coordinated benzothiazole ligand. To further examine the process a variable temperature ^{1}H NMR study was undertaken with spectra obtained in 10° increments from 23° to 63°. However, this study proved inconclusive. In order to encourage chelation, the second method of preparation was attempted. Two equivalents of $AgBF_4$ were stirred with the $Ru(bpy)_2Cl_2$ complex in 1:1 ethanol/acetone to remove the chloride anion and generate the adduct $Ru(bpy)_2(acetone)_2^{2+}$ before addition of the ligand. Even with this modification, the ^{1}H NMR spectrum of the resulting material was the same.

The complex was then analysed by electrospray MS, but this did not provide a definite structure of this complex. From the ^{1}H NMR evidence, we feel certain that the $Ru(bpy)_2^{2+}$ unit is intact, and hence it is likely that the ligand has rearranged. The elemental analysis of the complex was not supportive of the structure **12**. Because of the ambiguity over the structure, the mechanism of the fluxional process remains a mystery.

The complex $[Ru(bpy)_2(\mathbf{6})](PF_6)_2$ (**13**) was produced, in excellent yield (94%), by reaction of $Ru(bpy)_2Cl_2$ with ligand **6** in 3:1 ethanol/water. Complex **13** has, because of the unsymmetrical nature of the ligand, no internal symmetry. This led to a complicated ^{1}H NMR spectrum with 24 aromatic protons, 20 of which belong to 2-substituted pyridine rings. However, both rings of the ligand **6** could be positively identified by the cooperative use of 1-D TOCSY and ^{1}H nOe spectroscopy. The benzisoxazole ring was readily identified, as it does not contain a doublet with a smaller coupling constant (a H6 proton of a pyridyl ring), and a ^{1}H nOe from H4 of the benzisoxazole gave the chemical shift of H3' (Fig. 2.18). Irradiating H3' in a 1-D TOCSY experiment then gave the chemical shifts of H4', H5' and H6'.

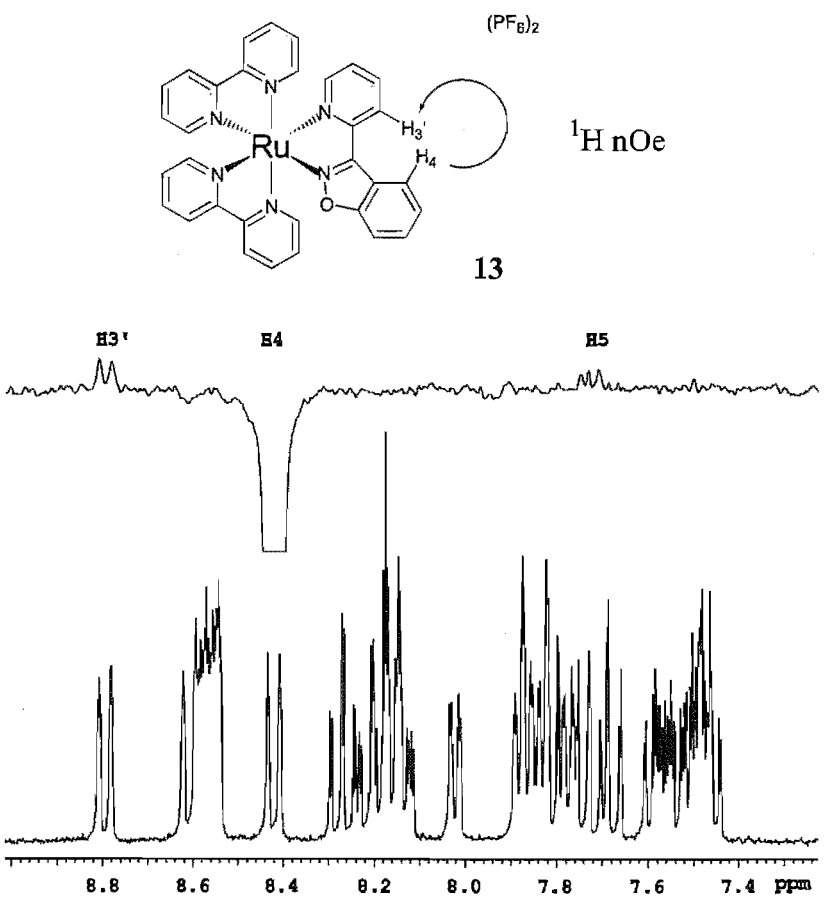

Fig. 2.18 ^{1}H NMR and ^{1}H nOe spectra of $[Ru(bpy)_2(\mathbf{6})](PF_6)_2$ (**13**).

Table 2.6 ^{1}H NMR Chemical Shifts[a] and Coordination Induced Shifts[b] of **6** and **13**.

	H4	H5	H6	H7	H3'	H4'	H5'	H6'
13	8.42	7.73	7.82	7.67	8.79	8.27	7.59	7.86
6	8.58	7.57	7.73	7.77	8.26	8.01	7.52	8.86
CIS	-0.16	+0.16	+0.09	-0.10	+0.53	+0.26	+0.07	-1.00

[a] For deuterated acetonitrile solutions. [b] CIS = ($\delta_{complex}$ - δ_{ligand}).

For $[Ru(bpy)_2L]^{2+}$ complexes negative CIS (upfield shifts) are generally as a result of some ring-current anisotropy (shielding) phenomena from other aromatic rings. This is demonstrated in complex **13** with the large upfield shift experienced by H6' (CIS -1.00 ppm). This shielding is from the pyridyl ring trans to the benzisoxazole (Fig. 2.18). Similarly, a shielding of H7 from the pyridyl ring of the bpy ligand that is *trans* to the pyridine ring of **6** could be expected. Table 2.6 indeed shows a negative CIS, but, because H7 is further from the pyridine ring the effect is much less and this is reflected in the CIS value of -0.10.

Based upon its upfield shift, it might seem that H4 also experiences some anisotropic shielding. Because of the cisoid conformation imposed by chelation, protons H4 and H3' are in an environment of high steric compression. To relieve this situation, the rings may be tilted relative to one another. In this case, H4 would lie above the pyridine ring and experience a small shielding effect from it. However, the H3' proton of the pyridyl ring should also experience a similar shielding from the benzene ring of the benzisoxazole. A positive CIS (downfield shift) of H3' to 8.79 ppm implies it does not experience any such shielding.

To explain this situation, rationalisation of the chemical shifts in the free ligand is necessary. This requires an understanding of the conformation of the ligand itself in solution. The chemical shift of H4, in the free ligand, is well downfield at 8.58 ppm. This information implies that proton H4 experiences a deshielding effect, and it is most likely that this is from the nitrogen of the pyridine ring (Fig. 2.19). Thus, the conformation of the ligand in solution is one where the nitrogens are *trans*, with respect to the inter-ring bond, and the molecule itself is near-planar. Therefore, H4 is not shielded by any ring-current anisotropy in complex **13**, but less deshielded when forced to adopt the cisoid conformation for chelation. This explanation is also consistent with the observed CIS of H3', which is shifted downfield (CIS +0.53) upon chelation to ruthenium.

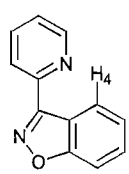

Fig. 2.19

The UV-vis spectrum of complex **13** (Fig. 2.20) shows a λ_{max} at 442 nm with a shoulder on the high-energy side at around 420 nm. The former is probably the (M)d—(L)π* transition and the latter (M)d—(bpy)π*. The (M)d—(L)π* transition is at higher energy than that of $Ru(bpy)_3^{2+}$ (452 nm), which suggests that the $\Delta E_{ox\text{-}red1}$ value for **13** should be greater than that for $Ru(bpy)_3^{2+}$. The cyclic voltammogram of complex **13** (Fig. 2.20) shows a reversible oxidation at 1.36 V and an irreversible reduction at -1.01 V. The reduction can be ascribed to electron transfer to ligand **6**, and may result in decomposition of the complex. Irreversible reductions of structurally related pyrazole-containing ligands have previously been shown to lead to complex decomposition.[8,76] The $\Delta E_{ox\text{-}red}$ value for **13** is 2.37 V, which is less than that in $Ru(bpy)_3^{2+}$ (2.59 V) and very similar to $[Ru(bpy)_2(\mathbf{1})]^{2+}$ (**7**) (2.33 V).

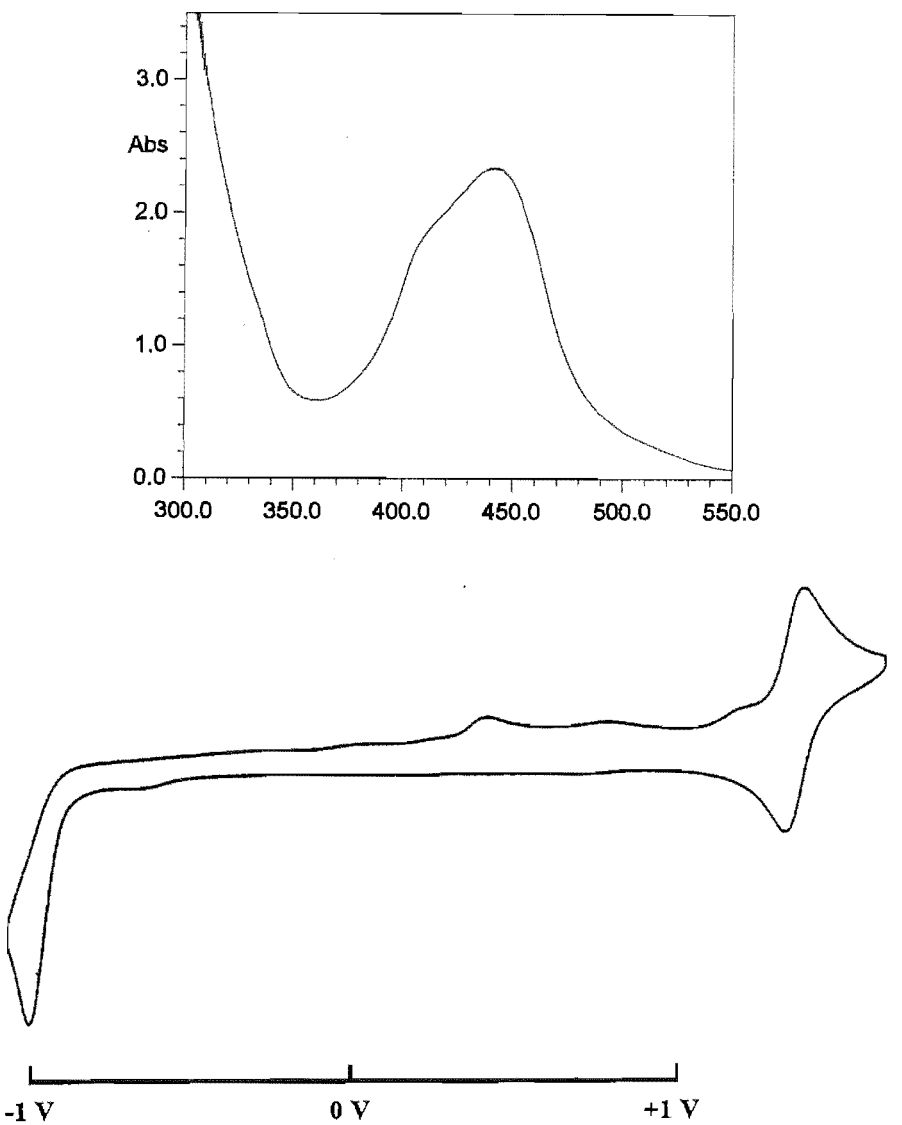

Fig. 2.20 UV-visible spectrum and cyclic voltammogram of $[Ru(bpy)_2(\mathbf{6})](PF_6)_2$ (**13**).

2.3.2 Complexes with other metal ions

Having studied the mononuclear ruthenium complexes, we thought it might be interesting to prepare and study some complexes of other metal ions with these ligands. To this end, selected complexes were prepared with Pd(II), Ag(I) and Cu(II). The extreme insolubility of ligand **2** was found to thwart any attempts at complex formation. Ligand **4** has been particularly well studied with neutral and cationic complexes of divalent transition metal ions, such as Ni(II), Cu(II), Zn(II), Co(II) and Hg(II), having been reported.[50c]

Palladium Complexes

When ligand **1** was reacted with 1 equiv. of lithium tetrachloropalladate (Li_2PdCl_4) in refluxing methanol, a tan complex of 1:1 stoichiometry [**1**.$PdCl_2$], (**14**), was formed in good yield (82%). FABMS indicated the dominant molecular ion was (**1**)Pd^+, and thus, the ligand is most probably acting as a N,N-chelating ligand (Fig. 2.21). The complex is soluble in strongly solvating solvents such as DMF, DMSO and $MeNO_2$ to give red/pink solutions. ^1H NMR of **14** in deuterated DMSO showed no change from that of the free ligand, indicating that in DMSO solution the complex dissociates.

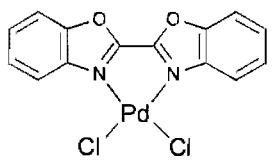

14

Fig. 2.21

When ligand **3** was reacted with Li_2PdCl_4 in methanol, an immediate precipitate developed and was filtered off. FABMS of the resulting solid suggested a chelating structure, as the molecular ion corresponding to (**3**)$PdCl^+$ was identified. Elemental analysis confirmed a 1:1 stoichiometry [**3**.$PdCl_2.H_2O$], and a monomeric chelating structure, (**15**), (Fig. 2.22) was proposed. The complex showed surprisingly good solubility in deuterated chloroform and a ^1H NMR spectrum was obtained. In six-membered chelate rings containing a methylene bridge, there exists the possibility of an agostic interaction between a methylene proton and the metal centre when the chelate ring is in a boat conformation.[77,78] The protons of the bridge are on the mirror plane which relates one half of complex **15** to the other, but they are diastereotopic, and hence should give rise to two signals. This was not seen in the ^1H NMR spectrum of **15**, and indicates that there is fast interconversion on the NMR timescale of the two possible boat forms. The chemical shifts and coordination induced shifts are presented in Table 2.7. The order of the ring protons was found by irradiation of the downfield doublet (H4) in a 1-D TOCSY experiment. The large positive CIS (+1.04) of the H4 protons is

testimony to the fact that the proximate chlorine deshields them. The H5 and H6 protons show small positive CIS values, and the protons of the methylene group have moved downfield 0.49 ppm as a result of the ligand chelating to palladium.

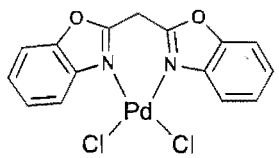

15

Fig. 2.22

Table 2.7 Chemical Shifts[a] and Coordination Induced Shifts[b] of **3** and **15**.

	H4	H5	H6	H7	CH_2
15	8.56	7.49	7.53	7.58	5.16
3	7.52	7.35	7.35	7.73	4.67
CIS	+1.04	+0.14	+0.17	-0.15	+0.49

[a] For deuterated chloroform solutions. [b] CIS = ($\delta_{complex}$ - δ_{ligand}).

Reaction of ligand **4** with Li_2PdCl_4 in refluxing methanol gave fine golden flakes that analysed as [**4**.$PdCl_2$.½H_2O], (**16**). FABMS provided evidence that the ligand was chelating with a molecular ion of (**4**)$PdCl^+$ being identified. The ^1H NMR spectrum of complex **16** was recorded in deuterated acetonitrile, but a spectrum of the ligand itself could not, and so no CIS could be calculated from this. A ^1H NMR spectrum was then recorded in deuterated DMSO, and this showed a mixture of free and complexed ligand, indicating an equilibrium between the two. The peaks due to the complex were easily distinguished from those of the free ligand as the complex has a downfield doublet (H4) brought about by the close proximity of these protons to the deshielding chlorine atom. A 1-D TOCSY irradiating this downfield doublet identified the rest of the ring protons. Again, as in the example of complex **15** above, the ^1H NMR spectrum showed only one signal for the protons of the methylene bridge. The chemical shifts and coordination induced shifts are presented in Table 2.8. The H4 protons of this complex are moved downfield as a result of deshielding from the chlorine atoms. All other ring protons show small positive CIS values. The methylene protons show a strong positive CIS value of +0.80 ppm.

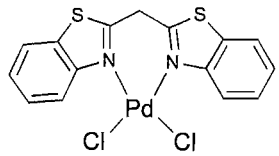

16

Fig. 2.23

Table 2.8 Chemical Shifts[a] and Coordination Induced Shifts[b] of **4** and **16**.

	H4	H5	H6	H7	CH_2
16	8.65	7.65	7.58	8.18	5.90
4	8.00	7.45	7.53	8.10	5.10
CIS	+0.65	+0.20	+0.05	+0.08	+0.80

[a] For deuterated dimethyl sulfoxide solutions. [b] CIS = ($\delta_{complex}$ - δ_{ligand}).

When ligand **6** was reacted with Li_2PdCl_4 in methanol a yellow complex, that analysed as [**6**.$PdCl_2$], (**17**), was formed in high yield (94%). The ^{1}H NMR spectrum of the complex was recorded in deuterated DMSO, and this showed a mixture of free and complexed ligand. The shifts of the complexed ligand were found by the irradiation of two signals at 9.11 ppm and 8.66 ppm in 1-D TOCSY experiments. The chemical shifts and coordination induced shifts are presented in Table 2.9. All the CIS values for this complex are positive, and this reflects the change in the adjacent substituent from a shielding pyridine ring in complex **13** to a deshielding chlorine atom. This leads to a positive CIS value of H6' (+0.24). Many of the other CIS values for **17** are similar to the shifts observed for the ruthenium complex **13**, and the reasons for these are the same as those discussed previously.

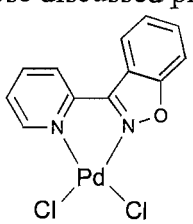

17

Fig. 2.24

Table 2.9 ^{1}H NMR Chemical Shifts[a] and Coordination Induced Shifts[b] of **17** and **6**.

	H4	H5	H6	H7	H3'	H4'	H5'	H6'
17	8.66	7.73	7.85	8.11	8.83	8.49	7.95	9.11
6	8.52	7.51	7.73	7.86	8.22	8.05	7.61	8.87
CIS	+0.14	+0.21	+0.12	+0.25	+0.61	+0.44	+0.34	+0.24

[a] For deuterated dimethyl sulfoxide solutions. [b] CIS = ($\delta_{complex}$ - δ_{ligand}).

Silver Complexes

A complex with ligand **1** and $AgNO_3$ was prepared by adding equimolar amounts of ligand **1** in chloroform to a solution of $AgNO_3$ in 1:1 chloroform/methanol. The resulting micro-crystals were a mauve colour and analysed as [**1**.$(AgNO_3)_2$] (**18**). Thus despite the fact that stoichiometric quantities of ligand and metal salt were mixed, the complex has formed has a 1:2 ligand:metal stoichiometry. This will be described as a [1 + 2] complex. The micro-crystals were too small for an X-ray structure analysis and, despite various attempts at recrystallisation, no crystals suitable for a structural investigation were obtained. ^{1}H NMR spectroscopy and FABMS were used to further characterise complex **18**. However, this and other attempts at characterisation of Ag(I) complexes described in this thesis by these methods gave no useful information. The Ag(I) ion is labile, and in the ^{1}H NMR spectrum no coordination induced shifts were observed, and in FABMS no molecular ions corresponding to any complexed ions were found.

When $AgNO_3$, dissolved in 1:1 methanol/water, was added to ligand **3** dissolved in methanol, the reaction solution immediately darkened. Upon standing, metallic silver was deposited around the sides of the vial, and the solution was filtered to remove metallic material every 24 hours until no more precipitated, then concentrated to dryness *in vacuo*. TLC showed the presence of two main components, one of which was the starting material. An EI mass spectrum identified the second major component as the dimeric product, 1,1',2,2'-tetra(2-benzoxazolyl)ethene, (**19**), (Fig 2.25). Also identifiable were alcohol and ketone oxidation products of the methylene-bridge of the starting ligand. This type of reaction has been previously observed for both ligands **3** and **4**.[50a] A possibility is that the silver acts to oxidise the methylene bridge in **3** to the corresponding ketone, which reacts *via* the Knoevengel reaction with another molecule of **3** to form the alkene **19**. Alternatively, the silver ion could act as a one-electron oxidant inducing radical coupling.

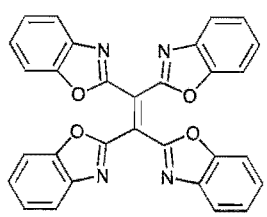

19

Fig. 2.25

Reacting $AgNO_3$ and **4** in refluxing methanol gave, after complete evaporation, needle-like crystals that analysed as [**4**.$AgNO_3$], (**20**), and some precipitated silver. The ^{1}H NMR spectrum of complex **20** in deuterated DMSO showed no difference from that of the free ligand, which indicated that the methylene bridge had not been oxidised.

Copper Complexes

Reaction of stoichiometric amounts of ligand **1** with $CuCl_2.2H_2O$ in chloroform/methanol gave purple cube-shaped crystals, (**21**), suitable for X-ray diffraction. The structure is shown in Fig. 2.26.

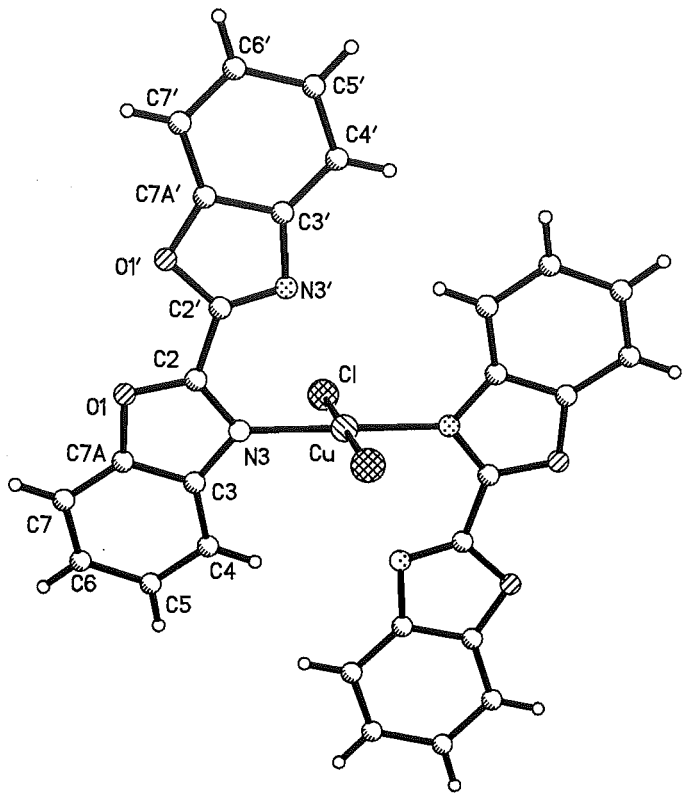

Fig. 2.26 Perspective view, with atom labelling of the asymmetric unit, of **21**. Selected bond lengths (Å) and angles (°): Cu-N3 1.979(7), Cu-Cl 2.261(2), N3-Cu-Cl 88.7(2), C2-N3 1.312(8), N3-C3 1.365(11), C3-C7A 1.414(11), C7A-O1 1.355(11), O1-C2 1.346(11),C2-N3-C3 104.8(6), C2-O1-C7A 104.7(5), C2-C2' 1.471(12), C2'-N3' 1.255(10), N3'-C3' 1.416(10), C3'-C7A' 1.417(12), C7A-O1' 1.355(11), O1'-C2' 1.350(10) C2'-N3'-C3' 104.4(6), C2'-O1'-C7A' 102.7(6).

The complex crystallises in the monoclinic space group $P2_1/c$, with the copper atom lying on a centre of inversion. The full structure is a [2 + 1] complex, with monodentate coordination of the heterocyclic ligands. The geometry about the copper is square planar, with the N3-Cu distance being 1.979(7)Å and the Cu-Cl bond distance 2.261(2)Å. The N3-Cu-Cl bond angle of 88.7(2)° defines the square planar environment of the copper.

Interesting is the conformation of the ligand in this complex. The ligand is essentially planar, although slightly bowed, with a mean deviation from the plane of 0.086(1)Å. The nitrogens of the coordinated and uncoordinated benzoxazole rings are *cis*, even though the ligand is only bound in a monodentate fashion. This is in contrast to the structure of the free ligand where the nitrogens are *trans* (see Fig. 2.3).[55] The Cu-N3' distance of 3.082(7)Å is

considered to be too long for a bonding interaction. Perhaps the reason for this conformation is an attractive interaction between N3' of one ligand and H4 of the other, as the distance of 2.806(7)Å is indicative of a weak hydrogen bond. The reason the ligand is not chelating may be based upon a steric argument, where the ligand may be too large to satisfactorily arrange in a *trans* fashion around the copper. This would be due to a steric interaction between the H4 protons that would result from this arrangement (Fig. 2.27). When two bpy ligands are in a *trans* arrangement around a metal atom, the ligands are significantly distorted from planarity, due to the interaction between their H6 protons.[79,80] As ligand **1** is larger than bpy, the H4 protons would be placed even closer, and would not allow two chelate rings to form.

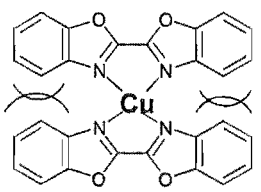

Fig. 2.27

The reaction of stoichiometric amounts of ligand **6** with $Cu(NO_3)_2.3H_2O$ in methanol gave large green block-shaped crystals, (**22**), one of which was cut and used for X-ray analysis. The structure is shown in Figure 2.28.

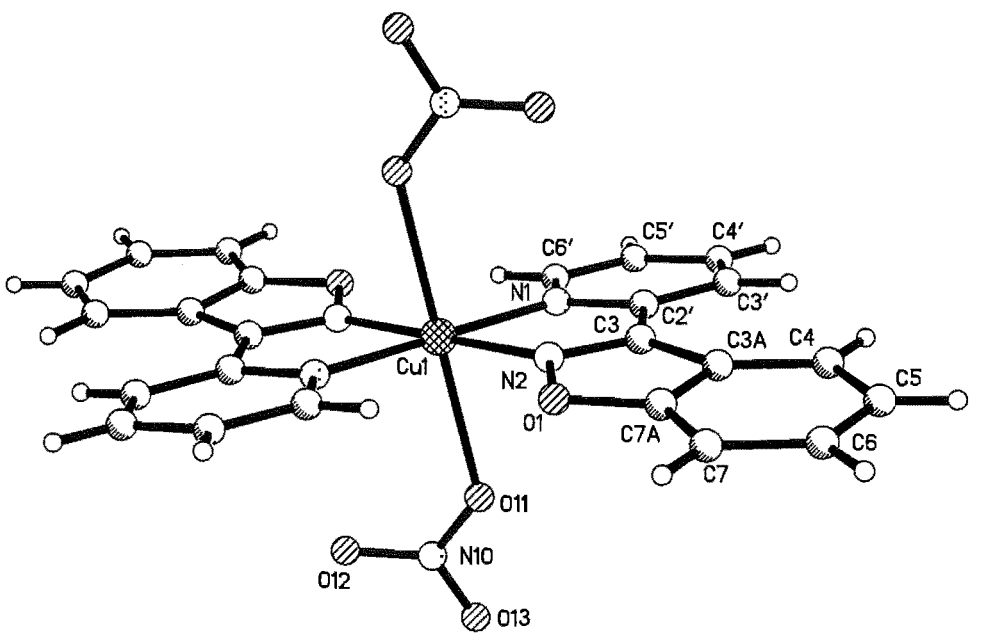

Fig. 2.28 Perspective view, with atom labelling of the asymmetric unit, of **22**. Selected bond lengths (Å) and angles (°): N1-Cu1 2.035(2), N2-Cu1 2.020(2), N1-Cu1-N2 78.8(1), O1-N2 1.391(2), N2-C2 1.318(2), O1-N2-C3 109.6(1), N2-O1-C7A 106.2(1), N1-Cu1-O11 85.16(6), N2-Cu1-O11 82.34(6).

The structure is another [2 + 1] complex, and has crystallised in the triclinic space group P-1. By virtue of the centre of inversion about Cu1, the rings of each ligand are *trans* with respect to each other in the complex. The ligand is chelating through N1 of the pyridine ring and N2 of the benzisoxazole, and is essentially planar, with a mean deviation from the plane of 0.080(3)Å. This supports the conclusion reached for complex **13** where the rings of the ligand are not tilted with respect to each other due to a steric interaction between H3' and H4. The bond lengths of the coordinating nitrogens are N1-Cu1 2.035(2)Å and N2-Cu1 2.020(2)Å with a bite angle N1-Cu1-N2 of 78.8(1)°. Two nitrate counter ions, each bound *via* an oxygen atom, complete the Jahn-Teller tetragonally distorted coordination sphere.

A search of the Cambridge Crystallographic Database revealed that this is the first reported X-ray crystal structure of a benzisoxazole-containing coordination complex. Structurally, this complex is very similar to one published in 1994 by Battaglia *et al.*[81] with the related ligand 4-(2-pyridyl)-1,2,3-triazolo[1,5-*a*]pyridine. A pictorial representation of this complex is shown in Fig. 2.29.

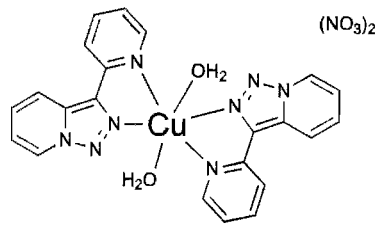

Fig. 2.29

2.4 Summary

In this chapter, four new ruthenium complexes were synthesised and investigated by a combination of ^{1}H NMR, ^{13}C NMR, UV-visible spectroscopy, cyclic voltammetry and X-ray crystallography. The results of these investigations proved that the heteroaromatic benzoxazole, benzisoxazole and benzothiazole rings lead to different properties for the $Ru(bpy)_2L^{2+}$ complexes when compared to $Ru(bpy)_3^{2+}$. Electrochemically, the benzoxazole and benzothiazole rings have a much lower reduction potential than bipyridine in the ruthenium complexes prepared. The irreversible first reduction of $[Ru(bpy)_2(\mathbf{6})](PF_6)_2$ (**13**) may indicate that the N-O bond in ligand **6** is electrochemically unstable. However, **6** was shown to be a useful chelating ligand, in what appears to be the first investigation of a ligand containing a 1,2-benzisoxazole component.

The ligands 2,2'-methylenebisbenzoxazole (**3**) and 2,2'-methylenebisbenzothiazole (**4**) have acidic methylene bridges due to the electron-withdrawing nature of the heterocyclic rings. This was evidenced by the conversion of ligand **3** to its deprotonated form when chelated to the ruthenium centre. This phenomenon has potential uses in the pH control over properties of complexes. This has been accomplished with other acidic hydrogens attached to nitrogen in pyrazole,[46] imidazole,[82] triazole,[83,84] and tetrazole rings.[9]

Chapter 3

Benzotriazoles

3.1 Introduction

In this chapter, the complexity of the heterocyclic ring system being examined has increased. Benzotriazole has a five-membered ring containing three heteroatoms, all of which are nitrogen, fused to a benzene ring. The ring system and ring numbering for benzotriazole itself are shown in Fig. 3.1. The coordination chemistry of benzotriazole and its deprotonated form, the benzotriazolate anion, has been thoroughly explored and reviewed.[85] A notable feature of both the protonated and deprotonated forms is their ability to coordinate to more than one metal ion. For example, the benzotriazolate anion has been shown to be able to coordinate to three metal centres *via* its three nitrogen atoms,[85] as depicted schematically in Fig. 3.2.

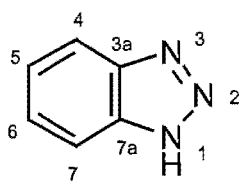

Fig. 3.1

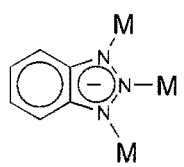

Fig. 3.2

Benzotriazole-containing ligands can be substituted in the 1- or the 2-position of the triazole ring. The coordination chemistry of 1-substituted benzotriazoles has also been explored and, in particular, 1-methylbenzotriazole has been examined in some detail by a group of Greek chemists.[86a-e] In general, the results of these investigations show that the N3 nitrogen atom of 1-methylbenzotriazole is the preferred, although by no means exclusive, nitrogen for coordination.

There has been some study of mononuclear iron[87] and ruthenium[88] complexes with benzotriazole, and more recently the electronic properties of a dinuclear ruthenium complex containing a benzotriazolate bridge has been examined.[89,90] The focus of this study is multidentate ligands, containing benzotriazoles substituted in the 1-position, that are capable of a chelating coordination mode. Ligands of this type have been little studied. However, the benzotriazolylborates represent a class of ligands that have been used in coordination chemistry. A molybdenum complex containing a tripodal tridentate tris(benzotriazol-1-yl)borate ligand has been characterised crystallographically,[91] and a pictorial representation of the complex is shown in Fig. 3.4a. The coordination chemistry of a bis(benzotriazol-1-yl)borate ligand has been investigated with ruthenium(II)[92] and more recently with rhodium(I).[93] The authors found that this ligand could bind in a chelating fashion through the N2 nitrogen atoms, as shown in Fig. 3.4b. It is instructive to note that a chelating relationship is impossible with the 1-substituted benzotriazole ligands for the present study when coordination occurs through the N3 atom. If this type of coordination occurred, the ligand is acting in a divergent manner, and would act as a bridge between different metal ions (Fig. 3.5).

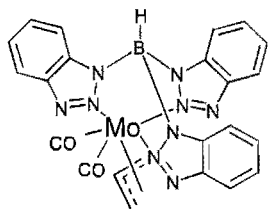

Fig. 3.4a

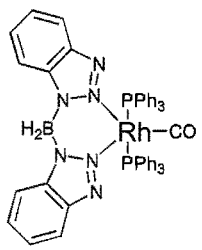

Fig. 3.4b

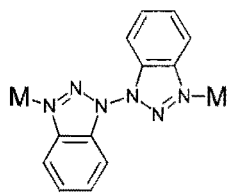

Fig. 3.5

One of the ligands in this study, 1,1'-bibenzotriazole, (**23**), has a structural similarity to 1,1'-biisoquinioline (biq). Upon chelation, biq is non-planar, due to the steric interaction between the H8 and H8' protons (Fig. 3.6). As a result, the coordinated ligand becomes chiral. In crystal structures of metal complexes involving this ligand, the rings of the ligand are splayed at *ca.* 37°.[94,95] In $Ru(bpy)_2^{2+}$ and $Os(bpy)_2^{2+}$ complexes, where because of the existing chirality, the resultant complexes with biq are diastereoisomeric. Furthermore, due to the fact that NMR differentiates the diastereomers, their existence was seen in ^1H NMR spectra, and the mechanism of interconversion between the diastereomeric forms was determined.[96-98] We wondered if this type of steric interaction between the H7 and H7'

protons would exist for **23** upon N2,N2'-chelation. It was also decided to prepare the 'hybrid' ligand 1-(1-isoquinolyl)benzotriazole, (**29**), and explore its potential for this interaction.

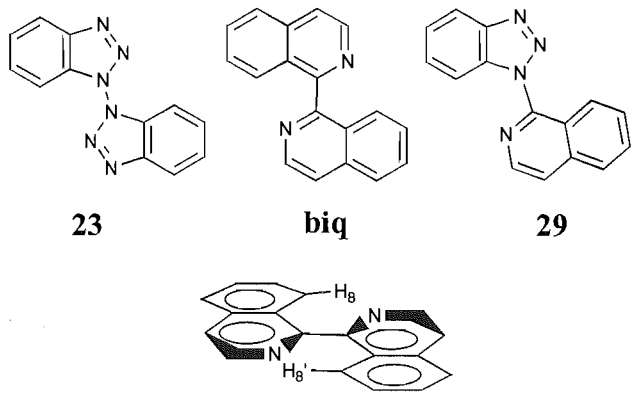

Fig. 3.6

The present study concerns the synthesis, characterisation, and electronic properties of a group of mononuclear ruthenium complexes bearing benzotriazole-containing ligands. Also investigated is the supramolecular chemistry of the ligands with copper(II), silver(I) and palladium(II).

3.2 Syntheses of Ligands

1,1'-Bibenzotriazole (**23**) was prepared in two steps, following reported literature preparations, which are summarised in Scheme 3.1.

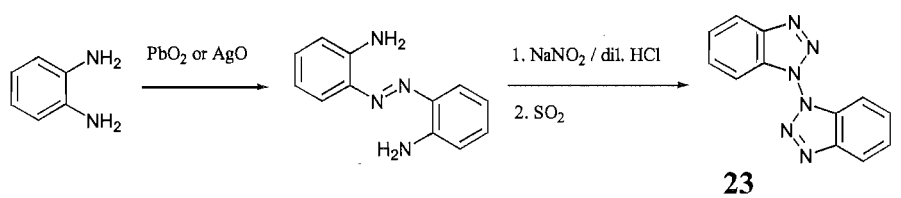

Scheme 3.1

1,2-Diaminobenzene was oxidised to 2,2'-diaminoazobenzene *via* the method of Carboni *et al.*[99] and that of Ortiz *et al.*;[100] however, the workup was changed in either case to that described by Skrabel *et al.*[101] Diazotisation of 2,2'-diaminoazobenzene by sodium nitrite in dilute hydrochloric acid, followed by reductive cyclisation using SO_2, as described by Harder *et al.*,[102] gave **23** in 40% yield from this reaction.

In the ^{1}H NMR spectrum of ligand **23** it was noticed that one of the two doublets was considerably upfield, at a chemical shift of 7.33 ppm. This signal was proposed to be due to the H7 protons, and this was confirmed by a GHSQC experiment. It seemed that the

benzotriazole rings of the biheterocycle were mutually shielding the H7 proton of the other ring. It was therefore of interest to study the conformation of this molecule in the solid state by single crystal X-ray crystallography. Crystals suitable for a structural study were grown by slow evaporation from an ethyl acetate solution of the compound. The structure is shown in Fig. 3.7.

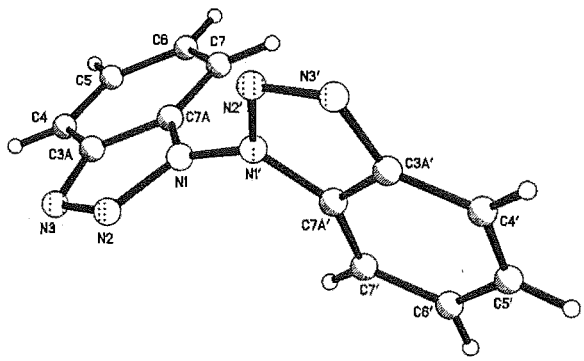

Fig. 3.7 Perspective view, with atom labelling of the contents of the asymmetric unit, of **23**. Selected bond lengths (Å) and angles (°): N1-N2 1.368(4), N2-N3 1.306(4), N1-N2-N3 107.1(3), C3A-C7A 1.397(5), C7A-N1 1.379(4), N2-N1-C7A 127.9(3), N1-N1' 1.366(4), N1'-N2' 1.392(4), N2'-N3' 1.294(4), N1'-N2'-N3' 107.5(3), C3A'- C7A' 1.389(5), C7A'-N1' 1.378(4).

The ligand crystallises in the chiral orthorhombic space group $P2_12_12_1$, with the asymmetric unit containing one full molecule. The bond lengths and bond angles of the rings are all within the range found previously for a 1-substituted benzotriazole.[103,104] Of interest is the N1-N1' bond length in this molecule as this distance has not been determined previously. From the X-ray analysis the value of 1.366(4)Å has been determined. Both rings of the ligand are planar (mean deviations from the plane of 0.005(1)Å for both rings), and are very nearly orthogonal to each other [84.5(1)°] (Fig. 3.7b). Surprisingly, the ligand has not adopted the *trans* coplanar conformation (Fig. 3.8), where there are two attractive intramolecular hydrogens bonds from the N2 nitrogens to the H7 hydrogens of the other ring. Also this conformation would maximise conjugation over the molecule.

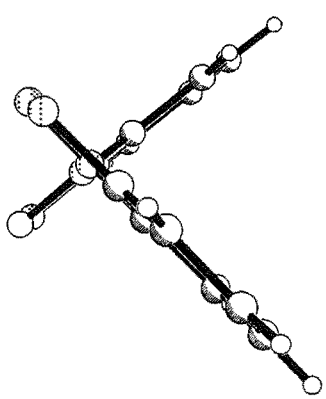

Fig. 3.7b

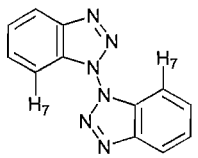

Fig. 3.8

This molecule demonstrates interesting molecular packing in the crystal structure, with π-π stacking along each of the three axis of the unit cell, as well as intermolecular hydrogens bonds from within a sheet. For example, along the a-axis the planar aromatic rings of the ligand stack in a head to tail manner, with the closest distance between the stacks being 3.475(5)Å. A perspective view along the a-axis is shown in Fig. 3.7c, which also shows the intermolecular hydrogen bond between the H6 proton of one benzotriazole and the N3 nitrogen of a different ligand within the same sheet [2.463(3)Å]. A reason that the molecule has not adopted the coplanar conformation of Fig. 3.8 may be that the effect of the extended π-π stacking outweighs the stability of conjugation gained by coplanarity.

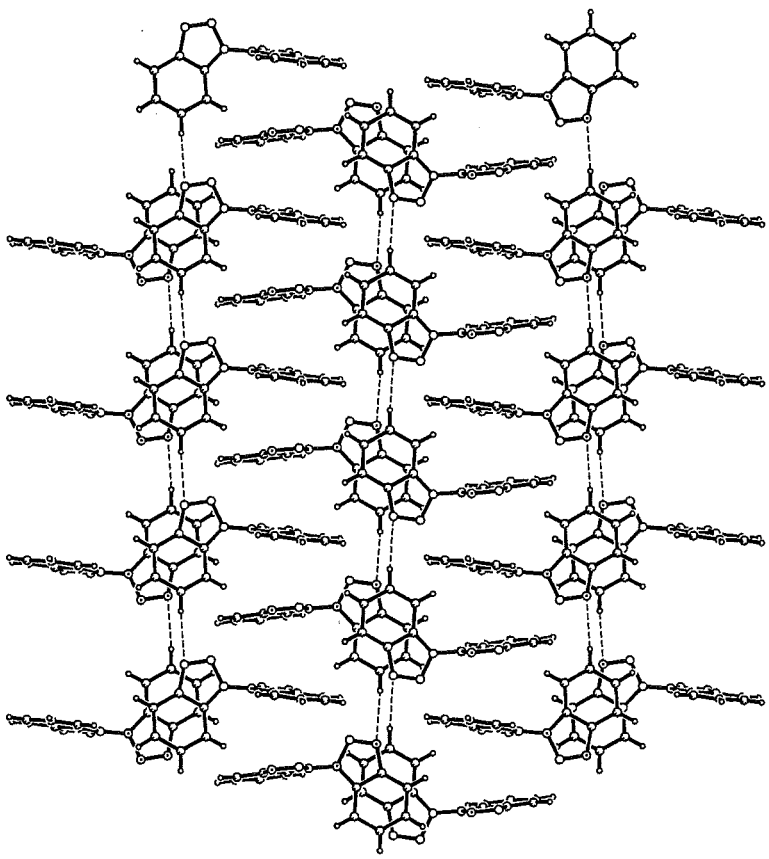

Fig. 3.7c View of the molecular packing along the a-axis in the crystal structure of **23**.

1,1'-Methylenebisbenzotriazole (**24**) was synthesised *via* a phase-transfer catalysed (PTC) reaction. Benzotriazole and diiodomethane were refluxed in a mixture of benzene and 40% aqueous NaOH, with tetrabutylammonium hydroxide as catalyst, as shown in Scheme 3.2.

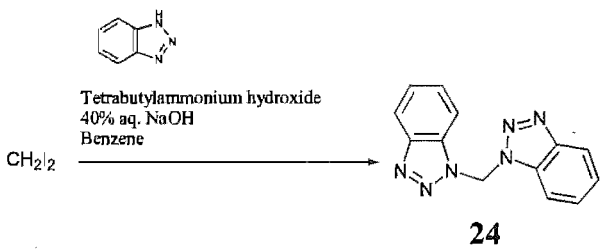

24

Scheme 3.2

This reaction produced a 6:4:1 ratio of isomers **24**, 1,2'-methylenebisbenzotriazole (**25**) and 2,2'-methylenebisbenzotriazole (**26**), respectively (Fig. 3.9). Ligand **24** had previously been prepared *via* a PTC reaction described by Avila *et al.*,[105] who also obtained a similar product ratio. Recrystallisation from toluene/hexane gave pure **24** in 27% yield.

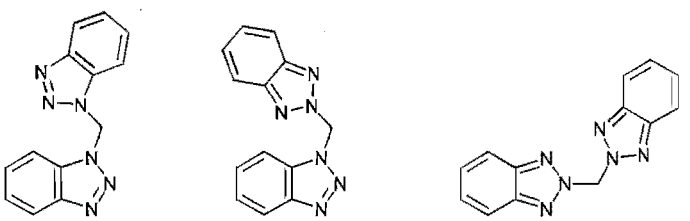

24 **25** **26**

Fig. 3.9

Some ligands containing only one benzotriazole ring were also prepared, *viz* 1-(2-pyridyl)benzotriazole, (**27**), 1-[(2-pyridyl)methyl]benzotriazole, (**28**), and 1-(1-isoquinolyl)benzotriazole, (**29**) (Fig. 3.10).

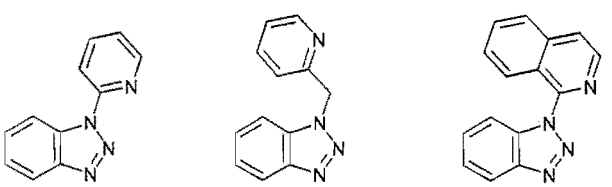

27 **28** **29**

Fig. 3.10

1-(2-Pyridyl)benzotriazole (**27**) was synthesised following the method of Katritzky,[106] except that 2-chloropyridine was used in place of 2-bromopyridine (Scheme 3.3). This resulted in a lower yield (67%) than that obtained with the bromopyridine (99%).

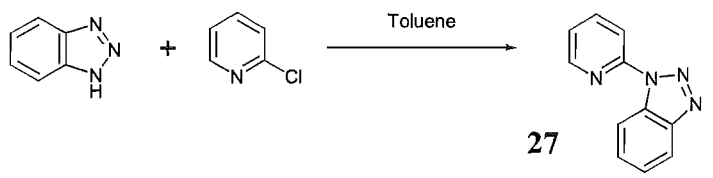

Scheme 3.3

1-[(2-Pyridyl)methyl]benzotriazole (**28**) was synthesised *via* a PTC reaction, with identical conditions to that described above for ligand **26**, as shown in Scheme 3.4.

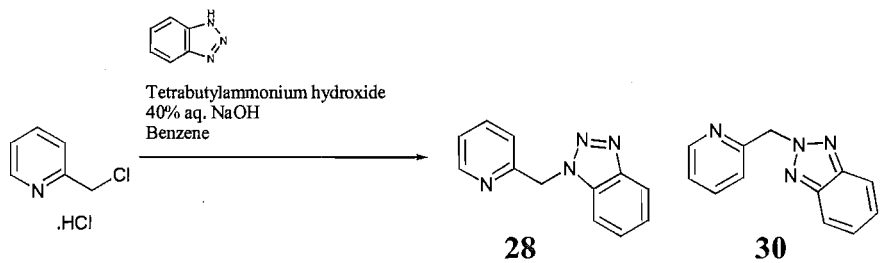

Scheme 3.4

A ^{1}H NMR spectrum of the crude reaction mixture revealed a 10:1 ratio of products **28** and 2-[(2-pyridyl)methyl]benzotriazole, (**30**). Recrystallisation from toluene gave pure **28** in 45% yield. Ligand **28** has previously been made by other methods.[107]

The synthesis of 1-(1-isoquinolyl)benzotriazole (**29**) was based on the method used to produce **27**, as shown in Scheme 3.5.

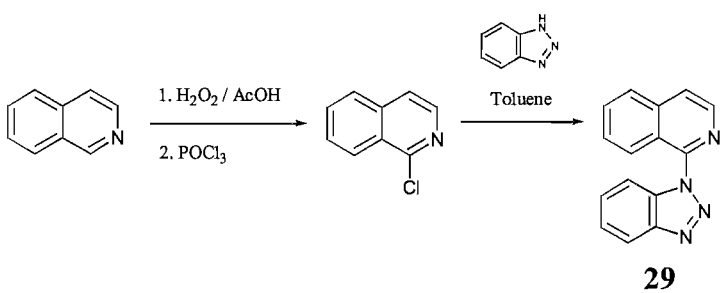

Scheme 3.5

1-Chloroisoquinoline was synthesised from isoquinoline by hydrogen peroxide oxidation in acetic acid, followed by chlorination in refluxing phosphorus oxychloride. The reaction of benzotriazole with 1-chloroisoquinoline in refluxing toluene produced the new

ligand **29** in 70% yield after recrystallisation. Ligand **29** was characterised by melting point, ^{1}H and ^{13}C NMR spectroscopy, EI mass spectrometry and elemental analysis.

NMR assignment of **29**.

A large part of the work described in this thesis involves the detailed analysis of ^{1}H NMR spectra of ruthenium complexes, particularly the changes in chemical shifts that coordination induces. To record the coordination induced shifts due to complexation, it is crucial that the signals of the ligand are correctly assigned. For this reason, it was important to assign totally the ^{1}H NMR spectrum of **29**.

To a first approximation, the ^{1}H NMR spectrum of **29** contains 10 different signals for the 10 different protons in the molecule, comprising 6 doublets and 4 triplets. The ^{1}H NMR spectrum of **29** is shown in Fig. 3.11. Nine different signals are observed in the spectrum. One signal, at *ca.* 7.8 ppm, can be recognised as the overlap of one doublet and one triplet.

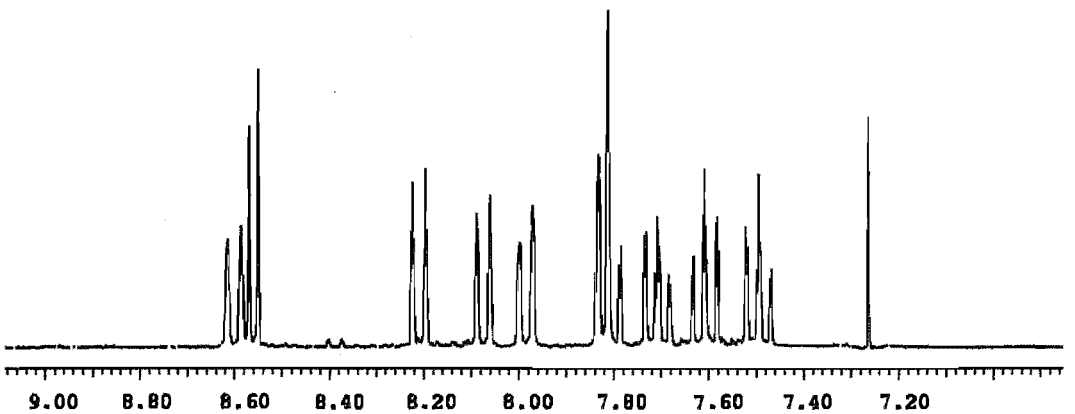

Fig. 3.11 ^{1}H NMR spectrum of **29**.

The first step in the ^{1}H NMR assignment was to separate the protons into their respective spin systems. This was done by 1-D TOCSY. Two four-spin systems were found with the expected doublet, triplet, triplet, doublet splitting pattern of 1,2-disubstituted benzene rings. These are at 8.21, 7.49, 7.61, 8.08 and 7.99, 7.81, 7.71, 8.60 ppm, which left two doublet signals at 8.58 and 7.82 ppm which must be H3' and H4' of the isoquinoline ring. 1-D TOCSY only gives an order around the ring, it does not allow the full assignment unless prior information, such as chemical shift or coupling constants, can positively identify one of the protons. What remained was to resolve which system belonged to the benzotriazole and which belonged to the isoquinoline, as well as obtaining the correct order around the rings. To accomplish this, one positive assignment for each system identified was needed. The benzotriazole ring system has a distinctive chemical shift for the C7 carbon at *ca.* 110 ppm. The identification of the proton signal belonging to C7 would allow the distinction of the benzotriazole *vs* isoquinoline four-spin proton system, and then allow for the correct assignment of the order around the benzotriazole ring from the 1-D TOCSY.

A ^{13}C NMR experiment was performed, with all 15 signals recorded. The signal of C7 was at 112.89 ppm, well separated from other signals in the spectrum. The next step was to correlate the protons to their respective carrier carbons by means of a GHSQC experiment. In the GHSQC spectrum, shown in Fig. 3.12, a correlation from the C7 carbon signal to the signal at 8.08 ppm in F2 identified H7 of the benzotriazole system, and so, the order and assignment of this ring was complete. The signals for the protons of the benzene isoquinoline ring are at 7.99, 7.81, 7.71 and 8.60 ppm. It seemed likely that the signal at 8.60 ppm was that of H8', based upon it being deshielded by the lone pair on N2 of the benzotriazole, implying the conformation was *trans* about the inter-ring bond with respect to N2 and N2' (Fig. 3.13). Based upon this assumption, the order around the isoquinoline ring was determined.

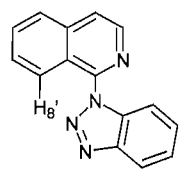

Fig. 3.13

Since the GHSQC spectrum allowed the assignment of all protonated carbons, the only other carbons to be assigned were quaternary. Comparison of the ^{13}C NMR spectrum of **29** with similar molecules allowed assignments of the quaternary carbons based upon chemical shift. For instance, C4A' (138.87 ppm) and C8A' (122.84 ppm) of the isoquinoline ring and C7A (133.37 ppm) of the benzotriazole were identified by comparison with isoquinoline[108] and with **27**. The only ambiguities which remained were the assignment of C1' and C3A to the remaining signals at 145.93 and 148.18 ppm. To resolve these, a GHMBC experiment was performed, and this was also used to confirm many of the assignments already made, particularly for H8', where in the GHMBC spectrum it should correlate to C4A'.

In the GHMBC spectrum, shown in Fig. 3.12, the signal from 8.60 ppm in F2 correlates to the C4A' carbon at 138.87, thereby confirming the proposal that this signal is H8. The ambiguity over C1' and C3A is also resolved from the correlations from the identified H7 and H5 protons to C3A, and the correlations from H3' and H8' to C1'.

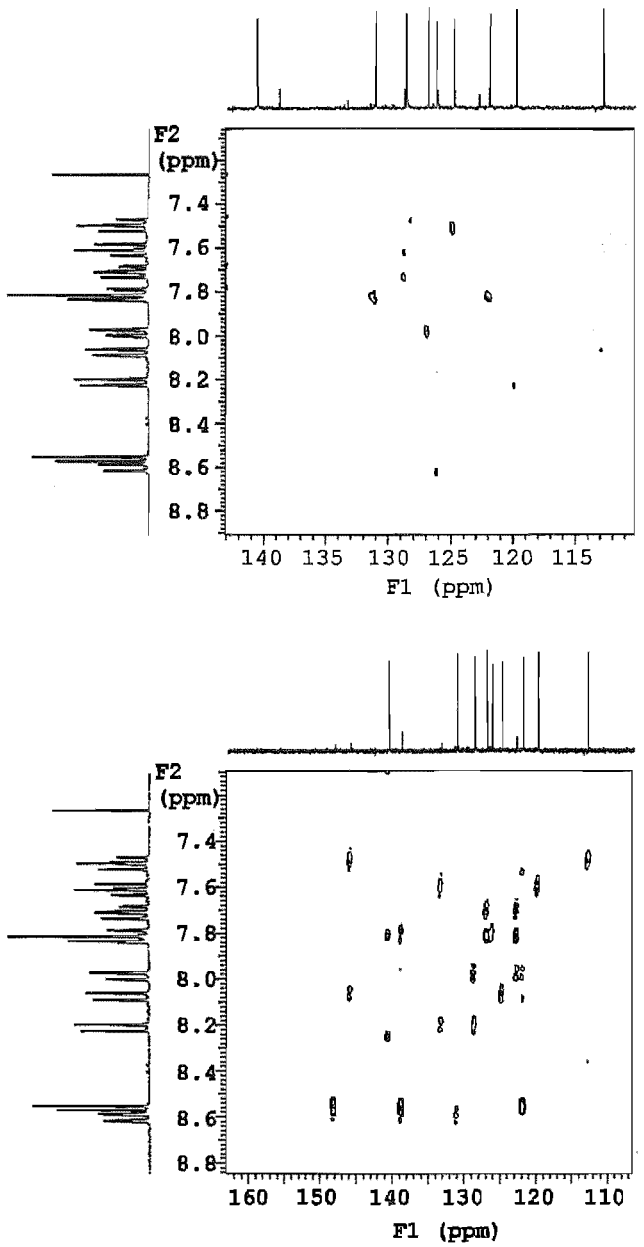

Fig. 3.12 GHSQC (top) and GHMBC spectra (bottom) of **29**.

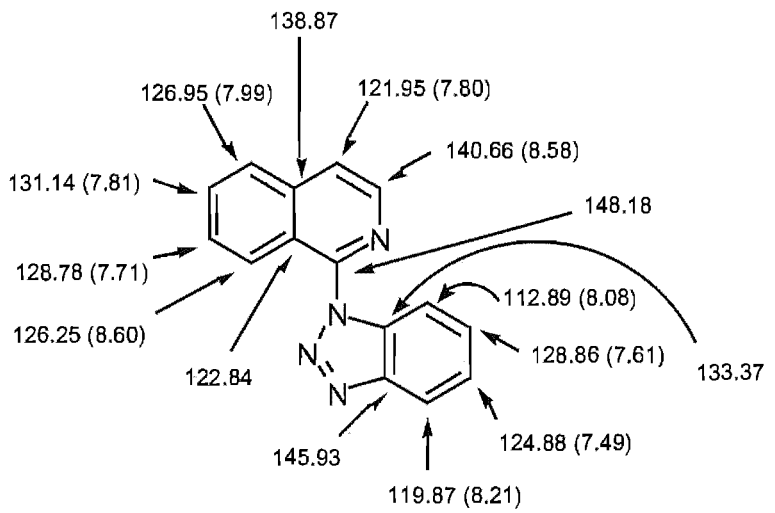

Fig. 3.14 ^{13}C (and ^{1}H NMR) chemical shifts for **29** in deuterated chloroform solutions.

3.3 Ruthenium Complexes

3.3.1 Synthesis and ^{1}H NMR

The reaction of ligand **23** with $Ru(bpy)_2Cl_2$ in 3:1 ethanol/water gave a dark coloured complex, in good yield, that was isolated as a hexafluorophosphate salt. This complex was found, by FABMS, to contain a coordinated chloride anion, as well as the ligand, and so was formulated as $[Ru(bpy)_2(\mathbf{23})Cl](PF_6)$, (**31**) (Fig. 3.15). Characterisation of this complex by ^{1}H NMR was aided by some easily identified signals in the spectrum (Fig 3.16). The proximate chlorine relationship described in Chapter 2 (Fig 2.15) was identified by the chemical shift of the bpy H6 at 10.18 ppm. Other signals that were recognised by their chemical shift were a downfield benzotriazole H4 at 9.12 ppm, which is also deshielded by the proximate chlorine, and another downfield bpy H6 at 9.04 ppm, which was assigned to the bpy H6 that resides over the coordinated benzotriazole ring (Fig 3.15). These signals provided an excellent starting point for characterisation by ^{1}H NMR, and allowed some determination of the conformation of the ligand in the complex. Irradiation of these and other signals in 1-D TOCSY experiments provided the chemical shifts of all the protons in the spectrum. As the bpy H3 signals are well separated in the spectrum, it was possible, by ^{1}H nOe experiments, to find the partner H3 proton of each bpy. In this manner, it was possible to assign totally the ^{1}H NMR spectrum of **31**.

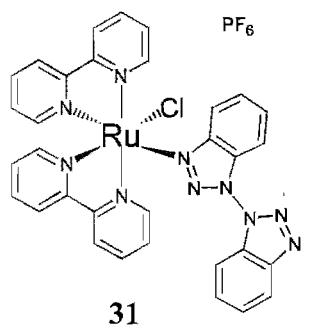

31

Fig. 3.15

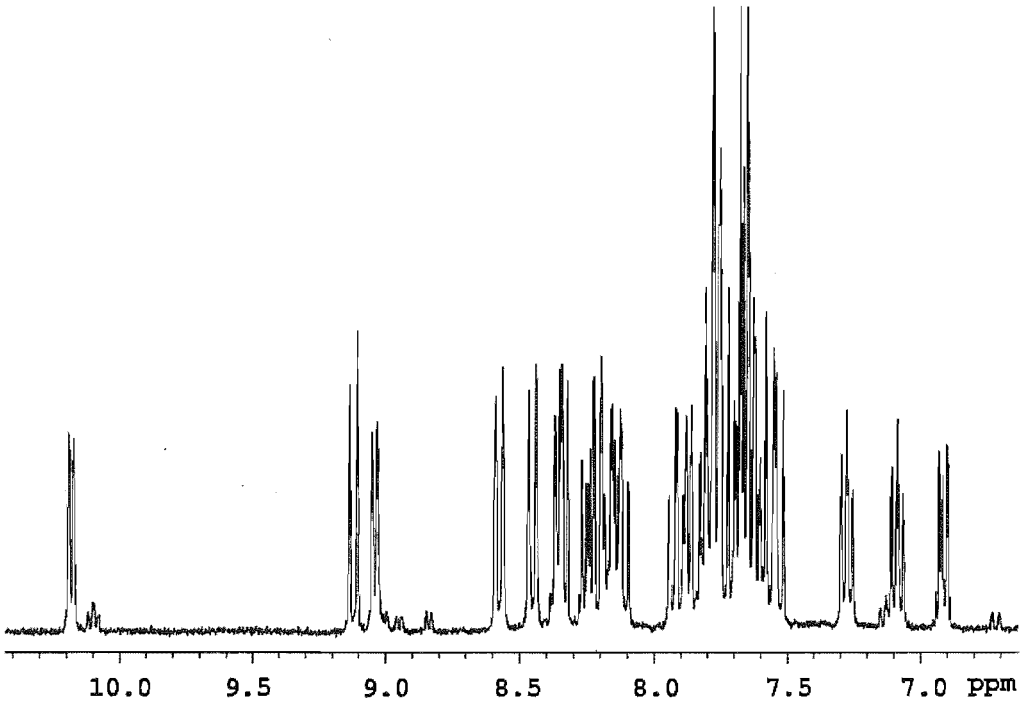

Fig. 3.16 ^{1}H NMR spectrum of [Ru(bpy)$_2$(**23**)Cl](PF$_6$) (**31**).

The chemical shifts and coordination induced shifts for complex **31** are given in Table 3.1. The only proton that experiences a significant CIS is H4 of the coordinated benzotriazole. For H4 to experience such a large positive CIS (+0.78 ppm), the coordinated benzotriazole ring must lie as shown in Fig. 3.15, where H4 is proximate to the chlorine atom. Importantly, the benzotriazole is postulated to be coordinated *via* the N3 nitrogen. If it were coordinated *via* N2, some of the signals of the uncoordinated ring would be expected to experience larger CIS, as was the case in the example in Chapter 2, *viz* complex [Ru(bpy)$_2$(**1**)Cl](PF$_6$) (**8**). The complex **31** is converted to [Ru(bpy)$_2$Cl(CH$_3$CN)](PF$_6$)$_2$ in acetonitrile solution, and some of the signals for this complex are seen in the above spectrum as the small signals present.

Table 3.1 ^{1}H NMR Chemical Shifts[a] and Coordination Induced Shifts[b] for **31** and **23**.

	H4	H5	H6	H7	H4'	H5'	H6'	H7'
31	9.12	7.65	7.78	7.57	8.36	7.70	7.80	7.53
23[c]	8.34	7.70	7.78	7.53				
CIS	+0.78	-0.05	0	+0.04	+0.02	0	+0.02	0

[a] For deuterated acetonitrile solutions. [b] CIS = ($\delta_{complex}$ - δ_{ligand}). [c] The free ligand in solution has 2-fold symmetry; hence H4= H4' etc.

The 3:1 ethanol/water conditions were also used in the reaction of ligand **24** with Ru(bpy)$_2$Cl$_2$. Again, a dark hexafluorophospate salt was obtained, in remarkably similar yield (82%) to complex **31**, and this was shown also by FABMS to contain a coordinated chlorine and was formulated as [Ru(bpy)$_2$(**24**)Cl](PF$_6$), (**32**). In the same manner as for the previous complex, the ^{1}H NMR spectrum of complex **32** could be totally assigned by 1-D TOCSY and

^{1}H nOe spectroscopy. The chemical shifts and coordination induced shifts for complex **32** are listed in Table 3.2.

Table 3.2 ^{1}H NMR Chemical Shifts[a] and Coordination Induced Shifts[b] for **32** and **25**.

	H4	H5	H6	H7	H4'	H5'	H6'	H7'	CH_2
32	8.88	7.47	7.71	8.07	8.10	7.45	7.68	7.78	7.57
25[c]	8.05	7.46	7.67	8.00					7.43
CIS	+0.83	+0.01	+0.04	+0.07	+0.05	-0.01	+0.01	-0.22	+0.14

[a] For deuterated acetonitrile solutions. [b] CIS = ($\delta_{complex}$ - δ_{ligand}). [c] The free ligand in solution has 2-fold symmetry; hence H4= H4' etc.

As was the case in the previous example, the ligand again acts in a monodentate fashion. The coordinated benzotriazole H4 experiences a similar CIS (+0.83) to that of complex **31** (+0.78), and thus, the ligand was assumed to be acting in the same mode of N3 coordination. The only other notable CIS value is that of H7'. The CIS of -0.22 ppm suggests that somehow H7' experiences some shielding. This shielding is most likely due to ring-current anisotropy. However, exactly which ring is shielding H7' was unable to be determined. A ^{1}H nOe experiment irradiating H7' gave an enhancement of H6', as expected, but no enhancement of any other protons in the complex. A possibility is that the shielding is from the benzene ring of the other benzotriazole, where the uncoordinated benzotriazole ring has 'folded under' the coordinated ring (Fig. 3.17).

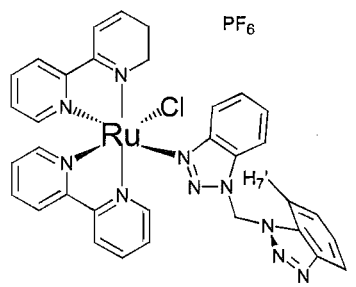

32

Fig. 3.17

Since complexes containing chelating benzotriazole ligands were desired, the reaction conditions were altered to encourage chelation. The $Ru(bpy)_2Cl_2$ complex was treated with two equivalents of $AgBF_4$ in acetone/ethanol before addition of the ligands **23** and **24**. Now, the corresponding reaction solutions were bright orange, instead of the dark purple colour of the ethanol/water reactions. Thus, it was hoped that the chelating complexes $[Ru(bpy)_2(\mathbf{23})](BF_4)_2$, (**33**), and $[Ru(bpy)_2(\mathbf{24})](BF_4)_2$, (**34**), (Fig. 3.18) had been formed.

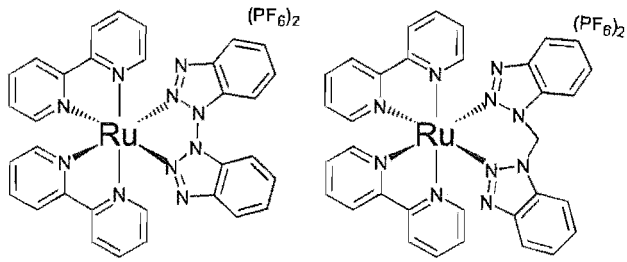

33 **34**

Fig. 3.18

Characterisation was attempted by ^{1}H NMR spectroscopy, in deuterated acetonitrile, for the product from the reaction with ligand **23**. The ^{1}H NMR spectrum of the complex showed changes when the complex was left in solution for a short time, indicating that ligand substitution was taking place, presumably with acetonitrile solvent replacing another ligand in the complex. ^{1}H NMR characterisation was then attempted in deuterated dichloromethane, a less nucleophilic solvent. The resulting ^{1}H NMR spectrum showed the presence of some monodentate impurity. However, some signals due to the chelating complex **33** could be assigned, including those of the bibenzotriazole ligand. The signals of the ligand were found *via* 1-D TOCSY and recognised by the absence of a bpy H6, with its characteristic small 3-bond coupling constant. The chemical shifts and coordination induced shifts determined for complex **33** are listed in Table 3.3.

Table 3.3 ^{1}H NMR Chemical Shifts[a] and Coordination Induced Shifts[b] for **33** and **23**.

	H4	H5	H6	H7
33	7.87	7.70	7.70	7.23
23	8.34	7.70	7.78	7.53
CIS	-0.47	0	-0.08	-0.30

[a] For deuterated dichloromethane solutions. [b] CIS = ($\delta_{complex}$ - δ_{ligand}).

Proton H4 shows the effect of ring-current anisotropy from the adjacent pyridine ring, as expected, with the CIS value of -0.47. The explanation for the negative CIS of H7 and H6 is also as a result of ring-current anisotropy, this time not from a pyridyl ring, but from the other benzene ring of the bibenzotriazole. Due to the cisoid nature of N2,N2'-chelation, the H7 protons are brought into an environment where they undergo a mutual steric interaction. To alleviate this steric interaction the rings of the ligand do not lie in the same plane, rather, they lie over one-another. As a result, the H6 and more so the H7 proton of each ring is shielded by ring-current anisotropy from the other benzene ring, and this is reflected in the larger negative CIS value of H7 relative to H6. As mentioned previously, this phenomenon has been reported for complexes of 1,1'-biisoquinoline.[94-98]

FABMS showed that the monodentate impurity was most likely the monoaqua complex $[Ru(bpy)_2(\mathbf{23})OH_2](BF_4)_2$, as molecular ions were identified in the mass spectrum

for $[Ru(bpy)_2(\mathbf{23})OH_2](BF_4)^+$ and $[Ru(bpy)_2(\mathbf{23})OH]^+$. This complex, of course, could be formed in the reaction or from the chelating complex **33**, as a result of ligand labilisation with subsequent substitution by adventitious water from the solvent. This result may, however, explain the result of the ^1H NMR in deuterated acetonitrile, where the above monoaqua complex is converted to the complex $[Ru(bpy)_2(OH_2)(CH_3CN)](BF_4)_2$. No attempts were made at stringent exclusion of water from the reaction conditions or NMR solvents, and further efforts at separation and purification of the reaction products proved futile.

$[Ru(bpy)_2(\mathbf{24})](BF_4)_2$, (**34**), was able to be separated and purified by column chromatography on alumina, albeit with some loss, after the $AgBF_4$ method, and was able to be characterised by FABMS, elemental analysis and ^1H NMR spectroscopy. Complex **34** is 2-fold symmetric, and thus only gives rise to 12 aromatic signals in the ^1H NMR spectrum, corresponding to the three different aromatic rings. In the ^1H NMR spectrum, the protons of the methylene bridge appear as a singlet, implying that there is rapid interconversion between boat conformers on the NMR timescale. The three different aromatic rings were identified by 1-D TOCSY, and that of the benzotriazole-containing ligand was distinguished as it does not contain the doublet of smaller coupling constant (bpy H6). One of the pyridine rings in **34** has its H6 further downfield than the other (8.27 ppm *vs* 7.84 ppm) and this was postulated to be the H6 proton that lies over the benzotriazole ring. The reason for this assignment was that the triazole ring being less aromatic than pyridine would shield this H6 proton less, and that the downfield position of the H6 proton would reflect this decrease in ring-current anisotropy. Confirmation that this downfield proton was over the benzotriazole was provided by a ^1H nOe experiment irradiating the signal for the methylene bridge. This experiment also provided information about the order around the benzotriazole ring. The relevant ^1H NMR data are listed in Table 3.4, and show that proton H4 experiences a small effect of ring-current anisotropy from the adjacent pyridine ring, and moves upfield upon chelation (CIS -0.21).

Table 3.4 ^1H NMR Chemical Shifts[a] and Coordination Induced Shifts[b] for **34** and **24**.

	H4	H5	H6	H7	CH_2
34	7.84	7.51	7.76	8.04	7.43
24	8.05	7.47	7.67	8.00	7.57
CIS	-0.21	+0.04	+0.09	+0.04	-0.14

[a] For deuterated dichloromethane solutions. [b] CIS = ($\delta_{complex}$ - δ_{ligand}).

The results thus far indicated that the N3 nitrogen atom of the benzotriazole was the stronger donor in the 1,1-substituted ligands **23** and **24**, as it was coordinating preferentially. Only by eliminating the chloride ion were the ligands encouraged to act in a chelating manner.

It was hoped that the influence of the pyridine and isoquinoline nitrogens would encourage chelation with the ligands **27**, **28**, and **29**. This was shown to be so by the relative

ease of synthesis of chelating mononuclear ruthenium complexes with these ligands. Using the 3:1 ethanol/water method, and only relatively short reflux times, chelating mononuclear ruthenium complexes $[Ru(bpy)_2(\mathbf{27})](PF_6)_2$, (**35**), $[Ru(bpy)_2(\mathbf{28})](PF_6)_2$, (**36**), and $[Ru(bpy)_2(\mathbf{29})](PF_6)_2$, (**37**), (Fig. 3.19) were formed in good yields (Table 3.5). FABMS and elemental analyses were correct for each of these complexes.

Table 3.5

	Reflux Time (Hrs)	Yield (%)
$[Ru(bpy)_2(\mathbf{27})](PF_6)_2$ (**35**)	4	88
$[Ru(bpy)_2(\mathbf{28})](PF_6)_2$ (**36**)	5	77
$[Ru(bpy)_2(\mathbf{29})](PF_6)_2$ (**37**)	15	87

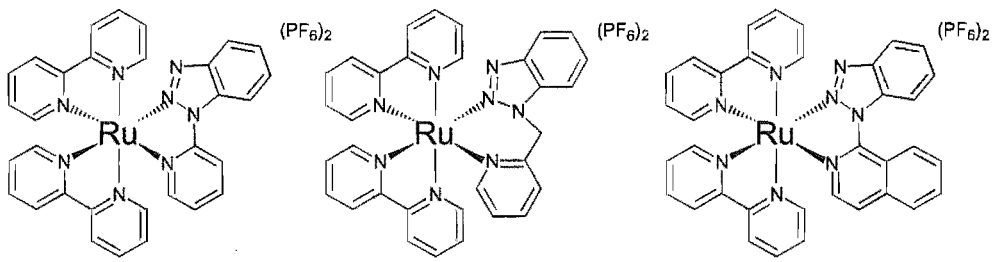

35 **36** **37**

Fig. 3.19

Each of these chelating complexes has, because of the unsymmetrical nature of the benzotriazole-containing ligand, no internal symmetry. This meant that the ^{1}H NMR spectra of complexes **35** and **36** would contain 24 different aromatic protons signals, while complex **37** would contain two more, giving 26 different aromatic proton signals in the ^{1}H NMR spectrum. Despite this complexity, the signals due to the benzotriazole-containing ligand were unambiguously assigned for **35** and **36**. Complex **37** provided a particularly challenging example for characterisation by ^{1}H NMR and total assignment was accomplished using 1- and 2-D NMR techniques. The following describes the NMR characterisation and interpretation of these complexes.

The situation faced for identifying the signals due to the ligand in complex **35** are the same as those described for complex **13** in Chapter 2. The ^{1}H NMR spectrum for complex **35** contains 24 different aromatic proton signals, 20 of which are due to 2-substituted pyridyl rings. However, fortunately, the same strategy of identifying the non-pyridyl ring in the complex and, by ^{1}H nOe, identifying the H3 proton of the pyridyl ring of the benzotriazole-containing ligand, was successful. The chemical shifts and coordination induced shifts are listed in Table 3.6. Further assignment of the bpy ligands was not attempted, because the signals for these were highly overlapped in the spectrum.

Table 3.6 ^{1}H NMR Chemical Shifts[a] and Coordination Induced Shifts[b] for **35** and **27**.

	H4	H5	H6	H7	H3'	H4'	H5'	H6'
35	8.05	7.71	7.91	8.40	8.57	8.32	7.51	7.84
27	8.16	7.56	7.72	8.69	8.30	8.09	7.47	8.68
CIS	-0.11	+0.15	+0.19	-0.29	+0.27	+0.23	+0.04	-0.84

[a] For deuterated acetonitrile solutions. [b] CIS = ($\delta_{complex}$ - δ_{ligand}).

Rationalisation of the CIS values of complex **35** are again based upon shielding arguments and a combination of σ-donation and back-bonding effects. The H6' and H4 protons are shielded by their respective adjacent pyridine rings of different bpy ligands, although H6' is shielded much more as it is closer. The chemical shift of H7 in the free ligand (8.69 ppm) suggests that the pyridine nitrogen is deshielding it. Upon chelation, the coordination induced conformational change of the ligand places H7 in a less deshielded environment, and the proton moves upfield (CIS -0.29 ppm). This is consistent with the CIS of H3', which moves downfield upon chelation. Proton H4' shows a positive CIS, which reflects a mixture of the σ-donation of the pyridine to the metal, which shifts the proton downfield, and the back-bonding ability of the ring, which accepts electron density from the metal, moving the proton upfield. It is this trade-off which determines the CIS of the H4 proton in ruthenium complexes, and typically, the CIS is +0.2 - +0.3. Interestingly the chemical shifts of H5 and H6 show smaller positive CIS, which perhaps indicates that the benzotriazole ring is accepting electron density from the metal.

In the reaction of ligand **28** with $Ru(bpy)_2Cl_2$ some monodentate product, $[Ru(bpy)_2(\mathbf{28})Cl](PF_6)$, (**38**), (Fig. 3.20), was also formed in low yield (14%). This was separated by chromatography, and identified by ^{1}H NMR to be coordinated *via* N3 of the benzotriazole. This assignment is based on the CIS value (Table 3.7) of the benzotriazole H4 and the pyridyl H3', which are both similar to those observed for the H4 and H7' protons, respectively, of the complex $[Ru(bpy)_2(\mathbf{25})Cl](PF_6)$ (**33**). As was the case for the monodentate complexes **31** and **32**, all the protons of complex **38** could be assigned to spin systems by way of 1-D TOCSY. Also, since there exists sufficient separation in the chemical shifts of the bpy H3's, ^{1}H nOe experiments allowed the complete ^{1}H NMR assignment of complex **38.**

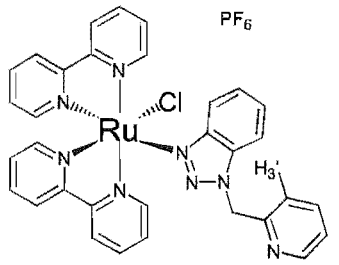

38

Fig. 3.20

Table 3.7 ^{1}H NMR Chemical Shifts[a] and Coordination Induced Shifts[b] for **38** and **28**.

	H4	H5	H6	H7	H3'	H4'	H5'	H6'	CH_2
38	8.84	7.40	7.57	7.72	6.97	7.72	7.32	8.42	5.72
28	8.08	7.37	7.45	7.57	7.25	7.62	7.23	8.53	6.04
CIS	+0.76	+0.03	+0.12	+0.15	-0.28	+0.10	+0.09	-0.11	-0.32

bpy H3	bpy H4	bpy H5	bpy H6
8.28	8.01	7.71	10.19
8.14	7.72	7.11	7.87
8.42	7.86	7.23	7.79
8.53	8.09	7.56	8.90

[a] For deuterated acetonitrile solutions. [b] CIS = ($\delta_{complex}$ - δ_{ligand}).

The ^{1}H NMR spectrum of [Ru(bpy)$_2$(**28**)](PF$_6$)$_2$, (**36**), is shown in Fig. 3.21. Of note is the appearance of the methylene bridge. In this unsymmetrical complex, the protons of the bridge are non-equivalent and close in chemical shift, and so split to form an AB-quartet. This was used to advantage for further ^{1}H NMR assignment. Irradiation of these signals in ^{1}H nOe experiments allowed the identification of the H3' and H7 protons of the ligand, which, coincidentally, both occur at the same chemical shift of 8.00 ppm. These experiments also identified the pyridine ring that is close to the axial proton of the bridge (Fig. 3.21). Furthermore, from the nOe's obtained, the axial and equatorial protons could be distinguished. Fortunately, in this chelating complex, the bpy H3 signals were sufficiently isolated to allow for ^{1}H nOe experiments to identify the pyridyl partners that make up the bpy ligands giving a complete assignment. The ^{1}H NMR data for **36** are listed in Table 3.8.

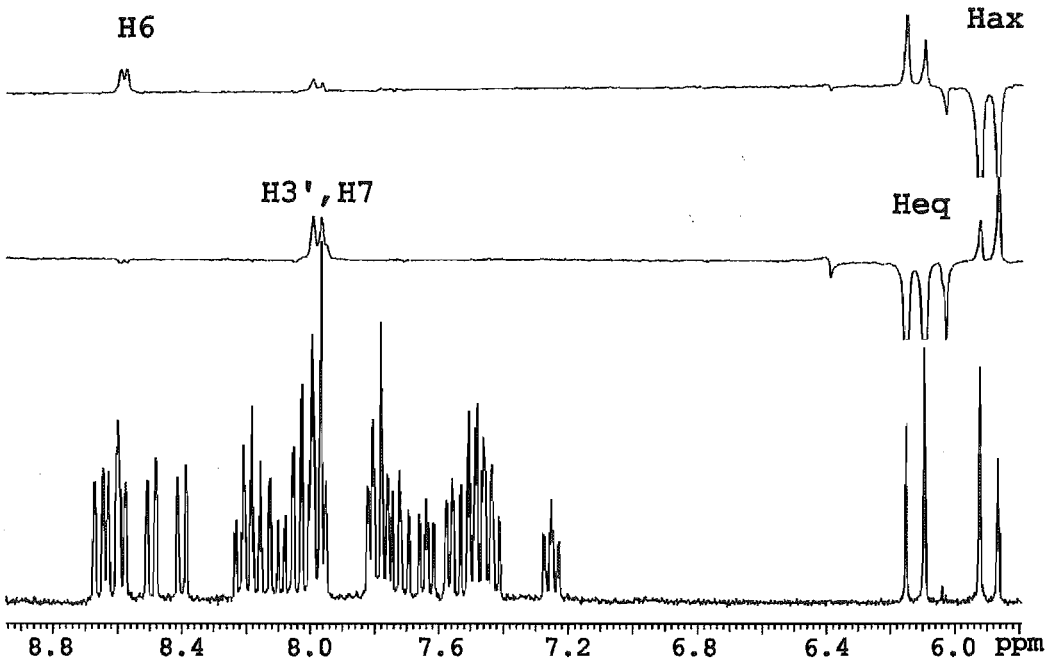

Fig. 3.21 ^{1}H NMR and ^{1}H nOe spectra of $[Ru(bpy)_2(\mathbf{28})](PF_6)_2$ (**36**).

Table 3.8 ^{1}H NMR Chemical Shifts[a] and Coordination Induced Shifts[b] for **36** and **28**.

	H4	H5	H6	H7	H3'	H4'	H5'	H6'	CH_2
36	7.80	7.51	7.71	8.00	8.00	7.97	7.25	7.70	5.91 / 6.13
28	8.08	7.37	7.45	7.57	7.25	7.62	7.23	8.53	6.04
CIS	-0.28	+0.14	+0.26	+0.43	+0.75	+0.35	+0.02	-0.83	-0.13 / +0.10

bpy H3	bpy H4	bpy H5	bpy H6
8.50	8.19	7.64	8.58
8.40	8.05	7.43	7.77
8.66	8.20	7.49	7.96
8.62	7.97	7.25	7.70

[a] For deuterated acetonitrile solutions. [b] CIS = ($\delta_{complex}$ - δ_{ligand}).

The negative CIS values of H4 and H6' are a result of shielding from the adjacent pyridine rings, again as H6' is closer it has a larger value. Proton H4' has a CIS value of +0.35, which suggests either a larger amount of σ-donation or a smaller amount of back-bonding to this ring than is usual. Also the benzotriazole shows significant positive CIS values for H6 and H5. This seemed to indicate that there might be a synergistic effect between the rings of the ligand. If the pyridine ring was accepting a smaller amount of back-bonding then perhaps this was because the benzotriazole was accepting more. The large positive CIS values for H3' and H7 are as a result of the coordination induced conformational change of the ligand. These two protons have been brought close together upon the ligand chelating to the ruthenium atom and are mutually deshielded.

Potentially, complexes of ligand **29** are capable of atropisomerism. When the ligand is chelating through the isoquinoline nitrogen and the N2 nitrogen of the benzotriazole, the

H7 and H8' protons are placed in an environment of high steric compression and, because of this, the rings may lie over one-another. In order to ascertain whether the rings of the ligand, in the complex **37**, were lying over one-another the identification of the signals due to the ligand was essential.

The signals due to H7 and H8' should be the most sensitive to the effects of atropisomerism. If the rings lie over one-another these protons should be shielded, whereas if the rings are coplanar they should be mutually deshielded. The ^{1}H NMR spectrum of complex **37** is shown in Fig. 3.22. The first thing of note is that there is no evidence of diastereoisomers in the spectrum, as two discrete sets of signals would be observed. This indicates that any such isomers must undergo rapid interconversion on the NMR timescale. In the approach taken for most of the ruthenium complexes, 1-D TOCSY was used to distinguish signals to as many different ring systems as possible. The identification of five 1,2-disubstituted rings and the identification of the two doublets (H3' and H4') of the isoquinoline was accomplished from 1-D TOCSY. A number of the rings could be easily assigned to the pyridyl rings of the bpy ligands, as they contained a doublet of smaller coupling constant. One, however, did not contain the doublet of smaller coupling constant, and so was either the benzotriazole or the isoquinoline. To identify this ring, the same strategy of correlating the H7 proton of the benzotriazole to its carrier carbon was used. The GHSQC spectrum of complex **37** is also shown in Fig. 3.22. The C7 carbon at 113.91 ppm gives a correlation to a signal at 8.07 ppm, which is one of the non bpy ring protons found *via* 1-D TOCSY, and so the benzotriazole ring was identified and assigned. This left only the protons of the isoquinoline four-spin system to be assigned. The chemical shift of proton H5' (8.25 ppm) was identified by irradiation of H4' in a ^{1}H nOe experiment. This signal is partially overlapped with a signal from a bpy H4 (c.o.m. 8.22 ppm), yet by selective irradiation of H5' and cancellation of the previously identified bpy ring, the signals due to the isoquinoline ring were definitively assigned.

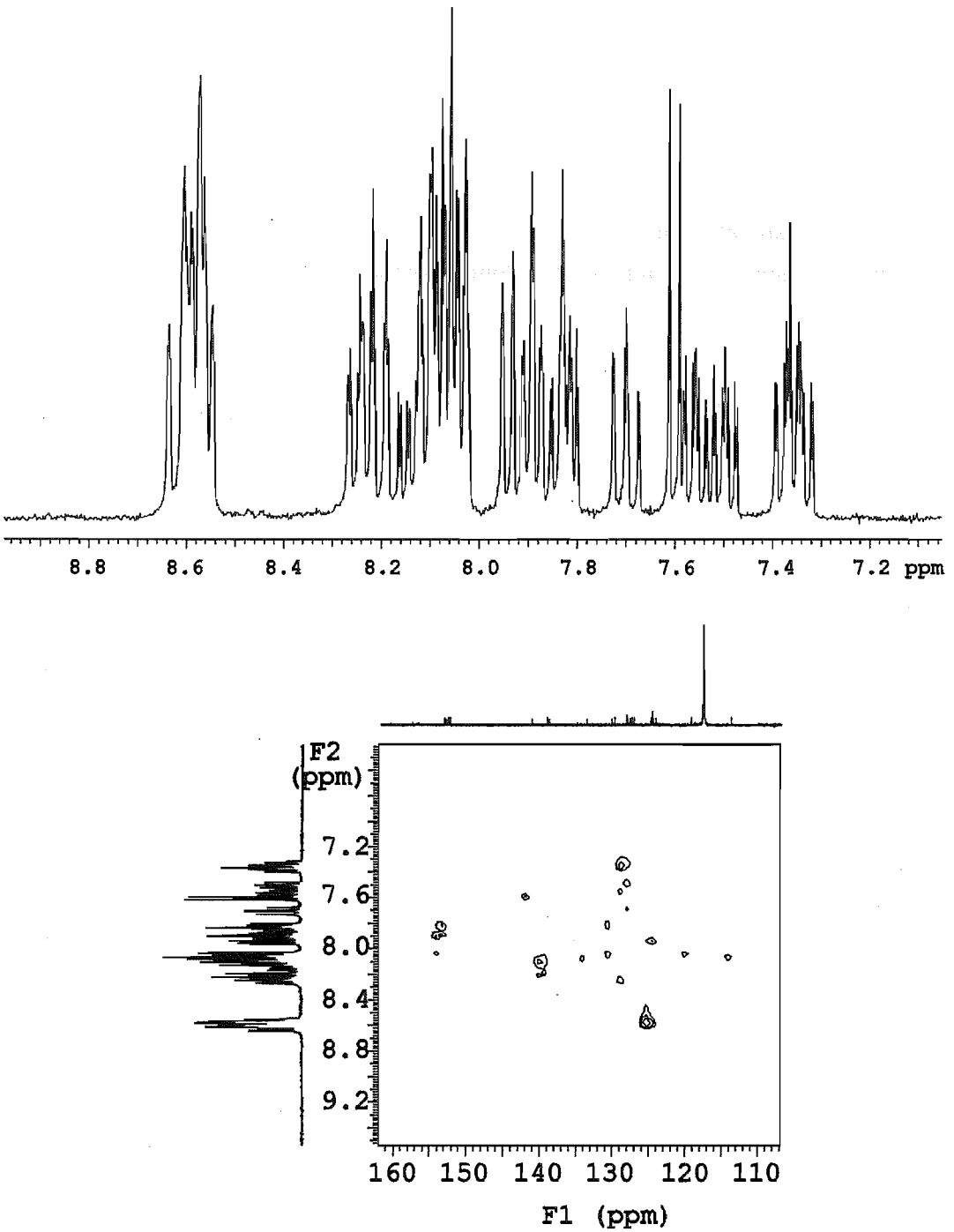

Fig. 3.22 ^{1}H NMR and GHSQC spectra of $[Ru(bpy)_2(\mathbf{29})](PF_6)_2$ (**37**).

Table 3.9 ^{1}H NMR Chemical Shifts[a] and Coordination Induced Shifts[b] for **37** and **29**.

	H4	H5	H6	H7	H3'	H4'	H5'	H6'	H7'	H8'
37	8.04	7.70	7.81	8.07	7.60	7.94	8.25	8.10	8.08	8.58
29	8.24	7.60	7.71	8.03	8.62	8.05	8.17	7.94	7.79	8.39
CIS	-0.20	+0.10	+0.10	+0.04	-1.02	-0.11	+0.07	+0.16	+0.29	+0.19

bpy H3	bpy H4	bpy H5	bpy H6
8.57	8.12	7.34	7.90
8.56	8.10	7.37	8.03
8.58	8.19	7.50	7.82
8.62	8.22	7.55	7.88

[a] For deuterated acetonitrile solutions. [b] CIS = ($\delta_{complex}$ - δ_{ligand}).

The CIS values of **37** can again be rationalised in a combination of through-space ring-current anisotropy and σ-donation/π back-bonding effects. The H4 and H3' protons are moved upfield as a result of ring-current anisotropy from their respective adjacent pyridine rings. As before, the CIS value of H4 is less than that observed for the other shielded proton, as it is further removed from the shielding pyridine. The H5 and H6 protons show small positive CIS values (+0.10). However, the most interesting CIS value of the benzotriazole ring is that of H7. If the rings of the ligand were coplanar, then the signal for this proton would be expected to be shifted downfield, resulting in a strong positive CIS value. As the CIS value for H7 is only small, this suggests that the ligand is in a non-planar conformation. Although H8 has a larger CIS value (+0.19), it is not strongly shifted and is therefore consistent with the above proposal.

The effect of attaching the five-membered benzotriazole ring to the 1-position of the isoquinoline is to reduce slightly the bite-angle of the resulting ligand relative to biq. This results in further separating the H7/H8' protons in ligand **29** relative to the H8/H8' protons of the biq ligand upon chelation. This obviously reduces the steric interaction, and is likely to lead to a reduction in the energy required to pass each other. Perhaps this is one reason why the existence of the diastereoisomers is not seen in the spectrum of **37**.

To further investigate the nature of the benzotriazole-containing ligands, it was decided to prepare a homoleptic complex. Based upon the results thus far, it seemed that ligand **28** would provide the best chance of forming a homoleptic complex. Therefore **28** was reacted with tetrakis(DMSO)dichlororuthenium [$Ru(DMSO)_4Cl_2$] in 3:1 ethanol/water. Over a two hour time period the colour of the solution changed from yellow to orange and to a dark red before becoming bright orange. At this time a solid started to form in the reaction mixture and so the reaction was stopped. The usual work-up procedure was followed, and the solvents were first removed *in vacuo* before attempting to redissolve the bright orange solid in water. However, the solid showed little solubility, indicating that some type of polymeric

complex had formed. The solid could be dissolved in DMSO and a ^{1}H NMR spectrum was recorded in deuterated solvent. The spectrum showed only signals corresponding to the free ligand, and this too was taken as further evidence of the formation of some complex other than the desired homoleptic complex.

3.3.2 UV-Visible Spectroscopy and Electrochemical Studies

Each of the complexes where the ligands acted in a monodentate fashion was studied by UV-visible spectroscopy. The results of the study are summarised in Table 3.10, while a representative UV-visible spectrum, for complex **38**, is shown in Fig. 3.23. In these chloro-containing complexes a MLCT occurs around 470-490 nm with other, possibly MLCT or MC, absorptions at 355-360 nm. No electrochemical measurements were made on these complexes.

Table 3.10 Absorption Maxima[a] with Molar Extinction Coefficients[b] for **31**, **32** and **38**.

	λ_{max} (ε)	λ_2 (ε)
[Ru(bpy)$_2$(**23**)Cl](PF$_6$) (**31**)	479 (8 650)	356 (7 800)
[Ru(bpy)$_2$(**24**)Cl](PF$_6$) (**32**)	471 (7 000)	361 (6 500)
[Ru(bpy)$_2$(**28**)Cl](PF$_6$) (**38**)	494 (5 600)	360 (7 000)

[a] In nanometers. [b] $M^{-1}cm^{-1}$.

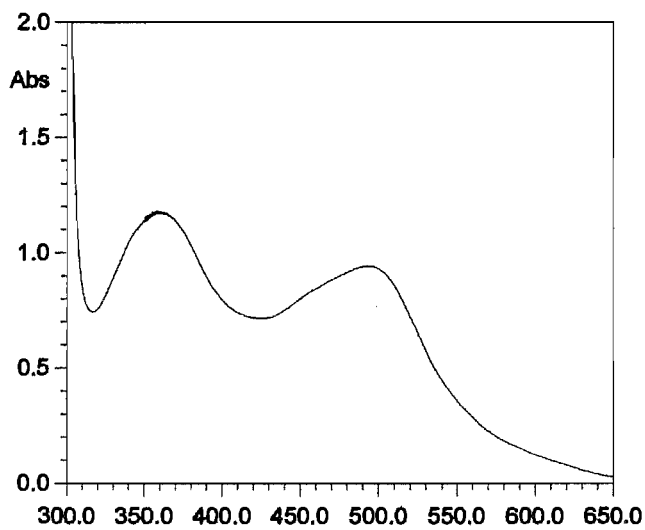

Fig. 3.23 UV-visible spectrum for [Ru(bpy)$_2$(**28**)](PF$_6$)$_2$ (**38**)

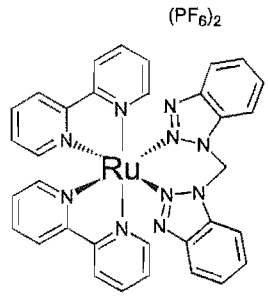

34

Fig. 3.24

UV-visible spectroscopy and cyclic voltammetry were used to investigate the chelating complex $[Ru(bpy)_2(\mathbf{25})](BF_4)_2$ (**34**). The UV spectrum of **34** shows λ_{max} at 368 nm (ε 9 800 $M^{-1}cm^{-1}$) with a shoulder around 420 nm. These transitions are ascribed to the (M)d—(L)π^* and (M)d—(bpy)π^* transitions, respectively. Importantly, this suggested that the bisbenzotriazole ligand would be harder to reduce than the auxiliary bpy ligands. Electrochemically, complex **34** exhibits a one-electron reversible redox couple at +1.50 V and two reversible one-electron reductions at -1.45 V and -1.60 V, which are both ascribed to the reductions of the bpy ligands. No reduction process was seen for the benzotriazole-containing ligand in the potential window examined (-2.00 V). Thus the electrochemistry and UV-visible data are consistent.

The three unsymmetrical chelating benzotriazole-containing complexes were investigated by UV-visible spectroscopy. The UV-visible spectrum for **35** is shown in Fig. 3.25, and is typical of the three complexes, with shoulders appearing on the high-energy side. The results of these investigations for **35**, **36** and **37** are summarised in Table 3.11, along with, for the sake of comparison, $Ru(bpy)_3^{2+}$ and $Ru(bpy)_2(biq)^{2+}$.[109]

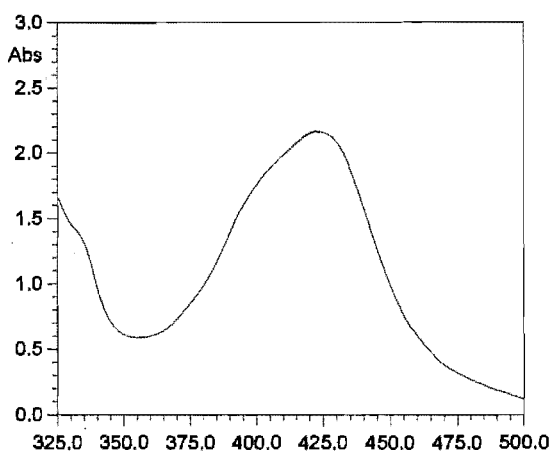

Fig. 3.25 UV-visible spectrum of $[Ru(bpy)_2(\mathbf{27})](PF_6)_2$ (**35**).

Table 3.11 Absorption Maxima[a] with Molar Extinction Coefficients[b] for **35**, **36** and **37**.

	λ_{max} (ε)
$Ru(bpy)_3^{2+}$	452 (13 600)
$[Ru(bpy)_2(\mathbf{27})](PF_6)_2$ (**35**)	422 (16 300)
$[Ru(bpy)_2(\mathbf{28})](PF_6)_2$ (**36**)	426 (11 300)
$Ru(bpy)_2(biq)^{2+}$	518 (7 500)
$[Ru(bpy)_2(\mathbf{29})](PF_6)_2$ (**37**)	429 (16 200)

[a] In nanometers. [b] $M^{-1}cm^{-1}$.

The λ_{max} for the complexes **35** and **36** are at shorter wavelength than that of $Ru(bpy)_3^{2+}$. This would suggest that the $\Delta E_{ox\text{-}red1}$ value, that is the HOMO-LUMO energy gap, will be larger in **35** and **36** than in $Ru(bpy)_3^{2+}$. Similarly, the λ_{max} for the complex **37** is at shorter wavelength than the corresponding $Ru(bpy)_2(biq)^{2+}$ complex.

The cyclic voltammograms of **35** and **36** are shown in Fig. 3.26, while the electrochemical studies for complexes **35**, **36** and **37** are summarised in Table 3.12, along with the redox potentials of $Ru(bpy)_3^{2+}$. As suggested by the UV-visible spectra, these complexes all show greater $\Delta E_{ox\text{-}red1}$ values than $Ru(bpy)_3^{2+}$. However, the reasons for this appear to differ between the various complexes.

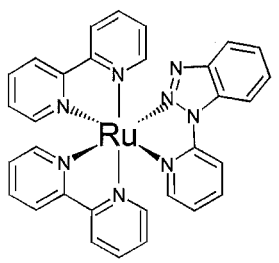

35

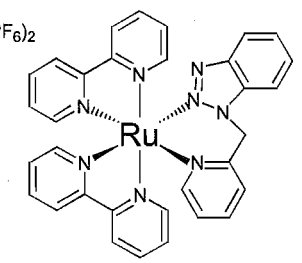

36

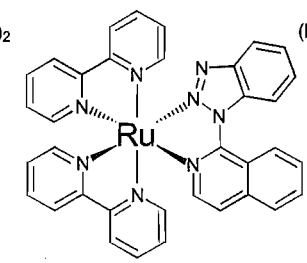

37

Table 3.12 Redox Potentials[a] of **35**, **36** and **37.**

	E_{ox}	E_{red1}	E_{red2}	E_{red3}	$\Delta E_{ox\text{-}red1}$
$Ru(bpy)_3^{2+}$	1.26	-1.33	-1.51	-1.77	2.59
$[Ru(bpy)_2(\mathbf{27})](PF_6)_2$ (**35**)	1.53	-1.39	-1.60	-	2.92
$[Ru(bpy)_2(\mathbf{28})](PF_6)_2$ (**36**)	1.30	-1.43	-1.64	-2.00[b]	2.73
$[Ru(bpy)_2(\mathbf{29})](PF_6)_2$ (**37**)[c]	1.47	-1.34	-1.72[b]	-1.93[b]	2.81

[a] In volts *vs* SCE in acetonitrile. [b] Irreversible reduction. [c] In volts *vs* SCE in dichloromethane.

The effect that the ligand **27** has had on complex **35** is to lower the electron density on the metal, thus making it harder to oxidise relative to $Ru(bpy)_3^{2+}$. There is a reasonable correlation of the first and second reduction potentials between complex **34** and $Ru(bpy)_3^{2+}$, and this would suggest that the reductions observed are most likely of the bpy ligands. No further reduction processes were observed in the potential range examined.

Interesting is the result for complex **36**, where the aromatic rings are separated by a methylene bridge. This complex has a much lower oxidation potential compared to the complexes **35** and **37**, where the heterocycles are directly linked, and therefore conjugated. The first two reductions are again most likely to be of the bpy ligands, with the third irreversible reduction at -2.00 V being that of the benzotriazole-containing ligand.

The introduction of the benzotriazole ring into the ligands **27** and **28** has dramatically affected the properties of the complexes compared to $Ru(bpy)_3^{2+}$, and indicates the difference in nature between benzotriazole and pyridine. The complexes **35** and **36** are harder to oxidise, which means the metal is less electron rich in each case, while the electron-rich triazole ligands are harder to reduce than the bpy ligands. These two features give rise to the larger $E_{ox\text{-}red1}$ values shown in Table 3.12.

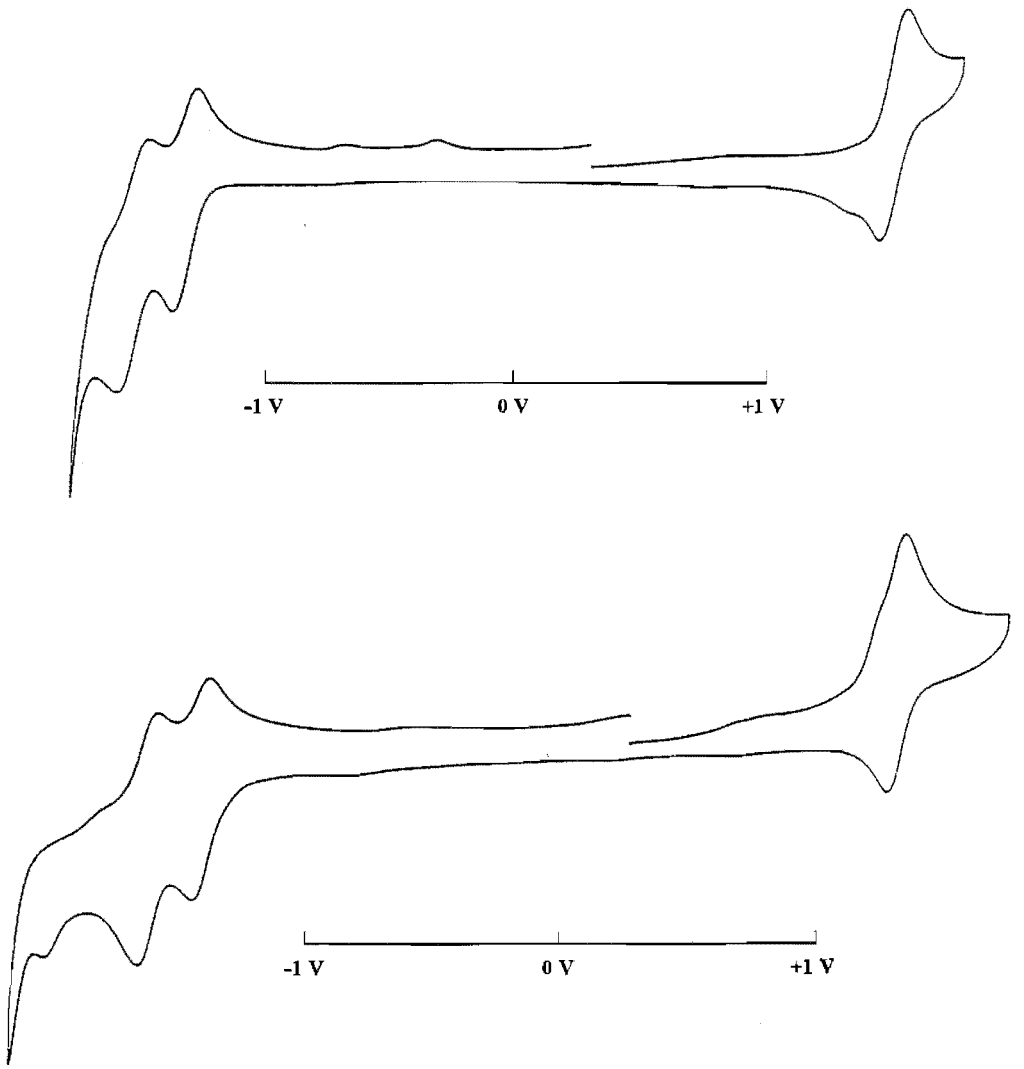

Fig. 3.26 Cyclic voltammograms of $[Ru(bpy)_2(\mathbf{27})](PF_6)_2$ (**35**) (top) and $[Ru(bpy)_2(\mathbf{28})](PF_6)_2$ (**36**).

The electrochemistry of $[Ru(bpy)_2(\mathbf{29})](PF_6)_2$ (**37**) was first examined in acetonitrile. Two closely spaced waves upon oxidation seemed to suggest that the complex was undergoing an eCe mechanism. An eCe mechanism is simply explained by having an intervening chemical step between a redox process. Different scan rates (Fig. 3.27) were used to probe this process. At the scan rate of 20 mVs^{-1}, the chemical step competes with the rate of the electrochemical measurement, and hence the redox wave is shifted to the left, indicating that the resulting complex formed after the chemical step has a redox potential less than that of **37**. At the scan rate of 500 mVs^{-1}, the electrochemical measurement is now faster than the chemical process and the true redox wave is observed. The mechanism was tentatively proposed to be that the benzotriazole ring of the ligand was released from the ruthenium upon oxidation, with an acetonitrile taking its place, and upon reversing the current the acetonitrile-containing complex was being reduced. No further investigation of this process was made. To possibly alleviate this problem, the electrochemistry was carried out in dichloromethane solution. This proved much more satisfactory, as the spurious redox wave was reduced considerably.

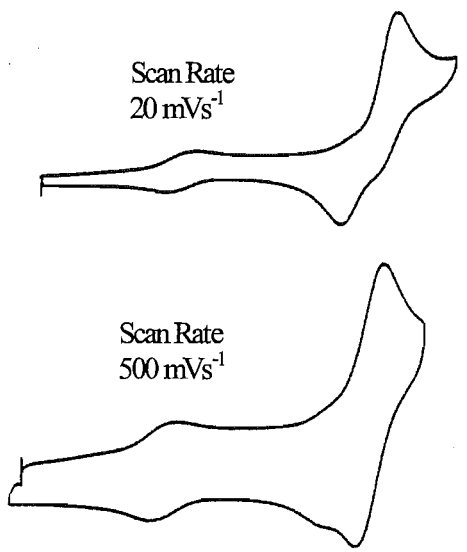

Fig. 3.27 Voltammograms for the oxidation of $[Ru(bpy)_2(\mathbf{29})](PF_6)_2$ (**37**)

The oxidation potential of this complex is much higher than in $Ru(bpy)_3^{2+}$, indicating the metal atom is again less electron rich. The first two reduction waves of complex **37** are most likely of the bpy ligands, with the third irreversible reduction that of ligand **29**. This seems to indicate that the isoquinoline ring has helped make the reduction of the benzotriazole-containing ligand at a less negative potential relative to the complex **35**, where no reduction was observed for the benzotriazole-containing ligand. This is consistent with the concept introduced in Chapter 2 where the effect of benzo-fusion is to lower the energy of the π^* orbital of the ligand.

The common element to the metal-based oxidations of **35**, **36** and **37** is the raised oxidation potential of these complexes, relative to $Ru(bpy)_3^{2+}$. This is, of course, due to the benzotriazole-containing ligand. The electron density on the metal may be reduced primarily in one of two ways. It may do so by the ligand being a poorer donor, relative to bpy, thus placing less electron density on the metal, or alternatively, the ligand may be better at back-bonding, that is accepting electron density from the metal. Having identified that the benzotriazole N3 is the more basic nitrogen perhaps the first suggestion is consistent with the observed chemistry.

3.4 Other Coordination Complexes

The aim of this section was to structurally characterise, by X-ray crystallography, some other complexes with the ligands used in this study. In particular, it was sought to confirm the postulation of preferential N3 coordination of benzotriazole. Complexes of all ligands were made with Cu(II), Ag(I) and Pd(II) salts, which are the three metal ions used throughout the work described in this thesis, for reasons already explained.

Ligand **23** was reacted with $CuCl_2.2H_2O$, $AgBF_4$ and $PdCl_2$ to give complexes with 1:1 stoichiometries [**23**.$CuCl_2.2H_2O$], (**39**), [**23**.$AgBF_4.½H_2O$], (**40**), and [**23**.$PdCl_2$], (**41**), respectively, as determined from elemental analyses. However, no information was gained from FABMS that would suggest discrete complexes, and, despite attempts at recrystallisation, crystals suitable for X-ray crystallography were unable to be grown for any of these complexes.

Green crystals were formed by slow evaporation from the methanolic reaction mixture of **24** and $CuCl_2.2H_2O$. These analysed as [**24**.$CuCl_2$], (**42**), and were of suitable quality for an X-ray structural investigation. The asymmetric unit of the structure is shown in Fig. 3.28a.

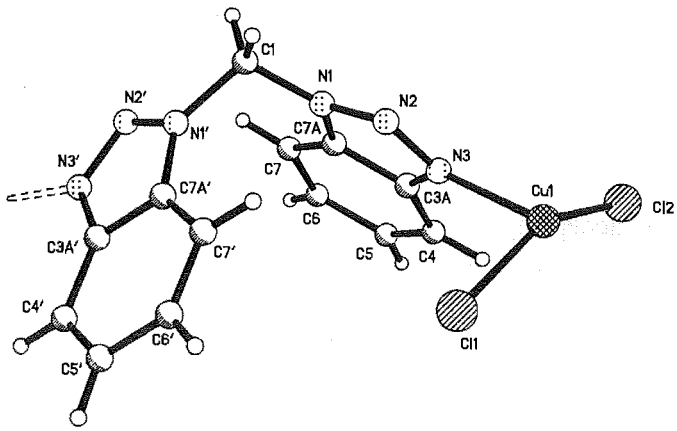

Fig. 3.28a Perspective view, with atom labelling of the contents of the asymmetric unit, of **42**. Selected bond lengths (Å) and angles (°): Cu1-N3 2.000(2), Cu1A-N3' 2.021(3), Cu1-Cl2 2.2137(9), Cu1-Cl1 2.2335(9), N1-N2 1.340(3), N2-N3 1.305(4), N3-C3A 1.377(4), N1-C1 1.452(4), N3-Cu1-Cl1 91.39(8), N3-Cu1-Cl2 94.72(8), Cl2-Cu1-Cl1 150.66(4), N2-N3-C3A 110.0(2), N1-C1-N1' 108.8(3).

The structure is a metallopolymer and has crystallised in the space group P-1. The asymmetric unit contains one copper dichloride unit and one ligand. In the metallopolymer, the ligand adopts a conformation where the meanplanes of each benzotriazole are at an angle of 98.5(4)° to each other, and with the methylene bridge being tetrahedral [108.8(3)°]. The ligand acts as a bridge separating the copper atoms in the chain by 9.250(1)Å. Each benzotriazole unit is coordinated *via* N3, with the Cu1-N3 bond length of 2.000(2)Å being slightly shorter than the Cu1A-N3' bond length [2.021(2)Å]. The geometry of the copper itself is perhaps best described as highly distorted tetrahedral. The angle across the copper to the coordinating N3's [149.31(12)°] and the Cl1-Cu-Cl2 bond angle of 150.66(4)° result in a 'flattened' tetrahedron, while the angles from N3 to the chloride anions are 91.39(8)° (N3-Cu1-Cl1) and 94.72(8)° (N3-Cu1-Cl2). The extended structure of **42** (Fig. 3.28b) shows that the polymeric chains pack with a weak, complementary, inter-chain interaction, [Cu-Cl 3.782(5)Å], between a coordinated chloride of one chain and the copper ion of another. This results in pairs of chains packing together, giving a 2-D ladder-like structure, and may be responsible for the 'flattened' tetrahedral arrangement around the copper.

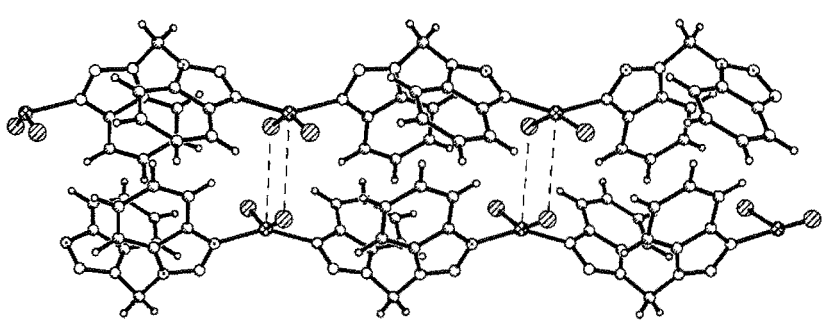

Fig. 3.28b Perspective view of the extended structure of **42**.

When ligand **24** was reacted with $AgNO_3$ in methanol, a complex precipitated from the reaction mixture almost immediately, which after recrystallisation from acetonitrile gave colourless crystals, (**43**), that were suitable for an X-ray diffraction analysis. The crystal structure is a one-dimensional metallopolymer, the asymmetric unit of which is shown in Fig. 3.29a, with the nitrate counterion omitted for clarity.

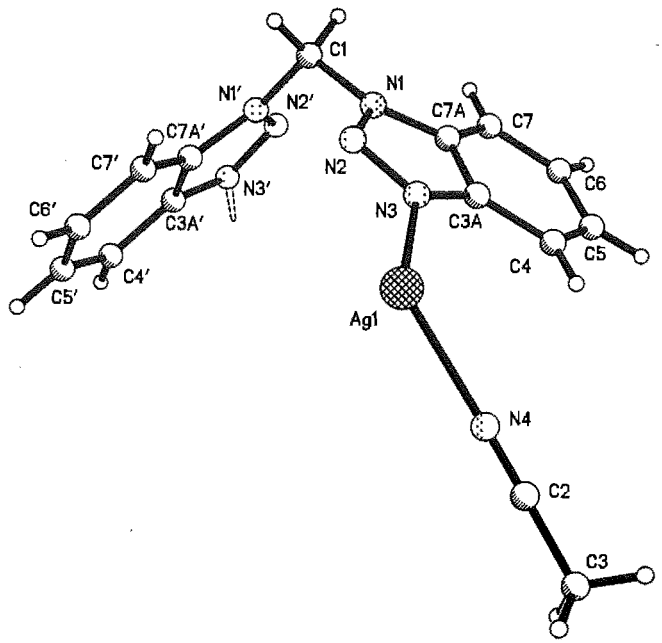

Fig. 3.29a Perspective view, with atom labelling of the contents of the asymmetric unit, of **43** with the non-coordinated nitrate counterion omitted. Selected bond lengths (Å) and angles (°): Ag1-N3 2.255(2), Ag1A-N3' 2.311(2), Ag1-N4 2.288(2), N1-N2 1.355(2), N2-N3 1.301(3), N3-N2-N1 107.8(2), N2-N3-C3A 109.4(2), N1-C1 1.452(3), N3-Ag1-N4 117.84(8), N3-Ag1-N3'A 124.93(7), N1-C1-N1' 110.2(2), N1'-N2' 1.355(2), N2'-N3' 1.300(3), N1'-C1 1.447(3), C3A'-C7A'-N1' 112.7(2), N2'-N3'-C3A' 109.1(2).

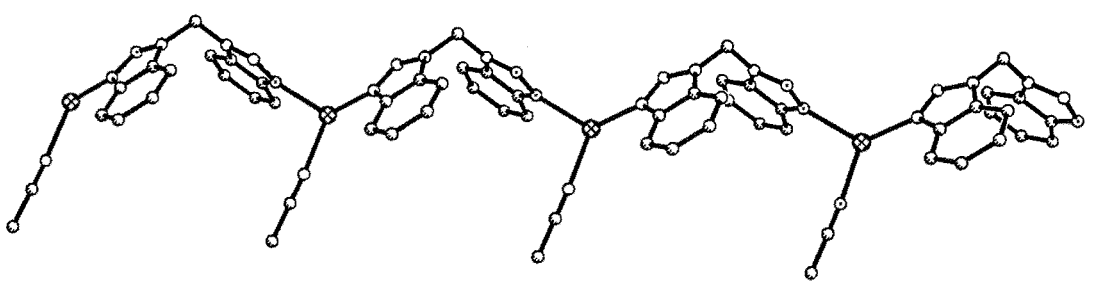

Fig. 3.29b Perspective view of the extended structure of **43**.

The conformation of the ligand in complex **43** is very similar to that in the previous crystal structure. The meanplanes of the benzotriazole units in the ligand subtend an angle of 84.1(5)° to each other, with the methylene bridge being close to tetrahedral [110.2(2)°]. Again the ligand is acting as a bridge between two metal ions, with each benzotriazole

coordinated *via* N3 to silver atoms [Ag1-N3 2.255(2)Å and Ag1A-N3' 2.315(2)Å]. A coordinated acetonitrile molecule completes the coordination sphere of the silver, and is essentially linear [N4-C2-C3 179.1(3)°] with a Ag1-N4 bond length of 2.288(2)Å. The nitrate counterion is not coordinated. The angle across the silver to the coordinating N3's is 124.93(7)°, which is smaller than that observed for the copper structure, perhaps because there are no inter-chain interactions present. The extended structure is simply a linear chain, comprised of silver atoms separated by V-shaped ligand spacers, [Ag1···Ag1A 9.212(1)Å].

A complex with $PdCl_2$ was also prepared. Ligand **24** was added to a solution of $PdCl_2$ dissolved in hot aqueous 2M HCl to give a tan solid, in high yield, which analysed as [**23**.$PdCl_2$], (**44**). Despite attempts to grow crystals for an X-ray analysis all efforts failed. ^1H NMR in deuterated DMSO gave no CIS, and FABMS was unable to find any discrete molecular ions. With this information, and the results of the previous crystal structures, the most likely structure for **44** is a metallopolymer (Fig 3.30).

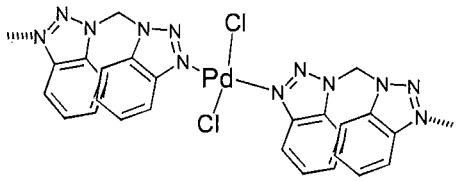

Fig. 3.30

The crystal structures of **42** and **43** with ligand **24** are dominated by the ligand conformation, and preferential N3 coordination disposes it to act as a V-shaped bridging ligand, with metallopolymers resulting. Based on these results, the complexes with ligand **23** (**38**, **39** and **40**) may also be metallopolymers with similar N3 coordination.

Large green single crystals, (**45**), grew from the methanolic reaction mixture of ligand **27** with $Cu(NO_3)_2.3H_2O$. The structure of the resulting complex is shown in Fig. 3.31.

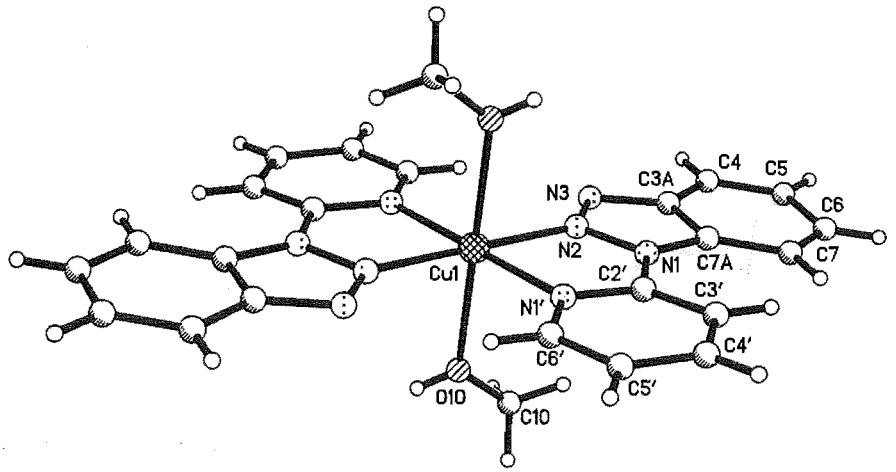

Fig. 3.31 Perspective view, with atom labelling of the contents of the asymmetric unit, of **45** with the non-coordinating nitrate counterions omitted. Selected bond lengths (Å) and angles (°): Cu1-N1' 2.033(2), Cu1-N2 2.047(2), Cu1-O10 2.298(2), N1-N2 1.369(3), N2-N3 1.303(3), N1-C2' 1.430(3), N1'-Cu1-N2 78.91(7), N1'-Cu1-O10 90.23(8), N2-Cu1-O10 91.71(8), N2-N1-C2' 117.1(2).

The structure is a [2 + 1] complex, which crystallises in the monoclinic space group $P2_1/n$. In the complex, a crystallographic centre of inversion at Cu1 relates the ligands, and so the arrangement around the copper is *trans*. Although the bulk sample analyses as $[(\mathbf{27})_2.Cu(NO_3)_2.MeOH.H_2O]$, refinement of the occupancy of the methanol CH_3 group converged to a value close to 1.0. Thus, the crystal used appears to have the stoichiometry $[(\mathbf{27})_2.Cu(NO_3)_2.2MeOH]$, as shown in Fig. 3.31, with the two non-coordinating nitrate counterions omitted. The ligand is chelating through N2 [Cu1-N2 2.047(2)Å] of the benzotriazole and N1' [Cu1-N1' 2.033(2)Å] of the pyridine ring giving a bite angle N1'-Cu1-N2 of 78.91(7)°.

This complex is structurally similar to the complex described in Chapter 2 with ligand **6** and copper(II) nitrate, *viz* **22**, and to that published by Battaglia *et al.*[81] The differences are that in this complex the apical positions are occupied by methanol solvate molecules whereas in complex **22** the nitrate counterions are in the apical positions and in the structure reported by Battaglia *et al.* the apical positions are occupied by water molecules.

Ligand **27** was also reacted with $AgNO_3$ in methanol to give colourless crystals, (**46**), that analysed as $[(\mathbf{27}).AgNO_3]$, suitable for X-ray diffraction. The complex is a symmetrical 12-membered [2 + 2] metallomacrocycle, which crystallises in the space group P-1, around a centre of inversion in the central cavity of the metallomacrocycle. Perspective views of the metallomacrocycle are shown in Fig. 3.32.

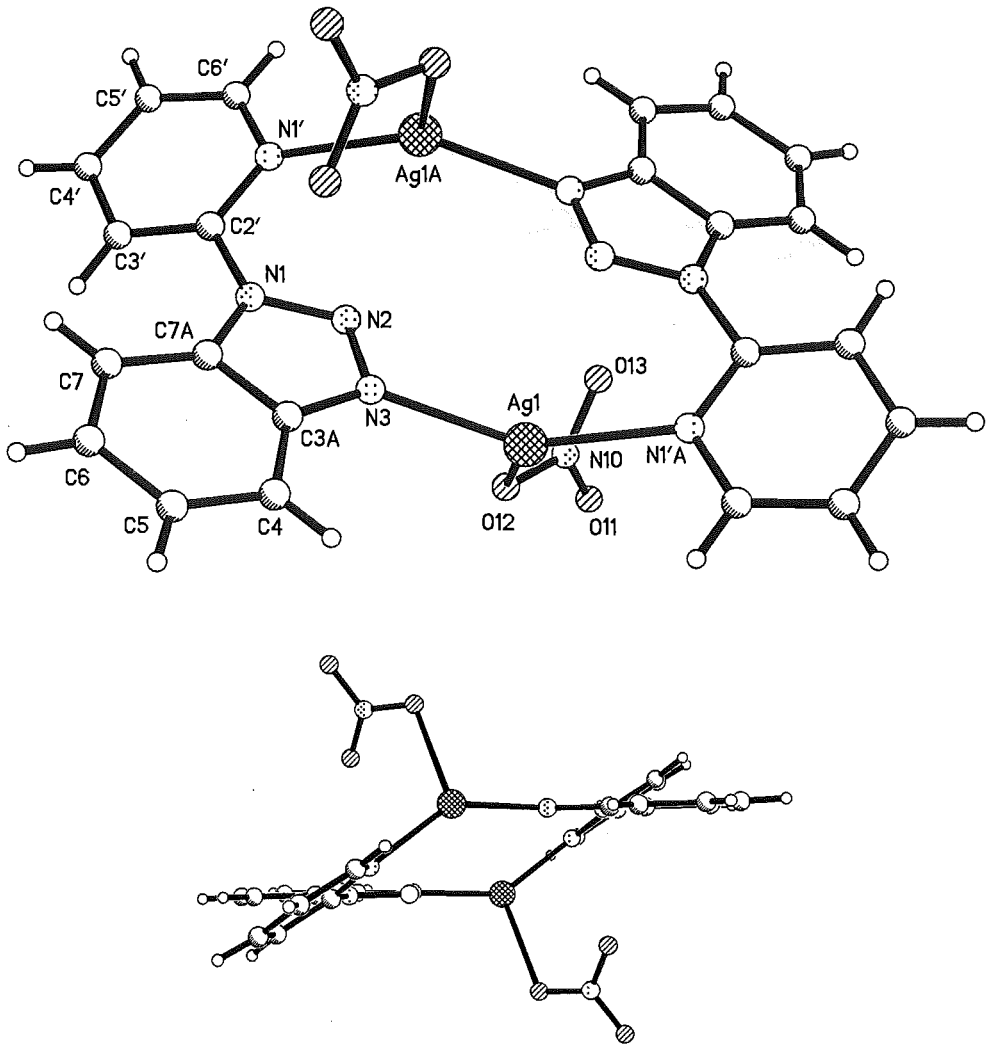

Fig. 3.32 Perspective views, with selected atom labelling, of **46**. Selected bond lengths (Å) and angles (°): Ag1-N3 2.251(2), Ag1-N1'A 2.291(2), Ag1-O12 2.592(2), N1-N2 1.367(3), N2-N3 1.309(3), N1-C2' 1.435(3), N3-Ag1-N1'A 143.37(7), N3-Ag1-O12 98.10(7), N1'A-Ag1-O12 114.04(7), N2-N1-C2' 118.6(2).

In this structure, the pyridine nitrogen (N1') and the benzotriazole N3 act as the donor atoms from the same ligand to two different silver ions. Thus, the ligand is acting in a bridging mode. The silver is tricoordinate, with a pyridine nitrogen coordinated from one ligand [2.291(2)Å] and a benzotriazole N3 from the other [2.251(2)Å]. The coordination of the silver atom is completed with a monodentate nitrate anion [2.592(2)Å]. The geometry about the silver can be described as a distorted T shape, with the N3-Ag1-N1'A bond angle of 143.37(7)° differing significantly from linearity. The two rings of the ligand are inclined at an angle of 33.5(3)° to each other. The N3-Ag1-N1'A angle at the silver and the angle between the planes of the two rings, define a rhombic cavity (Fig 3.32), with the silver atoms separated at a distance of 4.600(1)Å.

The palladium complex with **27** was also prepared in the same manner as that described for previous palladium complexes, and analysed as [**27**.$PdCl_2$.½H_2O], (**47**). However, no useful information from ^1H NMR or FABMS could be gained for **47**, and all efforts at recrystallisation failed to give crystals suitable for a structural analysis.

The green/blue crystals, which were recovered, by filtration, from the reaction of stoichiometric amounts of ligand **28** with $Cu(ClO_4)_2.6H_2O$ in methanol, analysed in the intriguing ratio [(**28**)$_3$.$Cu_2(ClO_4)_4.H_2O$]. FAB mass spectrometry gave molecular ions, in a 1:1 ratio, corresponding to $[(\mathbf{28})_2Cu(ClO_4)]^+$ and $[(\mathbf{28})_2Cu_2(ClO_4)]^+$. Together, these pieces of information suggested the formation of [2 + 1] and [2 + 2] complexes which had co-crystallised. Fractional recrystallisation from DMF afforded beautiful blue diamond-shaped crystals, (**48**), one of which was used for a structural investigation. The structure found by crystallography is of the [2 + 1] complex, as shown in Fig. 3.33.

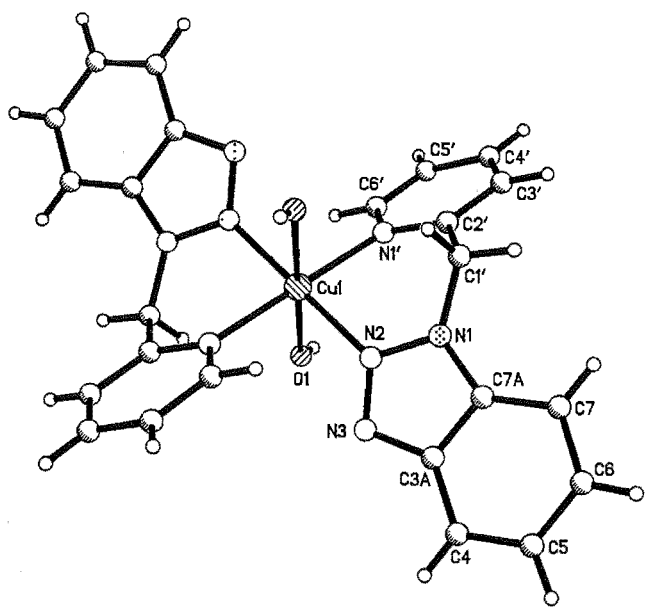

Fig. 3.33 Perspective view, with atom labelling of the contents of the asymmetric unit, of **48** with the non-coordinating perchlorate counterions and solvate molecules omitted. Selected bond lengths (Å) and angles (°): Cu1-N2 2.011(3), Cu1-N1' 2.034(4), Cu1-O1 2.369(4), N1'-Cu1-N2 87.5(1), N2-Cu1-O1 87.9(1), N1-N2 1.350(5), N2-N3 1.304(5), N1-C1' 1.461(5), C1'-C2' 1.507(5), N1-C1'-C2' 111.7(3).

Complex **48** is a [2 + 1] complex and has crystallised in the triclinic space group P-1. The asymmetric unit contains a copper atom, lying on a crystallographic centre of inversion, coordinated to a chelating ligand and a water, as well as a non-coordinating perchlorate counterion and DMF solvate molecule. The chelating benzotriazole-containing ligands being related through inversion are in a *trans* arrangement around the copper atom. The six-membered chelate ring of the ligand is in a boat conformation, providing a bite angle at the copper atom [N1'-Cu1-N2] of 87.5(1)°.

The reaction of ligand **28** with $AgNO_3$ in methanol gave a precipitate, which was filtered off and recrystallised from acetonitrile to produce colourless crystals, (**49**), of sufficient quality for an X-ray diffraction analysis. The structure is shown in Fig. 3.34.

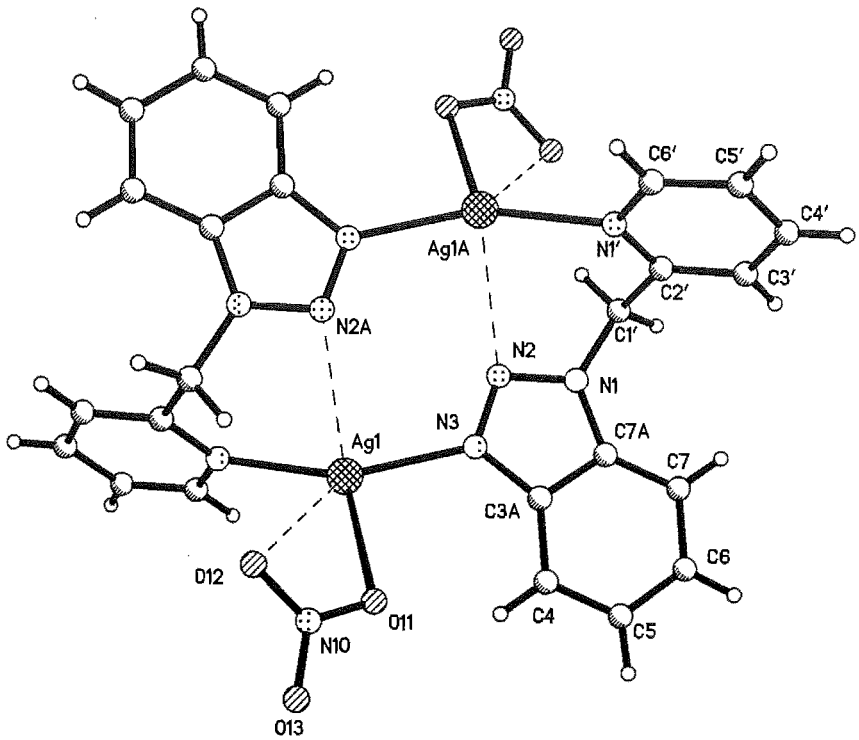

Fig. 3.34 Perspective view, with selected atom labelling, of **49**. Selected bond lengths (Å) and angles (°): Ag1-N3 2.222(2), Ag1A-N1' 2.228(2), Ag1-O11 2.527(2), N1-N2 1.345(3), N2-N3 1.308, N1-C1' 1.462(3), C1'-C2' 1.511(3), N3-Ag1-N1'A 152.96(8), N3-Ag1-O11 92.11(7), N1'A-Ag1-O11 114.87(7), N1-C1'-C2' 111.2(2), N3-N2-N1 107.9(2).

The complex is a [2 + 2] metallomacrocycle, similar to the complex **46.** This time, because of the methylene bridge, the metallomacrocycle is 14-membered. The introduction of the tetrahedral methylene group also results in a large change to the central cavity, with the silver-silver distance increasing to 4.942(1)Å relative to **46** [4.600(1)Å]. However, the geometry about the silver is remarkably similar to that found for the previous [2 + 2] structure, with the same number and type of donor atoms, with similar angles around the silver. In addition to the strong interactions between the silver atom and N3, N1A' and O11, the silver makes weaker contacts with N2A [2.922(3) Å] and O12 [3.060(2) Å].

Ligand **28** dissolved in methanol was added to a solution of $PdCl_2$ dissolved in hot aqueous 2M HCl. A yellow precipitate formed immediately and was collected by filtration. FABMS of the solid gave a molecular ion of $(\mathbf{28})_2Pd_2Cl_3^+$, which suggested the formation of another [2 + 2] metallomacrocycle. Crystals, (**50**), suitable for X-ray diffraction were grown

by vapour-diffusion of methanol into a DMF solution of the complex. The structure is shown in Fig 3.35a.

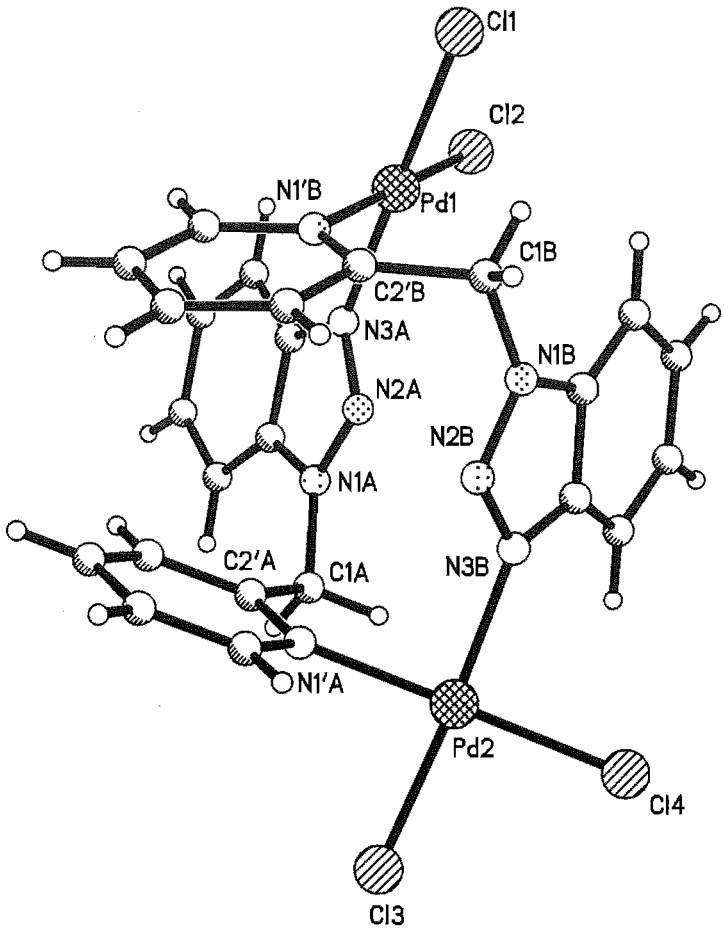

Fig. 3.35a Perspective view, with selected atom labelling, of **50** with the methanol solvate molecule omitted. Selected bond lengths (Å) and angles (°): Pd1-N3A 2.050(7), Pd1-N1'B 2.071(8), Pd1-Cl1 2.313(3), Pd1-Cl2 2.308(3), N3A-Pd1-N1'B 87.8(3), Pd2-N3B 2.052(8), Pd2-N1'A 2.056(8), Pd2-Cl3 2.299(2), Pd2-Cl4 2.300(3), N1'A-Pd2-N3B 88.8(3), N1A-C1A-C2'A 109.3(7), N1B-C1B-C2'B 110.6(8)

This complex crystallises in the space group $P2_1/c$, and contains in the asymmetric unit one [2 + 2] metallomacrocycle and a methanol solvate molecule, which has been omitted for clarity. The metallomacrocycle is 14-membered, the same as for the previous structure **49**, but because of the different geometric preference of palladium compared to silver, a very different topology results. Each palladium atom is square planar, with the chlorine atoms being *cis* at each metal centre. The angle to the coordinating benzotriazole N3 and pyridine N1 atoms, N3A-Pd1-N1'B 87.8(3)° and N1'A-Pd2-N3B 88.8(3)°, is significantly smaller than for the silver structure and has much to do with the different conformation of the metallomacrocycle. The methylene groups are tetrahedral and the torsional angle N2B-N1B-C1B-C2'B differs from the torsional angle N2A-N1A-C1A-C2'A. The benzotriazole rings of each ligand lie approximately orthogonal to each other, while the pyridine rings are almost

parallel. The influence of the metal geometry has increased the metal-metal separation, as the palladium-palladium distance of 6.739(1)Å is significantly larger than the silver-silver distance in the previous [2 + 2] structure [4.942(1) Å].

Interestingly, the chlorine atoms coordinated to each palladium do not share two-fold symmetry, and this results in the complex **50** being axially chiral. This structure also has an interesting conformation. The complex can be described as being in an 'armchair' arrangement (Fig. 3.35b), with the benzotriazole rings acting as the back and seat of the chair and the pyridyl rings providing the legs.

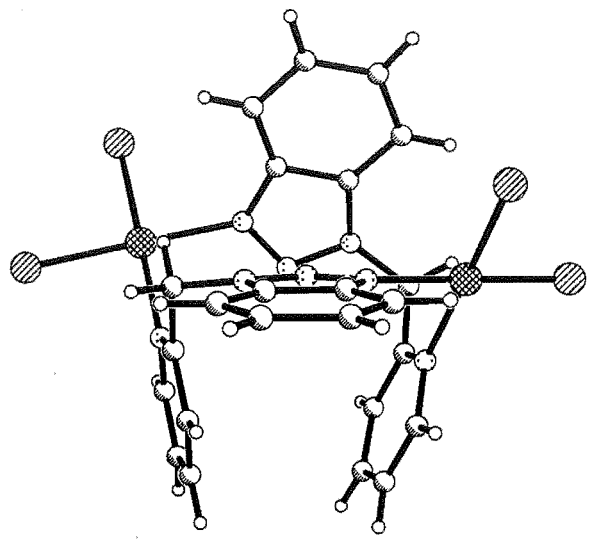

Fig. 3.35b

A copper complex with ligand **29** was prepared by adding a solution of $CuCl_2.2H_2O$, dissolved in 1:1 chloroform/methanol, to **29** dissolved in chloroform. After 1 day a tan solid had developed in the vial and this was filtered off. Vapour diffusion of diethyl ether into the filtrate precipitated more of the tan solid, resulting in a total yield of 89%. Elemental analysis of the solid confirmed a 1:1 stoichiometry, [**29**.$CuCl_2$] (**51**), but no information about the nuclearity of the complex was gained by FABMS. Recrystallisation from nitromethane gave thin orange plate-like crystals, and one of these was used for an X-ray diffraction study. Due to the thin crystal, the quality of the X-ray data was poor, and the refinement was only able to reduce the R-factor to 12%. However, the structure of the complex, shown in Fig. 3.36, could be determined unambiguously and is worthy of some discussion.

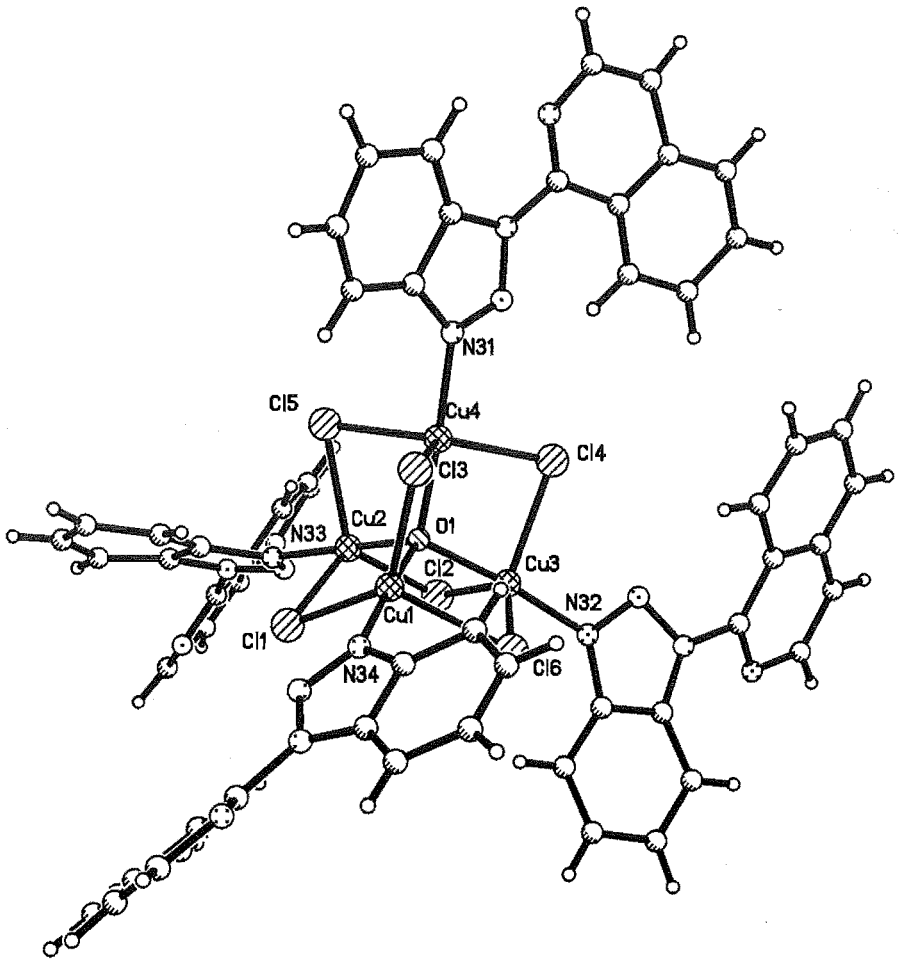

Fig. 3.36 Perspective view, with partial atom labelling of the asymmetric unit, of **51**. The hydrogen atoms and solvate molecules have been omitted for clarity.

The complex crystallises in the monoclinic space group C2/c, with eight molecules in the unit cell. Contained in the asymmetric unit is one full [4 + 4] metal complex as well as disordered nitromethane and water molecules, all of which have been omitted for clarity in Fig. 3.36. The complex contains a central Cu_4Cl_6 cluster encapsulating an oxo anion. Each of the four heterocyclic ligands in the complex coordinate in a monodentate fashion through the N3 nitrogen atom of the benzotriazole to a copper. The isoquinoline ring is not involved in the coordination. Each of the ligands has a *trans* arrangement with, respect to the heteroatoms about the inter-ring bond, and each possesses different angles between the meanplanes of their constituent aromatic rings ranging from 17° to 58°.

This is a surprisingly common type of cluster, as a search of the Cambridge Crystallographic Database found many structures containing the Cu_4Cl_6O core. Many contained simple appended ligands such as acetonitrile,[110] DMF,[111] DMSO,[112] pyridine,[113] and triphenylphosphine oxide.[114] One complex that has a similarity to the complex **51** is that

synthesised by Tosik *et al.*[115] where the central cluster has a benzimidazole bound *via* its N3 atom as the appended ligand.

Attempts to prepare a silver nitrate complex with ligand **29** were unsuccessful. Instead, $AgBF_4$ dissolved in methanol/chloroform was added to **29** dissolved in chloroform, and the resulting solution stored in the dark whereupon a white powder formed. Elemental analysis of this powder determined that the complex formed had a 1:1 stoichiometry, [**29**.$AgBF_4$.½H_2O], (**52**), yet despite various efforts to recrystallise complex **52** no crystals suitable for a structural study were obtained.

A palladium complex with ligand **29** was prepared by adding a methanolic solution of Li_2PdCl_4 to **29** dissolved in boiling methanol. The resulting yellow solid was filtered off and recrystallised from nitromethane to give a yellow microcrystalline solid (**53**). FABMS of **52** provided a molecular ion that corresponded to $(\mathbf{29})_2Pd_2Cl_3^+$, and so the formation of another [2 + 2] metallomacrocycle is proposed. A ^1H NMR spectrum recorded in deuterated DMSO showed no change from that of the ligand itself in the aromatic region, indicating that in DMSO solution the complex dissociates. A satisfactory elemental analysis of this complex was not obtained and this is attributed to an unknown exact composition of nitromethane (observed in the ^1H NMR spectrum) and water in the complex.

The results of this structural study are summarised in Table 3.13, and show that [2 + 1] structures were only found for the reactions with copper(II), where coordination is through the N2 nitrogen. Table 3.13 shows a prevalence of [2 + 2] metallomacrocycles, even for palladium(II) which, because of its preferred square planar coordination, was expected to give the best chance of chelating structures with these ligands. Unfortunately, some of the complexes were unable to be characterised by anything more than an elemental analysis, which is only able to determine the stoichiometry of the complex and not the structure.

Table 3.13

Ligand	Cu(II)	Pd(II)	Ag(I)
27	[2 + 1]	-	[2 + 2]
28	[2 +1] / [2 + 2]	[2 + 2]	[2 + 2]
29	[4 + 4] cluster	[2 + 2]	-

3.5 Summary

Monodentate, chelating and bridging coordination modes have been found for the ligands **23** and **24**. This has demonstrated the diversity of coordination modes that these ligands possess. The main feature of this study of these benzotriazole-containing ligands has been that they coordinate preferentially through the N3 nitrogen atom. This disposes 1-substituted benzotriazoles towards bridging ligands, rather than chelating ligands, upon coordination. The bibenzotriazoles, however, can be made to chelate and hence become N,N'-bidentate ligands; this was demonstrated in the ruthenium complexes, although this required more stringent reaction conditions.

The benzotriazole-containing ligands **27**, **28** and **29** displayed monodentate, bidentate and bridging coordinating properties. They acted as N,N'-bidentate ligands in the work with ruthenium. However, when complexes with other metal ions were made, with no restrictions on the coordination modes available, non-chelating structures were also found.

The inclusion of a benzotriazole ring into ligands **27**, **28** and **29** significantly altered the physicochemical properties of the ruthenium complexes prepared. The effect of the benzotriazole component was to reduce the electron density on the metal atom. This was postulated to be so in the ^{1}H NMR analysis of the complexes prepared, and verified by the electrochemical measurements. For example, in the complex $[Ru(bpy)_2(\mathbf{27})](PF_6)_2$ (**35**), which contains five pyridine rings and one benzotriazole, the oxidation potential was 1.53 V, which is 270 mV higher than that of $Ru(bpy)_3^{2+}$.

The interesting results of the benzotriazole-containing ligands reflect the geometrical arrangement of the ligands. With two strong donor atoms, namely the benzotriazole N3 and the pyridine or isoquinoline nitrogen, in geometric positions that make a chelating relationship between them impossible, the ligands act as components in metallomacrocycle formation.

In conclusion, the benzotriazole ring has been shown for the first time to be a useful component for incorporation into multidentate organic ligands, for use in coordination and metallosupramolecular chemistry.

Chapter 4

1,2,4-Heterodiazoles

4.1 Introduction

For Chapters 4 and 5, the emphasis is moved away from benzo-fused systems. The heterocyclic systems that will be investigated in Chapters 4 and 5 are two of the isomers of the heterodiazoles. Heterodiazoles are five-membered heterocycles containing 3 heteroatoms — two of which are nitrogen and the other either oxygen or sulfur, named oxadiazoles or thiadiazoles, respectively. There exist four possible substitution patterns in a five-membered ring with three such heteroatoms. These are shown with the ring numbering for each substitution pattern in Fig. 4.1.

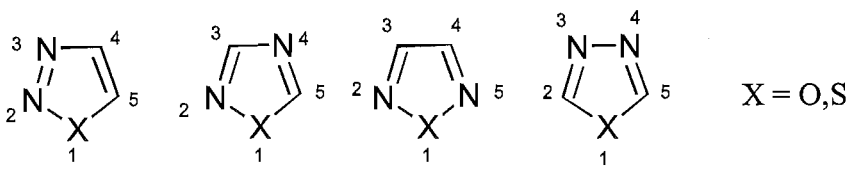

Fig. 4.1

Simple 1,2,3-oxadiazoles are unknown,[116] with the closest ring system being the zwitterionic sydnones (Fig. 4.2). 1,2,3-Thiadiazoles are, on the other hand, well-known. The usual method of synthesis of this heterocyclic system has been *via* the Hurd-Mori procedure.[117,118] By this method, the biheterocycle 4,4'-bi-1,2,3-thiadiazole (**54**) was recently synthesised, starting from butanedione, as shown in Scheme 4.1.[119]

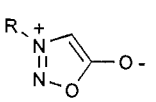

Fig. 4.2

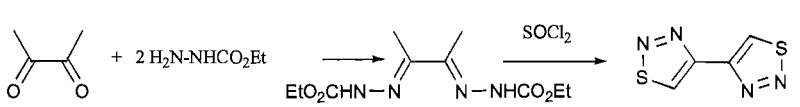

54

Scheme 4.1

Only one Xray crystal structure has been reported[120] for a coordination complex containing a 1,2,3-heterodiazole ligand. This complex, shown in Fig. 4.3a, contains a 1,2,3-thiadiazole as the heterocyclic ligand. Indeed, very little coordination chemistry has been explored with any of these heterocyclic ring systems. The 1,3,4-system has been by far the most investigated,[121-124] undoubtedly due to the ease of synthesis of this ring system compared to the others. The ring can be constructed starting from readily available materials, such as esters or acid chlorides and hydrazine, with subsequent ring closure using a dehydrating reagent. The appropriate choice of dehydrating agent can also be used to introduce the oxygen or sulfur into the ring. For example, 5,5'-diphenyl-2,2'-bi-1,3,4-oxadiazole[125] (**55**) and 5,5'-diphenyl-2,2'-bi-1,3,4-thiadiazole[126] (**56**) (Scheme 4.2) can both be synthesised from the same precursor by treatment with diphosphorus pentoxide (P_2O_5) and diphosphorus pentasulfide (P_2S_5), respectively. Of particular relevance to the present study was the preparation and study of a $Ru(bpy)_2^{2+}$ complex containing a 2,2'-bi-1,3,4-thiadiazole ligand (Fig. 4.3b).[127] The authors found that the thiadiazole ligand acted to withdraw electron density from the metal, and postulated that the presence of the sulfur atoms causes a strong enhancement of π back-bonding. In part, because of the coordination chemistry already reported for the 1,3,4-systems, these were not chosen for investigation in the present study.

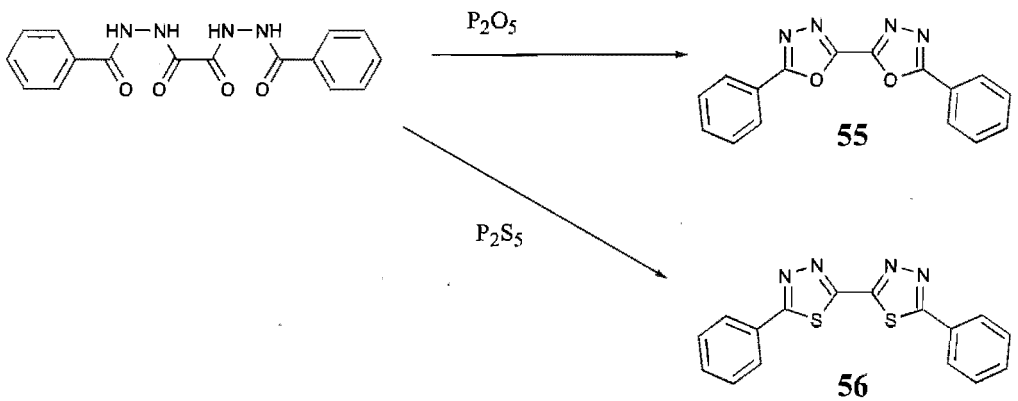

Scheme 4.2

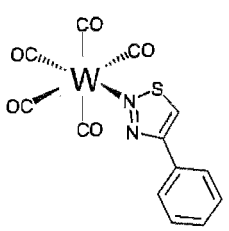

Fig. 4.3a

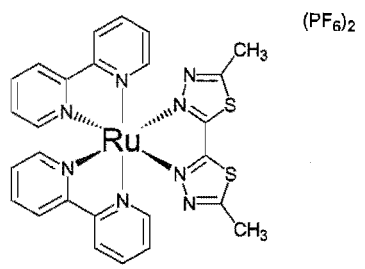

Fig. 4.3b

The purpose of the present study was, firstly, to examine the effect that such heterocyclic systems had on mononuclear ruthenium complexes and, secondly, to study the interactions between ruthenium centres bridged by a heterodiazole ring. Therefore the design of chelating ligands that would allow a systematic study of mono- and dinuclear ruthenium

complexes was necessary. It seemed a natural approach to attach other heterodiazoles, or pyridine rings, to the unsubstituted positions of the heterodiazole ring. In this fashion, a range of ligands could be synthesised that would allow control over the nuclearity of the complex through the available sites of chelation. The coordination chemistry of the 1,2,4- and 1,2,5-heterodiazoles was chosen for study, as they seemed to be the most well-suited to the construction of complexes of higher nuclearity. In this Chapter, the 1,2,4-heterodiazole systems are investigated, while Chapter 5 deals with the 1,2,5-systems.

Unlike the 1,3,4-systems, the 1,2,4-systems are unsymmetrical and hence isomers are possible with monosubstitution of the ring. We thought it would be interesting to see what effect, if any, this would have on the electrochemical properties of ruthenium complexes with such ligands. To this end, the preparation and study of some isomeric 1,2,4-heterodiazole-containing ligands was attempted.

With ligands containing a 3,3'-biheterodiazole core, as in 3,3'-bi-1,2,4-oxadiazole (**57**), there exist three possibilities for chelation of a single metal ion (Fig. 4.4). This ambidentate feature is an interesting aspect of the coordination chemistry of this system. Ligands containing the 3,3'-biheterodiazole core are also potentially able to bridge two metals, in one of the two modes shown in Fig. 4.4.

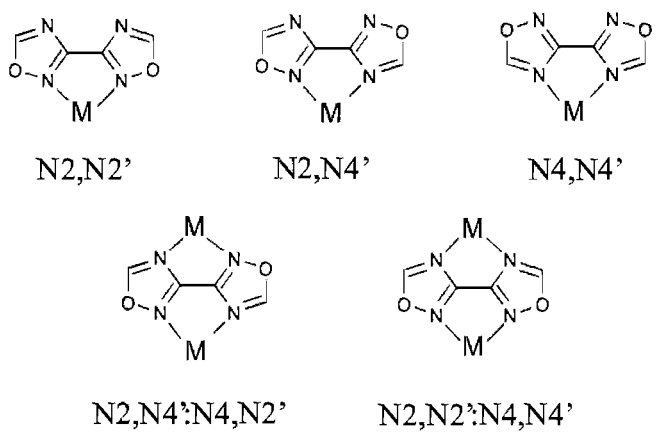

Fig. 4.4 Possible coordination modes of **57**.

This bisbidentate type of coordination is similar to the coordination mode demonstrated by a 2,2'-biimidazolate (Fig. 4.5), or 2,2'-bibenzimidazolate bridge. Of course, an oxadiazole ring does not contain the acidic NH proton of an imidazole and hence the ligand would bridge as a neutral, rather than anionic, species. Dinuclear complexes containing the biimidazolate bridge have been shown to exhibit strong metal-metal interactions.[128] Upon dinucleation, the metal-metal distance is only *ca.* 5.6 Å, and this is postulated to facilitate metal-metal interactions by direct orbital overlap of the two metals.

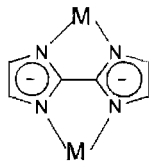

Fig. 4.5

The ligands selected for the present study are shown in Fig. 4.6. They are 3,3'-bi-1,2,4-oxadiazole (**57**), 5,5'-dimethyl-3,3'-bi-1,2,4-oxadiazole (**58**), 5,5'-diphenyl-3,3'-bi-1,2,4-oxadiazole (**59**), 5,5'-di(2-pyridyl)-3,3'-bi-1,2,4-oxadiazole (**60**), 5,5'-bi-1,2,4-oxadiazole (**61**), 3,3'-di(2-pyridyl)-5,5'-bi-1,2,4-oxadiazole (**62**), 2-(1,2,4-oxadiazol-3-yl)pyridine (**63**), 2-(1,2,4-oxadiazol-5-yl)pyridine (**64**), 2-(1,2,4-thiadiazol-5-yl)pyridine (**65**), 3,5-di(2-pyridyl)-1,2,4-oxadiazole (**66**) and 3,5-di(2-pyridyl)-1,2,4-thiadiazole (**67**).

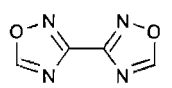

57

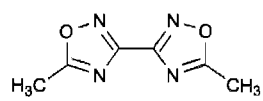

58

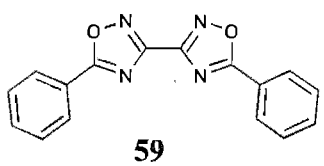

59

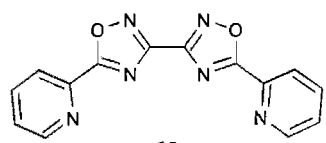

60

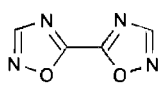

61

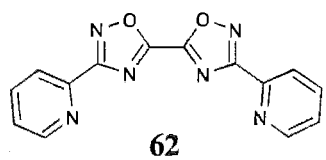

62

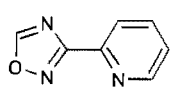

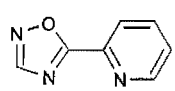

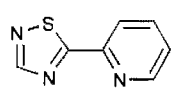

63 **64** **65**

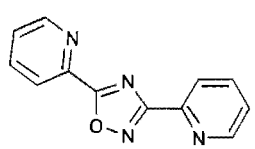

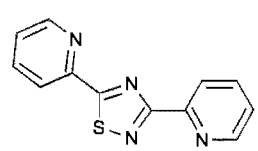

66 **67**

Fig. 4.6

A search of the Cambridge Crystallographic Database revealed only one crystal structure of a coordination complex containing a 1,2,4-heterodiazole,[129] and indicates the scarcity of use of these systems as ligands. The ligand is structurally related to 2,2':6',2"-

terpyridine and acted as a tridentate ligand. A pictorial representation of this complex is shown in Fig. 4.7.

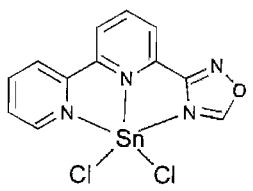

Fig. 4.7

There have been some reports of ruthenium complexes with 1,2,4-heterodiazole ligands. Orellana *et al.*[130] attempted to prepare a homoleptic ruthenium complex with the ligand 2-(1,2,4-oxadiazol-3-yl)pyridine (**63**), with a notable lack of success. However, these authors did successfully prepare a homoleptic ruthenium complex with the ligand 2-(1,2,4-thiadiazol-5-yl)pyridine (**65**),[130] which they also examined electrochemically.[131] The $Ru(bpy)_2^{2+}$ complex with ligand **65** has not been prepared, and this complex is important to the present study as it provides a basis for comparison of possible dinuclear $Ru(bpy)_2^{2+}$ complexes containing a 1,2,4-thiadiazole moiety. This is particularly relevant to any dinuclear ruthenium complex with ligand **67**.

In contrast to the few studies of the 1,2,4-heterodiazoles, 1,2,4-triazoles have been well studied.[132-135] Of relevance to the present study are the investigations into the dinuclear complexes of several related ligands. For instance, 3,5-di(2-pyridyl)-1,2,4-triazole (**68**), (Fig. 4.8), and 5,5'-di(2-pyridyl)-3,3'-bi-1,2,4-triazole (**69**), (Fig. 4.9), have structural similarities to the ligands **66/67** and **60/62**, respectively. Ligand **68** has been well-studied, with many dinuclear complexes having been prepared and investigated by a variety of techniques.[136-144] The triazole ring contains an acidic proton and in dinuclear complexes of **68** bridges in the fashion shown in Fig. 4.8, where the triazole is anionic and coordination occurs in the less sterically demanding N1,N4 manner. This is similar to the only mode in which N,N'-chelating dinuclear complexes involving ligands **66/67** can bridge two metals (Fig. 4.8), although the heterodiazole ligands would not bridge as anionic species.

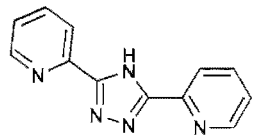

68

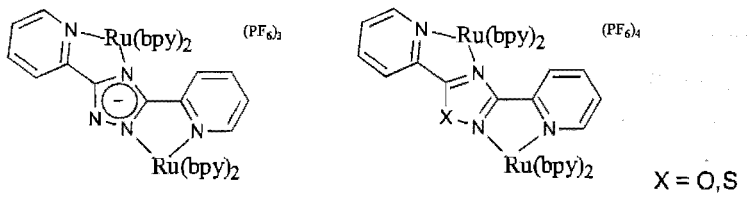

Fig. 4.8

The ligand 5,5'-di(2-pyridyl)-3,3'-bi-1,2,4-triazole (**69**) has recently been shown to be able to form trinuclear complexes with three chelating $Ru(bpy)_2^{2+}$ units (Fig. 4.9).[145] Given this successful polynuclear construction there was particular interest in the synthesis of ligands **60** and **62**.

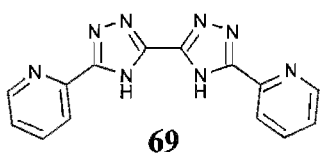

69

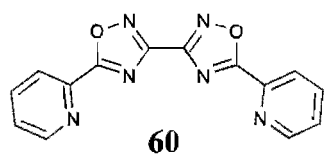

60

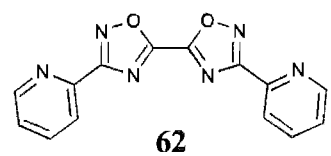

62

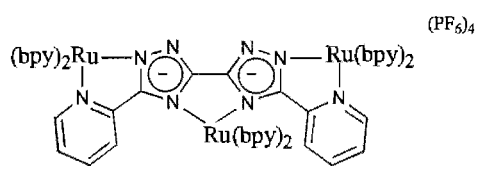

Fig. 4.9

In work with ruthenium complexes 1,2,4-triazoles have been shown to be good σ-donors and poor π-acceptors. This results in a lowering of the oxidation potential of the complex, but the electron-rich triazole ligands themselves are harder to reduce than bpy ligands. No such work has been reported for 1,2,4-heterodiazoles and the present study aims to explore the electronic nature and properties of these heterocyclic systems in chelating ligands.

4.2 Syntheses of Ligands

For the ligands containing a 3,3'-bi-1,2,4-oxadiazole core, oxamidoxime[146] proved a valuable starting material, as did 2-picolylamidoxime[147] for the oxadiazole ligands with appended pyridine rings. These molecules were synthesised according to the reported procedures and are shown in Fig. 4.10.

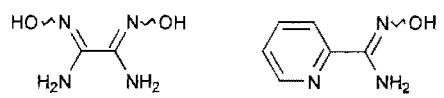

Fig. 4.10

Ligand **57** was synthesised *via* the method of Adrianov *et al.*,[148] which involves a boron trifluoride promoted double cyclisation of oxamidoxime in hot triethyl orthoformate, as shown in Scheme 4.3. By this method ligand **57** was produced in 76% yield.

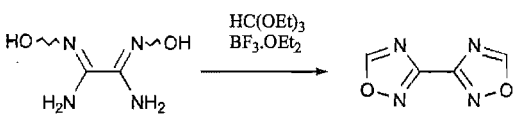

57

Scheme 4.3

5,5'-Dimethyl-3,3'-bi-1,2,4-oxadiazole (**58**) and 5,5'-diphenyl-3,3'-bi-1,2,4-oxadiazole (**59**) are both known molecules, having been first synthesised over 100 years ago.[149] The methods described by Zinkeisen,[149] summarised in Schemes 4.4 and 4.5, were followed to produce **58** and **59**, respectively. In both cases, oxamidoxime is reacted with an excess of reactant (acetic anhydride and benzoyl chloride) which also acts as a dehydrating agent. The reactions required long reflux times, and the yields were rather low (20-40%).

In line with our interest in the solid state structures of the biheterocycles produced in this work, the crystal structure of **59** was determined, and is shown in Fig. 4.11.

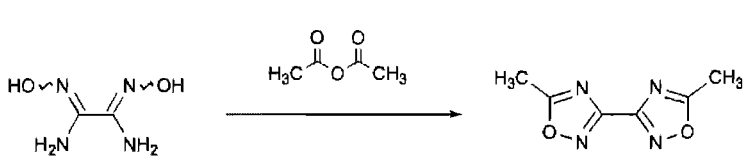

58

Scheme 4.4

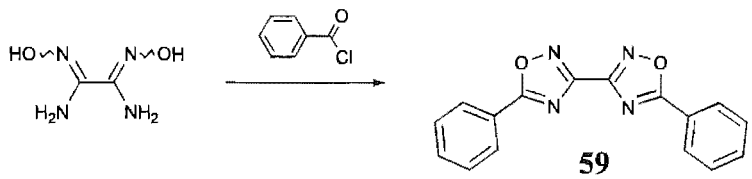

Scheme 4.5

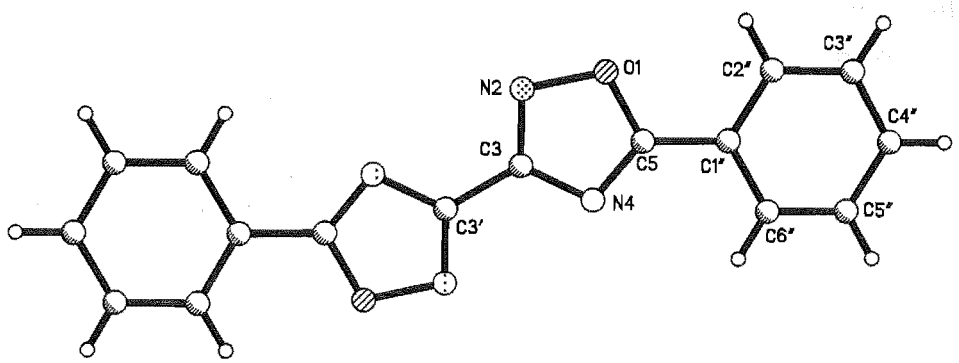

Fig. 4.11 Perspective view, with atom labelling of the contents of the asymmetric unit, of **59**. Selected bond lengths (Å) and angles (°): O1-N2 1.415(3), N2-C3 1.308(3), C3-N4, 1.369(4), N4-C5 1.306(4), C5-C1" 1.447(4), C5-O1 1.356(3), C3-C3' 1.462(6), C5-O1-N2 106.7(2), C3-N2-O1 102.3(2), N2-C3-N4 116.0(3), N2-C3-C3' 121.0(3), N4-C3-C3' 123.0(3), N4-C5-C1' 129.0(3), C5-N4-C3 102.4(2), O1-C5-C1' 118.4(3).

Ligand **59** crystallises in the monoclinic space group $P2_1/c$, with a centre of inversion located in the middle of the inter-ring bond separating the oxadiazole rings. The ligand is perfectly planar, with a mean deviation from the plane of only 0.043(1)Å. Each phenyl ring may be encouraged to lie in the plane of the oxadiazole ring to which it is bonded, by the two attractive hydrogen bonding interactions of the *ortho* hydrogens of the phenyl rings with the O1 and N4 heteroatoms. Also, the bioxadiazole core is in a *trans* coplanar conformation, again maximising conjugation. The distances and angles around the oxadiazole ring are similar to the distances found for other molecules containing a 1,2,4-oxadiazole ring.[150-152] As this molecule crystallises in the space group $P2_1/c$, it packs with the characteristic herringbone array (Fig. 4.11b), with the distance separating the planar aromatic molecules being 3.49(7)Å.

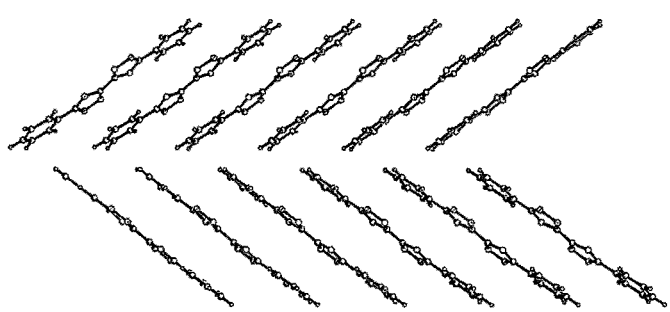

Fig. 4.11b Perspective view of the herringbone array.

In an attempt to prepare 5,5'-di(2-pyridyl)-3,3'-bi-1,2,4-oxadiazole (**60**), oxamidoxime was heated in an excess of ethyl picolinate (Scheme 4.6). After 30 minutes the solution had become discoloured and a solid had formed in the reaction mixture, so the reaction was stopped and analysed by TLC and ^{1}H NMR. These both showed no sign of any product that could be identified as **60**. Attempted catalysis of this reaction by boron trifluoride or triethylamine did not aid the formation of ligand **60**. As it was desirable to retain oxamidoxime, which provides the 3,3'-bioxadiazole core, the reaction partner was changed to be more reactive. Picolinic acid was converted into its acid chloride by reaction with thionyl chloride, and reacted with oxamidoxime (Scheme 4.6). The product of this reaction was the iminoester, where the two oxime oxygen atoms have acted as nucleophiles. The first attempt to cyclise the iminoester was by heating at 250°C, but the only product recovered from this reaction was picolinic acid. Cyclisation was then attempted in polyphosphoric acid (PPA). The ^{1}H NMR spectrum of the material isolated showed only one pyridine ring in the product, and signals consistent with an amidoxime. FABMS indicated that the molecular formula was $C_8H_7N_5O$, and so the product was formulated as shown in Scheme 4.6, where cyclisation of one ring had occurred but the other had cleaved to generate an amidoxime. As a simple synthesis was not found, it was decided not to pursue the preparation of **60** any further.

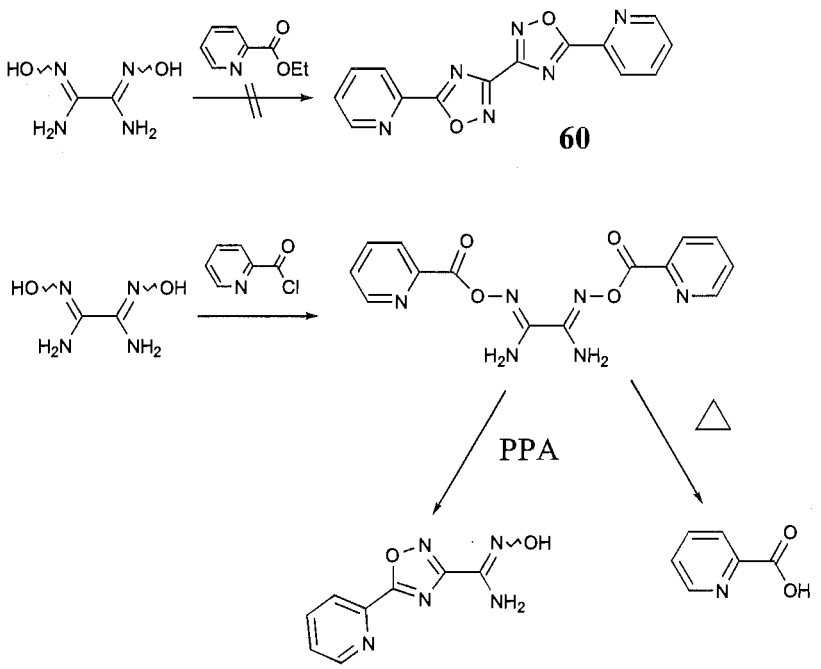

Scheme 4.6

A synthesis of the ligand 5,5'-bi-1,2,4-oxadiazole (**61**) has not been reported.[75] A possible synthesis of this biheterocycle is the reaction of diethyl oxalate with formamidoxime (Scheme 4.7).

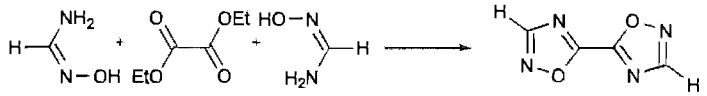

61

Scheme 4.7

Two equivalents of the amidoxime were suspended in diethyl oxalate, containing a catalytic amount of boron trifluoride, and gently heated until the amidoxime dissolved (*ca.* 50°C). At this point a violent reaction ensued, with almost all of the contents of the reaction flask being lost out the top of the attached reflux condenser. The reaction was repeated while maintaining the temperature below 50°C, and at no point was there a clear solution, yet the colour changed from a white to a yellow suspension, and thus it was hoped that at least some reaction had taken place. A ^{1}H NMR spectrum of the crude material showed no evidence for double cyclisation to produce any of the desired biheterocycle **61**, or that possible mono- or uncyclised intermediates (Fig. 4.12) were present. EIMS of the crude material also found no molecular ions that corresponded to any of the anticipated products, and so this synthesis was abandoned.

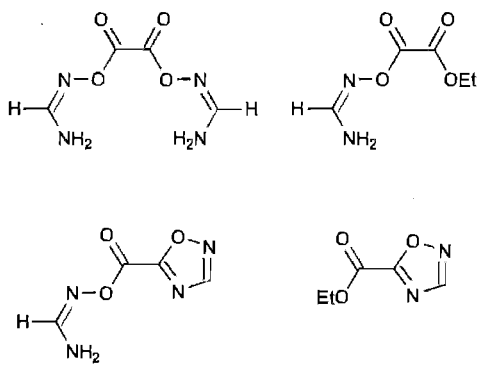

Fig. 4.12 Some possible products from the reaction of formamidoxime with diethyl oxalate.

The synthesis of 3,3'-di(2-pyridyl)-5,5'-bi-1,2,4-oxadiazole (**62**) was also based upon a double cyclisation reaction, involving 2-picolylamidoxime with diethyl oxalate (Scheme 4.8). Two equivalents of the amidoxime were added to diethyl oxalate heated to 160°C in the presence of a catalytic amount of boron trifluoride. From this reaction, the new ligand **62** was isolated in 26% yield, along with 3,5-di(2-pyridyl)-1,2,4-oxadiazole (**66**) in 25% yield.

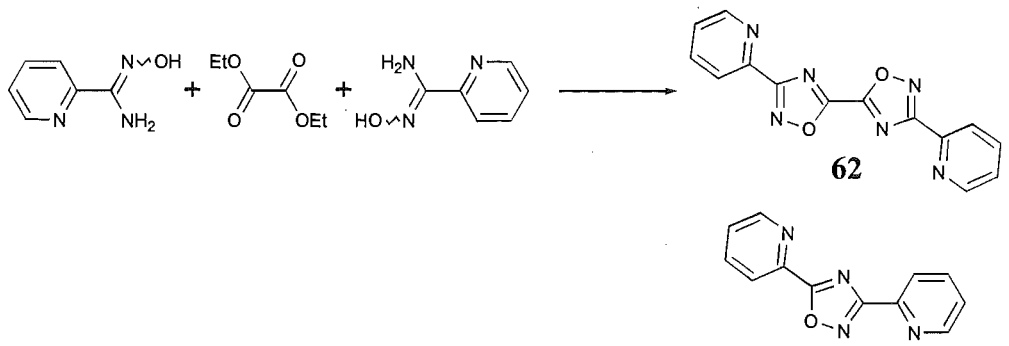

62

66

Scheme 4.8

2-(1,2,4-Oxadiazol-3-yl)pyridine (**63**) has previously been prepared by Paudler *et al.*[153] This is an important ligand for the present study, and so was synthesised for use in this work. In view of the excellent boron trifluoride promoted cyclisation to give ligand **57**, 2-picolylamidoxime was heated in an excess of triethyl orthoformate in the presence of a catalytic amount of boron trifluoride (Scheme 4.9). From this reaction, **63** was isolated in 82% yield, a considerably better yield than that obtained by Paudler *et al.* (39%), who did not use boron trifluoride.

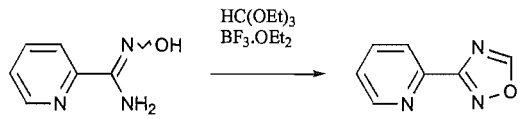

63

Scheme 4.9

Synthesis of the isomeric ligand, 2-(1,2,4-oxadiazol-5-yl)pyridine (**64**), was also attempted. The method of synthesis was based upon a general procedure for 5-monosubstituted 1,2,4-oxadiazoles, developed by Lin *et al.*[154] A reaction scheme for the synthesis is shown in Scheme 4.10. Picolinamide was heated in a slight excess of N,N'-dimethylformamide dimethyl acetal to generate an acyl amidine intermediate, which was reacted *in situ* with acidic aqueous hydroxylamine. This 'one-pot' reaction gave the intermediate **70** in 69% yield after recrystallisation. The procedure for the cyclisation step was to heat the intermediate **70** in a mixture of acetic acid and dioxane. However, the colourless crystalline solid collected from the reaction mixture was not the expected ligand **64**. The ^{1}H NMR spectrum of the material (shown in Fig. 4.13) has no signal for the proton of the oxadiazole ring, and a number of broad signals are observed that are consistent with hydrogens attached to nitrogen or oxygen. The chemical shifts are also different from those of the starting material, also shown in Fig. 4.13, and another indicator that a reaction had occurred was the change in melting point. These pieces of information indicated that a molecular rearrangement had taken place. To determine the molecular constitution, the elemental analysis and mass spectrum of the molecule were obtained. These both determined

that the molecular constitution of the molecule was unchanged, but that the mass spectrum was considerably different.

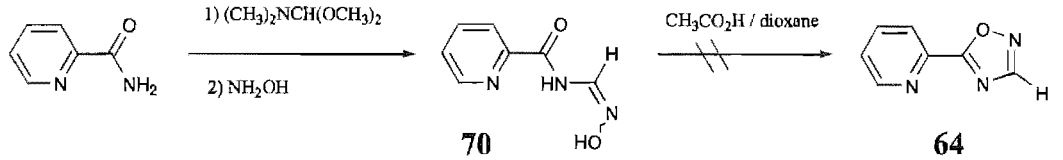

70 **64**

Scheme 4.10

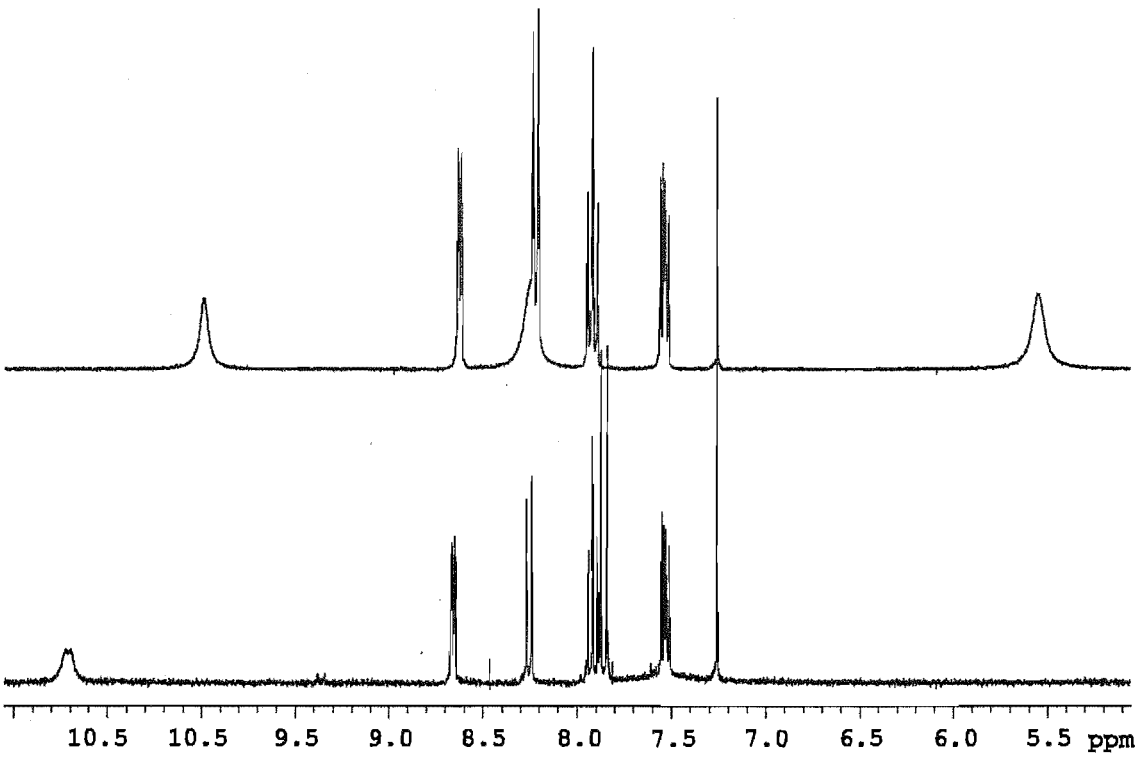

Fig. 4.13 ^{1}H NMR spectra for **70** (bottom) and the rearrangement product.

The mass spectrum of **70** shows the fragmentations depicted schematically in Fig. 4.14. For the rearranged product the molecular ion at 165 a.m.u. does not have the cleavage path that would suggest the loss of the oxime (31 a.m.u.), but instead loses 16 a.m.u., which could be an oxygen atom or an NH_2 group. Also observed are the fragment ions that correspond to the picolinamide ion (122 a.m.u.), the pyridyl carbonyl species (106 a.m.u.), and the pyridyl cation (78 a.m.u.).

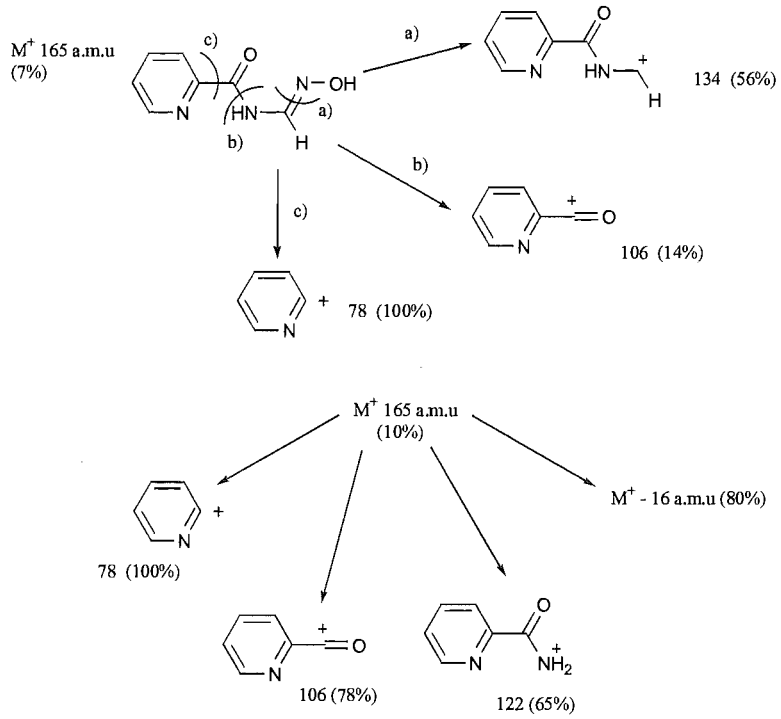

Fig. 4.14

The IR spectrum also revealed that the rearrangement product contained two carbonyl groups, one similar to that of the starting material. Based upon all the experimental information we feel that the molecule that best fits all the experimental data is one containing a urea functionality (Fig. 4.15). Surprisingly, there has been little published work on pyridylureas with the only literature being a patent[155] and a recently published series of papers by Masiero *et al.*[156] Fortunately, Masiero *et al* synthesised the urea-containing molecule in Fig. 4.15 by an unrelated route. By the comparison with the ^{1}H NMR data provided an identical match was found, confirming the structure of the product from the reaction of **70** and acetic acid.

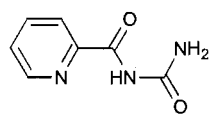

Fig. 4.15

Another possible synthesis of ligand **64** is the reaction of formamidoxime with the ethyl ester of picolinic acid (Scheme 4.11). This reaction was first attempted by simply heating the amidoxime in neat ester, and was monitored by TLC. The TLC plate showed no change of the reaction mixture, even after 16 hours at reflux. The reaction was repeated with the addition of boron trifluoride, which had been so successful previously, but still no product was seen by TLC or in ^{1}H NMR spectra. The reaction conditions were varied to include different solvents (ethanol, toluene, and xylene), with or without catalysts (boron trifluoride and triethylamine), all with no success.

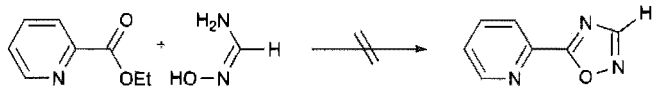

64

Scheme 4.11

3,5-Di(2-pyridyl)-1,2,4-oxadiazole (**66**) has previously been prepared by Liete *et al.*,[157] and was also isolated as a by-product in the synthesis of 3,3'-di(2-pyridyl)-5,5'-bi-1,2,4-oxadiazole (**62**) above. The method of synthesis employed by Liete *et al.*[157] was the reaction of 2-picolylamidoxime with acetic acid. From this reaction, 2-(5-methyl-1,2,4-oxadiazo-3-lyl)pyridine, the ligand **66**, and an unidentified component were isolated (Scheme 4.13). Symmetrical 3,5-diaryl-1,2,4-oxadiazoles can also be prepared by simply heating the corresponding arylamidoxime alone,[158] and this was the method used to synthesise **66** in the present work. 2-Picolylamidoxime was heated neat at 210°C for 30 minutes and **66** was obtained as the only product in 50% yield after recrystallisation.

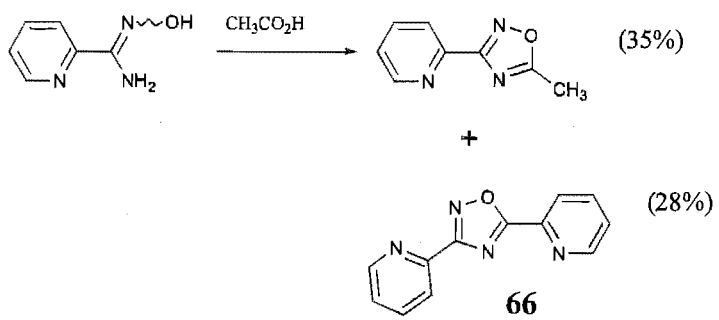

66

Scheme 4.13

As mentioned in the introduction, 2-(1,2,4-thiadiazol-5-yl)pyridine (**65**) is a known molecule.[131] The paper[131] reporting the synthesis of **65** was extremely light on experimental detail, quoting only a yield (35%) and reference to a general procedure followed.[159] Interestingly, in this paper by Lin *et al.*[159] the 3- and 4-substituted thiadiazolylpyridines were synthesised, but the 2-substituted isomer was not. An outline of the reaction scheme used, adapted for the present case, is shown in Scheme 4.12. Thiopicolinamide is reacted with N,N'-dimethylformamide dimethyl acetal to give the thioacyl amidine **71**, which is converted to the desired 1,2,4-thiadiazole by treatment with hydroxylamine-O-sulfonic acid in an alcoholic medium containing pyridine.

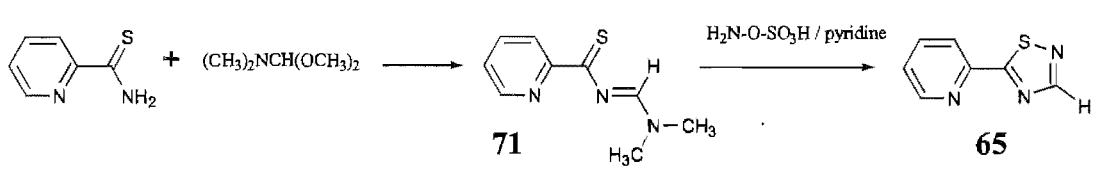

71 65

Scheme 4.12

Accordingly, thiopicolinamide[160] was combined with N,N'-dimethylformamide dimethyl acetal in a vial and left (accidentally) over a long weekend. A ^{1}H NMR spectrum of the material isolated, in 54% yield after workup, is shown in Fig. 4.16. Clearly, this is not the expected thioacyl amidine **71**, as no singlet for the formamidine proton is observed in the spectrum. The spectrum does contain the expected splitting pattern for a 1,2-disubstituted ring. However, two noticeable features of this spectrum suggested that this ring was no longer a pyridine. The position of these signals were much further upfield (*ca.* 1 ppm) than is usual for pyridine rings, and the usual coupling constant of a pyridine H6 (5.6 Hz) was missing. Thus, it seemed likely that another molecular rearrangement had taken place. Also in the spectrum are two signals in the methyl region, in a 6:3 ratio at 2.87 ppm and 2.38 ppm, respectively. The signal at 2.87 ppm was assumed to be the dimethylamino moiety that had been retained in the product.

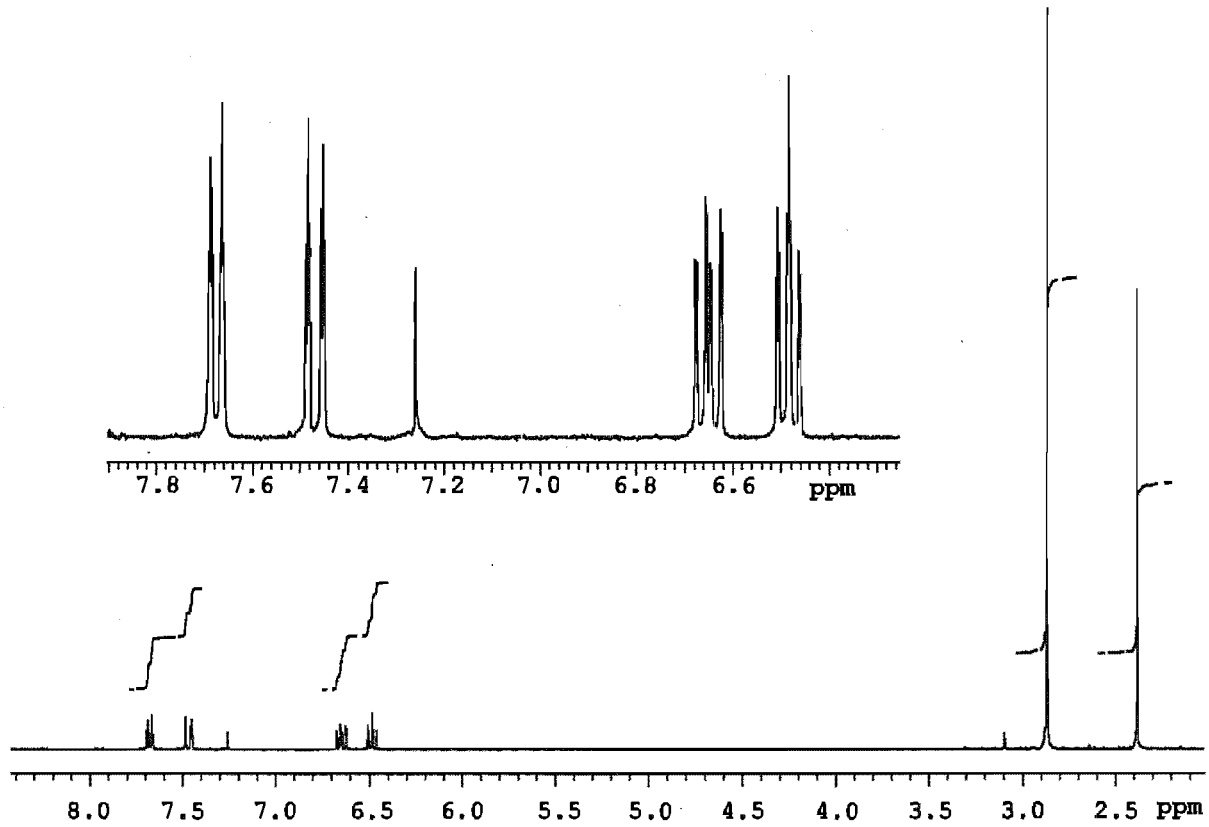

Fig. 4.16 ^{1}H NMR spectrum of rearrangement product.

To identify this product, an EI mass spectrum was first obtained. This gave a molecular ion at 207.1 a.m.u., and was identified by a high-resolution measurement as $C_{10}H_{13}N_3S$. With this information, the formation of a novel product, **72** (Fig. 4.17), with an imidazo[1,5-*a*]pyridine heterocyclic system, was proposed. Conformation of this proposal was by the complete ^{1}H and ^{13}C NMR assignments of this molecule (Fig. 4.17), and by comparison of these with the NMR spectra of a similar molecule containing an imidazo[1,5-*a*]pyridine system.[161]

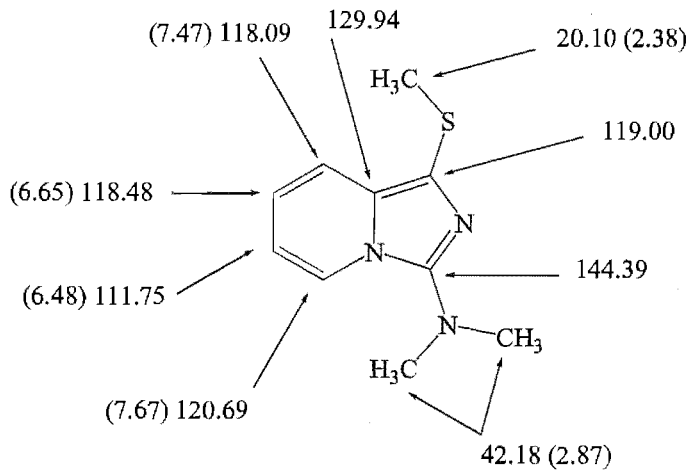

Fig. 4.17 ^{13}C NMR (and ^{1}H) chemical shifts of **72** in deuterated chloroform.

The reaction was repeated, on a much smaller scale, and followed by ^{1}H NMR. Fig. 4.19 shows the aromatic region of the spectrum over the time period 0-2 hours. In Trace I a spectrum of the starting thioamide is shown. In Trace II, taken after 35 minutes, it is clearly seen that all the starting thioamide has been consumed, and that only one product, presumably the thioacyl amidine **71**, is present. Certainly this is consistent with the observed signal at 8.70 ppm for the proton of the amidine carbon. After 2 hours (Trace III), a considerable amount of cyclised product is formed. Clearly, the thioacyl amidine **71** forms then cyclises, and this led to a proposed mechanism for the formation of **72** (Fig. 4.18). The first step is the formation of **71**, the pyridine nitrogen then acts as an intramolecular nucleophile to the amidine carbon, with subsequent electron rearrangement. Subsequent proton transfer results in the formation of a thiol. In the initial condensation methanol is produced, and the thiol is methylated to give **72**. The imidazo[1,5-*a*]pyridine system has previously been constructed using intramolecular cyclisations involving a pyridine ring.[162]

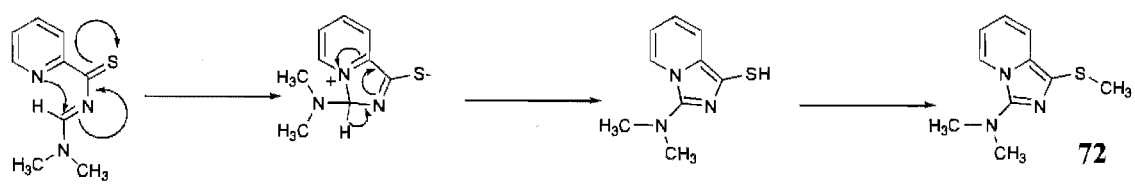

Fig. 4.18 Proposed mechanism for the formation of **72**.

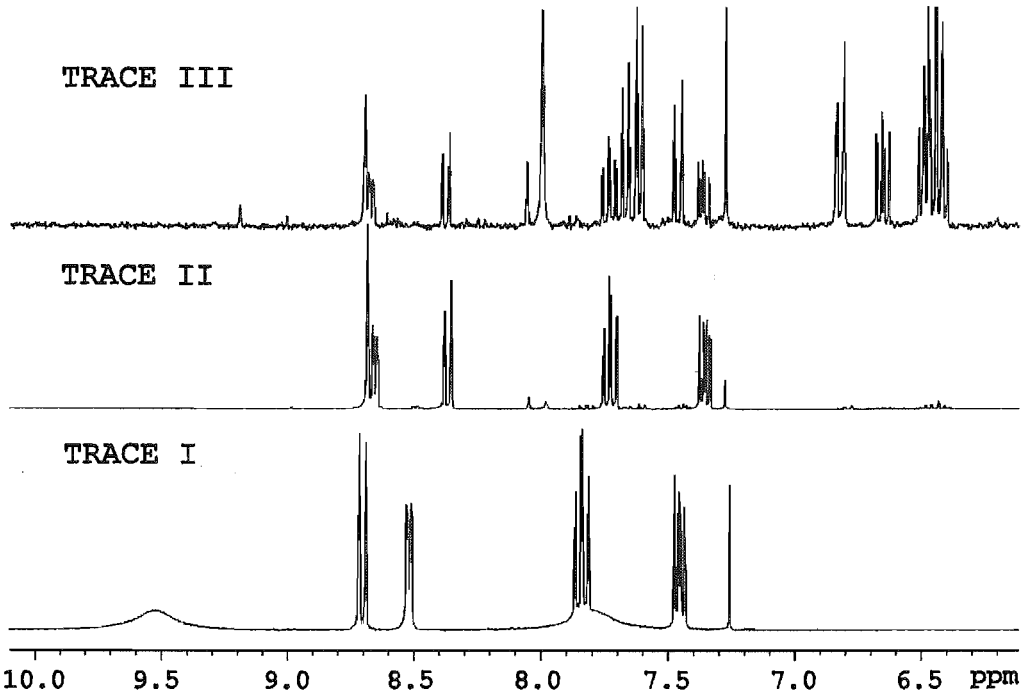

Fig. 4.19 ^{1}H NMR spectra of the reaction of N, N'-dimethylformamide dimethyl acetal with thiopicolinamide.

In order to circumvent the formation of **72**, it seemed appropriate to combine the two steps of the synthesis into a 'one-pot' procedure. Thiopicolinamide and N,N'-dimethylformamide dimethyl acetal were combined and allowed to stand for 30 minutes before hydroxylamine-O-sulfonic acid, in a mixture of methanol/ethanol, and pyridine were added and the resulting mixture allowed to stir at room temperature for 5 hours. By this method **65** was obtained in 75% yield after purification, a considerable improvement over the previously quoted yield of 35%.

3,5-Diaryl-1,2,4-thiadiazoles are conveniently prepared by the oxidation of arylthioamides.[163] Meltzer *et al.*[164] have prepared the 3- and 4-substituted dipyridyl-1,2,4-thiadiazoles but curiously not the 2-substituted isomer. The method of Meltzer was used in an attempt to prepare 3,5-di(2-pyridyl)-1,2,4-thiadiazole (**67**), starting from the previously prepared precursor thiopicolinamide, as shown in Scheme 4.14.

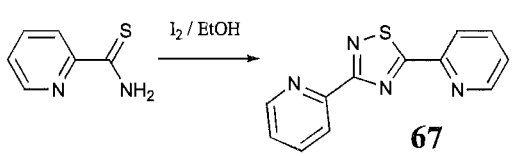

Scheme 4.14

The ^{1}H NMR spectrum of the material isolated after workup is shown in Fig. 4.20. Clearly, the product contains three pyridyl rings and two NH type peaks. Thus in the reaction the thioamide has not cyclodimerised to give the thiadiazole, but has cyclotrimerised. A high-resolution EI mass spectrum provided the molecular formula $C_{18}H_{14}N_6$ for this product. In an

attempt to identify exactly what this product was, we turned to X-ray crystallography. Small single crystals were grown by the slow evaporation of an acetone solution of the compound. The crystal structure revealed that the molecule had a central 1,3,5-triazine core with the 2-substituted pyridine rings appended in the 2, 4, and 6 positions. Unfortunately, however, the crystal structure could not fully elucidate the placement of the two NH protons, and hence the tautomer present. 2,4,6-Tris(2-pyridyl)-1,3,5-triazine (Fig. 4.21) is a known and well-used ligand,[165-168] and is conveniently prepared by trimerisation of 2-cyanopyridine.[169] It seems likely that the product of the thiopicolinamide reaction is one of the tautomers of the corresponding dihydrotriazine.

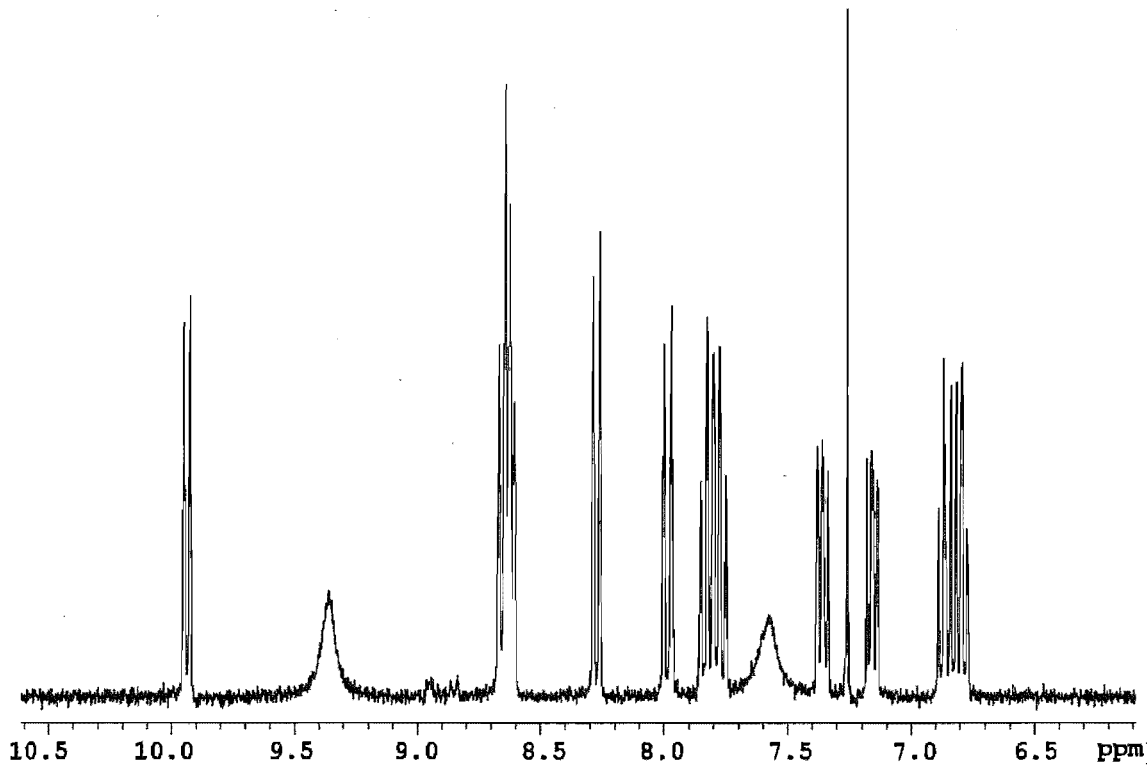

Fig. 4.20 ^{1}H NMR spectrum of the trimerisation product.

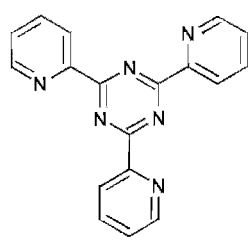

Fig. 4.21

With the iodine method proving unsuccessful, some other oxidising agents that have been used with success for the oxidation of thioamides to 1,2,4-thiadiazoles were tried. These attempts included hydrogen peroxide in pyridine solution,[170] and sodium nitrite in acetic acid.[171] However, in each case, none of the desired 1,2,4-thiadiazole could be identified in TLC or ^{1}H NMR spectra.

To avoid an oxidation procedure, an alternative method of synthesis of **67** was tried. The generation of nitrile sulfides, by thermal decarboxylation of aryl(1,3,4-oxathiazol-2-ones), in the presence of nitriles has been shown to lead to the formation of diaryl-1,2,4-thiadiazoles, by intermolecular [3 + 2] cycloaddition (Scheme 4.15).[172]

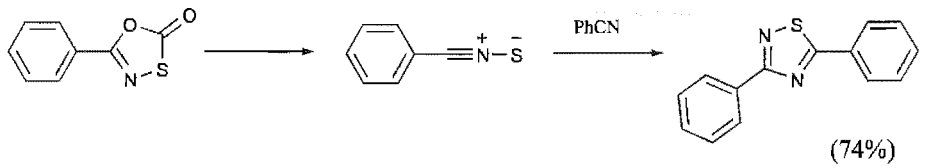

Scheme 4.15

To prepare the appropriate 5-(2-pyridyl)-1,3,4-oxathiazol-2-one, picolinamide was reacted with chlorocarbonyl sulfenyl chloride in chloroform, following the general method described by Muhlbauer *et al.*[173] This reaction gave the desired oxathiazolyl-2-one in only 12% yield (Scheme 4.16). The oxathiazolyl-2-one was then added in small portions to an excess of redistilled 2-cyanopyridine heated to 200°C. However, although a new small component could be identified in the reaction mixture by TLC this could not be isolated after chromatography. Thus the synthesis of **67** was finally abandoned.

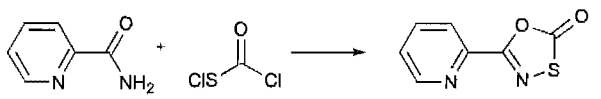

Scheme 4.16

4.3 Metal Complexes

The first goal of the investigation into the coordination chemistry of 1,2,4-systems was to ascertain which mode of bonding the ligands containing a 3,3'-bi-1,2,4-oxadiazole core would adopt when chelating to a single metal ion. The three possible modes are shown in Fig. 4.22. Two of the modes are symmetrical (N2,N2' and N4,N4') and the other is unsymmetrical (N2,N4'). It was originally anticipated that the N2,N2' mode might be preferred, given that it possesses an ∝-diimine arrangement so common for chelating biheterocycles, and might also be favoured for steric reasons.

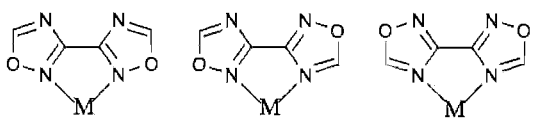

Fig. 4.22

Palladium(II) adopts a square planar geometry almost exclusively, and readily chelates to biheterocycles. For this reason, palladium(II) was chosen as the first metal ion to be used for this investigation. Ligand **57** was reacted with one equivalent of $PdCl_2$ dissolved in hot aqueous 2M HCl. Yellow plates, suitable for X-ray diffraction, grew from the reaction mixture. The structure contained some disorder, which could not be satisfactorily modelled, and the structure as a whole could not be refined to an acceptable level. However, the ligands bound to the metal could be determined unambiguously. A pictorial representation of the complex (**73**) is shown in Fig. 4.23, and shows that the complex contains a chelating ligand and two coordinated chlorine atoms. One ring of the ligand has ring-opened, regenerating an amidoxime, which coordinates to the metal through the oxime nitrogen, and importantly, the unopened ring is coordinated *via* the N4 nitrogen atom. This suggested that perhaps N4,N4' chelation would be the preferred mode of chelation by **57**.

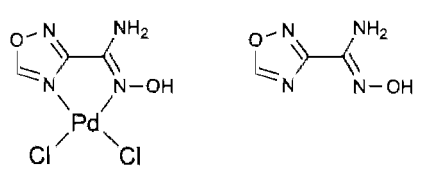

73 **74**

Fig. 4.23

The ^{1}H NMR spectrum of the complex was recorded in deuterated acetonitrile and, by the selective monocyclisation of oxamidoxime,[148] the free ligand, (**74**), was produced and a ^{1}H NMR spectrum recorded, allowing the calculation of the CIS values (Table 4.1). The oxadiazole H5 shows a positive CIS, consistent with its proximity to the chlorine atom.

Table 4.1 ^{1}H NMR Chemical Shifts[a] and Coordination Induced Shifts[b] for **73** and **74**.

	H5	NH_2	OH
73	9.65	6.85	[c]
74	9.06	5.80	8.58
CIS	+0.59	+1.05	

[a] For deuterated acetonitrile solutions. [b] CIS = ($\delta_{complex}$ - δ_{ligand}). [c] Not recorded.

Moussebios *et al.*[174] have shown that 1,2,4-oxadiazoles are converted to amidoximes upon treatment with acid. So instead of the acidic conditions of the previous reaction, a methanolic solution of Li_2PdCl_4 was added to a methanolic solution of ligand **57**. Again, the reaction mixture furnished crystals, (**75**), suitable for crystallography, and one of these was used for X-ray analysis. The structure is shown in Fig. 4.24.

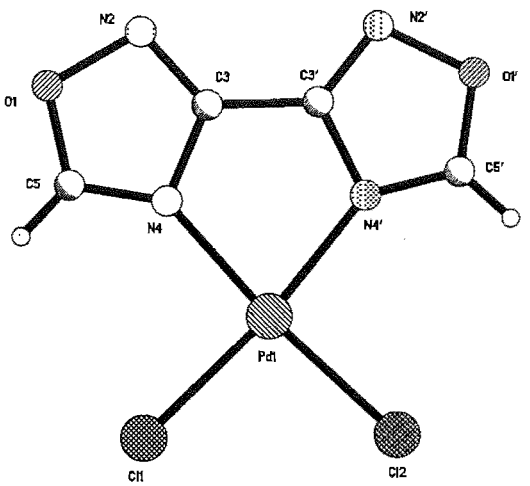

Fig. 4.24 Perspective view, with atom labelling of the contents of the asymmetric unit, of **75**. Selected bond lengths (Å) and angles (°): Pd1-N4 2.031(3), Pd1-N4' 2.046(3), Pd1-Cl1 2.270(1), Pd1-Cl2 2.276(1), N4-Pd1-N4' 79.8(1), Cl1-Pd1-Cl2 92.82(4), O1-C5 1.334(4), O1'-C5' 1.335(4), O1-N2 1.417(4), O1'-N2' 1.423(4), N2-C3 1.295(4), N2'-C3' 1.290(5), C3-N4 1.371(5), C3'-N4' 1.386(4), N4-C5 1.289(4), N4'-C5' 1.297(5), C5-O1-N2 107.5(3), C5'-O1'-N2' 107.3(3), C3-N2-O1 102.0(3), C3'-N2'-O1' 102.3(3), N2-C3-N4 115.0(3), N2'-C3'-N4' 115.3(3), C3-N4-C5 103.5(3), C3'-N4'-C5' 102.6(3), N4-C5-O1 112.0(3), N4'-C5'-O1' 112.5(3).

The complex crystallises in the orthorhombic space group Pnma, with a full molecule in the asymmetric unit. This structure unambiguously determined the mode of coordination as N4,N4'. The values for the bond lengths and angles for the 1,2,4-oxadiazole rings in this complex are similar to those found for the other coordination complex containing a 1,2,4-oxadiazole.[129]

Ligand **57** was also reacted with an excess of Li_2PdCl_4 in the hope of forming a dinuclear complex. However, the complex that formed in this attempt, as determined by elemental analysis, was the above mononuclear complex **75**.

Given that **57** is a multidentate ligand, and is potentially capable of coordinating to more than one metal at a time, it was decided to explore **57** in the context of metallosupramolecular chemistry. To this end, the coordination chemistry of ligand **57** was investigated with $AgNO_3$. A complex of 1:1 stoichiometry [**57**.$AgNO_3$], (**76**), was prepared by mixing methanolic solutions of $AgNO_3$ and ligand **57**. Recrystallisation of the resulting complex from acetonitrile gave colourless single crystals suitable for an X-ray diffraction study. The asymmetric unit of the structure is shown in Fig. 4.25a.

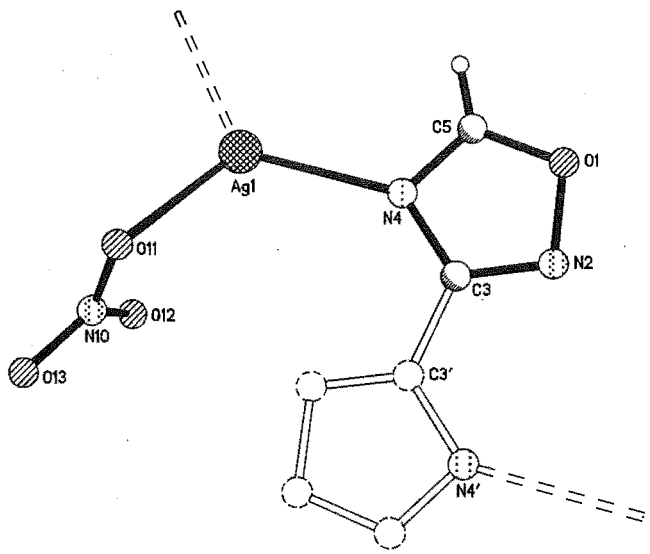

Fig. 4.25a Perspective view, with atom labelling of the contents of the asymmetric unit, of **76**. Selected distances (Å) and angles (°): Ag1-N4 2.384(2), Ag1-O11 2.370(3), O1-N2 1.417(3), N2-C3 1.309(3), C3-N4 1.384(3), N4-C5 1.301(3), C3-C3' 1.478(5), O11-Ag1-N4 111.33(5), N4-Ag1-N4' 131.82(9), C5-O1-N2 106.6(2), C3-N2-O1 102.6(2), N2-C3-N4 115.2(2), C3-N4-C5 102.0(2), N4-C5-O1 113.6(2).

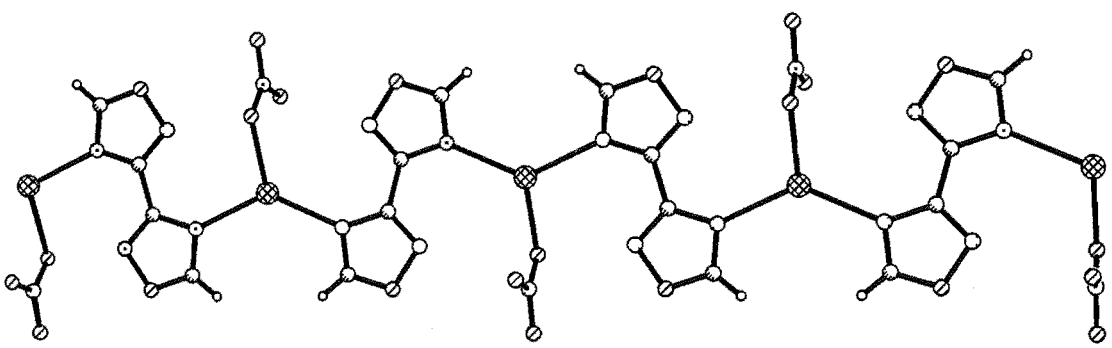

Fig. 4.25b Perspective view of the extended structure of **76**.

The asymmetric unit contains one half ligand, coordinated to the silver atom *via* its N4 nitrogen, and a nitrate anion coordinated *via* an oxygen atom to the silver. The silver atom and the four atoms of the nitrate anion all lie on a mirror plane and the occupancy of these atoms is ½. The silver atom is tricoordinate, and the geometry of the coordination can be

described as a distorted T-shape. The angle around the silver for the coordinating N4 atoms of different ligands [N4-Ag1-N4' 131.82(9)°] results in the coordination being far from linear. By virtue of the centre of inversion in the centre of the inter-ring bond, the rings of the ligand are strictly coplanar and *trans*. The two symmetry elements provide this one-dimensional metallopolymer with a central axis, about which the nitrate anions oscillate with the polymer itself weaving about in a wave-like fashion (Fig. 4.25b).

Having determined that the N4,N4'-mode was preferred for ligand **57**, it was of interest to examine the bonding of the ligand **58**, where the preferred N4 nitrogen of the oxadiazole is crowded by the neighbouring methyl group. This might result in a N2,N2' chelate, and would represent an example of steric control over the regioselectivity of complex formation. One equivalent of $PdCl_2$ dissolved in hot aqueous 2M HCl was added to ligand **58** dissolved in methanol, and the resultant solution left to stand. Fine golden rods, that analysed as [**58**.$PdCl_2$], (**77**), formed in the next few days, but unfortunately these crystals were too small for an analysis by X-ray diffraction. Importantly, there was no evidence for a ring-opened product in the ^1H NMR spectrum. However, as the chemical shift of the methyl groups in the complex was close to that of the free ligand, the spectrum proved inconclusive, indicating either that ligand dissociation had occurred or that N2,N2'-chelation had very little effect on the chemical shift of the methyl groups. N4 coordination would place the protons of the methyl groups considerably closer to the chlorine atom than would the H5 protons of ligand **57** (Fig. 4.26). Thus they would be much more sensitive to the effects of shielding by the chlorine atom, and only a large positive CIS in one or both groups would be evidence to suggest N4 coordination.

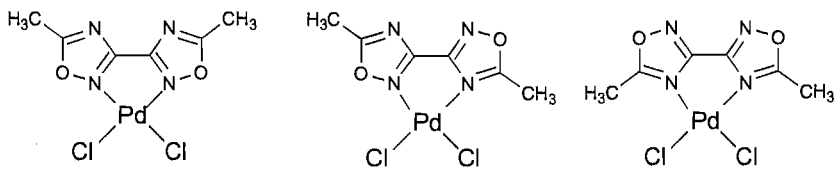

N2,N2' N2,N4' N4,N4'

Fig. 4.26

To determine how other ligands containing a 1,2,4-heterodiazole would chelate, some coordination complexes were prepared with 2-(1,2,4-oxadiazol-3-yl)pyridine (**63**) and 2-(1,2,4-thiadiazol-5-yl)pyridine (**65**) (Fig. 4.27). Both **63** and **65** are capable of two modes of chelation. For ligand **63**, N1,N2'- or N1,N4'-chelation is possible, while for ligand **65**, N1,S1' and N1,N4' are the possible modes of chelation. Several features could be ascertained by the formation and characterisation of chelating complexes with these simple ligands, and these features could be used to predict the coordination of complexes of higher nuclearity with the extended ligands. Accordingly, palladium(II) and copper(II) complexes were prepared with both of these ligands.

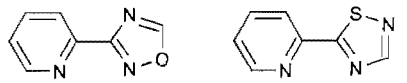

63 **65**

Fig. 4.27

When ligand **63** was reacted with Li_2PdCl_4 in methanol, a yellow complex precipitated from solution in high yield (95%), and analysed as [**63**.$PdCl_2$], (**78**). The complex was recrystallised from nitromethane, and the golden yellow needle-like crystals formed were filtered off. Unfortunately, the crystals were not large enough for crystallography, so ^1H NMR spectroscopy was employed as a tool in characterisation. The mode of chelation (N1,N2' or N1,N4') (Fig. 4.28) could be most easily distinguished by the chemical shift of the oxadiazole H5' proton. In the N1,N4' mode, the oxadiazole proton points toward the adjacent chlorine atom, and would be expected to be deshielded by this electronegative element, giving a strong positive CIS. Alternatively, the H5' proton in the N1,N2' mode points away from the chlorine atom and would be expected to experience no such deshielding effect. Thus it would be expected to have only a small CIS value.

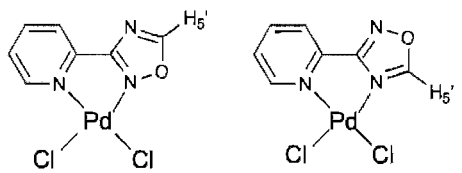

N1,N2'- N1,N4'-

Fig. 4.28

The chemical shifts and coordination induced shifts for **78** are shown in Table 4.2. From the shifts, particularly the strong CIS value of H5', chelation is deduced to be through the N1,N4'-mode.

Table 4.2 ^1H NMR Chemical Shifts[a] and Coordination Induced Shifts[b] for **78** and **63**.

	H3	H4	H5	H6	H5'
78	8.41	8.41	7.96	9.08	10.73
63	8.12	8.04	7.62	8.77	9.77
CIS	+0.29	+0.37	+0.34	+0.31	+0.86

[a] For deuterated dimethyl sulfoxide solutions. [b] CIS = ($\delta_{complex}$ - δ_{ligand}).

To prepare the copper complex two equivalents of ligand **63** was reacted with $Cu(NO_3)_2.3H_2O$ in methanol and after a few days crystals, (**79**), suitable for a structural study were obtained directly from the reaction solution. The structure is shown in Fig. 4.29.

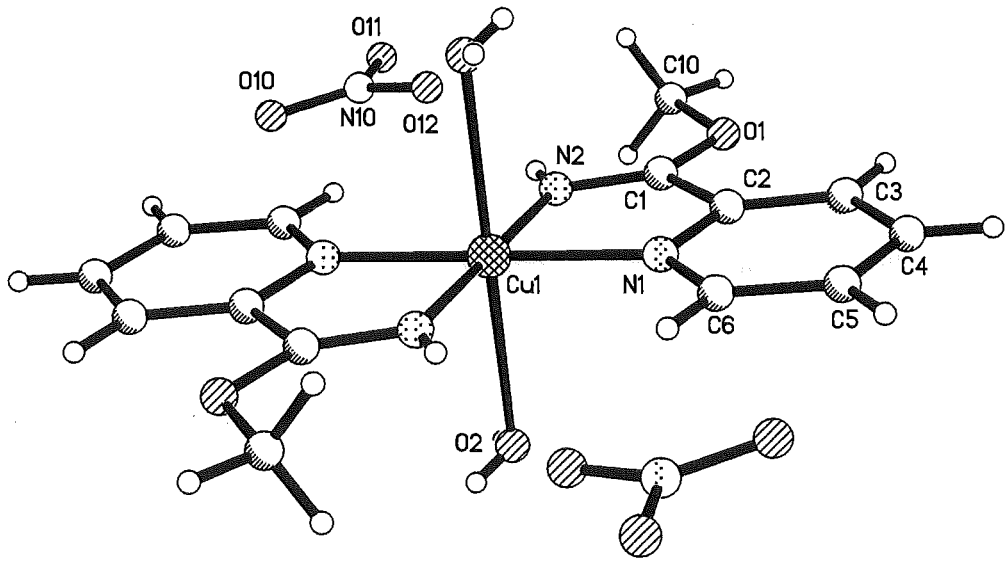

Fig. 4.29 Perspective view, with atom labelling of the contents of the asymmetric unit, of **79**. Selected distances (Å) and angles (°): Cu1-N1 2.020(2), Cu1-N2 2.012(2), N1-Cu1-N2 80.9(1), Cu1-O2 2.561(3), C1-N2 1.280(3), C1-O1 1.327(3), C1-C2 1.488(3), O1-C10 1.451(3).

Complex **79** crystallises in the space group P-1, with a centre of inversion located at Cu1. This results in a *trans* arrangement of the ligands in the complex, as well as relating the non-coordinated nitrate counterions through the centre of inversion. The structure shows that the ligand has rearranged, with the oxadiazole ring being cleaved, and that an iminoester has formed. Eloy *et al.*[175] have shown that, upon standing, 3-substituted 1,2,4-oxadiazoles decompose to the corresponding nitrile. It seems that this process has occurred, and that the solvent has reacted with the nitrile to produce the iminoester, which has then chelated to the copper. This rearrangement once again demonstrates the instability of the 1,2,4-oxadiazole ring.

Reacting $CuCl_2.2H_2O$ with ligand **63** in methanol gave another copper complex. Immediately, a light lime green precipitate formed, in quantitative yield, and this was collected by filtration. Elemental analysis of the complex determined a 1:1 stoichiometry [**62**.$CuCl_2$], (**80**). Unfortunately, no crystals suitable for a crystallographic study could be grown.

A palladium(II) complex with ligand **65** was prepared and purified in the same manner as the palladium(II) complex for ligand **63** described above. The golden needle-like crystals, (**81**), obtained from the nitromethane recrystallisation analysed as [**65**.$PdCl_2$], but were not suitable for X-ray crystallography. Again, ^{1}H NMR spectroscopy was employed as a characterisation tool. The mode of chelation (N1,S1' or N1,N4') (Fig. 4.30) could, as before, be most easily distinguished by the chemical shift of the proton on the heterodiazole ring. In

one mode (N1,N4'), the thiadiazole proton points toward the deshielding chlorine atom, whereas in the other mode (N1,S1'), it points away from the chlorine atom. On the basis of the CIS value the mode of coordination could potentially be distinguished.

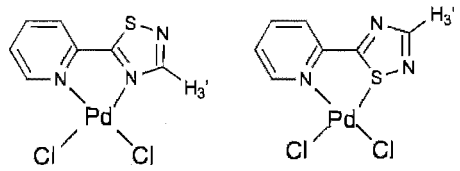

N1,N4'- N1,S1'-

Fig. 4.30

The ^{1}H NMR spectrum of the complex **81** was recorded in deuterated DMSO, and it showed a mixture of free and complexed ligand. In comparison with the spectrum of the free ligand, the signals due to the complex were identified. The chemical shifts and coordination induced shifts are given in Table 4.3. The H4, H5 and H6 protons of the pyridine ring in complex **81** show similar CIS values to the previous palladium complex **78**. The CIS value of H3 is more than twice that of the CIS of H3 in the previous complex **78**, and this was assumed to be because this proton was close to the large sulfur atom - indicating N1,N4'-chelation.

Table 4.3 ^{1}H NMR Chemical Shifts[a] and Coordination Induced Shifts[b] for **81** and **65**.

	H3	H4	H5	H6	H3'
81	8.78	8.43	7.95	9.03	9.14
65	8.17	8.08	7.65	8.72	9.02
CIS	+0.61	+0.35	+0.30	+0.31	+0.12

[a] For deuterated dimethyl sulfoxide solutions. [b] CIS = ($\delta_{complex}$ - δ_{ligand}).

A copper complex was prepared by reacting ligand **65** with $CuCl_2.2H_2O$ in methanol. This gave an immediate precipitate of a light green complex in quantitative yield, and the elemental analysis of this complex determined a 1:1 stoichiometry, [**65**.$CuCl_2$], (**82**). Recrystallisation by vapour diffusion of diethyl ether into a methanol/DMSO solution of the complex provided crystals suitable for X-ray crystallography. The structure is shown in Fig. 4.31.

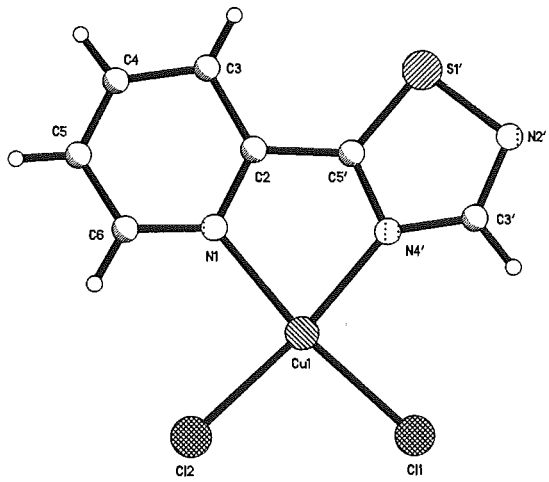

Fig. 4.31 Perspective view with atom labelling of **82**.

This complex crystallises in the monoclinic space group C2/c, and has a chelating ligand and two chlorines coordinated to a copper atom in a square planar coordination environment. The ligand is coordinating through the pyridine nitrogen and N4' of the 1,2,4-thiadiazole ring. In this structure, there was evidence of some disorder with respect to the orientation of the ligand. The ligand as a whole was found to exist also in the opposite orientation within the crystal, and this was found to be so about 15% of the time. Attempted modelling of this disorder was unsuccessful, and also due to the presence of diffuse solvent the structure could only be refined to an R-factor around 8.5%. Nevertheless, this study proved that chelation was through the N1,N4'-mode for this complex. The molecular packing for this structure indicated that the molecules pack in sheets, with weak Cu-Cu interactions [*ca.* 3.8Å] between the sheets, and interaction between the chlorine atoms of one complex to the sulfur atom of another within the sheet. A search of the Cambridge Crystallographic database revealed no X-ray crystal structures of 1,2,4-thiadiazole-containing coordination complexes. Indeed, very few X-ray crystal structures of molecules containing this heterocyclic ring have been reported.[176-179]

These results suggest that there might exist some predictive control over the coordination modes that the extended ligands would have upon formation of complexes of higher nuclearity. For example, it was expected that the ligand 3,3'-di(2-pyridyl)-5,5'-bi-1,2,4-oxadiazole (**62**) would form dinuclear complexes in the form of N4,N1"-μ-N4',N1"', as shown in Fig. 4.32.

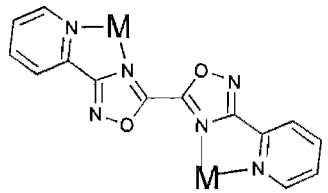

Fig. 4.32

In order to gain some insight into the exact nature of the metal-ligand interactions in complexes of these ligands, a study of their coordination chemistry with ruthenium(II) was undertaken. The first ruthenium complex prepared was with ligand **57**. Using the standard 3:1 ethanol/water reaction conditions, $Ru(bpy)_2Cl_2$ was first refluxed for an hour before addition of the ligand. Reflux was continued for another hour before the reaction was stopped and the cationic products isolated as hexafluorophosphate salts. A ^1H NMR spectrum of the material obtained after workup was very confusing. No singlet corresponding to the oxadiazole H5 proton was immediately obvious, and the spectrum definitely indicated the presence of more than one complex. Interestingly, there were also signals corresponding to ethoxy groups. FABMS of the material was unable to identify any ions that corresponded to the desired $[Ru(bpy)_2(\mathbf{57})](PF_6)_2$ complex (Fig. 4.33) and so further purification and identification of the products was not attempted.

It seemed that the ligand had again undergone rearrangement. To test whether the rearrangement was metal-catalysed, the ligand was refluxed alone in 3:1 ethanol/water. A ^1H NMR spectrum of the resulting products showed a mixture of starting material and products containing the ethoxy-type peaks seen in the ^1H NMR spectrum of the ruthenium complex. This proved that the ligand was unstable to the refluxing 3:1 ethanol/water reaction conditions. Hence, the alternative procedure, using $AgBF_4$ as the silver salt, was attempted. Analysis by FABMS and ^1H NMR spectroscopy of the crude material obtained from this reaction again provided no evidence for the formation of the desired complex $[Ru(bpy)_2(\mathbf{57})](BF_4)_2$.

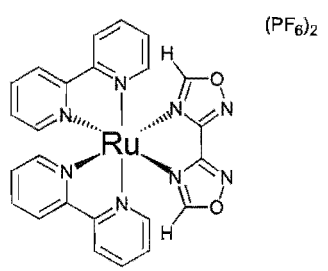

Fig. 4.33

At this time we interpreted the results obtained for ligand **57** as suggestive that monosubstituted 1,2,4-oxadiazoles may be unstable to such reaction conditions. It was hoped that the disubstituted ligand **59** would be more stable. Due to the low solubility of ligand **59**,

a long reflux time was required in the reaction with $Ru(bpy)_2Cl_2$. A low yield (45%) of complex was obtained, and this was purified by chromatography on alumina. The ^1H NMR spectrum of this complex is shown in Fig. 4.34. From the appearance of the spectrum, it is obvious that a symmetrical chelating complex has formed. Of note is the existence of a broad signal at 10.8 ppm, which is typical of the chemical shifts of oxime protons found in this work, and so it seemed that the oxadiazole rings had again ring-opened. To get an idea of the molecular constitution of the complex, a high-resolution FAB mass spectrum was obtained. The dominant molecular ion was at 707.1 a.m.u. corresponding to $C_{36}H_{29}N_8O_2Ru^+$, with the only higher cluster at 853.1 a.m.u., which corresponds to the addition of HPF_6. As the $Ru(bpy)_2^{2+}$ unit is intact, this leaves $C_{16}H_{14}N_4O_2$ as the molecular formula for the ligand, which represents the addition of 4 hydrogen atoms. In light of the molecular formula obtained, and the presence of an acidic hydrogen in the ^1H NMR spectrum, two possible products were considered (Fig. 4.35). In one product, an oxime functional group is present, while the other contains an acyl amidine. Exactly which of these is present in the complex is unknown, but the favoured possibility is the amidine as no singlet signal can be seen for a proton attached to the carbon of an imine in the ^1H NMR spectrum. Also, the N-O bond in oxadiazoles is the most susceptible to cleavage and breakage at this point would give the amidine product.

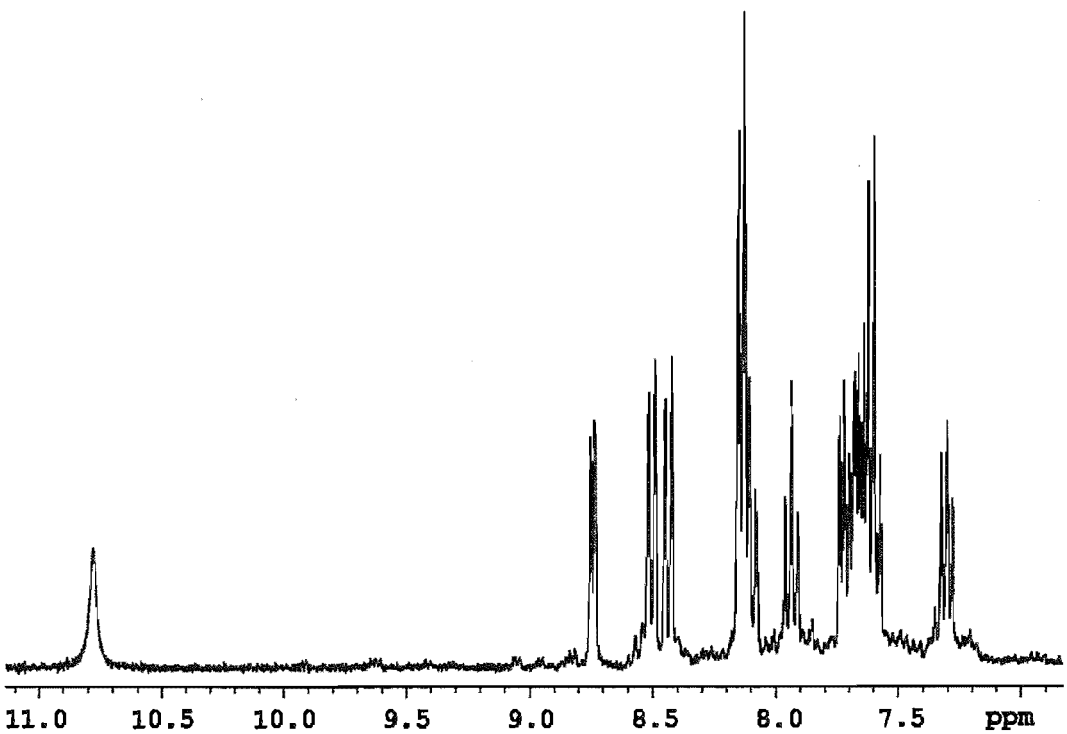

Fig. 4.34 ^1H NMR spectrum of the rearrangement product from the reaction of $Ru(bpy)_2^{2+}$ and ligand **59**.

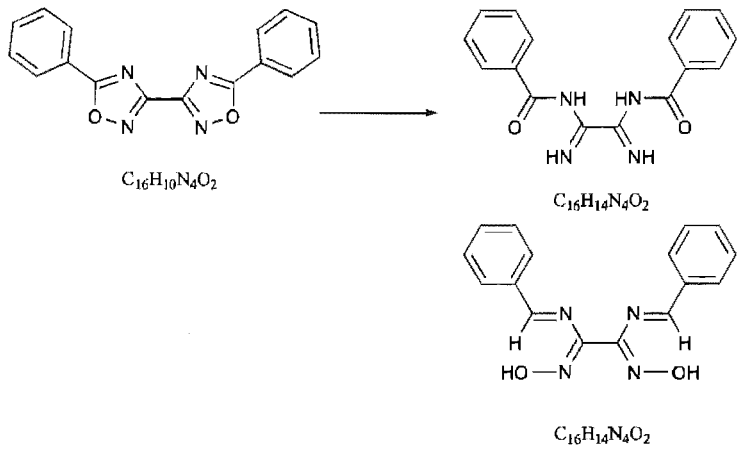

Fig. 4.35

It was at this stage that the precursors oxamidoxime, (OAO), and 2-picolylamidoxime, (PAO), (Fig. 4.10), were reacted with $Ru(bpy)_2Cl_2$ and $Ru(dmb)_2Cl_2$, respectively, under the standard 3:1 ethanol/water reaction conditions. This was done to study their behaviour under FABMS conditions, and to get an idea of the chemical shifts of the oxime and amine protons in the ^1H NMR spectrum. From the ^1H NMR spectra and from the elemental analyses of these complexes it was determined that chelating complexes had formed, and that they were both bis(hexafluorophosphate) salts. In the ^1H NMR spectra of both complexes, the oxime proton was not observed, which is in contrast to the spectra seen thus far. This was taken as more evidence that the downfield proton may be an amidine proton and not that of an oxime. Under the FAB mass spectral conditions the complex $[Ru(bpy)_2(OAO)](PF_6)_2$ gave the dominant molecular ion of $C_{22}H_{21}N_8O_2Ru^+$ ($[Ru(bpy)_2(OAO)]^+$ minus a proton) with again the only higher cluster being the addition of HPF_6. This is consistent with losing PF_6^- then HPF_6 from the neutral complex. The complex $[Ru(dmb)_2(PAO)](PF_6)_2$ also underwent the same loss of PF_6^- then HPF_6 in the mass spectrometer. Thus the behaviour of these complexes simulated that found for the ring opened products, lending support to the molecular formula determination above.

It was with some trepidation that the reactions with the other 1,2,4-oxadiazole ligands in the 3:1 ethanol/water reaction conditions were performed. The results of the reactions for ligands **62** and **63** in ethanol/water are conveniently and concisely summarised in Scheme 4.17. Neither of the 1,2,4-oxadiazole ligands was unchanged in these reactions. The decomposition products were characterised, and the technique of FABMS proved particularly useful for this purpose. The decomposition product of the ligands in these reactions was the same. The alternative reaction conditions were then used for the reaction of ligand **63**. However, ^1H NMR and FABMS showed the presence of the same decomposition product. The alternative conditions using the silver salt in acetone/ethanol were unsuitable for the reaction with **62** as this molecule has very low solubility in these solvents. As a last attempt, the conditions that had been used for the preparation of ruthenium complexes with the

triazole-based ligand **69**[145] (Fig. 4.9) were used for ligand **62**. This was unsuccessful as ^{1}H NMR spectroscopy and FABMS again identified the amidine decomposition product.

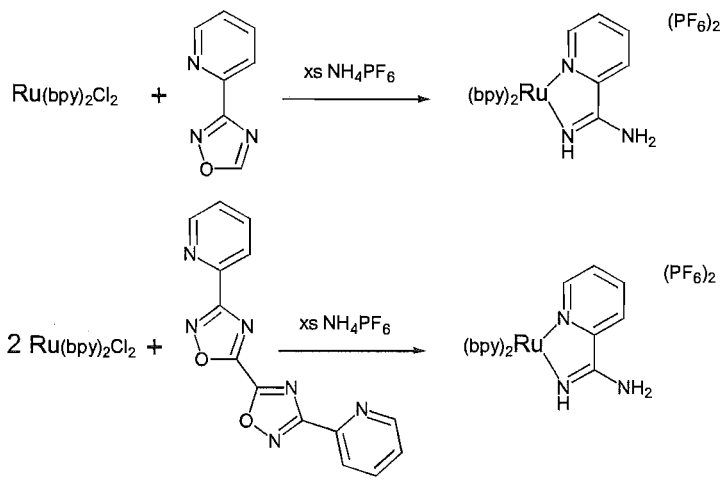

Scheme 4.17

The results for the reaction of $Ru(dmb)_2Cl_2$ with ligand **66** in ethanol/water were slightly more interesting in that the ligand had only ring-opened and not cleaved (Scheme 4.18). The reaction was repeated using the silver reaction conditions, and again ^{1}H NMR and FABMS identified that the same product had formed. Perhaps some stabilisation would be offered by dinucleation of the ligand, and therefore ligand **66** was reacted with two equivalents of $Ru(bpy)_2Cl_2$ in refluxing 3:1 ethanol/water. The product of this reaction, isolated as a hexafluorophosphate salt, was shown by FABMS to contain two $Ru(bpy)_2^{2+}$ units and was postulated to be the dinuclear complex shown in Scheme 4.18. The ^{1}H NMR spectrum of this material was very complicated. However, one piece of information could be gleaned from the spectrum; the presence of two signals in the downfield region corresponding to the NH protons is consistent with the formation of diastereoisomers.

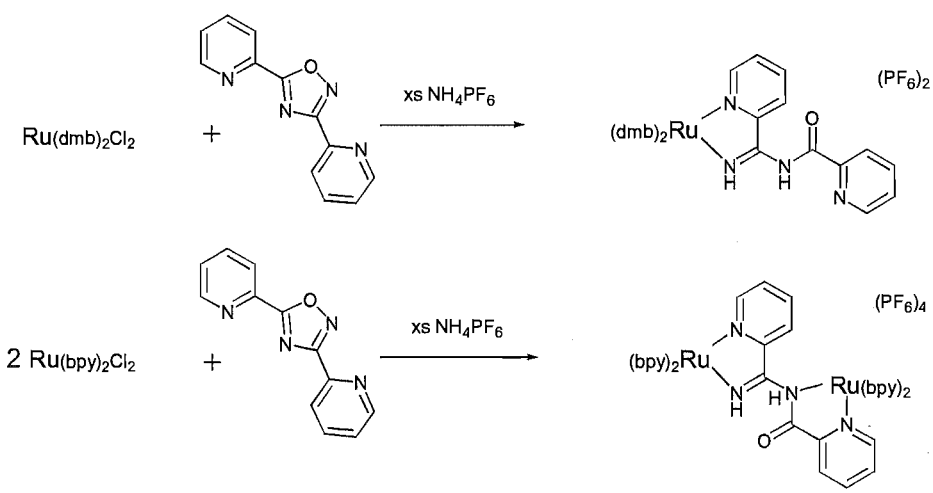

Scheme 4.18

The first ruthenium complex prepared with the thiadiazole ligand (**65**) was with $Ru(dmb)_2Cl_2$ in the 3:1 ethanol/water conditions. Pleasingly, characterisation by FABMS and elemental analysis revealed that a chelating complex, (**83**), had formed in an excellent yield of 96%. From the CIS values (Table 4.4), particularly the large upfield shift of H3', it was deduced that the thiadiazole ligand was chelating through N1,N4', as shown in Fig. 4.36. Of further note is the small positive CIS of H4. As the CIS of this proton reflects the σ-donor π-back-bonding trade off, the value of +0.10 would seem to indicate one of two things: either the pyridine is donating less to the metal or is accepting an unusually large amount of π-back donation.

Table 4.4 ^{1}H NMR Chemical Shifts[a] and Coordination Induced Shifts[b] for **83** and **65**.

	H3	H4	H5	H6	H3'
83	8.59	8.14	7.55	7.85	8.28
65	8.23	8.04	7.59	8.73	8.84
CIS	+0.36	+0.10	-0.04	-0.88	-0.56

[a] For deuterated acetonitrile solutions. [b] CIS = ($\delta_{complex}$ - δ_{ligand}).

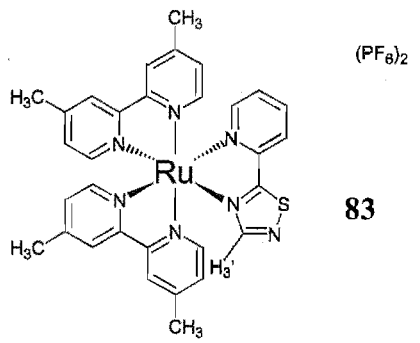

83

Fig. 4.36

The complex $[Ru(bpy)_2(\mathbf{65})](PF_6)_2$, (**84**), was prepared in the same manner as above and was characterised by FABMS and elemental analysis. The ^{1}H NMR spectrum of **84** is shown in Fig. 4.37. In previous complexes, *viz.* **13** and **35**, the cooperative use of 1-D TOCSY and ^{1}H nOe spectroscopy allowed the positive identification of the ligand of interest in the complexes. Because the thiadiazole proton points away from the pyridine ring of the ligand (Fig. 4.36), the strategy used previously is inappropriate. This only left the comparison of the CIS values of complex **83** to identify the pyridine ring of the thiadiazole-containing ligand in **84**. This made the identification of all the protons of the complex **84** important. Unfortunately, none of the identified spin systems in complex **83** gave a sufficiently good correlation to that of the pyridine ring of the thiadiazole ligand in complex **83** to be able to be assigned with certainty.

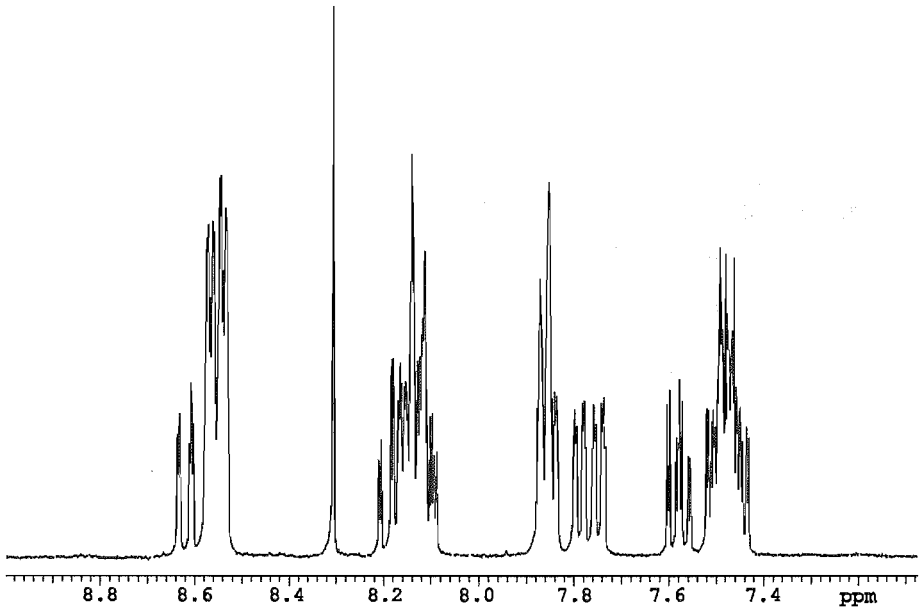

Fig. 4.37 ^{1}H NMR spectrum of [Ru(bpy)$_2$(**65**)](PF$_6$)$_2$ (**84**).

UV-visible spectroscopy and cyclic voltammetry were then used to investigate complexes **83** and **84**. The UV-visible spectrum and cyclic voltammogram of **84** are shown in Fig. 4.38, while the results of these studies are summarised in Table 4.5.

Table 4.5 Absorption Maxima[a] and Redox Potentials[b] of complexes **83** and **84**.

	λ_{max}	E_{ox}	E_{red1}	E_{red2}	E_{red3}	$\Delta E_{ox\text{-}red1}$
$Ru(bpy)_3^{2+}$	452	+1.26	-1.33	-1.51	-1.75	2.59
83	494	+1.18	-1.08	-1.69	-1.88	2.26
84	487	+1.29	-1.02	-1.58	-1.92	2.31

[a] In nanometers for acetonitrile solutions. [b] In volts *vs* SCE in acetonitrile.

When compared to $Ru(bpy)_3^{2+}$, the substitution of a single pyridine ring with a 1,2,4-thiadiazole has significantly changed the redox and electronic properties of the resulting complex. The thiadiazole-containing complexes **83** and **84** have their λ_{max} at longer wavelength, and the HOMO-LUMO energy gap has been considerably reduced, as evidenced by the smaller $E_{ox\text{-}red1}$ values for these complexes, as compared to $Ru(bpy)_3^{2+}$. The complex **83** is easier to oxidise than complex **84** by 110 mV. This is attributable to the well-known effect of replacement of bpy with dmb.[180] The electron donating effect from the methyl groups of the dmb ligands adds electron density to the metal, and this allows for easier oxidation (the removal of an electron) of the metal. The effect of adding a methyl group is to lower the oxidation potential by approximately 25 mV per group, and this is seen in complexes **83** and **84** as the complex **83** possesses 4 methyl groups (2 for each dmb ligand) and the oxidation potential is lowered by 110 mV.

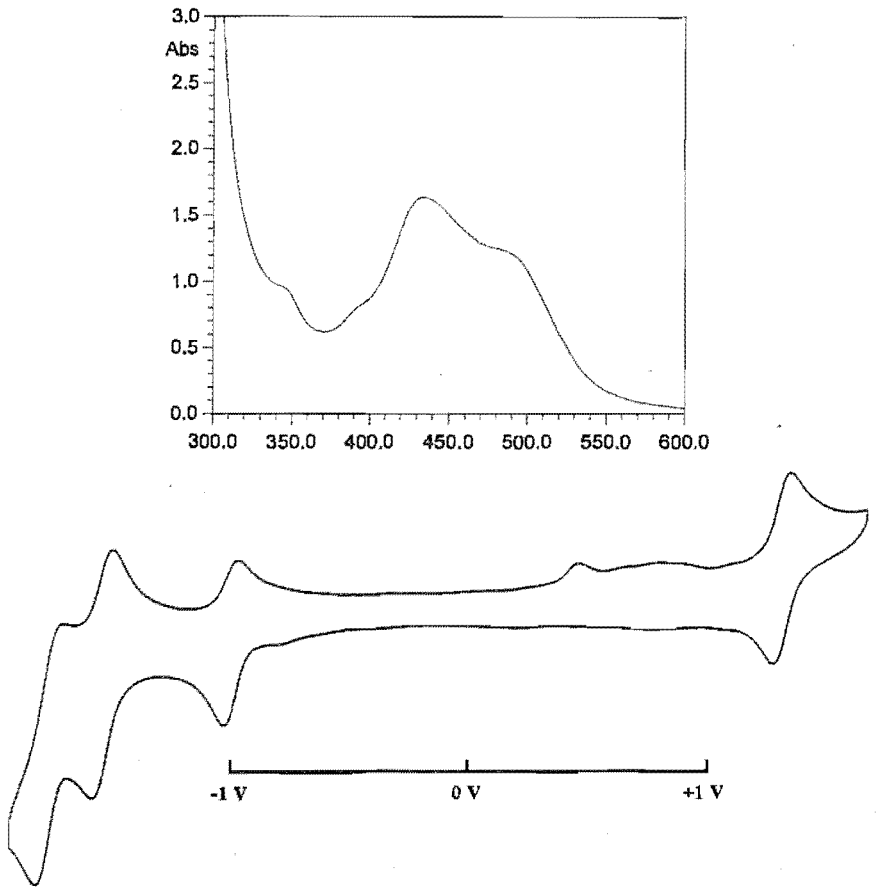

Fig. 4.38 UV-visible spectrum and cyclic voltammogram of $[Ru(bpy)_2(\mathbf{65})](PF_6)_2$ (**84**).

Given the disappointing results of the 1,2,4-oxadiazoles, it was decided to investigate another unexplored heterocyclic system. 1,4,2,5-Dioxadiazines have not been used as ligands. Despite being such an exotic ring system, 1,4,2,5-dioxadiazines are surprisingly easily constructed. De Sarlo[181] has synthesised 3,6-diaryl-1,4,2,5-dioxadiazines, in high yields, by the pyridine catalysed dimerisation of nitrile oxides. Given the interesting properties of dinuclear complexes containing 2,5-di(2-pyridyl)pyrazine, (**85**), and 3,6-di(2-pyridyl)tetrazine, [182-188] (**86**), we thought that by the replacement of CH by N and O, using a 1,4,2,5-dioxadiazine as the central six-membered ring (Fig. 4.39), this study could be systematically extended by employing the new ligand **87**.

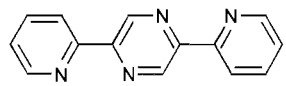

85

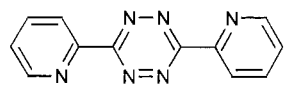

86

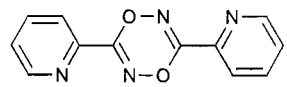

87

Fig. 4.39

To synthesise the desired ligand, the appropriate precursor needed to be prepared (Scheme 4.19). 2-Pyridinecarboxaldehyde was converted into the corresponding oxime by reaction with hydroxylamine, and treatment of the oxime with chlorine in chloroform solution gave the hydroximinolyl chloride as the hydrochloride salt in quantitative yield. Two equivalents of triethylamine and an excess of pyridine (4-5 equiv.) were added to an ethanolic solution of the hydrochloride salt. After work-up two products were identified in TLC, separated by chromatography and assigned by ^{1}H NMR. In subsequent preparations, separation and purification was achieved by simple recrystallisation to produce ligand **87** in modest yields of 55-60%. Characterisation of this new ligand was by melting point, ^{1}H and ^{13}C NMR spectroscopy, EIMS and elemental analysis.

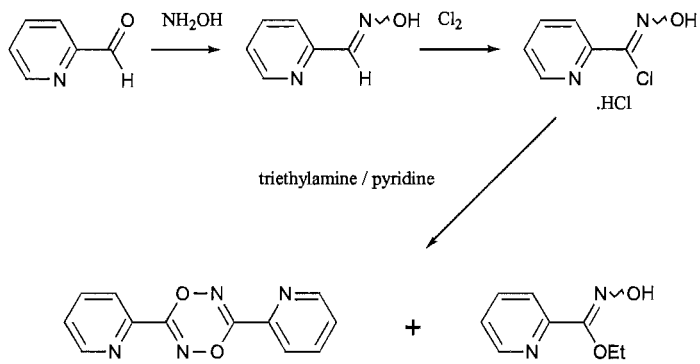

87

Scheme 4.19

As the dinuclear $Ru(bpy)_2^{2+}$ complex with this ligand would only contain 2-substituted pyridine rings, ligand **87** was reacted with two equivalents of $Ru(dmb)_2Cl_2$ under the standard 3:1 ethanol/water conditions. This would hopefully allow the ready identification of the pyridine rings of the ligand in the ^{1}H NMR spectrum. The cationic products of the reaction were collected as hexafluorophosphate salts and purified by chromatography on alumina. Two bands were separated on the column, and were analysed by ^{1}H NMR spectroscopy. This ascertained that they were different mononuclear complexes each containing five different

pyridine rings. In the first band, the sixth coordination site was ^{1}H NMR silent, while the second complex had a broad signal at *ca.* 6.5 ppm reminiscent of a NH_2 peak seen for the complexes isolated previously. The samples were then positively identified by FABMS as complexes containing picolinate and picolinamide (Scheme 4.20).

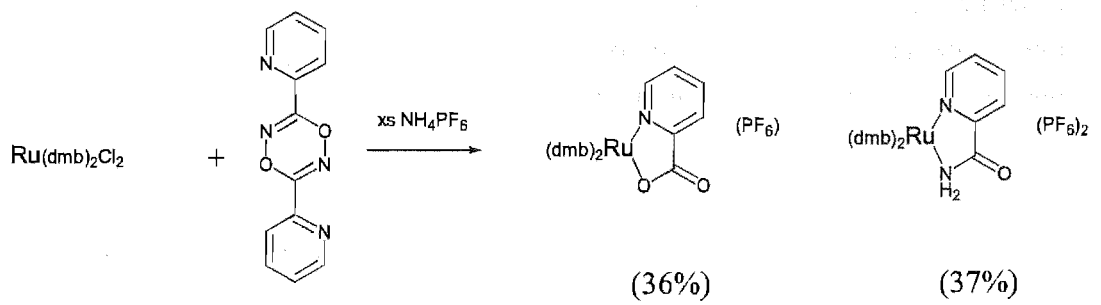

Scheme 4.20

In an attempt to see if this ligand was able to bridge two metal ions, ligand **87** was reacted with two equivalents of $CuCl_2.2H_2O$ in methanol. Upon addition, an immediate precipitate formed leaving a green solution, indicating that complete uptake of the metal ion was not achieved. The elemental analysis of the complex was not consistent with either a [1 + 1] or a [1 + 2] stoichiometry, but something in between, suggesting a mixture of the two complexes.

A silver nitrate complex was prepared in the same manner as previous silver complexes. The colourless complex analysed as [**87**.$AgNO_3$], (**89**), and formed in an excellent yield of 96%. Despite various attempts to recrystallise this complex to gain crystals suitable for an X-ray analysis no such crystals were grown.

4.4 Summary

In this chapter, the synthesis of a new 1,2,4-oxadiazole-containing ligand (**62**) was described, as well as improved syntheses of three previously reported ligands (**63**, **65** and **66**). Other attempts at the syntheses of desired ligands led to the discovery of a novel fused heterocyclic compound containing an imidazo[1,5-*a*]pyridine ring (**72**), and the formation of an unexpected 1,3,5-triazine-containing product from the reaction of thiopicolinamide and iodine. Other unsuccessful attempts at ligand preparations were also discussed.

The characterisation of the chelating palladium complexes prepared confirmed the preference for coordination of the N4 nitrogen over the N2 nitrogen in 3-substituted 1,2,4-oxadiazoles. Also the polymeric structure of the silver nitrate complex with 3,3'-bi-1,2,4-oxadiazole (**57**) was determined by X-ray crystallography. This structure too had coordination to the metal from the N4 atom.

Despite the favourable features that the 1,2,4-oxadiazole heterocyclic system offers, in retrospect it was an unfortunate choice, as it proved unsuitable for the construction of ruthenium complexes by the methods used in this work. Also, a number of complexes formed and characterised arose from decomposition of the 1,2,4-oxadiazole rings in the ligands. These included an acid induced ring opening and a product where, after decomposition, a subsequent reaction with solvent provided a chelating ligand. These both demonstrate the instability of this heterocyclic system. On the other hand, the 1,2,4-thiadiazole system, although more synthetically challenging, proved to be much more stable. A preliminary investigation into this system proved interesting. Electrochemically, the 1,2,4-thiadiazole ring brought the π^* energy level of ligand **65** to lower energy relative to bpy, resulting in a lower reduction potential of the ligand in the complex. Thus, in contrast to the unstable 1,2,4-oxadiazole system, the 1,2,4-thiadiazole ring is a useful component for incorporation into chelating ligands and has a significant effect upon the electronic properties of the resulting complexes.

A new, novel, 1,4,2,5-dioxadiazine ligand was successfully synthesised. Disappointingly, the brief exploration into the coordination chemistry of this system proved fruitless, with no crystal structures to determine if the dioxadiazine ring participates in coordination, and with the ligand cleaving under the 3:1 ethanol/water reaction conditions in the attempted preparation of a dinuclear ruthenium complex.

Chapter 5

1,2,5-Heterodiazoles

5.1 Introduction

This chapter deals with another isomer of the heterodiazoles. Again the ligands contain a five membered ring with three heteroatoms — two of which are nitrogen and the other either oxygen or sulfur. The ring system and ring numbering for a 1,2,5-system are shown in Fig. 5.1.

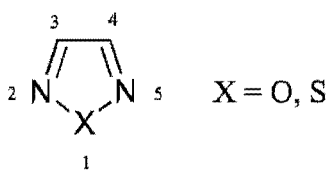

Fig. 5.1

The first point of consideration was, again, the rational design of chelating ligands containing these heterocycles that would allow a systematic study of mononuclear and dinuclear complexes. As in Chapter 4, linking other heterodiazoles or pyridines to the unsubstituted positions of a heterodiazole ring was chosen as the approach. The ligands for this study are 2-(1,2,5-oxadiazol-3-yl)pyridine (**90**), 3,4-di(2-pyridyl)-1,2,5-oxadiazole (**91**), 4,4'-di(2-pyridyl)-3,3'-bi-1,2,5-oxadiazole (**92**), 2-(1,2,5-thiadiazol-3-yl)pyridine (**93**), 3,4-di(2-pyridyl)-1,2,5-thiadiazole (**94**) and 4,4'-di(2-pyridyl)-3,3'-bi-1,2,5-thiadiazole (**95**) (Fig. 5.2).

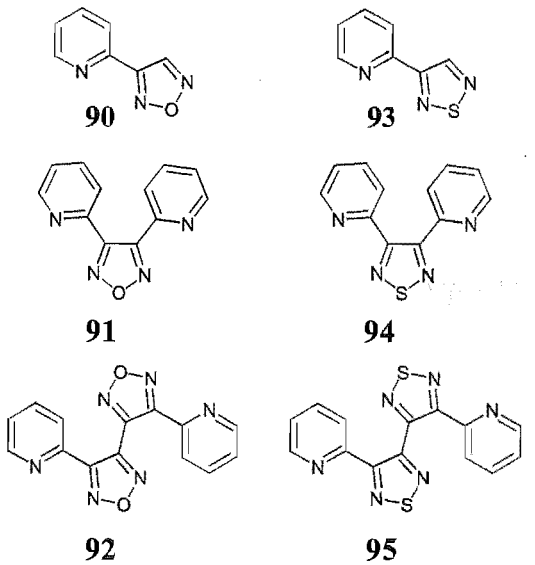

Fig. 5.2

Ligands **90** and **93** are the building blocks for these families of oxadiazoles and thiadiazoles. Extension through the 4-position of the heterodiazole, in each case by a pyridine, gives **91** and **94**, whereas **92** and **95** are the 'dimer' ligands of **90** and **93**. The preparation of mononuclear ruthenium complexes with **90** - **95** would provide a basis for comparison of the properties of the dinuclear complexes.

Ligands **91** and **94** have a structural similarity to 2,3-di(2-pyridyl)pyrazine, (**96**), and 4,6-di(2-pyridyl)pyrimidine, (**97**), (Fig. 5.3), both of which have been very well studied.[10,189] In dinuclear complexes involving ligand **96**, the pyridine rings of the ligand are kilted with respect to the central pyrazine ring because of the steric clash between the H3 protons of the pyridyl rings. This leads to disruption of overlap of the π-systems within the ligand. Even so, dinuclear ruthenium complexes of **96** exhibit metal-metal interactions (ΔEp 170 mV).[190] Ligand **97** is a sterically less demanding ligand than **96**. The pyridyl rings of the ligand are further separated, leading to reduced steric interaction, which is much better for the stability of dinuclear complexes. Ligand **97** also has a shorter metal-metal distance than **96** but, despite these favourable features, the metal-metal interaction in dinuclear ruthenium complexes of **97** is slightly less (ΔEp 160 mV).[191]

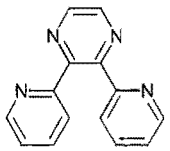

96

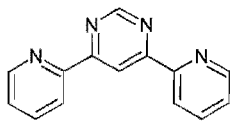

97

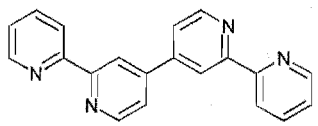

98

Fig. 5.3

Replacing the central six-membered diazine rings with a five-membered heterodiazole has some important consequences geometrically and electronically. Firstly, the angle across a five-membered ring is greater than that in a six-membered ring (72° *vs* 60°), and this fact should help reduce the steric interaction for the dinuclear complexes of **91** and **94** relative to those encountered in the dinuclear complexes with ligand **96**. Another favourable outcome of replacing the central six-membered ring with a five-membered ring is that the distance across the five-membered ring is less. This will result in the metal-metal distance being decreased relative to dinuclear complexes containing **96** and comparable to those containing **97**. Electronically, the diazines and the heterodiazoles are very different. The diazines are a class of π-deficient heterocycles while the heterodiazoles are π-excessive. This electronic difference is expected to impart significantly different properties to the dinuclear complexes of **91** and **94** relative to those of **96** and **97**.

In a similar fashion, binuclear complexes of **92** and **95** can be compared to the binuclear complexes of 2,2':4',4":2",2'"-quaterpyridine, (**98**) (Fig. 5.3), a ligand that facilitates weak, but detectable, metal-metal interactions.[76,192]

Previous studies of the coordination chemistry of 1,2,5-heterodiazoles have been mainly restricted to 2,1,3-benzothiadiazoles[193,194] and simple derivatives of them.[195,196] The studies of Munakata *et al.*[194] were investigations into potential metallopolymeric networks with simple 2,1,3-benzothiadiazoles and Cu(II) salts. A study by Kaim *et al.*[197] examined the properties of dinuclear molybdenum pentacarbonyl complexes bridged by 2,1,3-benzothiadiazole and 2,1,3-benzoselenadiazole rings.

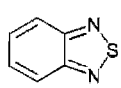

2,1,3-benzothiadiazole

The coordination chemistry of 1,2,5-oxadiazoles has been even less well investigated with only one report in the literature.[198] To summarise, all of the reported studies on the

1,2,5-heterodiazole systems have been of simple monocyclic ligands and not those capable of a chelating coordination mode. This is in contrast to the present study, where the aim was to study the electronic properties of these heterocycles in new chelating heterocyclic ligands.

This chapter describes the preparation and characterisation of four new ligands, as well as the attempted preparations of two other ligands. Also described is a metallosupramolecular complex with one of the ligand precursors, as well as an interesting, new, ring-opening ring-closing (RORC) reaction. Mononuclear ruthenium complexes, homodinuclear ruthenium complexes, heterodinuclear ruthenium-palladium and heterodinuclear ruthenium-platinum complexes are prepared, characterised and examined electrochemically.

5.2 Syntheses of Ligands

Two established methods for the synthesis of 1,2,5-oxadiazoles are the cyclodehydration of α-dioximes and the deoxygenation of 1,2,5-oxadiazole-2-oxides (Scheme 5.1).[199] Both of these synthetic procedures were employed in the syntheses of the 1,2,5-oxadiazole-containing ligands.

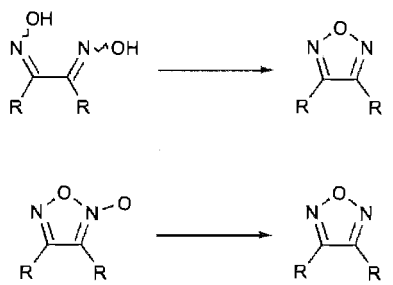

Scheme 5.1

To produce the ligand **90**, 2-acetylpyridine was first oximated by amyl nitrite in sodium ethoxide solution to give the desired oxime, and this was then reacted with hydroxylamine, based on a procedure for the phenyl analogue,[200] to give the α–dioxime in 17% overall yield for these two steps. Unfortunately, the α–dioxime was not cyclised with one equivalent of acetic anhydride as has been reported for the phenyl analogue.[201]

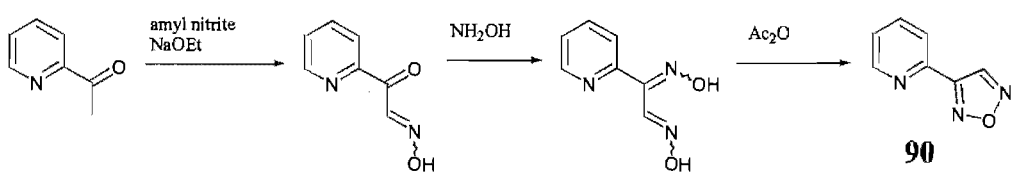

90

Scheme 5.2

Ligand **91** was produced in two steps starting from the commercially available 2,2'-pyridil, as shown in Scheme 5.3. An α-dioxime was prepared by reacting the diketone with an excess of aqueous hydroxylamine, and heating the dioxime at 185°C for 7 hours in a sealed tube effected cyclisation. The yields of the two reactions were 42% and 33%, respectively, giving an overall yield for the two steps of 14%. This new 1,2,5-oxadiazole-containing ligand was characterised by melting point, ^{1}H and ^{13}C NMR spectroscopy, EI mass spectrometry and elemental analysis.

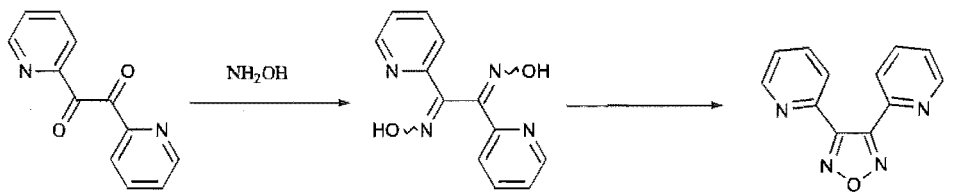

91

Scheme 5.3

A closely related molecule to **91** was also synthesised, originally with the intention of subsequent deoxygenation to give **91**. 3,4-Di(2-pyridyl)-1,2,5-oxadiazole-2-oxide, (**99**), is a known molecule[202] and was prepared by the literature procedure as shown in Scheme 5.4.

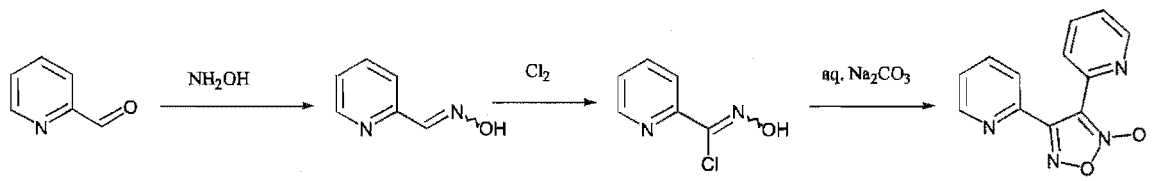

99

Scheme 5.4

Ligand **99** is also potentially capable of forming dinuclear complexes. It must, however, do so using two different donor sets, as shown in Figure 5.4. The chelate ring sizes would also be different in dinuclear complexes containing **99**. The N5-N1" chelate is five-membered, while the O2-N1' is six-membered. Complexes of this type have been little-studied, perhaps due to their intrinsically more complex nature. In this study, the mononuclear ruthenium complex of ligand **99** could be compared to the mononuclear complex of **91**, perhaps allowing some rationalisations about the nature of the 1,2,5-oxadiazole-2-oxide ring compared to the 1,2,5-oxadiazole ring.

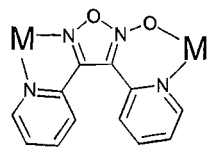

Fig. 5.4

Preparation of ligand **92** was based upon a procedure used for the diphenyl analogue,[203] and the method is summarised in Scheme 5.5. Bis(2-pyridoyl)-1,2,5-oxadiazole-2-oxide, (**100**), was synthesised according to the reported literature procedure starting from 2-acetylpyridine.[204] In the paper by Ponzio[203] a tin reduction was used to deoxygenate the 1,2,5-oxadiazole-2-oxide ring. This was found to be unsatisfactory for the present case, as only picolinic acid was recovered from the reaction. Deoxgenation of 1,2,5-oxadiazole-2-oxides has been accomplished by reaction with phosphites,[205,206,226] and this type of reaction was attempted for **100**. However, suitable conditions for this reaction were not found. When **100** was stirred in benzene at room temperature with one equivalent of triethyl phosphite under an atmosphere of nitrogen, the reaction solution turned dark brown. Analysis of the reaction mixture by TLC and ^{1}H NMR showed no sign of any change that would indicate the formation of a new product. When the reaction conditions were changed to refluxing benzene still no reaction occurred. This suggested that the reaction would need more forcing conditions. Deoxgenation of unstrained 1,2,5-oxadiazole-2-oxides has been effected by heating them in a neat solution of the phosphite,[207,208] and so **100** was refluxed in an excess of triethyl phosphite. This time TLC showed that all the starting material had been consumed in the reaction. However, no deoxygenated product could be isolated from the reaction mixture. One of the drawbacks of using an excess of phosphite is that further deoxygenation can occur. For instance, 1,2,5-oxadiazole-2-oxides can be converted to nitriles.[226] No further attempts were made to synthesise **92**.

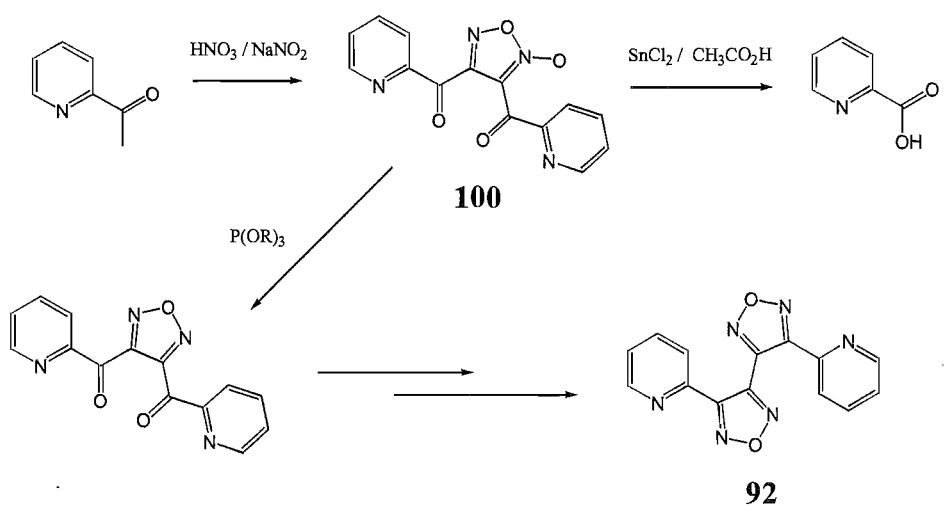

Scheme 5.5

1,2,5-Thiadiazoles are available *via* several methods of synthesis.[209] The most general of these has been the action of disulfur dichloride (S_2Cl_2) on α–diamines or dioximes.[210] Rees *et al.*[211] have recently provided a new method for the synthesis of 1,2,5-thiadiazoles based on reactions of the inorganic heterocycle trithiazyl trichloride ($S_3N_3Cl_3$) with alkenes and alkynes. This reaction is, as they have shown, applicable to a range of substrates.[212,213] Retrosynthetic analysis of the desired thiadiazole-containing ligands in Fig. 5.2 provided some easily accessible substrates (Fig. 5.5) for use in this type of reaction.

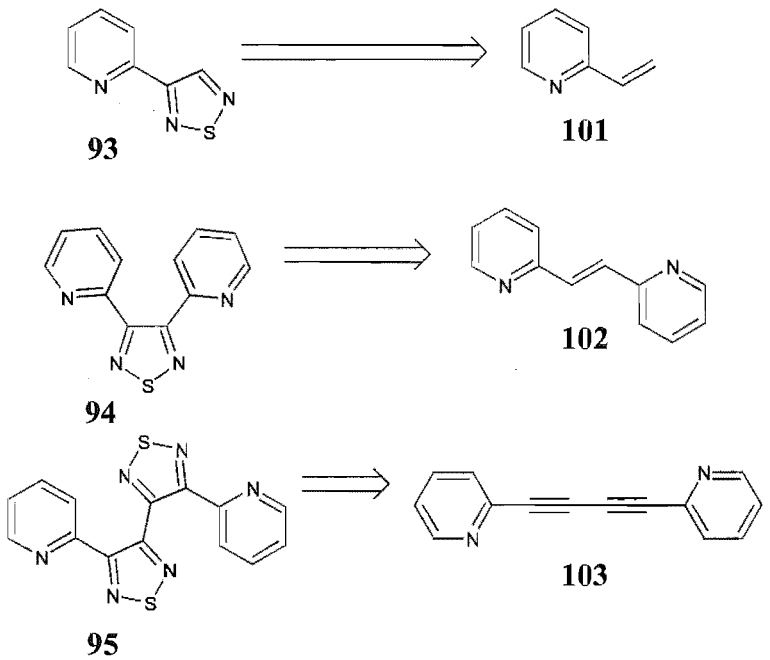

Fig. 5.5

The first substrate, 2-vinylpyridine (**101**) is commercially available and was purchased from Aldrich. 1,2-Di(2-pyridyl)ethene (**102**) was prepared by refluxing 2-methylpyridine with pyridine-2-carboxaldehyde in the presence of acetic anhydride as described by Newkome *et al.*[214] 1,4-Di(2-pyridyl)buta-1,3-diyne (**103**) is a known compound,[215] and was prepared, in this work, by a three-step sequence starting from 2-vinylpyridine. 2-Vinylpyridine was brominated then dehydrobrominated following a literature procedure,[216] to produce 2-ethynylpyridine, which was oxidatively coupled using $CuCl/O_2$ in acetone *via* the method described by Hay[217] to give **103** in 66% yield.

The reactions of **101** - **103** with $S_3N_3Cl_3$[218,219] were performed by a general method. $S_3N_3Cl_3$ was suspended or dissolved in dry toluene and added dropwise with stirring to the unsaturated substrate dissolved in a mixture of dry pyridine and dry toluene. The solutions turned green (dark red in the case of 2-vinylpyridine) and a precipitate generally formed. The mixture was set to reflux for a time before the reaction was stopped and the product isolated. Table 5.1 gives the reaction times and yields for these reactions.

Table 5.1

Substrate	$S_3N_3Cl_3$[a]	Reflux time[b]	Product	Yield(%)
101	1	4	**93**	43
102	1	18	**94**	49
103	2.5	7	**95**	17

[a] Molar equivalents. [b] In hours.

The yields of the thiadiazoles are only modest, but are comparable to the yields obtained by this method for similar substrates. As examples, N-vinylphthalimide reacts with $S_3N_3Cl_3$ to give 3-phthalimido-1,2,5-thiadiazole in 35% yield, 1,2-diphenylethene gave a 28% yield of thiadiazole and 1,4-diphenylbuta-1,3-diyne a 70% yield of bithiadiazole. However, this one-step procedure has significant advantages over alternative synthetic approaches to the ligands. No attempts at optimising these reactions were made. These new 1,2,5-thiadiazole-containing ligands were characterised by melting point, ^1H and ^{13}C NMR spectroscopy, EI mass spectrometry and elemental analysis.

As ligand **95** contains a bi-1,2,5-thiadiazol-3-yl subunit, we decided to study the conformation of this molecule in the solid state by X-ray diffraction, thereby extending the small study of the biheterocyclic species produced in the course of this work. Suitable crystals were grown for this study by slow evaporation of an ethanol solution of the compound. The structure is shown in Fig. 5.6a.

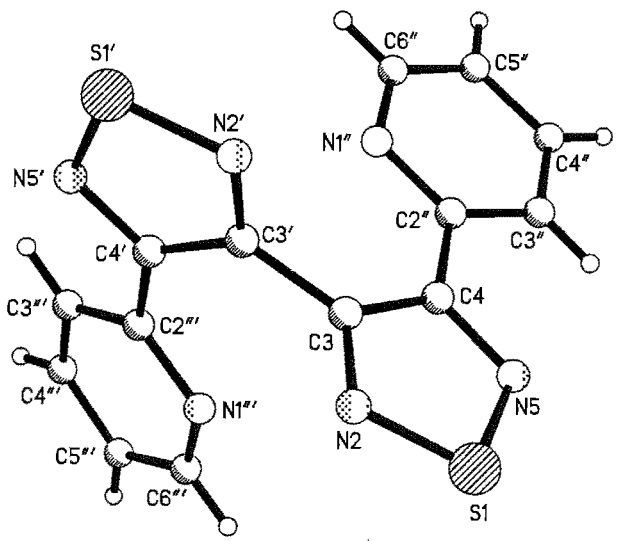

Fig. 5.6a Perspective view, with atom labelling of the contents of the asymmetric unit, of **95**.

Although a full set of data was collected the refinement did not converge to an acceptable R-factor (10.5%). Subsequently, it was found that the data collected for this structure was affected by a fault in the CCD area detector. A crystal will be resubjected to a

structural analysis when the area detector is restored to full working order. For the time being, a discussion of the structure is given without analysis of the bond length parameters.

The ligand crystallises in the triclinic space group P-1, with one full molecule in the asymmetric unit. Interestingly, the 1,2,5-thiadiazole rings are approximately orthogonal to each other [84.6°], leading to the ligand being split into two different halves at the inter-ring bond separating these rings. For one half, the thiadiazole (S1-N5) and its pyridine ring (N1"-C6") are coplanar, while for the other half there exists a twist of the pyridine away from the plane of the thiadiazole [17.8°] (Fig. 5.6b). The conformation of each thiadiazole ring and its pyridine is *trans* with respect to the nitrogen atoms. This is perhaps as a result of an intramolecular hydrogen-bonding interaction between the H3 proton of the pyridine ring and N5 of the thiadiazole. There is conjugation of the π-systems over each coplanar unit, but this does not extend over the whole molecule, due to the non-planarity of the central biheterocyclic subunit. The angle of 84.6° between the thiadiazole rings is reminiscent of the angle between the benzotriazole rings [84.5(5)°] found in the crystallographic study of 1,1'-bibenzotriazole (**23**) (Fig. 3.6a-c).

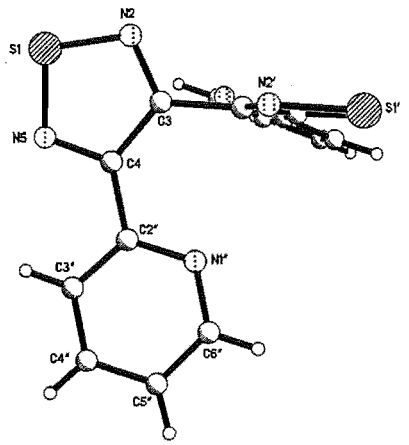

Fig. 5.6b

As an aside, it was realised that **103** had not been previously used as a ligand. However, its isomer 1,4-di(4-pyridyl)buta-1,3-diyne has been well studied. It displays interesting coordination chemistry having been used in the construction of molecular frameworks, such as criss-cross grids[220] and molecular ladders,[221] where it acts as a linear bridge between metal centres separating them by *ca.* 17Å.

It was therefore decided to explore the coordination chemistry of ligand **103** with $AgNO_3$. Reaction of **103** with $AgNO_3$ in methanol gave a fawn coloured solid, in good yield (83%), that analysed as [**103**.$AgNO_3$], (**104**). In order to distinguish between various cyclic or polymeric structures that are possible with this stoichiometry, an X-ray structure analysis was carried out. Crystals suitable for an investigation were grown by slow evaporation of an

acetonitrile solution of this complex. The asymmetric unit and a view of the extended structure are shown in Fig. 5.7a and 5.7b, respectively.

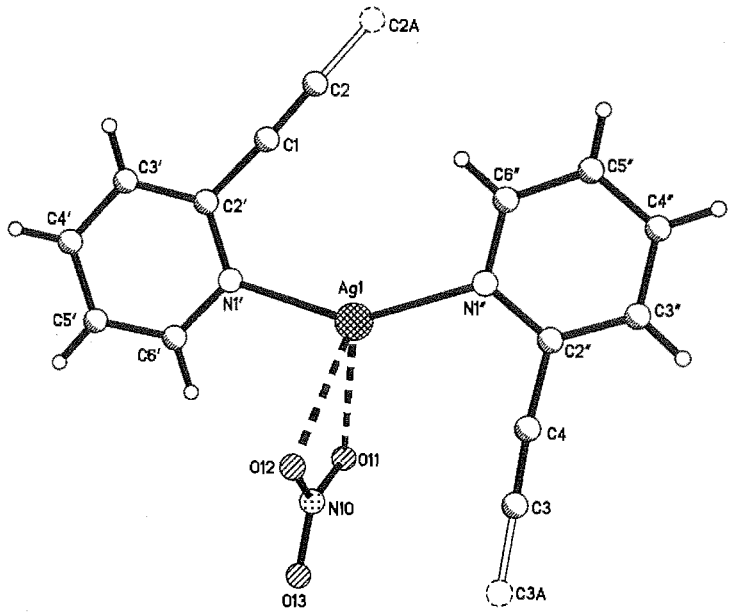

Fig. 5.7a Perspective view, with atom labelling of the contents of the asymmetric unit, of **104**. Selected bond lengths (Å) and angles (°): Ag1-N1' 2.246(2), Ag1-N1" 2.203(2), Ag1-O11 2.642(2), Ag1-O12 2.570(2), N1'-Ag1-N1" 146.17(6), C2'-C1 1.438(3), C1-C2 1.202(3), C2-C2A 1.386(4), C2'-C1-C2 176.5(2), C1-C2-C2A 178.4(3), C2"-C4 1.429(3), C4-C3 1.207(3), C3-C3A 1.364(4), C2"-C4-C3 172.4(2), C4-C3-C3A 178.4(3).

The asymmetric unit comprises a silver atom coordinated to two different half ligands and a weakly chelating nitrate anion. The geometry of one of the ligands is very similar to that of the free ligand,[222] while the other deviates from linearity at C4 [C2"-C4-C3 172.4(2)°]. By virtue of the crystallographic centres of inversion, the two pyridine rings of each ligand are strictly coplanar and have the nitrogens disposed in a transoid conformation. Within this structure the two independent ligands bridge silver atoms with separations of 8.832(1) and 8.666(1)Å, distances approximately half of those found with the isomeric ligand 1,4-di(4-pyridyl)buta-1,3-diyne. The whole structural motif bears a close resemblance to that recently described for a silver(I) complex of 2,2'-dicyanodiphenylacetylene.[223]

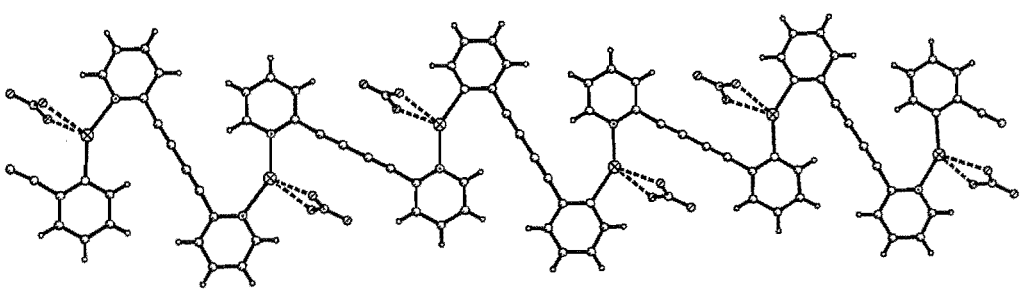

Fig. 5.7b Perspective view of the extended structure of **104**.

5.3 Mononuclear Complexes

The focus of this study is to examine the properties of complexes containing a 1,2,5-heterodiazole ligand and also to study dinuclear complexes containing ruthenium polypyridyl units bridged by a 1,2,5-heterodiazole ring. The properties of dinuclear complexes are best determined by comparison with their mononuclear complexes. It is, therefore, important to study the mononuclear complexes, and understand their properties before attempting to study and rationalise the interactions in dinuclear complexes. To this end, mononuclear complexes with **93**, **91**, and **94** were first prepared and examined.

Ligand **93** and one equivalent of $Ru(bpy)_2Cl_2$ were reacted in refluxing 3:1 ethanol/water and the cationic products isolated as hexafluorophosphate salts. Purification of the resulting dark red product, by chromatography on alumina, separated a small head band before a larger reddy-brown fraction. FABMS confirmed the small head band was a complex containing a chloride anion and the ligand, and so, was formulated as $[Ru(bpy)_2Cl(\mathbf{93})](PF_6)$ (**107**). Characterisation of this complex by ^1H NMR was attempted, but the complex underwent decomposition in solution with the ligand undergoing dissociation. Some information about the nature of the complex was able to be determined before decomposition. The signal for the thiadiazole proton was easily recognised in the spectrum by its chemical shift and singlet appearance. Interestingly, it appeared at 8.69 ppm in the spectrum, a CIS value (CIS = $\delta_{complex}$ - δ_{ligand}) of -0.67 ppm, meaning it has shifted upfield upon complexation. The most likely explanation for this observed CIS is that H4' is experiencing some shielding from ring-current anisotropy. Coordination *via* N5 of the thiadiazole, with the H4' proton facing towards a neighbouring pyridine, would have this effect (Fig. 5.8).

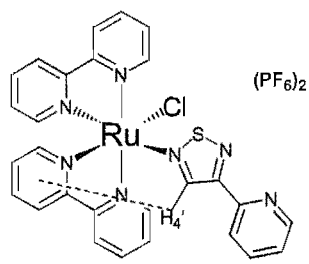

107

Fig. 5.8

The second fraction collected was the desired $[Ru(bpy)_2(\mathbf{93})](PF_6)_2$ complex (**108**). The ^1H NMR spectrum of **108** is shown in Fig. 5.9. The H4' of the ligand is easily assigned to the singlet at 9.55 ppm, giving a CIS (CIS = $\delta_{complex}$ - δ_{ligand}) of +0.29 ppm, meaning it has moved downfield upon complexation. However, this is the only signal easily assigned as the other spectral signals are highly overlapped, with the only separation in chemical shifts being the H6's of the pyridyl rings at around 7.8 ppm. Even then, some of these signals are partially

overlapped or not very well separated. Nevertheless, using careful 1-D TOCSY the assignment of signals to 4 of the 5 different pyridyl rings in this complex was achieved. This example nicely demonstrates the true power of the 1-D TOCSY experiment. With a spectrum such as this, a technique such as ^{1}H-^{1}H COSY would have been almost useless, as the mass of overlapped signals would have made the extraction of information from a spectrum very difficult indeed.

In previous examples (*viz.* **13** and **35**), the cooperative use of 1-D TOCSY and ^{1}H nOe spectroscopy allowed the positive identification of the signals due to the pyridine ring of the ligand of interest. This strategy was again used in this case. A ^{1}H nOe experiment irradiating H4' was performed and an enhancement found at 8.61 ppm. However, two H3 protons, previously identified by the 1-D TOCSY, were found to be at the same chemical shift as this enhancement. With this result, the positive identification of the signals due to the pyridine ring of the thiadiazole ligand was not possible.

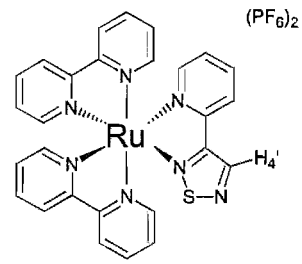

108

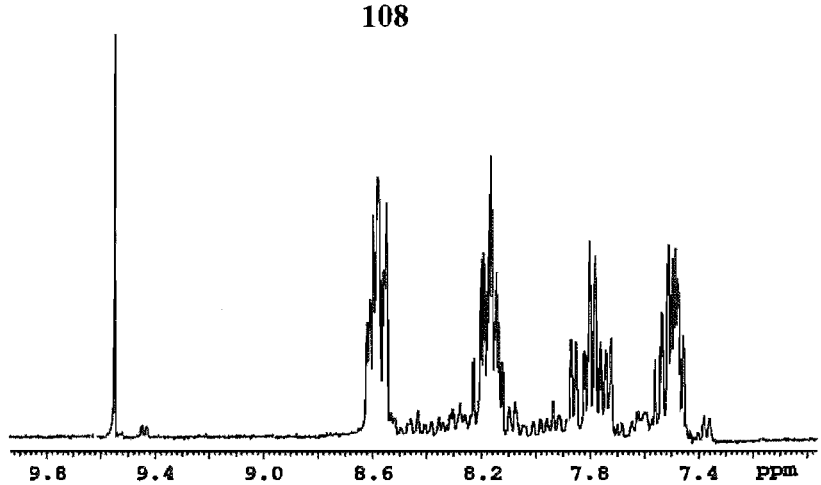

Fig. 5.9 ^{1}H NMR spectrum of $[Ru(bpy)_2(\mathbf{93})](PF_6)_2$ (**108**).

Ligand **91** and one equivalent of $Ru(bpy)_2Cl_2$ were reacted in 3:1 ethanol/water to give an orange complex, (**109**), in high yield (92%), which was isolated as the hexafluorophosphate salt. The ^{1}H NMR spectrum of complex **109** is shown in Fig. 5.10. By 1-D TOCSY six different rings were identified in the complex, and it was deduced that the ligand is chelating through the nitrogen of a pyridine ring and N2 of the oxadiazole. Hence, the ligand has an uncoordinated pyridine ring (Fig. 5.11). Unlike the other H6 protons, the H6 of the uncoordinated ring (H6') experiences no ring-current anisotropy effects and is very

much downfield of the others at the chemical shift of 9.03 ppm. The other distinctive proton in the spectrum is at 9.86 ppm and is assigned as H3 of the coordinated pyridine ring of the oxadiazole-containing ligand. This assignment was based upon the assumption that the pyridine nitrogen of the uncoordinated ring deshields this proton. Therefore, the conformation in solution is one where the uncoordinated ring lies in the same plane as the chelate ring with the nitrogen atom pointing towards H3 of the coordinated ring (Fig. 5.11). Confirmation that these were indeed the rings of the oxadiazole-containing ligand was by the preparation of the analogous $[Ru(dmb)_2(\mathbf{91})](PF_6)_2$ complex, (**110**). The chemical shifts and coordination induced shifts for **109** and **110** are listed in Table 5.2. Both of these complexes were also characterised by FABMS and elemental analysis.

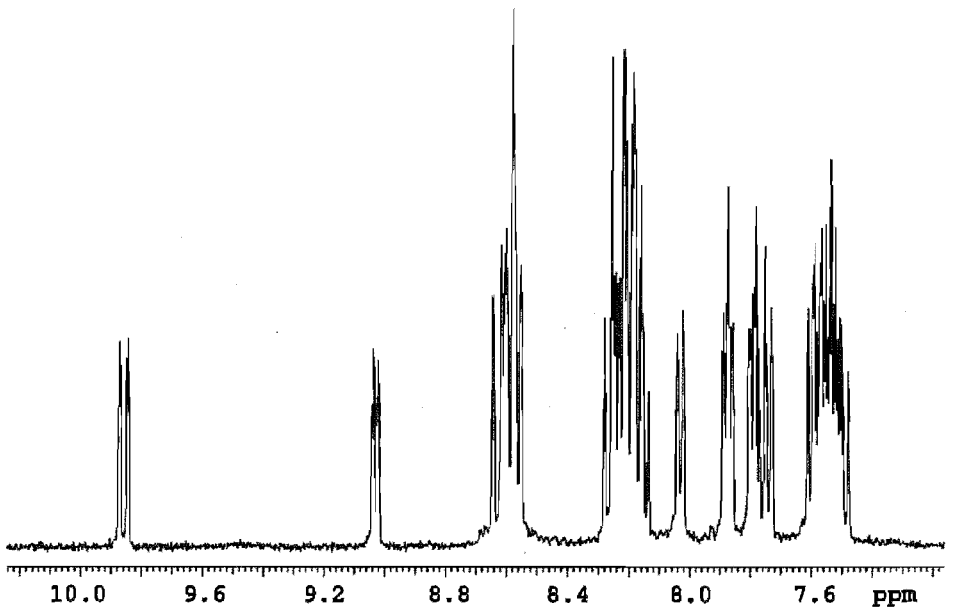

Fig. 5.10 ^{1}H NMR spectrum of $[Ru(bpy)_2(\mathbf{91})](PF_6)_2$ (**109**).

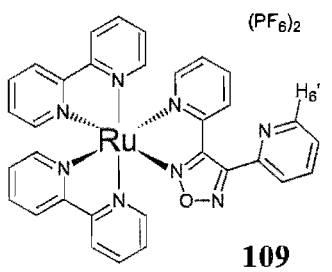

109

Fig. 5.11

Table 5.2 ^{1}H NMR Chemical Shifts[a] and Coordination Induced Shifts[b] of **91**, **109** and **110**.

	H3	H4	H5	H6	H3'	H4'	H5'	H6'
109	9.86	8.22	7.59	7.88	8.27	8.16	7.76	9.03
91[c]	7.91	7.97	7.53	8.60				
CIS	+1.95	+0.25	+0.06	-0.72	+0.36	+0.19	+0.24	+0.43
110	9.80	8.17	7.56	7.85	8.25	8.18	7.76	9.02
91[c]	7.91	7.97	7.53	8.60				
CIS	+1.89	+0.20	+0.03	-0.75	+0.34	+0.21	+0.23	+0.42

[a] For deuterated acetonitrile solutions. [b] CIS = ($\delta_{complex}$ - δ_{ligand}). [c] The free ligand in solution shows 2-fold symmetry; hence H3 = H3' etc.

[Ru(bpy)$_2$(**94**)](PF$_6$)$_2$, (**111**), was prepared, in high yield (87%), by reaction of ligand **94** with one equivalent of Ru(bpy)$_2$Cl$_2$, as described for the previous complexes. Again by 1-D TOCSY, identification and assignment of the six different rings was possible. Those of the thiadiazole-containing ligand were easily assigned by the now recognisable chemical shifts of the H6' proton of the uncoordinated ring and the deshielded H3 of the coordinated ring. The ^{1}H NMR data for this complex are shown in Table 5.3.

Table 5.3 ^{1}H NMR Chemical Shifts[a] and Coordination Induced Shifts[b] of **94** and **111**.

	H3	H4	H5	H6	H3'	H4'	H5'	H6'
111	9.02	8.03	7.49	7.86	8.09	8.12	7.74	8.90
94[c]	7.82	7.91	7.43	8.47				
CIS	+1.20	+0.12	+0.06	-0.61	+0.27	+0.21	+0.31	+0.43

[a] For deuterated acetonitrile solutions. [b] CIS = ($\delta_{complex}$ - δ_{ligand}). [c] The free ligand in solution shows 2-fold symmetry; hence H3 = H3' etc.

The UV-visible spectra of **109** (Fig. 5.12) and **110** were, as expected, very similar in appearance. The λ_{max} for each of these complexes is centred at *ca.* 435 nm with shoulders on the high energy side around 400 nm.

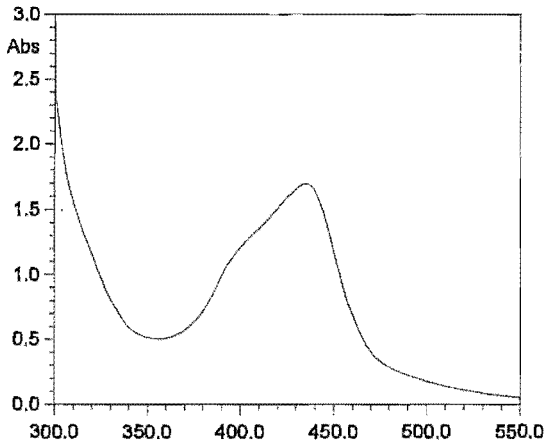

Fig. 5.12 UV-visible spectrum of $[Ru(bpy)_2(\mathbf{91})](PF_6)_2$ (**109**).

Each of the mononuclear complexes **108** - **111** were investigated by cyclic voltammetry, and the results of these investigations are summarised in Table 5.4, while Fig. 5.13 shows the cyclic voltammograms of complex **109** and complex **111**. Table 5.4 also includes the redox potentials and absorption maxima of the 2,3-di(2-pyridyl)pyrazine (**96**) and 4,6-di(2-pyridyl)pyrimidine (**97**) $Ru(bpy)_2^{2+}$ complexes for the sake of comparison.

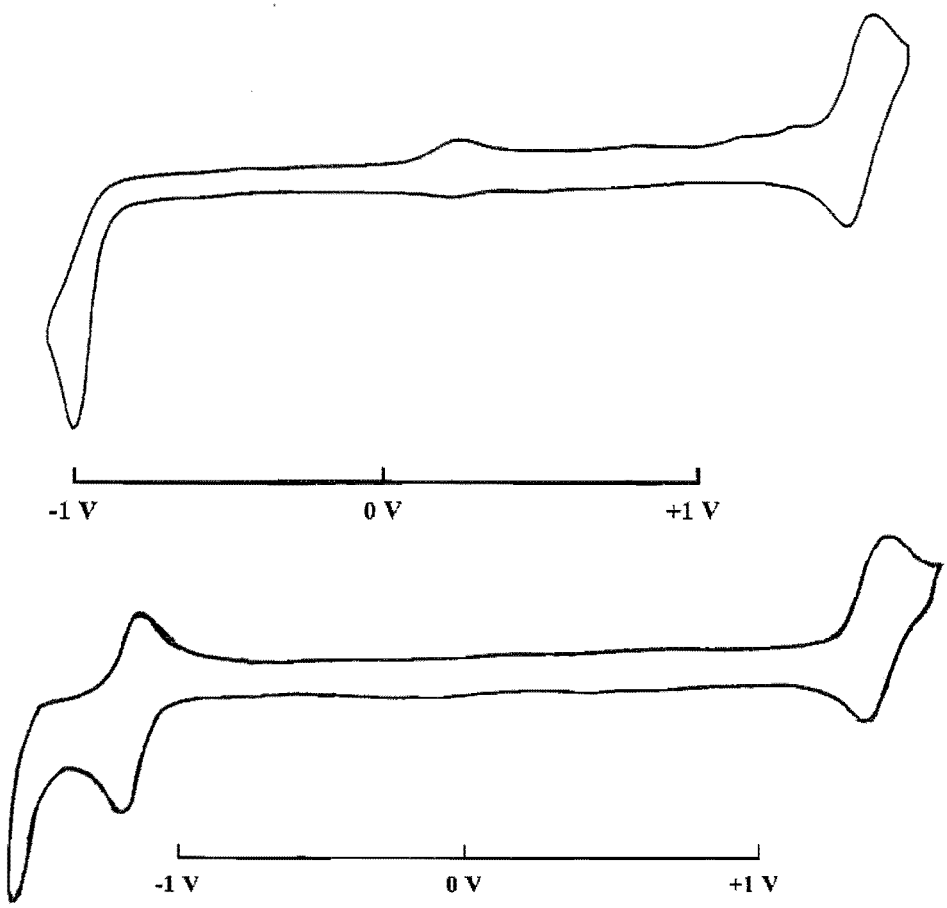

Fig. 5.13 Cyclic voltammograms of $[Ru(bpy)_2(\mathbf{91})](PF_6)_2$ (**109**) (top) and $[Ru(bpy)_2(\mathbf{94})](PF_6)_2$ (**111**).

Table 5.4 Absorption Maxima[a] and Redox Potentials[b] of **108**, **109**, **110** and **111**.

	λ_{max}	E_{ox}	E_{red1}	E_{red2}	E_{red3}	$E_{ox\text{-}red1}$
$Ru(bpy)_2(\mathbf{91})^{2+}$ (**109**)	435	1.51	-0.97[c]	-	-	2.48
$Ru(dmb)_2(\mathbf{91})^{2+}$ (**110**)	434	1.40	-1.08[c]	-	-	2.48
$Ru(bpy)(\mathbf{93})^{2+}$ (**108**)	455	1.36	-1.19	-1.55[c]	-	2.55
$Ru(bpy)_2(\mathbf{94})^{2+}$ (**111**)	454	1.37	-1.18	-1.53[c]	-	2.55
$Ru(bpy)_2(\mathbf{96})^{2+}$	492	1.28	-1.03	-1.55	-1.76	2.31
$Ru(bpy)_2(\mathbf{97})^{2+}$	475	1.31	-1.06	-1.55	-1.74	2.37

[a] In nanometers. [b] In volts *vs* SCE in acetonitrile. [c] Irreversible reduction.

The oxadiazole-containing complexes **109** and **110** show an excellent correlation between the UV-visible spectroscopy and the electrochemistry. The reason for the higher oxidation potential of the complex **109**, compared to the oxidation potential of complex **110**, is the well-documented effect of replacement of bpy with dmb as discussed in Chapter 4.[180] However, even with this difference the $\Delta E_{ox\text{-}red1}$ value is the same for each complex, which is consistent with the λ_{max} values. Both **109** and **110** have an irreversible first reduction which, based upon the potential, is assigned to the oxadiazole ligand.

Comparison of the UV-visible and electrochemical properties of the thiadiazole-containing complexes **108** and **111**, reveals that replacement of ligand **93**, which is unsubstituted at the 4-position of the thiadiazole, with the ligand **94** has little or no effect on the UV-visible or electrochemical properties of the complex. Again, the UV-visible and electrochemical data are totally consistent.

The heterodiazole-containing complexes **108**, **109**, **110** and **111** have larger HOMO-LUMO gaps than the pyrazine- and pyrimidine-containing complexes. This mainly arises because the heterodiazole complexes are harder to oxidise. The electronegative oxygen atom in complexes **109** and **110** acts to reduce the electron density of the ruthenium atom, raising the oxidation potential of the complex. The explanation for the lower oxidation potential for complexes **108** and **111** is that the sulfur is not as electronegative as oxygen, and does not reduce the electron density of the metal as much, and so these complexes are easier to oxidise.

An important electrochemical difference between the 1,2,5-systems is the reversibility of the first reductions. We thought the difference might possibly lie in the molecular orbitals concerned for the different systems. It was thought that some explanation might be forwarded by the examination of the heterodiazole systems, as they were assumed to be primarily responsible for the observed properties of the complexes. In an attempt to understand this problem, the use of *ab initio* calculations was turned to. As a first approximation Extended Hückel Molecular Orbital (EHMO) calculations[224] were performed for the parent heterocyclic systems. The results indicated that the HOMO of the 1,2,5-oxadiazole ring is a σ-bonding

orbital and the LUMO an antibonding π orbital (Fig. 5.14). Reduction of the 1,2,5-oxadiazole ring involves adding an electron to this antibonding orbital, which perhaps explains the irreversibility of this system. It is natural to then ask why the reductions are reversible for the 1,2,5-thiadiazole system. The EHMO calculations for this ring indicate that the HOMO is again σ-bonding and the LUMO π-antibonding but, importantly, the LUMO resides almost totally on the sulfur atom alone (Fig. 5.15). Possibly, the electrochemically added electron resides principally upon the sulfur atom, and can be reversibly removed from it in these complexes.

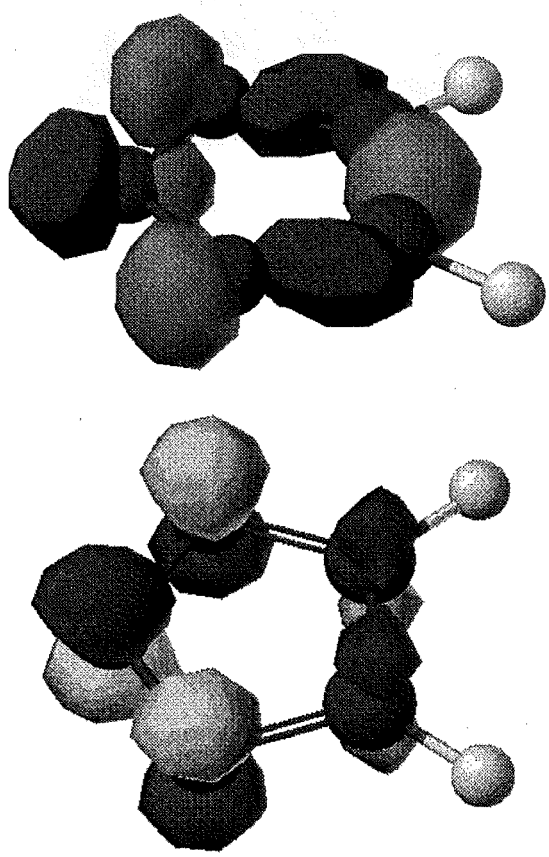

Fig. 5.14 HOMO (top) and LUMO (bottom) molecular orbitals of the parent 1,2,5-oxadiazole ring.

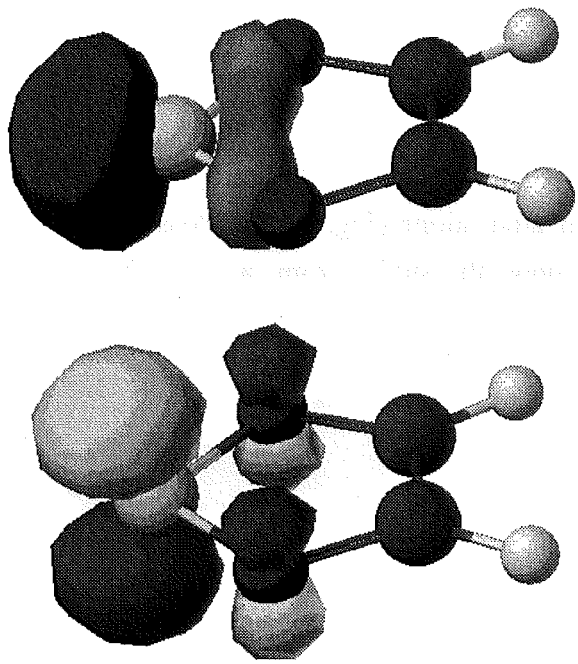

Fig. 5.15 HOMO (top) and LUMO (bottom) molecular orbitals of the parent 1,2,5-thiadiazole ring.

There have been few *ab initio* studies on these types of compounds. A recent study[225] determined that the 1,2,5-oxadiazole system was the least delocalised of the isomeric oxadiazoles, and postulated that the electronegative oxygen atom prevents the electrons in its p_Z orbital from interacting effectively with the rest of the π electron system of the ring. Thus, it seems the 1,2,5-oxadiazole system has a high diene character. Perhaps it can be expected that the thiadiazoles are more 'aromatic' than oxadiazoles, in the same way that thiophene is more aromatic than furan.

At this point, it seemed appropriate to prepare homoleptic ruthenium complexes using ligands **91** and **94**. This might allow for more insight into the electronic nature of the heterocycles. With three symmetrical bidentate ligands coordinated to a single metal ion, there exists only two enantiomeric forms, Λ and Δ. When the ligand is unsymmetrical, the formation of meridional (mer) and facial (fac) diastereoisomers are possible. This is shown in Fig. 5.16 where A and B represent different ends of the same ligand. Typically, in the preparation of homoleptic complexes with unsymmetrical ligands, the mer- and fac- isomers form in a statistical ratio of 3:1.

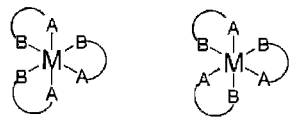

mer- fac-

Fig. 5.16

Ligands **91** and **94** were reacted with $Ru(DMSO)_4Cl_2$ in 3:1 ethanol/water. The desired homoleptic complexes, $[Ru(\mathbf{94})_3](PF_6)_2$, (**112**) and $[Ru(\mathbf{91})_3](PF_6)_2$, (**113**), were isolated and purified *via* the usual procedures. The ^1H NMR spectrum of **112** is shown in Fig. 5.17, and, from the appearance of the two separated H6 signals at 7.86 ppm and 8.00 ppm, the isomers have not formed in the 3:1 ratio. No attempts to assign the spectrum were made. As the H3 protons of the coordinated pyridine rings are downfield (*ca.* 8.9 ppm) it seems that the same phenomenon of deshielding that was evidenced in the ^1H NMR identification of $[Ru(bpy)_2(\mathbf{94})](PF_6)_2$ (**111**) is also present for each of the ligands in the complex **112**. Thus it exists in solution in the conformation shown in Fig. 5.18. Complex **112** was further characterised by FABMS and elemental analysis. The ^1H NMR spectrum of **113** was too complicated to assign totally, but it did have some signals that indicated the formation of the mer- and fac- isomers in a 3:1 ratio. These signals were from the deshielded H3 protons of the coordinated pyridine rings. Complex **113** was also characterised by FABMS.

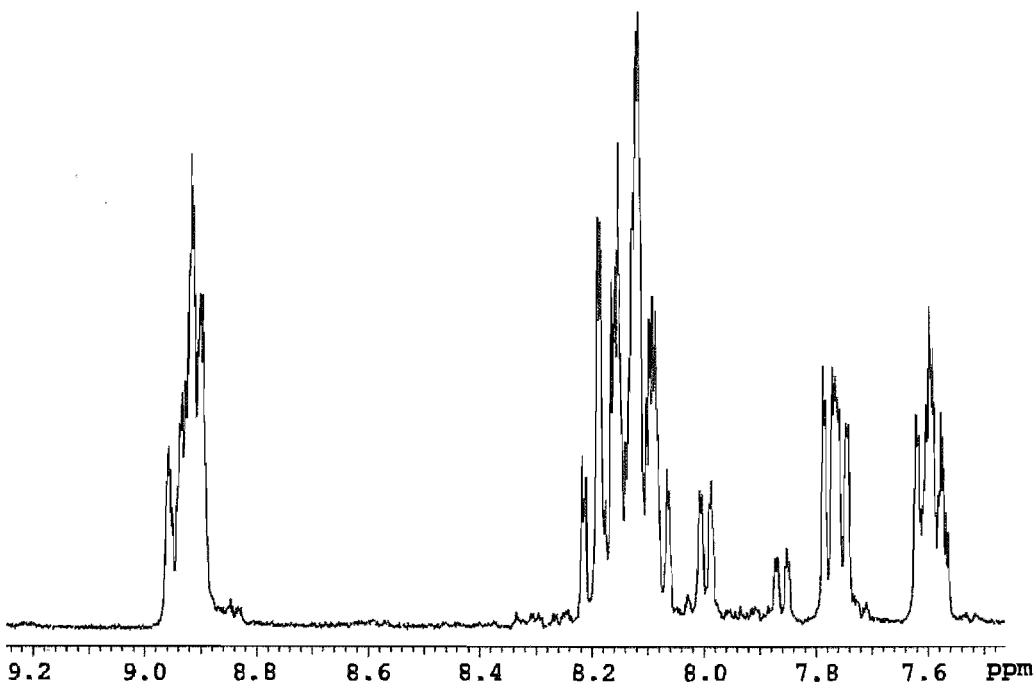

Fig. 5.17 ^1H NMR spectrum of $[Ru(\mathbf{94})_3](PF_6)_2$ (**112**).

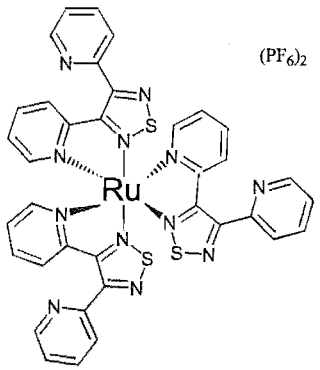

mer-112

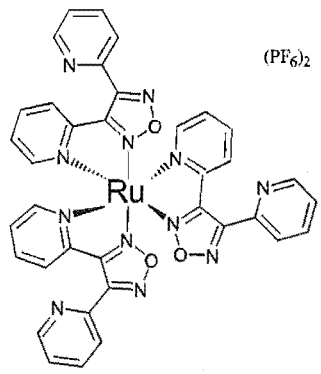

mer-113

Fig. 5.18

To probe the nature of the metal-ligand interactions in these homoleptic ruthenium complexes, UV-visible spectra were obtained. These proved enlightening when used in comparison with the UV-visible spectra of the corresponding heteroleptic $[Ru(bpy)_2L]^{2+}$ (L = **91** and **94**) complexes. The UV-visible spectrum of $[Ru(\mathbf{94})_3](PF_6)_2$ (**112**) is shown along with the UV-visible spectrum of $[Ru(bpy)_2(\mathbf{94})](PF_6)_2$ (**111**) in Fig. 5.19. For complex **111** the spectrum consists of a MLCT at 454 nm with a shoulder on the high-energy side at approximately 420 nm. In the spectrum of **112**, the shoulder of the heteroleptic complex corresponds well with the λ_{max} for complex **112** at 435 nm. This seemed to suggest that in complex **111** the MLCT [(M)d—(L)π*] was at 420 nm and that the (M)d—(bpy)π* transition was at the longer wavelength of 455 nm. Similarly, for the complexes $[Ru(bpy)_2(\mathbf{91})](PF_6)_2$ (**109**) and $[Ru(\mathbf{91})_3](PF_6)_2$ (**113**) (Fig. 5.20), the λ_{max} for the homoleptic complex corresponds well to the shoulder of the heteroleptic complex, indicating the shoulder at approximately 400 nm for complex **109** is the (M)d—(L)π* transition, and that the (M)d—(bpy)π* transition was at the longer wavelength of 435 nm.

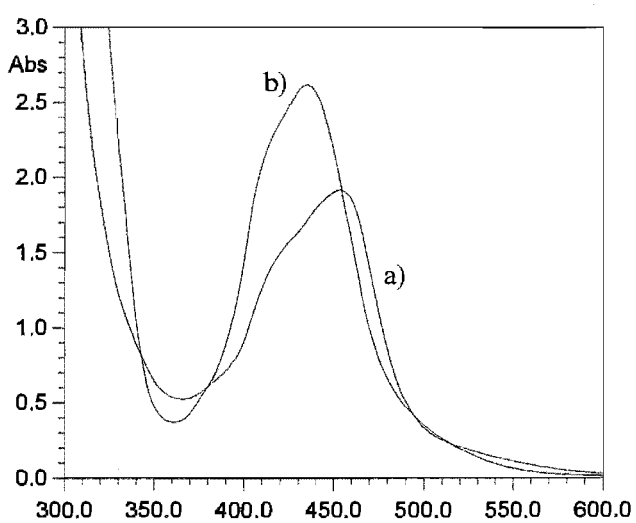

Fig. 5.19 UV-visible spectra of a) $[Ru(bpy)_2(\mathbf{94})](PF_6)_2$ (**111**) and b) $[Ru(\mathbf{94})_3](PF_6)_2$ (**112**).

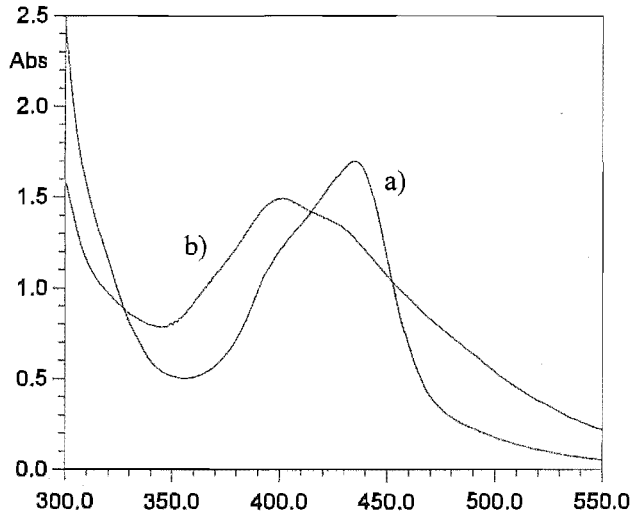

Fig. 5.20 UV-visible spectra of a) $[Ru(bpy)_2(\mathbf{91})](PF_6)_2$ (**109**) and b) $[Ru(\mathbf{91})_3](PF_6)_2$ (**113**).

Electrochemical measurements were also made on these homoleptic complexes and provided more interesting results. No oxidation process of the ruthenium was observed for either **112** or **113** in the potential range examined (+2.1 V), highlighting the electron deficient nature of the ruthenium atom in these complexes. Upon scanning to negative potentials, the complexes each undergo one irreversible redox process. For complex **112** an irreversible reduction occurs at –0.73 V, while complex **113** is reduced at –0.41 V.

Thus, the effects of the heterodiazole-containing ligands are clear. They are poor donors of electron density to the metal, resulting in the raised oxidation potentials of the ruthenium complexes and by virtue of the incorporated heterocyclic oxygen or sulfur atoms, electron deficient. This behaviour is in direct contrast to the effects of heterocyclic rings incorporating nitrogen heteroatoms only. With these types of heterocyclic systems the effect upon the metal atom is to increase the electron density upon it, therefore lowering the oxidation potential whilst the electron rich heterocycles are harder to reduce than the bipyridine ligands. Thus the incorporated oxygen and sulfur atoms have inverted the reactivity demonstrating that, by structural modification of heterocyclic structure, in this case molecular replacement, properties of complexes can be dramatically altered.

The molecule di(2-pyridyl)-1,2,5-oxadiazole-2-oxide (**99**) was also reacted with $Ru(bpy)_2Cl_2$ under the standard refluxing 3:1 ethanol/water conditions. The expected product from this reaction, after workup, was $[Ru(bpy)_2(\mathbf{99})](PF_6)_2$ (Fig. 5.21), (**114**), where coordination is through N5 of the oxadiazole and the pyridine nitrogen to form a five-membered chelate. Furthermore, it seemed logical to expect that the conformation of the ligand would be similar to that of the corresponding 1,2,5-oxadiazole (Fig. 5.11), and that the ^1H NMR spectrum would resemble that of complex **109** (Fig. 5.9). Some slight changes to the spectrum were expected. For instance, the N-oxide group of the 1,2,5-oxadiazole-2-oxide (Fig. 5.21) might influence the H3' proton of the uncoordinated ring.

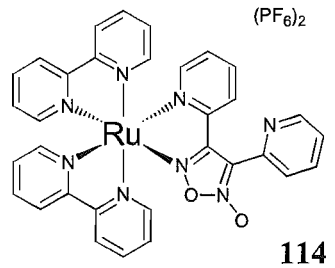

114

Fig. 5.21

However, the complex isolated, in 90% yield, has the ^{1}H NMR spectrum shown in Fig. 5.22. The important difference is that the signal for H6' is not in the expected position (*ca.* 9 ppm). However, there did seem to be the expected downfield H3 signal at 9.55 ppm. By 1-D TOCSY six different four-proton spin systems were identified. One of the rings identified differed from the others in that it did not show the usual coupling constant of a pyridine H6. The proton of this ring is visibly different from the other H6's at the chemical shift of 7.34 ppm. It seemed likely that the ligand had rearranged, so that this ring was no longer a pyridine. To test that it was indeed the ligand rearranging, the reaction was repeated with the $Ru(dmb)_2Cl_2$ precursor, to produce the complex **116**. Importantly, all dmb auxiliary ligands were unaffected, and excellent agreements of the chemical shifts for the ligand in each complex were obtained (Table 5.6, pg 145). FABMS of complexes **115** and **116** also provided an important result; the molecular ion suggested that the ligand had retained its molecular constitution. So, in the rearrangement, the ligand had not lost or gained any atoms. To determine the structure of the complex an X-ray crystal structure investigation was conducted. Small single crystals suitable for X-ray diffraction were grown by slow evaporation of a CH_2Cl_2 solution of complex **115**. Figure 5.23 shows the structure of the rearranged product.

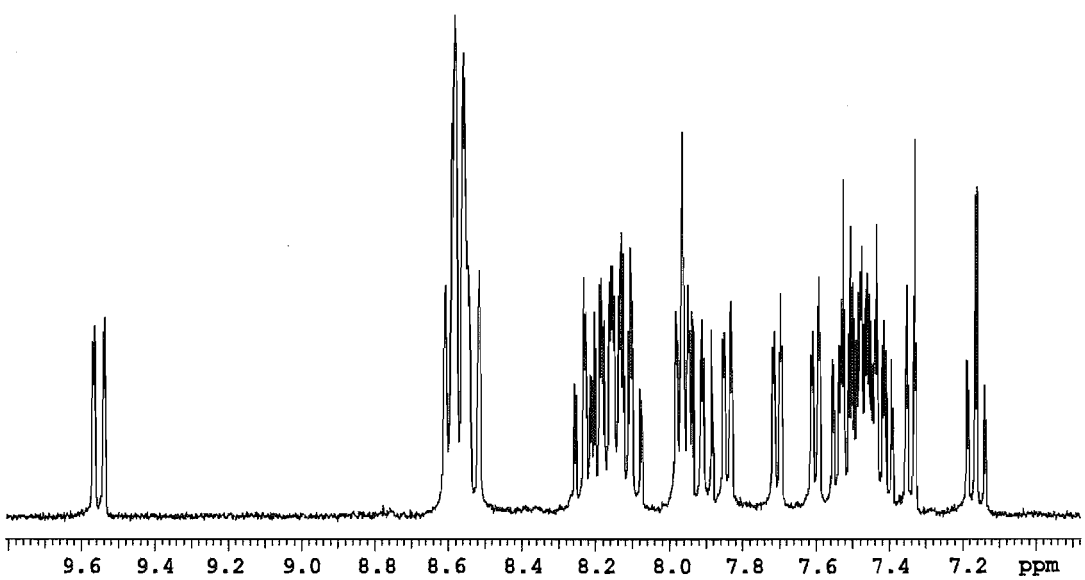

Fig. 5.22 ^{1}H NMR spectrum of **115.**

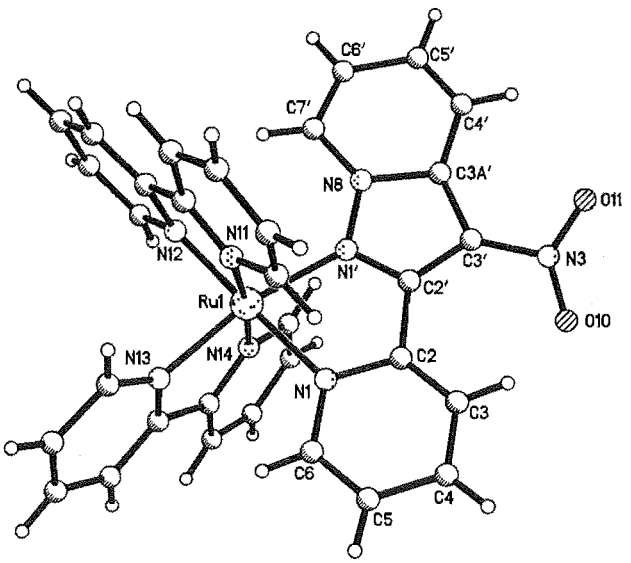

Fig. 5.23 Perspective view, with selected atom labelling, of the complex **115** without the counterions and solvate molecules.

The complex crystallises in the monoclinic space group C2/c, with one cationic complex, two hexafluorophosphate counterions and water and dichloromethane solvate molecules in the asymmetric unit. For clarity, the counterions and solvate molecules are not shown in Fig. 5.23. Due to the small crystal, the data set collected was weak, and also the structure contains some diffuse solvent, and both of these factors contributed to an unsatisfactory refinement converging to an R-factor of 7.4%. However, the crystallographic study has succeeded in unambiguously identifying the rearranged ligand. The ligand has rearranged from 3,4-di(2-pyridyl)-1,2,5-oxadiazole-2-oxide to 2-(2-pyridyl)-3-nitro-pyrazolo[1,5-*a*]pyridine. Perhaps the simplest explanation for the formation of this product is shown in Fig. 5.24.

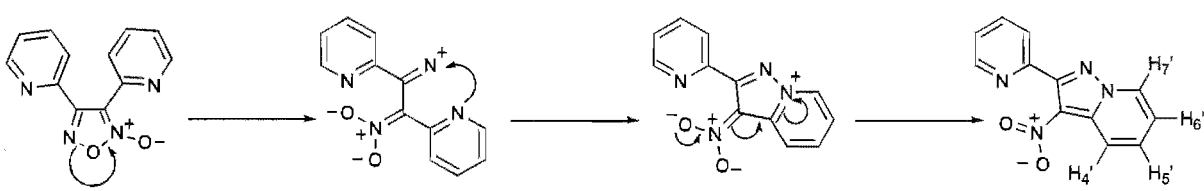

Fig. 5.24

The N5-O1 bond is broken heterolytically, with the electrons moving to the more electronegative element oxygen. The generated intermediate is then attacked by the nucleophilic nitrogen atom of the pyridine attached to what was formally C3 of the 1,2,5-oxadiazole-2-oxide ring. Rearrangement of the electron skeleton, as shown, leads to the pyrazolo[1,5-*a*]pyridine system. This mechanism is a ring-opening ring-closing (RORC) sequence. 1,2,5-Oxadiazole-2-oxides have a rich history of involvement in many different heterocyclic ring transformations.[199,226] However, this seems to be the first reported

rearrangement mediated by a transition metal. Thermal and photochemical isomerisations of 1,2,5-oxadiazole-2-oxides involve breakage of the O1-N2 bond, and this has been assumed to give dinitroso intermediates. Under forcing thermal conditions, 1,2,5-oxadiazole-2-oxides undergo retro-1,3-dipolar cycloaddition, which involves not only breakage at the O1-N2 bond but also the C3-C4 bond.[199,226] Recently there has been a theoretical and experimental study on the rearrangements of nitrobenzofuroxans (nitrobenzo-1,2,5-oxadiazole-2-oxides).[227] This process also involves O1-N5 bond rupture, similar to that proposed for the above process.

The RORC sequence reported here is also a previously unreported synthesis of pyrazolo[1,5-*a*]pyridines, which have previously been constructed in several different ways.[228] The methods that pertain to the present case are those that effect ring closure between the heteroatoms. These methods include the oxidation of pyridylethylamine by potassium ferricyanide,[229] which gives the parent heterocyclic system. The generation of nitrenes, by reaction of phosphites with nitro[230] and nitroso[231] containing compounds, in the presence of a suitably disposed pyridine ring, also leads to ring closure between the heteroatoms. These two methods most closely resemble the proposal forwarded above. A method that offers considerable versatility is the reaction of N-amino(2-methyl)pyridines with acid derivatives or synthetic equivalents.[232] The dual electrophilic/nucleophilic character of hydroxylamine-O-sulfonic acid has also been utilised in the construction of the pyrazolo[1,5-*a*]pyridine ring.[233] These procedures are potentially adaptable for a possible synthesis of the ligand in complexes **115** and **116** (Scheme 5.6). In some cases, the 3-position of the ring requires subsequent nitration to produce the desired ligand, and this is readily achievable for this system using mild nitrating conditions.[228] There has been some investigation in the field of medicinal chemistry of molecules containing the pyrazolo[1,5-*a*]pyridine moeity,[234] as they have receptor binding activity for adenosine.[235]

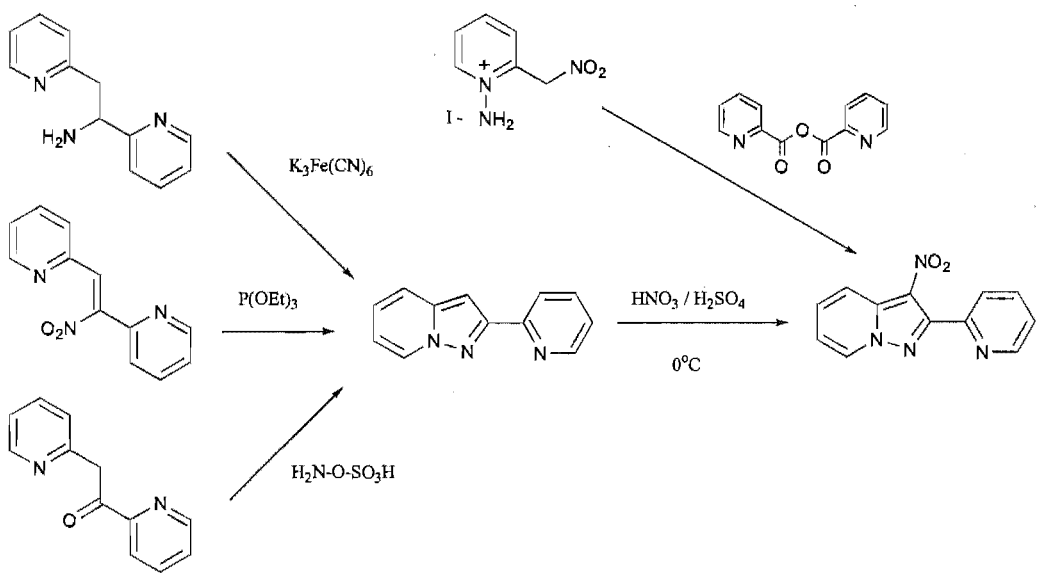

Scheme 5.6

The structural identification of the ligand allowed the assignment of the ^{1}H NMR spectra for the complexes. The chemical shifts for the resulting rearranged ligand in the complexes are given in Table 5.6. The proton that did not share the H6 coupling constant is H7' of the pyrazolo[1,5-*a*]pyridine ring, and this proton is shielded in the complexes **115** and **116** by the adjacent pyridyl ring. The H6 protons are also shielded, and occur at the positions expected for pyridyl H6's in these types of ruthenium complexes. The reason for the downfield position of the H3 proton is the deshielding it experiences from the neighbouring nitro group (See Fig. 5.23).

Table 5.6 ^{1}H NMR Chemical Shifts[a] for the ligand in complexes **115** and **116**.

	H4'	H5'	H6'	H7'	H3	H4	H5	H6
115	8.57	7.91	7.16	7.34	9.55	8.23	7.50	7.84
116	8.57	7.91	7.18	7.37	9.53	8.20	7.48	7.83

[a] For deuterated acetonitrile solutions.

Possibly the RORC process was thermodynamically controllable, and so, the reaction was repeated using milder reaction conditions with a silver salt, a lower temperature (35-40°C) and a shorter reaction time. After purification, the ^{1}H NMR spectrum (Figure 5.25) showed that two products had formed in a ratio of 4:1, with the major product being the already identified RORC product **115**. The minor product has the chemical shifts that are reminiscent of the complexes **109** and **110**, where the H6 proton of the uncoordinated ring at 9.00 ppm is now evident, as is a H3 proton at a downfield position (9.29 ppm) which could well be H3 of the coordinated ring. These were both irradiated in 1-D TOCSY experiments and found to have similar chemical shifts to the oxadiazole ligand in complex **109**. With this information, it seems entirely reasonable to propose that complex **114** (Figure 5.21) is formed in the reaction, but undergoes irreversible rearrangement to the pyrazolo[1,5-*a*]pyridine. Evidence that this is a facile process, is the high conversion to the rearranged product (*ca.* 80%) even with the mild conditions of 35-40°C.

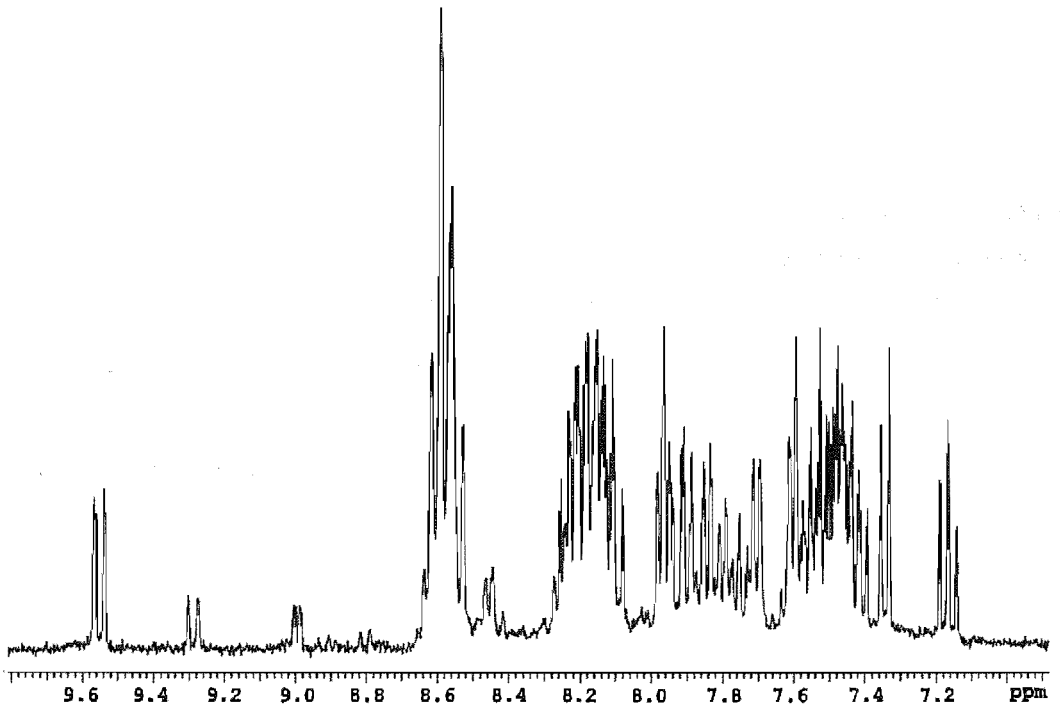

Fig. 5.25

To test that the rearrangement was metal-catalysed, ligand **99** was refluxed alone in 3:1 ethanol/water. The material was then analysed by recording its ^{1}H NMR spectrum, and this showed no change from that of the starting material, indicating that the process was metal-catalysed. As a further investigation, the ligand was refluxed in combination with another metal salt (nickel perchlorate), before the organic component was analysed by ^{1}H NMR. Although the resulting spectrum was a little broadened, perhaps due to the presence of some paramagnetic Ni(II), it was clear that the ligand had not rearranged.

Having serendipitously prepared these complexes it was decided to study them further by performing UV-visible spectroscopic and electrochemical measurements. Table 5.7 summarises both the UV-visible and electrochemical studies, and the UV-visible spectrum and cyclic voltammogram of complex **115** is shown in Fig. 5.26.

Table 5.7 Absorption Maxima[a] with Molar Absorption Coefficients[b] and Redox Potentials[c] of **115** and **116**.

	λ_{max} (ε)	E_{ox}	E_{red}	$E_{ox\text{-}red}$
115	443 (15 900)	+1.28	-0.97	2.25
116	438 (15 500)	+1.18	-1.00	2.18

[a] In nanometers. [b] $M^{-1}cm^{-1}$. [c] In volts *vs* SCE in acetonitrile.

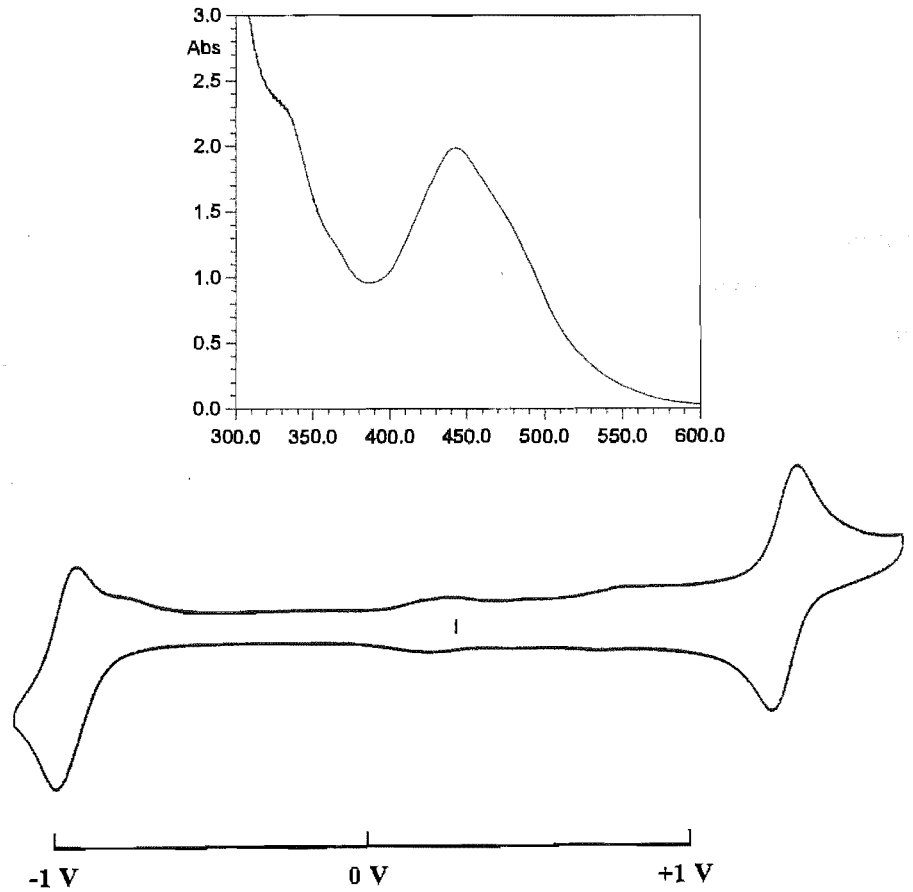

Fig. 5.26 UV-visible spectrum and cyclic voltammogram of **115**.

The complexes undergo redox couples at +1.28 and +1.18 V for **115** and **116**, respectively. This difference is again a result of the electron donating effect from the dmb ligands as discussed previously.[180] Each complex has a fully reversible one-electron reduction at -0.97 and -1.00 V, respectively, that is attributable to the pyrazolo[1,5-*a*]pyridine ligand. Further multiple electron reductions are evident in the cyclic voltammograms of both complexes, but assignment of the redox waves is difficult, as there is considerable overlap. A possibility is that the nitro group in the ligand is also participating in the electrochemistry.

Complexes containing benzo-fused systems have been much studied,[236-240] and have been shown to possess different properties to the unfused analogues. However, ligands containing other fused systems, such as the pyrazolo[1,5-*a*]pyridine ring, have been little studied and yet offer a wide range and scope as ligands for study. The results obtained suggested that ligand **99** might display other interesting coordination chemistry. Accordingly, coordination complexes with $PdCl_2$, $CuCl_2.2H_2O$, and $AgNO_3$ were prepared.

Five and six membered ring chelates are common with palladium(II) complexes. With ligand **99** there is the possibility, as mentioned previously, to form either a six-membered chelate *via* O2 and N1', or a five-membered chelate *via* N5 and N1" (Fig. 5.27). It was anticipated that the H6' and H6" protons of the molecule could be used diagnostically to

identify which of the chelates had formed. For example, in either case, only one of H6' or H6" would be deshielded by the proximate chlorine in the ^{1}H NMR spectrum, with the other changing little in chemical shift. Irradiation of the deshielded H6 in a 1-D TOCSY experiment would determine the chemical shifts of the other protons in the ring. A GHMBC experiment could then correlate the H3 proton to the appropriate quaternary carbon (C3 or C4) of the 1,2,5-oxadiazole-2-oxide, which show a separation in chemical shift. This was the anticipated method by which the distinction of the chelate could be made.

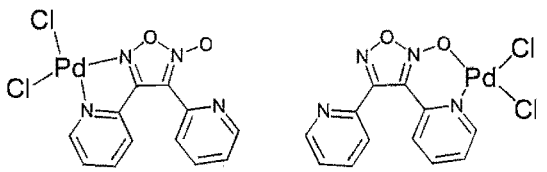

N5,N1" O2,N1'

Fig. 5.27

When Li_2PdCl_4 was reacted with ligand **99** in methanol a yellow complex, (**117**), was formed in high yield (95%), that analysed as [**99**.$PdCl_2$]. FABMS provided a molecular ion of (**99**)$PdCl^+$, which indicated that the complex was monomeric. ^{1}H NMR of the complex in deuterated DMSO gave an unexpected spectrum, shown in Fig. 5.28, where both the H6' and H6" protons are deshielded, indicating that both pyridine rings of the ligand are coordinated to palladium. This suggested that another mode of coordination was taking place. The one that seemed most likely, given the FABMS result, was the formation of a seven-membered metallocycle (Fig. 5.29) with N1',N1" coordination.

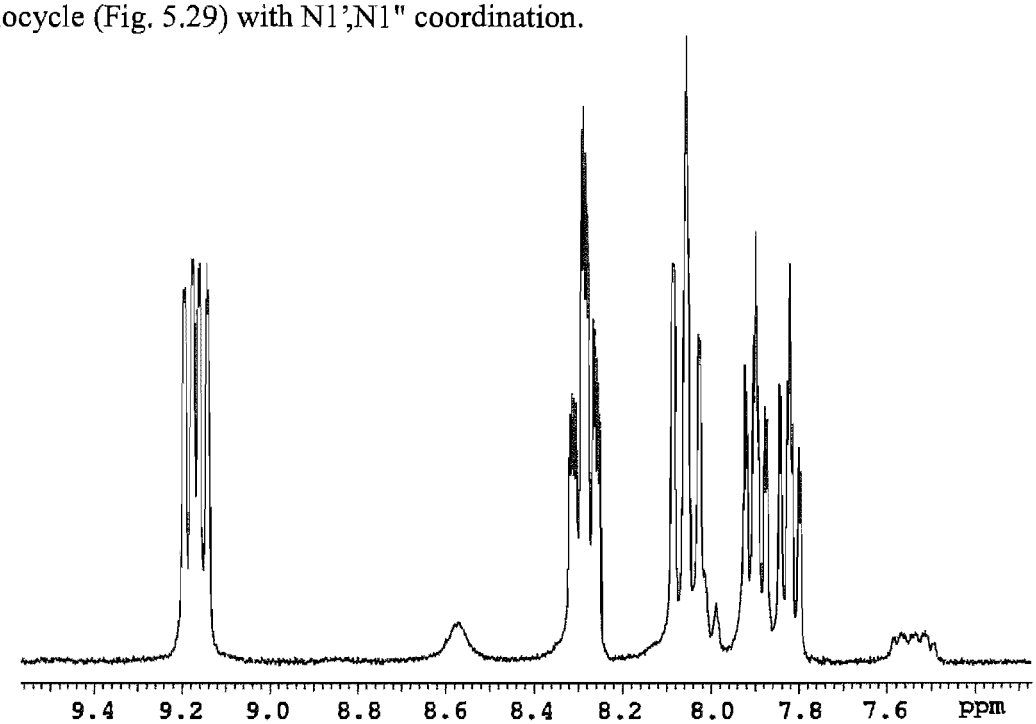

Fig. 5.28 ^{1}H NMR spectrum of **117**.

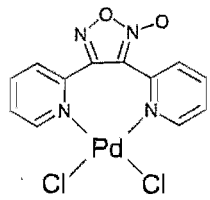

N1',N1"

Fig. 5.29

By 1-D TOCSY the signals due to each spin system in the complex were identified by irradiation of the isolated H5 protons at the chemical shifts of 7.82 ppm and 7.90 ppm. The chemical shifts and coordination induced shifts for **117** are shown in Table 5.8, and were assigned by assuming that the most downfield H6 proton in the free ligand is also the most downfield H6 proton in the complex. The small broad peaks that are apparent in the spectrum are due to the presence of some dissociated free ligand.

Table 5.8 ^{1}H NMR Chemical Shifts[a] and Coordination Induced Shifts[b] of **99** and **117**.

	H3	H4	H5	H6	H3'	H4'	H5'	H6'
117	8.03	8.27	7.82	9.14	8.07	8.28	7.90	9.18
99	7.91	8.01	7.51	8.55	7.87	8.01	7.56	8.56
CIS	+0.12	+0.26	+0.31	+0.59	+0.20	+0.27	+0.34	+0.62

[a] For deuterated dimethyl sulfoxide solutions. [b] CIS = ($\delta_{complex}$ - δ_{ligand}).

The CIS values are very similar for the two rings, although it should be noted that the CIS values for H3'-H6' are all slightly larger than the corresponding values for H3-H6. The H6 and H6' protons are deshielded by their proximity to the chlorine atoms attached to the palladium, resulting in the large positive CIS values. The values for H4/H4' and H5/H5' are significant and indicate σ-donation to the metal.

When ligand **99** and $CuCl_2.2H_2O$ are mixed in methanol, green crystals, (**118**), that analyse as [**99**.$CuCl_2$] are formed. To unambiguously determine the structure a crystal was subjected to an X-ray crystal structure analysis. The asymmetric unit of the structure is shown in Fig. 5.30a.

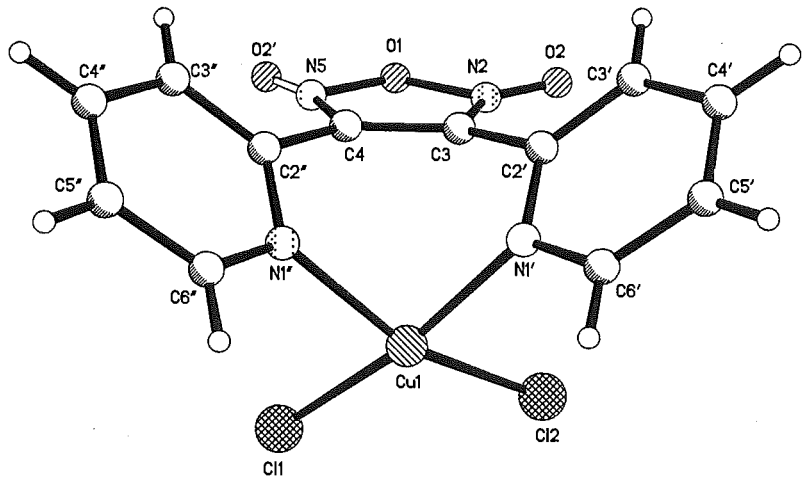

Fig. 5.30a Perspective view, with atom labelling of the contents of the asymmetric unit, of **118**. Selected bond lengths (Å) and angles (°): N1'-Cu1 2.023(3), N1"-Cu1 2.047(3), Cl1-Cu1 2.332(1), Cl2-Cu1 2.583(1), N1'-Cu1-N1" 87.2(1), N1'-Cu1-Cl1 167.4(1), N1'-Cu1-Cl2 85.1(1), Cl1-Cu1-Cl2 93.81(4), O1-N2 1.436(4), O1-N5 1.375(4), N5-O2 1.740(10), N2-C3 1.331(4), C3-C4 1.422(4), N5-C4 1.328(4), N5-O1-N2 108.8(3).

The most notable feature of this structure is the formation of the seven-membered chelate ring, as proposed above for the palladium complex. The chelate ring is puckered, with the planes of the coordinated pyridine rings making an angle of 69.6(5)° between each other. Because of the tilt of the pyridine rings, the copper atom lies well below the plane defined by the 1,2,5-oxadiazole-2-oxide ring [2.131(4)Å]. The seven-membered chelate ring provides a bite angle at the copper (N1'-Cu1-N1") of 87.2(1)°. There is some disorder of the 1,2,5-oxadiazole-2-oxide ring, with O2 having partial occupancies on N2 and N5. This disorder was successfully modelled and the partial occupancy was found to be around 15%. The full structure is a chloro-bridged [2 + 2] dimer (Fig. 5.30b), by virtue of the centre of inversion in the centre of the four-membered Cu_2Cl_2 ring. Such cyclic dimers are common for copper(II) chloride complexes.[241] The coordination geometry of the copper itself can be described as square pyramidal with the μ-chloro occupying the apical position.

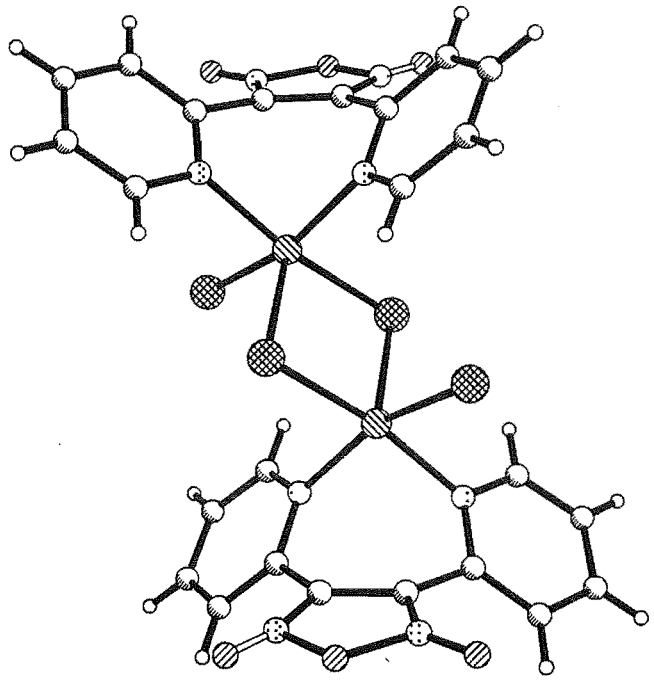

Fig. 5.30b Perspective view of the dimeric structure of **118**.

When ligand **99** and $AgNO_3$ are mixed in methanol a colourless complex is formed, in high yield (86%), which analyses as [**99**.$AgNO_3$], (**119**). The ^1H NMR spectrum of the complex was obtained in deuterated acetonitrile, and this proved that the ligand had not undergone any rearrangement. However, crystals suitable for a structural characterisation were unable to be grown.

It is interesting that in the coordination complexes of **99** with copper and palladium, the 1,2,5-oxadiazole-2-oxide ring has played no part in the coordination. In both structures the ligand is coordinated to the metal ion through the pyridine donors, with the formation of a seven-membered ring, rather than the formation of a smaller chelate. To test if this was a general phenomenon some other complexes were synthesised and investigated with ligands **91** and **93** and **94**.

A palladium(II) complex was prepared by reacting ligand **93** with Li_2PdCl_4 in methanol, giving a yellow complex, (**120**), in high yield (91%). The ^1H NMR spectrum of the complex showed a mixture of free and complexed ligand, indicating an equilibrium between the two. The signals for the complex were determined after comparison with the spectrum of the free ligand. The CIS values (Table 5.9) show that the H6 proton of the pyridine ring shows a small positive value consistent with it being deshielded by the adjacent chlorine. The CIS value (+0.42) of H4 of the pyridine ring indicates the σ-donation effect from the pyridine to the metal. The thiadiazole ring proton (H4') has moved downfield upon complexation and

this is likely to be both a deshielding effect due to its proximity to H3 and an electronic effect. The CIS value for this proton in the complex $[Ru(bpy)_2(\mathbf{93})](PF_6)_2$ **108** was +0.29 ppm.

Table 5.9 ^{1}H NMR Chemical Shifts[a] and Coordination Induced Shifts[b] for **120** and **93**.

	H3	H4	H5	H6	H4'
120	8.57	8.44	7.88	8.93	9.76
93	8.16	8.02	7.55	8.74	9.43
CIS	+0.41	+0.42	+0.33	+0.19	+0.33

[a] For deuterated dimethyl sulfoxide solutions. [b] CIS = ($\delta_{complex}$ - δ_{ligand}).

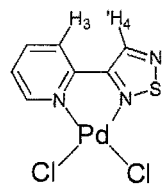

120

Fig. 5.31

A palladium complex was prepared in the above manner using ligand **91**. A yellow complex, (**121**), formed in high yield (95%), and analysed in a 1:1 stoichiometry [**91**.$PdCl_2$]. The ^{1}H NMR spectrum was recorded in deuterated dimethyl sulfoxide and showed the presence of a deshielded H6 proton and another signal for a H6 proton at a chemical shift very close to that of the free ligand. The integration of these signals was the same, and this left some doubt about the nature of the bonding in the complex, as this situation is consistent with either a five-membered chelate or an equilibrium between a seven-membered chelate and dissociated free ligand. Two pieces of information led to the assignment that the seven-membered chelate had formed. The first was the large CIS value (Table 5.10) of the deshielded H6 (+0.56). This is only consistent with the formation of the seven-membered ring, as it places the H6 protons of the pyridine rings closer to the chlorine atoms attached to the palladium. If the five-membered chelate had formed then the CIS would not be as large (for example, see the CIS of H6 in the previous complex). Also there is no desheilding effect from the pyridine nitrogen of the uncoordinated ring upon the H3 proton of the coordinated ring, as was seen for previous five-membered chelates with this ligand. Thus, the fact that the signals had such a close integration appears to be merely a coincidence. The chemical shifts and coordination induced shifts for all signals are given in Table 5.10. The CIS values for **121** show the same general features as the values found for the seven-membered chelate with ligand **99**, *viz.* complex **117**, and the reasons for these are the same as those proposed for **117**.

Table 5.10 ^{1}H NMR Chemical Shifts[a] and Coordination Induced Shifts[b] for **121** and **91**.

	H3	H4	H5	H6
121	8.05	8.26	7.86	9.15
91	7.89	8.00	7.56	8.59
CIS	+0.16	+0.26	+0.30	+0.56

[a] For deuterated dimethyl sulfoxide solutions. [b] CIS = ($\delta_{complex}$ - δ_{ligand}).

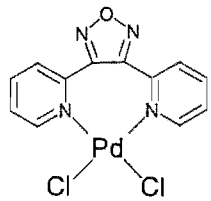

121

Fig. 5.32

A palladium complex with ligand **94** was prepared in the same fashion as above, and the yellow complex, (**122**), analysed as [**94**.$PdCl_2$]. The ^{1}H NMR spectrum was recorded in deuterated dimethyl sulfoxide and again showed a mixture of free and complexed ligand, but integration of the signals due to each were not the same and so the formation of the seven-membered chelate was again evident. The coordination induced shifts for complex **122** are given in Table 5.11, and show similar features to those of complex **121** for exactly the same reasons. However, the CIS values are all less positive that the corresponding values for **121**.

Table 5.11 ^{1}H NMR Chemical Shifts[a] and Coordination Induced Shifts[b] for **122** and **94**.

	H3	H4	H5	H6
122	8.93	8.19	7.79	9.08
94	7.91	8.10	7.55	8.72
CIS	+0.16	+0.09	+0.24	+0.36

[a] For deuterated dimethyl sulfoxide solutions. [b] CIS = ($\delta_{complex}$ - δ_{ligand}).

A platinum complex was prepared by adding a nitromethane solution of bis(dimethyl sulfoxide)dichloroplatinum [$(DMSO)_2PtCl_2$] to ligand **94** dissolved in nitromethane. The yellow micro-crystals, (**123**), which were recovered by filtration, in high yield (91%), analysed as [**94**.$PtCl_2$]. Recording the ^{1}H NMR spectrum of this complex was attempted in deuterated dimethyl sulfoxide, but this only succeeded in precipitated the $(d_6\text{-}DMSO)_2PtCl_2$ complex and liberating the ligand.

In an attempt to synthesise a dinuclear complex, ligand **94** was reacted with two equivalents of copper(II) nitrate in methanol. Sky blue crystals, (**124**), suitable for

crystallography were afforded directly from the reaction mixture. The structure is shown in Fig. 5.33.

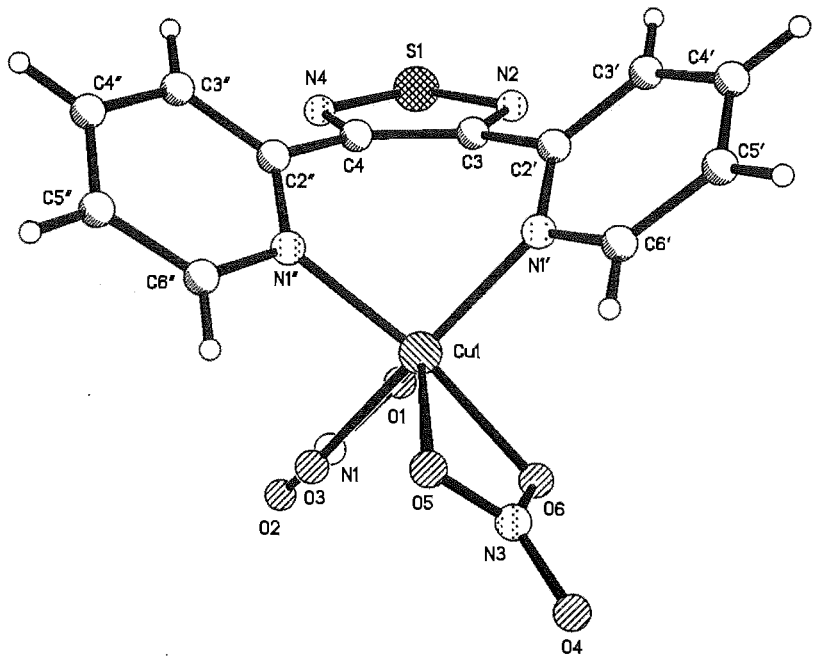

Fig. 5.33 Perspective view, with atom labelling, of **124**. Selected bond lengths (Å) and angles (°). Cu1-N1' 2.002(2), Cu1-N1" 1.979(2), N1'-Cu1-N1" 93.74(6), Cu1-O5 2.413(2), Cu1-O6 2.014(1), O5-Cu1-O6 58.02(5), O1-Cu1-O3 58.03(6), Cu1-O1 2.373(2), Cu1-O3 2.028(1), S1-N2 1.633(2), S1-N5 1.629(2), N2-C3 1.330(3), C3-C4 1.446(3), C4-N5 1.327(3).

The crystal structure revealed that a mononuclear complex with a seven-membered chelate ring had formed. The ligand is coordinating to the copper by the pyridine nitrogens [Cu1-N1' 2.002(2)Å and Cu1-N1" 1.979(2)Å], making a large bite angle [93.74(6)°] at the metal atom. The two nitrate anions are chelating, with one of the coordinating oxygens of each nitrate bonded more strongly than the other, and complete the pseudo-octahedral coordination of the copper atom. The structural conformation of the ligand is remarkably similar to the structure found earlier with ligand **99** and copper(II) chloride, *viz.* **118**. The seven-membered chelate again provides a similar angle between the pyridines [66.3(5)°], and the copper atom lies below the plane of the thiadiazole ring [1.997(3)Å]

The results of the palladium and copper complexes with ligands **91** and **94** indicated that the heterodiazole rings were not participating in coordination, and that, as with ligand **99**, the formation of the seven-membered chelate was favoured over the formation of a smaller chelate. Of interest was an investigation into the coordination chemistry of these ligands with silver(I), where there is a very different geometric preference. To this end, ligand **94** and $AgNO_3$ were reacted in methanol. The resulting precipitated material was recrystallised from acetonitrile to give colourless crystals, (**125**), one of which was used for an X-ray analysis. A

perspective view of the asymmetric unit is shown in Fig. 5.34a, while the extended structure is shown in Fig. 5.34b.

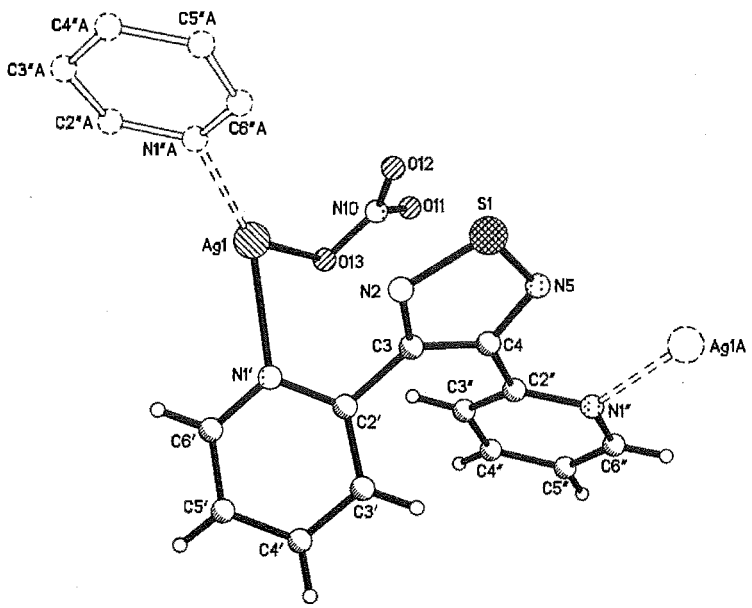

Fig. 5.34a Perspective view, with atom labelling, of **125**. Selected bond lengths (Å) and angles (°). Ag1-N1' 2.305(2), Ag1-N1"A 2.235(2), N1'-Ag1-N1"A 136.54(8), Ag1-O13 2.412(3), O13-Ag1-N1' 81.48(8), S1-N2 1.633(2), S1-N5 1.633(2), N2-S1-N5 98.6(1), N2-C3 1.333(4), S1-N2-C3 107.6(2), C3-C4 1.434(4), N2-C3-C4 113.2(2), C4-N5 1.334(4), C3-C4-N5 112.9(3), C4-N5-S1 107.7(2), C3-C2' 1.493(4), C4-C2" 1.478(4).

The complex is a one-dimensional metallopolymer, and has crystallised in the monoclinic space group $P2_1/n$. The asymmetric unit contains a silver atom, bonded to a monodentate nitrate anion, and one ligand coordinated to the silver *via* a pyridine nitrogen. The ligand is coordinated to the silver by the pyridine nitrogen only, with the thiadiazole ring again not participating in coordination. The ligand acts in a bridging fashion through each of its pyridine nitrogens, separating two silver atoms in the polymeric chain by 7.401(1)Å. The conformation of the ligand can be defined by the angles between each of the meanplanes of the three planar aromatic rings. The two pyridine rings are of a similar pitch relative to the central 1,2,5-thiadiazole ring [45.9(4)° and 31.3(4)°], but have the nitrogens in the opposite orientation, leading to the metallopolymer having an undulating character. The silver atom is tricoordinate with the angle between the coordinating nitrogens 136.54(8)°. The angle at silver between the nitrate anion and N1' is 81.48(8)°, and this is considerably smaller than the N1"A-Ag1-O13 angle [141.77(8)°], which gives the silver a geometry that is neither trigonal planar nor distorted T-shape.

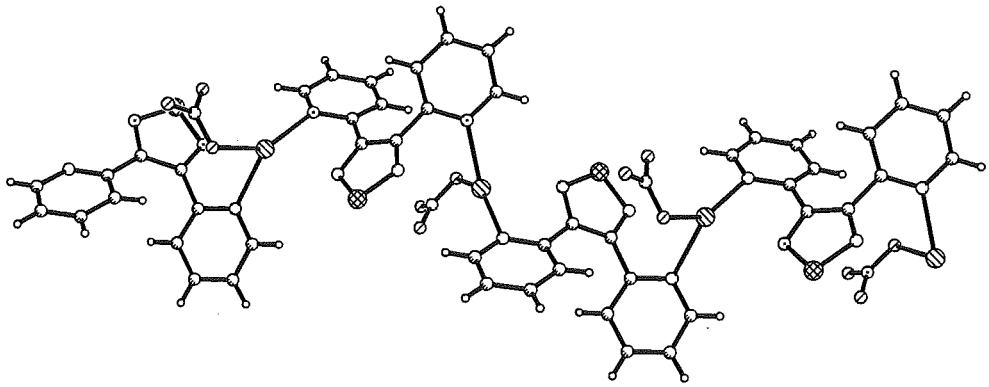

Fig. 5.34b Perspective view of the extended structure of **125**.

5.4 Dinuclear Ruthenium Complexes

Having prepared and examined mononuclear ruthenium complexes, some homodinuclear complexes of ruthenium with ligands **91**, **94**, and **95** were prepared. In dinuclear complexes containing two octahedral metal centres there exists the possibility of diastereoisomerism between racemic, (ΛΛ / ΔΔ), and meso, (ΛΔ), forms (Fig. 5.35). Each of the diastereoisomers contains a 2-fold element of symmetry, with the racemic diastereomer having a 2-fold rotational axis, whereas the meso contains an internal mirror plane. The meso and racemic forms are diastereoisomeric, and are therefore potentially distinguishable by NMR.

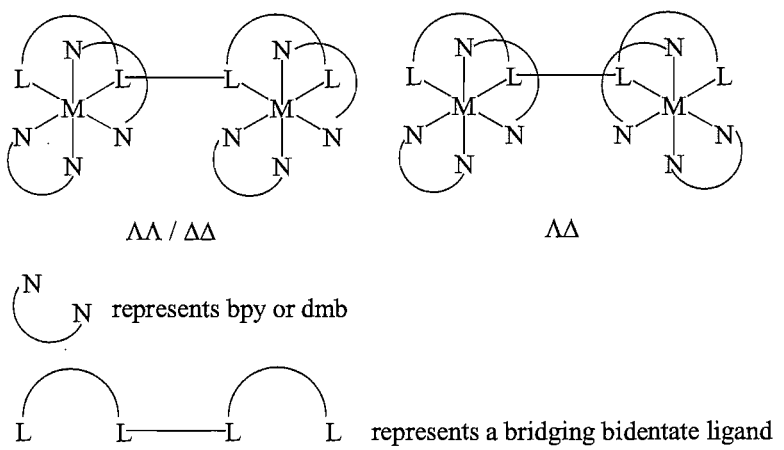

Fig. 5.35

In anticipation that the ^{1}H NMR spectrum of the dinuclear complexes of ligands **91** and **94** with $Ru(bpy)_2Cl_2$ would be difficult to assign, the first complex prepared was with the 4,4'-dimethyl derivative $Ru(dmb)_2Cl_2$. This perhaps would at least allow identification of the pyridine rings of the bridging ligand. The dinuclear complex $[(dmb)_2Ru(\mathbf{91})Ru(dmb)_2](PF_6)_4$, (**126**), was prepared by reacting ligand **91** with an excess of $Ru(dmb)_2Cl_2$ in refluxing 3:1

ethanol/water, with conversion to the hexafluorophosphate salt during work-up. In the reaction, the mononuclear complex **110** was also formed and this was separated from the desired dinuclear complex **126** by chromatography on alumina using 100:1 CH_2Cl_2/MeOH as eluant. After purification by vapour-diffusion recrystallisation of diethyl ether into an acetonitrile solution of the complex, complex **126** was characterised by FABMS which confirmed a dinuclear complex.

In the ^{1}H NMR spectrum of complex **126**, the pyridine rings of the thiadiazole-containing ligand were found by 1-D TOCSY by irradiation of the most downfield signal at 8.96 ppm. From this signal two pyridine rings were identified, consistent with the formation of diastereoisomers. The only difference in the chemical shifts between the diastereoisomers is in the H6 protons. Integration of these separated resonances revealed that the diastereoisomeric complexes had formed in a 6:5 ratio. However, they could not be specifically assigned to either the meso or racemic forms. The chemical shifts and coordination induced shifts for complex **126** are presented in Table 5.12.

Table 5.12 ^{1}H NMR Chemical Shifts[a] and Coordination Induced Shifts[b] of **126** and **91**.

	H3	H4	H5	H6
126	8.96	8.33	7.66	7.90
				7.98
91	7.91	7.97	7.53	8.60
CIS	+1.05	+0.36	+0.13	-0.70
				-0.62

The CIS values show a large positive shift of the H3 protons for each complex of +1.05 ppm. This is a chelation-induced change in chemical shift. The dinucleation by the ligand has forced all three rings of the ligand to be coplanar, or very nearly so, which has brought the H3 protons of the ligand to be close together in space (Fig. 5.36), and in this conformation the rings deshield each other. The CIS value of +0.36 for the H4 protons is indicative of one of the effects of σ-donation or π back-bonding dominating the other. The usual upfield CIS is seen for the H6 protons.

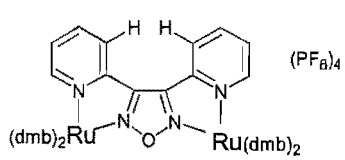

126

Fig. 5.36

The dinuclear complexes $[(bpy)_2Ru(\mathbf{91})Ru(bpy)_2](BF_4)_4$, (**127**), and $[(bpy)_2Ru(\mathbf{94})Ru(bpy)_2](PF_6)_4$, (**128**), (Fig. 5.37) were also prepared and purified in the same

manner as complex **126**. The reaction times and yields for these three complexes are shown in Table 5.13. The formation of the dinuclear complexes required a longer reflux time (*ca.* 24 hrs) than the corresponding mononuclear complexes (*ca.* 4 hrs). FABMS and elemental analyses were correct for the dinuclear complexes **127** and **128**.

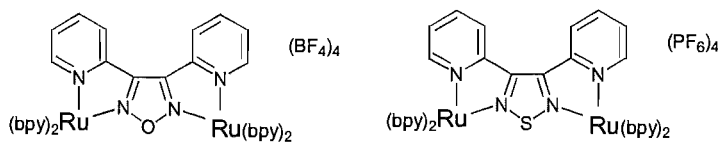

127 **128**

Fig. 5.37

Table 5.13

Complex	Reflux Time (hrs)	% Yield
126	24	35
127	24	31
128	24	47

In the same manner as for complex **126**, the rings of the ligand were found for complex **127** by the irradiation of the most downfield multiplet in a 1-D TOCSY experiment. The signals for each diastereoisomer were resolved in the experiment, although cannot be assigned to a specific isomer. No further ^{1}H NMR assignment of this complex was attempted due to the complicated nature of the spectrum. Keene *et al.*[242,243] have separated such diastereoisomers by ion-exchange chromatography. Separation may have considerably aided further ^{1}H NMR identification in this case, but, as the signals due to the oxadiazole ligand were clearly found, this was not deemed to be necessary. The relevant NMR data are presented in Table 5.14. Not surprisingly, the CIS values are very similar to complex **126**, and the reasons for these are the same.

Table 5.14 ^{1}H NMR Chemical Shifts[a] and Coordination Induced Shifts[b] of **127** and **91**.

	H3	H4	H5	H6
127	8.96	8.35	7.69	7.99
	8.95		7.67	7.91
91	7.91	7.97	7.53	8.60
CIS	+1.05	+0.38	+0.16	-0.61
	+1.04		+0.14	-0.69

[a] For deuterated acetonitrile solutions. [b] CIS = ($\delta_{complex}$ - δ_{ligand}).

It is not unreasonable to expect that the meso and racemic diastereoisomers may form in a 1:1 ratio. However, in the case of complex **128**, there exists a 3:1 ratio of diastereoisomers. Each complex contains 40 protons, related by 2-fold symmetry, and so the

spectrum has 40 different proton signals. Because of the large diastereoisomeric excess, and the highly symmetrical nature of the spectrum (Fig. 5.38), the individual ^{1}H NMR spectrum of the diastereoisomers could be distinguished and assigned to either the major or minor form. Table 5.15 gives the chemical shifts and coordination induced shifts for the major, **128a**, and minor, **128b**, diastereoisomers.

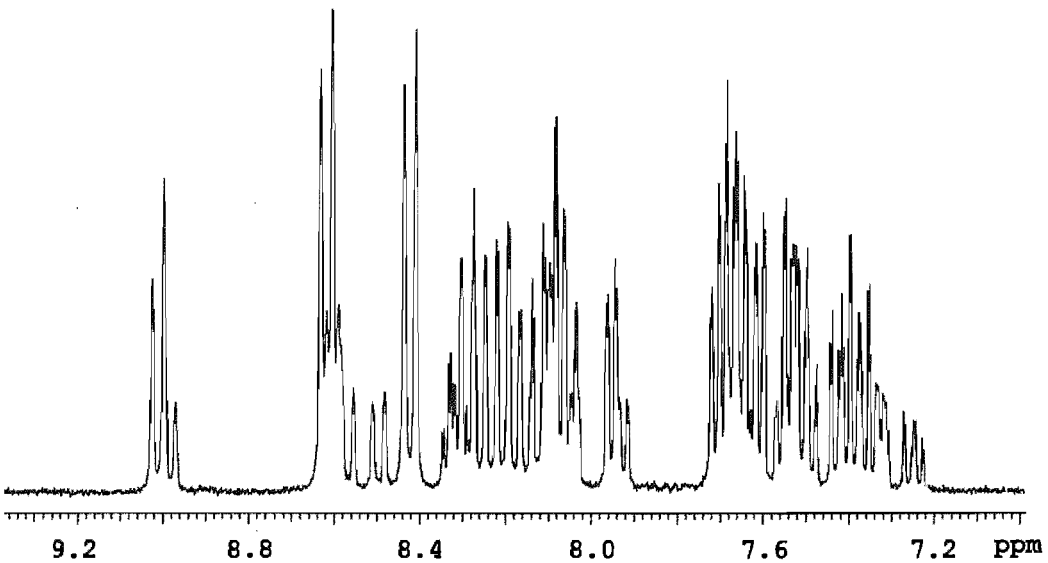

Fig. 5.38

Table 5.15 ^{1}H NMR Chemical Shifts[a] and Coordination Induced Shifts[b] of **94** and **128a/128b**.

	H3	H4	H5	H6
128a	9.00	8.30	7.66	7.95
94	7.82	7.91	7.43	8.47
CIS	1.18	0.39	0.23	-0.52
	H3	H4	H5	H6
128b	8.98	8.27	7.62	7.92
94	7.82	7.91	7.43	8.47
CIS	1.16	0.36	0.18	-0.49

[a] For deuterated acetonitrile solutions. [b] CIS = ($\delta_{complex}$ - δ_{ligand}).

The UV-visible spectra of complexes **126**, **127** and **128** show the effect of chelation of a second $Ru(bpy)_2^{2+}$ unit, with the lowest energy MLCT being red-shifted in each complex relative to the corresponding mononuclear complex. As an example, the λ_{max} for complex **127** is at 497 nm, whereas in the mononuclear complex **109** it was at 435 nm. This corresponds to a lowering of the LUMO in dinuclear complexes compared to mononuclear complexes. The UV-visible spectra of $[(bpy)_2Ru(\mathbf{91})Ru(bpy)_2](PF_6)_4$ (**127**) and $[(bpy)_2Ru(\mathbf{94})Ru(bpy)_2](PF_6)_4$ (**128**) are shown in Fig. 5.39 and some important UV-visible data for all three dinuclear complexes are presented in Table 5.16.

Table 5.16 UV-visible parameters[a] for **126**, **127** and **128**.

	λ_{max} (ε)[b]	$\lambda_2(\varepsilon)$
126	498 (15 000)	409 (18 700)
127	497 (11 600)	405 (18 200)
128	531 (16 000)	420 (17 800)

[a] In acetonitrile solutions. [b] M^{-1} cm^{-1}.

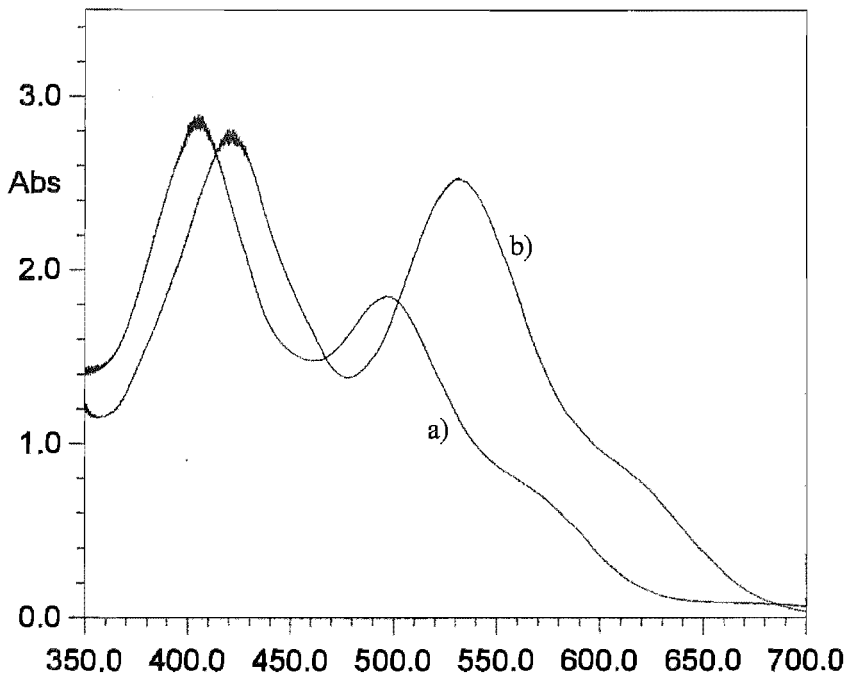

Fig. 5.39 UV-visible spectra of a) $[(bpy)_2Ru(\mathbf{91})Ru(bpy)_2](BF_4)_4$ (**127**) and b) $[(bpy)_2Ru(\mathbf{94})Ru(bpy)_2](PF_6)_4$ (**128**).

The UV-visible spectrum of **127** consists of two distinct peaks at 405 nm [(M)d-(bpy)π^*] and 497 nm [(M)d-(L)π^*], the latter, which is less intense, also having a broad low intensity shoulder at longer wavelength. The UV-visible spectrum for **128** has the same general features, with the (M)d-(bpy)π^* transition occurring at 420 nm, and the (M)d-(L)π^* transition at 531 nm also with a broad low intensity shoulder at longer wavelength.

The dinuclear complexes were each examined by cyclic voltammetry, and the cyclic voltammograms of complex **127** and **128** are shown in Fig. 5.40, while the data for all three complexes are shown in Table 5.17.

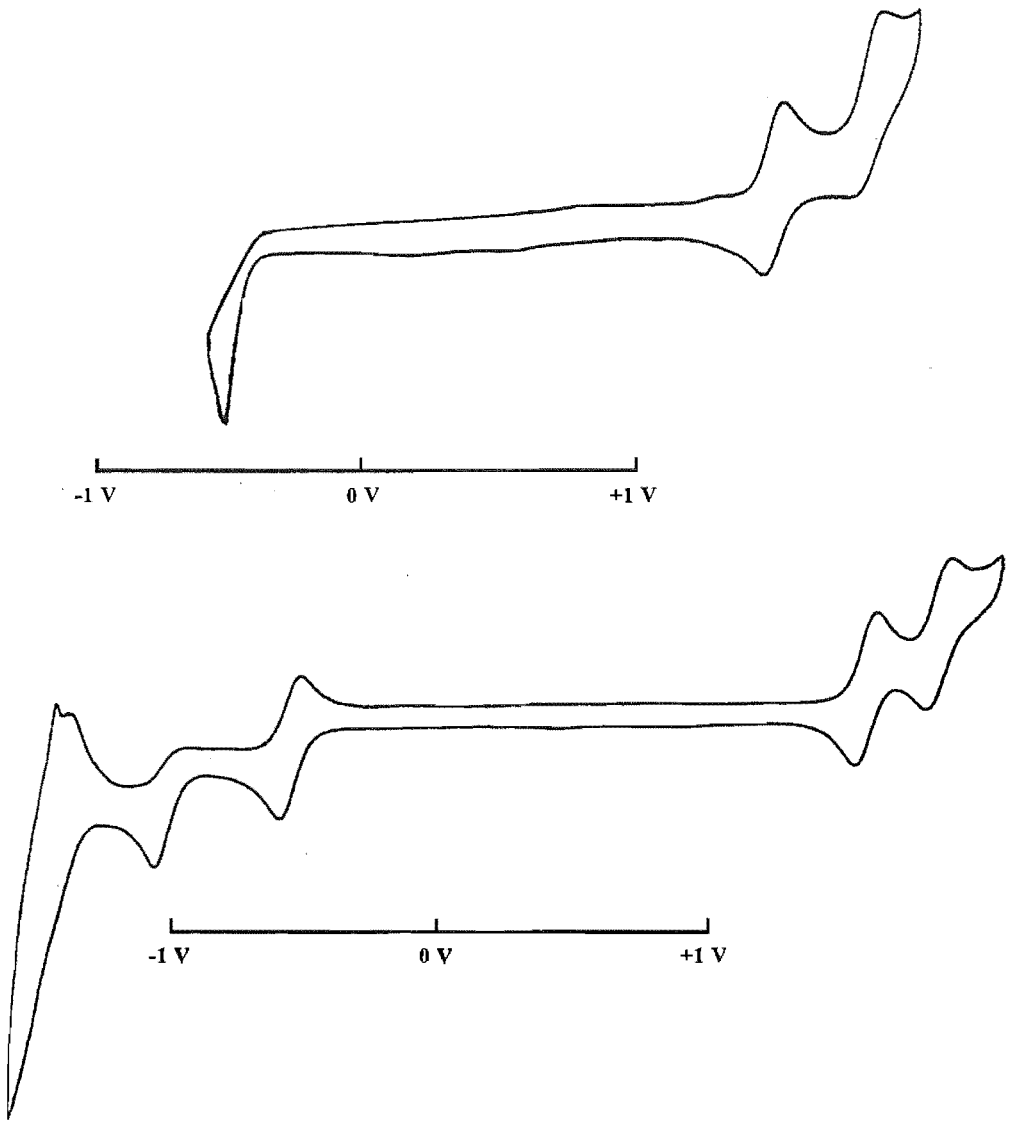

Fig. 5.40 Cyclic voltammograms for $[(bpy)_2Ru(\mathbf{91})Ru(bpy)_2](BF_4)_4$ (**127**) (top) and $[(bpy)_2Ru(\mathbf{94})Ru(bpy)_2](PF_6)_4$ (**128**).

Table 5.17 Redox Potentials[a] of complexes **127**, **126**, and **128**.

	E_{ox1}	E_{ox2}	E_{red1}	E_{red2}	$E_{ox1\text{-}red1}$
127	+1.48	+1.82	-0.53[b]	-	2.01
126	+1.42	+1.80	-0.58	-	2.00
128	+1.41	+1.67	-0.62	-1.08[b]	2.03

[a] In volts *vs* SCE in acetonitrile. [b] Irreversible reduction.

Electrochemically, complex **127** exhibits two one-electron oxidations at 1.48 and 1.82 V, a peak separation of 340 mV (ΔEp = 340 mV). This indicates a large metal-metal interaction when compared to the dinuclear complexes $[(bpy)_2Ru(\mathbf{96})Ru(bpy)_2]^{4+}$ (ΔEp = 170 mV)[45,183] and $[(bpy)_2Ru(\mathbf{97})Ru(bpy)_2]^{4+}$ (ΔEp = 160 mV)[191] and indicates the stability of the mixed valence [Ru(II)-Ru(III)] complex. A measure of stability is the comproportionation constant Kc, given by the formula $Kc = \exp[\Delta E^{1/2}(mV)/25.69\ mV]$ for which complex **127** has a value of 5.6×10^5. Examination in the negative potential region revealed a single

irreversible reduction process at -0.53 V for the complex **127** and this is assigned to the bridging ligand.

The electrochemical examination of **128** revealed the complex undergoes two one-electron reversible oxidations at 1.41 V and 1.67 V, which is a smaller peak separation (ΔEp = 260 mV) than was seen for **127**. The comproportion constant for complex **128** is 2.5 x 10^4. The first reduction at -0.62 V is fully reversible and is centred on the bridging ligand. The second reduction at -1.08 V is irreversible and is also bridging ligand based. The electrochemistry of complex **128** became somewhat complicated by adsorption processes at the electrode surface. This has been encountered before in work with sulfur-containing ligands.[45] However, further 2-electron reduction processes were found at -1.60 V and -1.86 V, and by analysis of peak heights and peak-to-peak separations, were assigned as the simultaneous one-electron reductions of the auxiliary bpy ligands.

Some of the important factors governing metal-metal interactions are the metal-metal distance, the electron density of the LUMO at the coordinating centres,[188,244] and of course, the nature of the bridge. With short internuclear metal-metal separations, it has been proposed that electron transfer may be through the direct orbital overlap of the metal d orbitals (Fig. 5.41). This point has been particularly made for dinuclear complexes containing a 2,2'-bipyrimidine[188,245] or 2,2'-biimidazolate bridge.[128] In other bridging ligands the geometry is such that direct metal d orbital overlap is not possible, so that communication must be mediated through the π-system of the bridging ligand, and this is the case with the present examples. The metal-metal interactions of the homodinuclear complexes just described are of a strong nature, with ΔEp = 340 mV for **127** and ΔEp = 260 mV for **128,** which indicates good communication of the metals through the bridging ligand. Molecular models suggested a distance of *ca.* 6.0Å for the dinuclear complexes **126**, **127** and **128**.

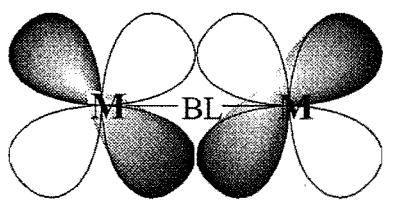

BL represents a bidentate bridging ligand, such as 2,2'-bipyrimidine or 2,2'-biimidazolate.

Fig. 5.41

As mentioned in the introduction to this chapter, the ligands **91** and **94** have a structural similarity to **96** and **97**. However, the replacement of the central diazine rings with a heterodiazole would alter the distance between the metals (more so in the case of **96**), and importantly the electronic nature of the bridge. The degree of aromaticity of the bridge has

been postulated to facilitate interaction between the metals. As was mentioned previously, the 1,2,5-oxadiazoles are only 'aromatic' in that they contain 6 π electrons, with the oxygen atom contributing little of its electron density into the ring,[225] and the heterocyclic 1,2,5-oxadiazole system is perhaps better described as being diene-like. The thiadiazoles may be, because of the greater polarisability of the larger sulfur atom, a more delocalised system. However, this being the case, the low aromatic character of the bridge has not restricted the electronic communication between the metals. In fact, on the basis of the electrochemical results obtained, the low aromatic character has served to facilitate the interaction!

Two dinuclear ruthenium complexes were also prepared using ligand **95**. Refluxing **95** with 3-4 equivalents of $Ru(dmb)_2Cl_2$ or $Ru(bpy)_2Cl_2$ gave the dinuclear complexes $[(dmb)_2Ru(\mathbf{95})Ru(dmb)_2]^{4+}$, (**129**), and $[(bpy)_2Ru(\mathbf{95})Ru(bpy)_2]^{4+}$, (**130**), respectively, which were isolated as the hexafluorophosphate salts. None of the possible trinuclear ruthenium complexes were formed. This is perhaps indicative of a transoid or orthogonal conformation between the thiadiazole rings, due to the free rotation about the 3,3'-inter-ring bond. The dinuclear complexes exist as shown in Fig 5.42. Both complexes were formed in excellent yields by the standard 3:1 ethanol/water method (Table 5.18).

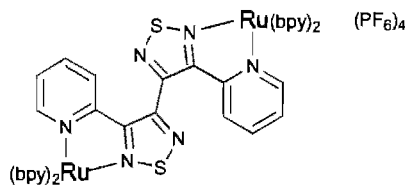

130

Fig. 5.42

Table 5.18

Complex	Reflux time (Hrs)	Yield (%)
129	18	95
130	18	96

The aromatic region of the ^1H NMR spectrum of complex **129** is shown in Fig. 5.43. By irradiation of the most downfield doublet at 8.12 ppm in a 1-D TOCSY experiment, only one ring for the ligand was identified in the spectrum. This indicates that if the meso and racemic diastereoisomers have formed, they must have the same influence upon the rings of the ligand. The chemical shifts and coordination induced shifts for **129** and **95** are listed in Table 5.19. Due to the unusually highfield position of the pyridine H6 protons in the ligand **95**, the CIS of the H6 protons in the complex **129** is smaller than that usually observed for such ruthenium complexes. The H4 protons of the complex also show a smaller than usual shift, and this is again due to one of the effects of π back donation or σ donation dominating the other.

Table 5.19 ^{1}H NMR Chemical Shifts[a] and Coordination Induced Shifts[b] for **129** and **95**.

	H3	H4	H5	H6
129	8.12	7.92	7.51	7.86
95	7.97	7.74	7.20	8.10
CIS	0.15	0.18	0.31	-0.24

[a] For deuterated acetonitrile solutions. [b] CIS = ($\delta_{complex}$ - δ_{ligand}).

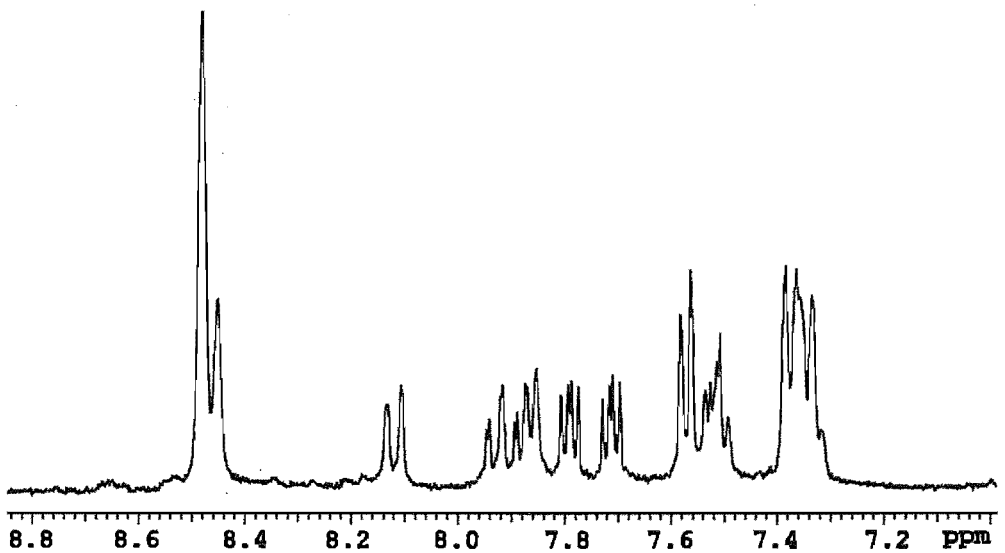

Fig. 5.43 ^{1}H NMR spectrum of $[(bpy)_2Ru(\mathbf{95})Ru(bpy)_2](PF_6)_4$ (**129**).

The ^{1}H NMR spectrum of complex **130** was too difficult to assign. The ^{1}H NMR spectrum effectively contains ten different 2-substituted pyridine rings, five for each diastereoisomer, all of the signals of which appear to be overlapped in the spectrum. To determine which of these signals were due to the thiadiazole-containing ligand was not possible. It is reasonable to expect that the chemical shifts in **130** would be similar to those of **129**. One technique that has been used with success in cases such as this, is the replacement of bpy with d_8-bpy. The drawbacks of this technique are the high cost of d_8-bpy and the loss of information that other protons in the spectrum carry. Characterisation of **130** was by FABMS and elemental analysis, both of which confirmed a dinuclear complex.

The UV-visible spectrum of **129** (Fig. 5.44) shows a λ_{max} at 471 nm whereas in the mononuclear complex it is at 454 nm. This suggests that the metal-metal interaction is smaller in complex **129** than in the complex **126**, for which the λ_{max} was 531 nm. The (M)d—(bpy)π^* transition is also evident at 420 nm and is less intense than the MLCT transition into the bridging ligand.

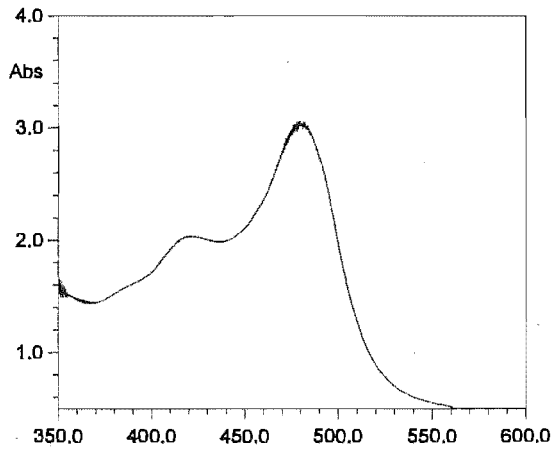

Fig. 5.44 UV-visible spectrum of $[(bpy)_2Ru(\mathbf{95})Ru(bpy)_2](PF_6)_4$ (**129**).

The electrochemical investigations of complexes **129** and **130** are summarised in Table 5.20, while the cyclic voltammogram for complex **130** is shown in Fig. 5.45. Both complexes undergo simultaneous two-electron oxidations, meaning the metal-metal interaction is small. In the negative potential region, the first two reduction waves are closely spaced, and are assigned to the bridging ligand **95** in each complex. Perhaps the first added electron has the effect of influencing the second, making the latter slightly harder to add to the bridging ligand. The complexes then undergo a third reduction process, most likely a two-electron reduction, that is irreversible, and at which point adsorption processes at the electrode surface are encountered, as evidenced by the stripping curve in the voltammogram.

The complex **129** has a lower oxidation potential, which is again attributable to the electron donating methyl groups of the auxiliary dmb ligands. This difference is primarily responsible for the smaller $E_{ox\text{-}red1}$ value of **129** compared to **130**. As the distance between the two metals has increased, the metal-metal interaction has decreased. This result has been seen for many dinuclear ruthenium complexes, including those of 2,2':4',4":2",2'"-quaterpyridine (**98**),[76,192] where the metal-metal interaction is diminished relative to those containing the bridging ligands **96** and **97**, which have smaller internuclear distances. Also, the metal-metal interaction may be decreased as a result of rotation about the 3,3'-inter-ring bond, which disrupts a planar π system of the ligand, precluding mediation *via* the bridging ligand.

Table 5.20 Redox Potentials[a] of complexes **129** and **130**.

	E_{ox}	E_{red1}	E_{red2}	E_{red3}	$E_{ox\text{-}red1}$
129	+1.31[b]	-1.02	-1.14	-1.75[c]	2.33
130	+1.41[b]	-0.98	-1.10	-1.62[c]	2.39

[a] In volts *vs* SCE in acetonitrile. [b] Two-electron process. [c] Irreversible reduction.

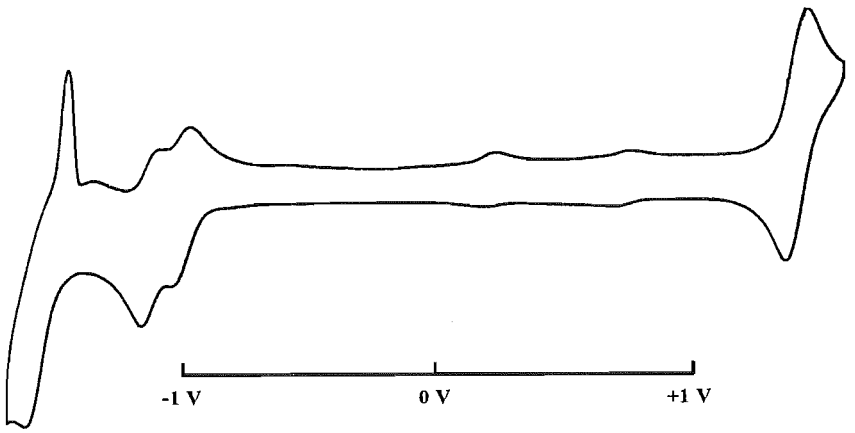

Fig. 5.45 Cyclic voltammogram of $[(bpy)_2Ru(\mathbf{95})Ru(bpy)_2](PF_6)_4$ (**130**).

5.5 Heterodinuclear Complexes

The mononuclear complexes **109**, **110** and **111** are amenable for the construction of heterodinuclear complexes. As a further investigation, some heterodinuclear ruthenium/palladium and ruthenium/platinum complexes were prepared and examined.

The first attempt at preparing a dinuclear ruthenium-palladium complex was by adding a methanolic solution of Li_2PdCl_4 to complex **111** dissolved in hot acetone/ethanol. An immediate precipitate formed and was collected by filtration. FABMS showed that the precipitated complex was the chloride salt, (**131**), formed by the reaction shown below.

$$Li_2PdCl_4 + [(bpy)_2Ru(\mathbf{94})](PF_6)_2 \longrightarrow [(bpy)_2Ru(\mathbf{94})PdCl_2]Cl_2 + 2LiPF_6$$

Complex **131** is sparingly soluble in acetonitrile, and a ^1H NMR spectrum was recorded in deuterated solvent. The spectrum of **131** is shown in Fig. 5.46, and the relevant NMR data for **131** are shown in Table 5.26. The appearance and position (9.38 ppm) of a pyridine H6 proton (H6') easily distinguished the pyridine ring of the thiadiazole-containing ligand coordinated to palladium. The chemical shifts of the other protons of this ring were found by 1-D TOCSY from the irradiation of this signal. Interestingly, the H3 proton of this ring (H3') was more upfield than expected. Irradiation of another isolated signal in the spectrum, at 7.68 ppm, provided the other ring of the ligand. This ring too had a signal for H3 that was at unusually high field. With both H3 protons of the complex being shielded, the pyridine rings of the ligand were proposed to be providing the ring-current anisotropy shielding the H3 proton of the other ring (Fig. 5.47).

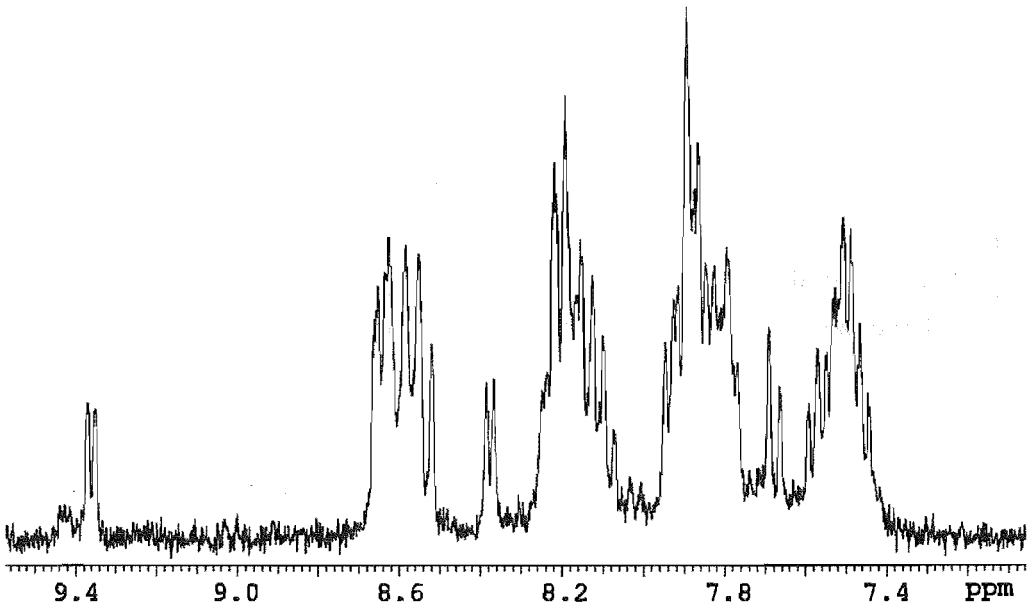

Fig. 5.46 ^{1}H NMR spectrum of $[(bpy)_2Ru(\mathbf{94})PdCl_2]Cl_2$ (**131**).

Table 5.26 ^{1}H NMR Chemical Shifts[a] and Coordination Induced Shifts[b] for **94** and **131**.

	H3	H4	H5	H6	H3'	H4'	H5'	H6'
131	7.68	7.86	7.46	7.93	7.87	8.21	7.79	9.35
94[c]	7.82	7.91	7.43	8.47				
CIS	-0.14	-0.05	+0.03	-0.54	+0.05	+0.30	+0.36	+0.88

[a] For deuterated acetonitrile solutions. [b] CIS = ($\delta_{complex}$-δ_{ligand}). [c] The free ligand in solution shows 2-fold symmetry; hence H3 = H3'.

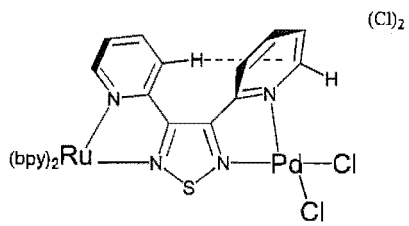

131

Fig. 5.47

By the preparation and ^{1}H NMR characterisation of the ruthenium-palladium complex, $[(dmb)_2Ru(\mathbf{91})PdCl_2]Cl_2$ (**132**), starting with the 4,4'-dimethyl-2,2'-bipyridine precursor **110**, the signals assigned to the rings of the thiadiazole ligand in complex **131** were confirmed by comparison. The relevant ^{1}H NMR data for complex **132** is given in Table 5.27. Importantly, the CIS values show a good correlation to those found above.

Table 5.27 ^{1}H NMR Chemical Shifts[a] and Coordination Induced Shifts[b] for **91** and **132**.

	H3	H4	H5	H6	H3'	H4'	H5'	H6'
132	7.88	7.93	7.52	7.88	8.06	8.26	7.85	9.33
91[c]	7.91	7.97	7.53	8.60				
CIS	-0.03	-0.04	-0.01	-0.72	+0.15	+0.39	+0.32	+0.73

[a] For deuterated acetonitrile solutions. [b] CIS = ($\delta_{complex}$-δ_{ligand}). [c] The free ligand in solution shows 2-fold symmetry; hence H3 = H3'.

In order to perform electrochemical measurements the chloride anion needed to be exchanged for a non-redox active counterion, and this was attempted using a metathesis reaction. The chloride salt was suspended in water, containing an excess of NH_4PF_6, and stirred for two days. However, FABMS indicated the presence of chloride counterions and no satisfactory elemental analyses were obtained. To alleviate this problem a different method of synthesis was used.

When an equimolar amount of bis(benzonitrile)dichloropalladium [$(PhCN)_2PdCl_2$] in chloroform was added to mononuclear ruthenium complex **111** dissolved in dichloromethane at room temperature, a product precipitated out of solution in near quantitative yield. FABMS of the resulting solid gave a molecular ion that suggested the complex contained a $PdCl_2$ fragment as well as a coordinated benzonitrile and so was formulated as [$(bpy)_2Ru$(**94**)$Pd(PhCN)Cl_2$]$(PF_6)_2$, (**133**). A ^{1}H NMR spectrum in deuterated acetonitrile showed that **133** had some very similar chemical shifts compared to the precursor ruthenium complex. In particular, the H6 of the uncoordinated ring and the H3 of the coordinated ring had both changed very little in chemical shift. Therefore the resulting complex was proposed as shown in Fig. 5.48, where the palladium has coordinated to the N5 of the thiadiazole in a monodentate fashion. Importantly, the complex still contains an uncoordinated pyridyl ring, which is consistent with the chemical shifts observed.

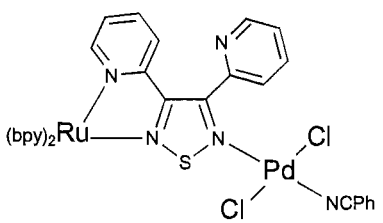

133

Fig. 5.48

When the reaction conditions are changed to refluxing acetone/ethanol the desired chelating complex, **134**, is formed. Also, the complex **133** could be converted to the **134** by the same conditions (Scheme 5.7).

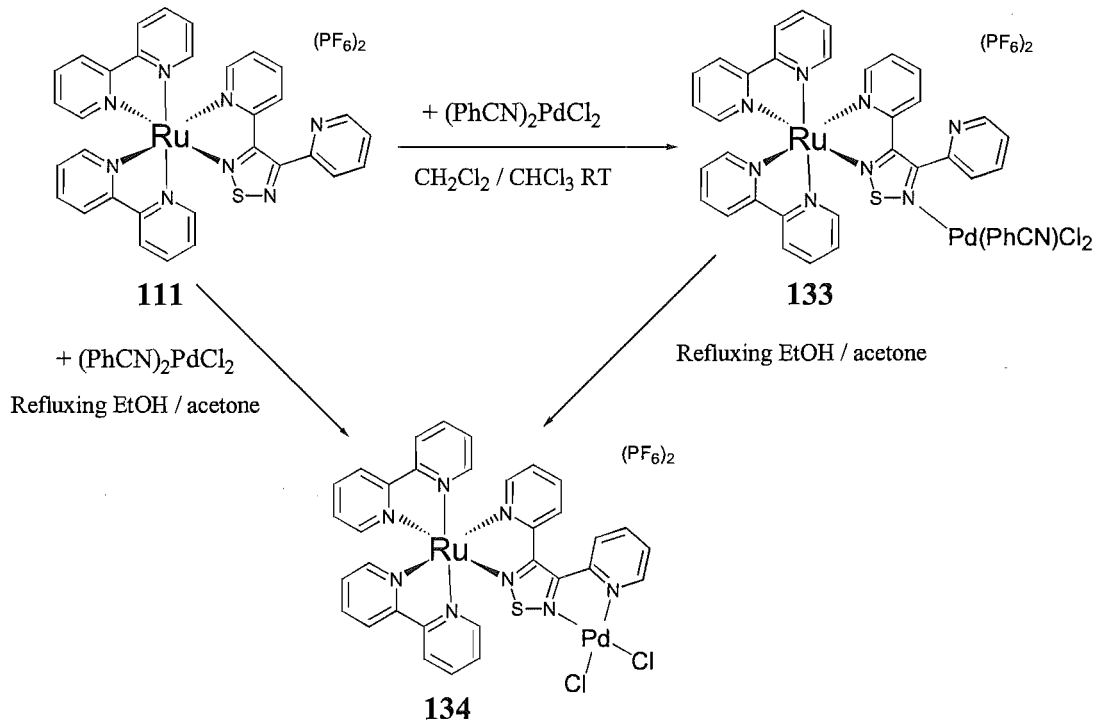

Scheme 5.7

A ruthenium-platinum complex was prepared by reacting equimolar amounts of the mononuclear ruthenium complex **111** with $(DMSO)_2PtCl_2$ in acetone/nitromethane at room temperature (Scheme 5.8). Careful inspection of the ^1H NMR spectrum revealed that a downfield H6 proton was close in chemical shift to the ruthenium precursor, and this indicated that the complex formed contained an uncoordinated pyridine ring of the ligand. This proton was irradiated in a 1-D TOCSY experiment and the chemical shifts of all protons of the ring did not suggest coordination. Also, the presence of DMSO was observed in the spectrum. The FAB mass spectrum of this complex indicated coordinated DMSO and elemental analysis confirmed this. As above it seemed the metal fragment was coordinated to the thiadiazole N5 in a monodentate fashion. The complex was then heated at reflux in ethanol/nitromethane, in the hope of converting it to the desired chelating complex. However, FABMS again indicated the presence of coordinated DMSO. Accordingly, the complex was formulated as $[(bpy)_2Ru(\mathbf{94})PtCl_2(DMSO)](PF_6)_2$ (**136**). The H6 proton of the pyridyl ring coordinated to the platinum was identified in the spectrum by its appearance and downfield position (9.07 ppm). This proton had changed in chemical shift and suggested another mode of coordination. Irradiation of this signal gave the chemical shifts of the other protons of the ring. From the CIS values of this ring (Table 5.22), in particular H4', it was deduced that the platinum fragment was now coordinated to the pyridine ring. The proton signals for the other pyridine ring of the thiadiazole-containing ligand was found by irradiation of a downfield signal at 8.86 ppm in a 1-D TOCSY experiment. In general, the signals for the bpy ligands were grouped together in the ^1H NMR spectrum with considerable overlap. No attempts to assign any of the individual bpy ring systems were therefore made.

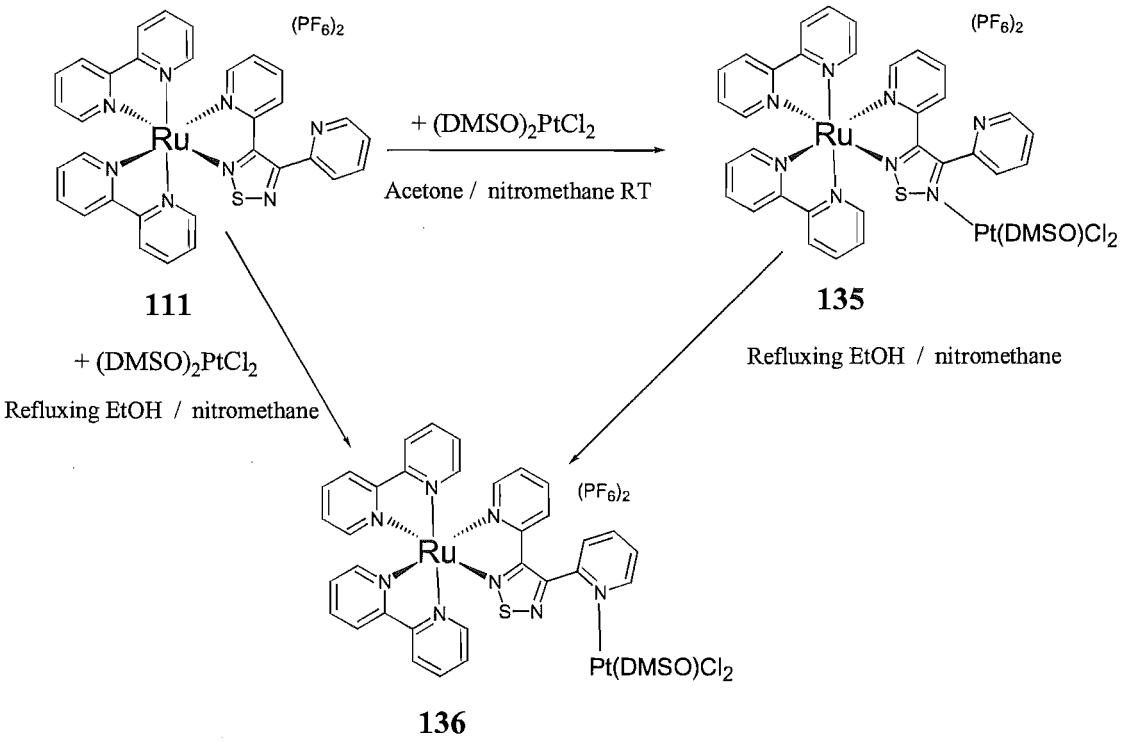

Scheme 5.8

Table 5.22 ^{1}H NMR Chemical Shifts[a] and Coordination Induced Shifts[b] for **94** and **136**.

	H3	H4	H5	H6	H3'	H4'	H5'	H6'
136	8.86	8.25	7.62	7.95	8.76	8.50	7.83	9.07
94[c]	7.82	7.91	7.43	8.47				
CIS	+1.04	+0.34	+0.19	-0.52	+0.94	+0.59	+0.40	+0.60

[a] For deuterated acetonitrile solutions. [b] CIS = ($\delta_{complex}$-δ_{ligand}). [c] The free ligand in solution shows 2-fold symmetry; hence H3 = H3'.

Both H3 and H3' show the effect of being deshielded and are moved downfield. This may be as a result of the pyridine coordinated to the platinum existing in the conformation shown in Scheme 5.8. The CIS value of H4' reflects the strong effect of σ-donation, when the metal does not participate in back-bonding. This difference is illustrated in the comparison of the CIS values of H4 with H4'. The CIS value of the H4 proton is tempered with the effect of back-bonding, resulting in a smaller CIS value of +0.34. Complex **136** was also prepared directly from **111**, as shown in Scheme 5.8.

The incorporation of the $PtCl_2$(DMSO) fragment has a marked effect on the UV-visible spectrum of the complex. The UV-visible spectrum (Fig. 5.46) of **136** shows three MLCT transitions. The transitions occur at 514 nm, 458 nm and 423 nm and are assigned, based on previous complexes, to the (M)d—(L) π*, (M)d—(bpy)π* and (M)d—(L) π* transitions, respectively. The influence of the platinum is to induce another MLCT transition at lower energy. As this transition is at 514 nm, this suggested that the electrochemistry

would show a first reduction of the bridging ligand at a potential close to that of the homodinuclear ruthenium complex **128** (λ_{max} 531 nm).

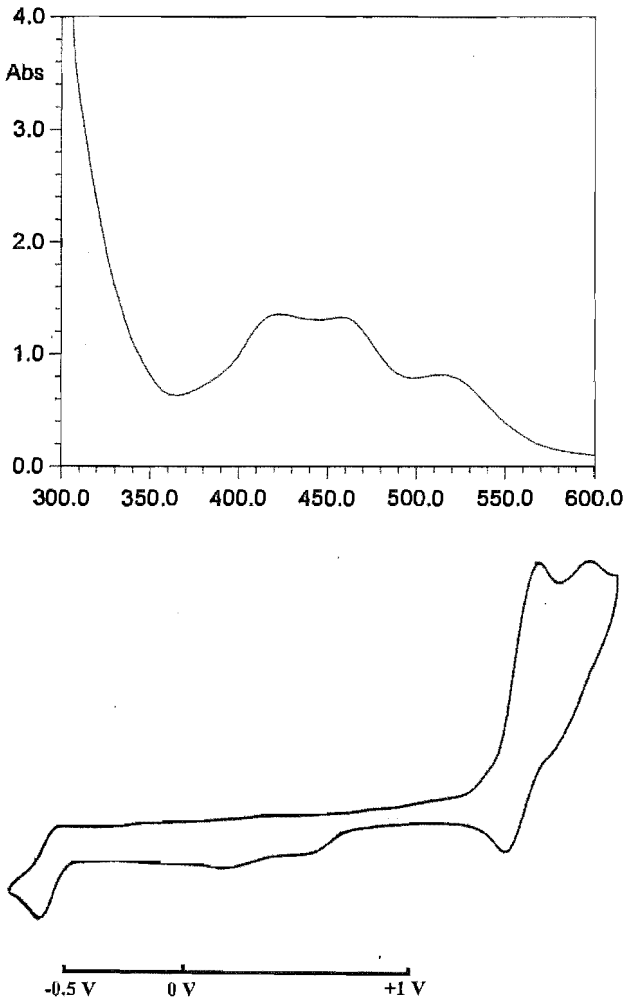

Fig. 5.46 UV-visible spectrum and cyclic voltammogram of $[(bpy)_2Ru(\mathbf{94})PtCl_2(DMSO)](PF_6)_2$ (**136**).

Indeed, the cyclic voltammogram of complex **136** (Fig. 5.46) did show an irreversible first reduction of the bridging thiadiazole-containing ligand (-0.60 V) at a potential close to that of the homodinuclear ruthenium complex (-0.62 V). The platinum atom undergoes a two-electron oxidation at +1.41 V, and surprisingly this is a reversible process. For a related heterodinuclear ruthenium/platinum complex, with **96** as the bridging ligand, this redox process is irreversible.[246] The oxidation potential of the ruthenium atom is at +1.67 V, which is similar to the second oxidation potential of the homodinuclear ruthenium complex **128**.

5.6 Summary

This chapter has included the syntheses of four new ligands, 3,4-di(2-pyridyl)-1,2,5-oxadiazole **91**, (1,2,5-thiadiazol-3-yl)pyridine **93**, 3,4-di(2-pyridyl)-1,2,5-thiadiazole **94**, and 4,4'-di(2-pyridyl)-3,3'-bi-1,2,5-thiadiazole **95**. Also the attempted preparations of two other 1,2,5-oxadiazole-containing ligands were discussed. The three thiadiazoles were synthesised following a procedure recently described by Rees *et al.*, thereby extending this method. Ligand **95** was also studied in the solid state by X-ray diffraction and was found to exist with an approximately orthogonal relationship between the 1,2,5-thiadiazole rings. A silver nitrate complex was prepared with one of the ligand precursors - 1,4-di(2-pyridyl)buta-1,3-diyne **103**, and characterised crystallographically, resulting in the discovery of a metallopolymeric structure. This is the first example of a metal complex using this molecule as a ligand.

Also incorporated into this study was the known molecule 3,4-di(2-pyridyl)-1,2,5-oxadiazole-2-oxide **99**. This ligand was found to undergo a new RORC reaction mediated by the $Ru(bpy)_2^{2+}$/$Ru(dmb)_2^{2+}$ cations, which resulted in the formation of complexes containing a pyrazolo[1,5-*a*]pyridine ligand. The resulting complexes were studied and the pyrazolo[1,5-*a*]pyridine system was found to lower the first reduction potential of the ligand in the complexes when compared to $Ru(bpy)_3^{2+}$. Presently, we are unaware of any other complexes containing this ring system having been studied. Palladium and copper complexes were subsequently prepared with **99** and, by a combination of ^1H NMR and X-ray crystallography, were found to form seven-membered chelates in preference to a possible five-membered chelate. By the preparation of palladium and copper complexes with structurally related ligands (**91** and **94**) this was found to be a general phenomenon.

The ligands **91**, **93** and **94** were shown to be able to form five-membered chelates in the work with the $Ru(bpy)_2^{2+}$ cation and for Pd(II) with **93**. The results for the $Ru(bpy)_2^{2+}$ cation are in no doubt related to the steric requirements placed upon complex formation by the existing metal complex. The seven-membered chelate, with its large bite-angle at the metal atom, is simply unable to fit into the space available. The UV-visible spectroscopy and electrochemical measurements provided insight into the electronic nature of the heterocyclic systems and the ruthenium complexes. For these complexes, the oxidation potential is raised considerably by the incorporation of just one heterodiazole ring. For example, the complex $[Ru(bpy)_2(\mathbf{91})](PF_6)_2$ **109** undergoes metal-based oxidation at +1.53 V, which is 270 mV higher than in $Ru(bpy)_3^{2+}$ (+1.26 V). The heterodiazole ligands are also more easily reduced than bpy in the complexes, highlighting their electron deficient nature.

A factor previously considered important for electronic communication in dinuclear complexes is the aromaticity of the bridge. Although *ab initio*[225] studies suggest the 1,2,5-oxadiazole ring contains little aromatic character, the dinuclear ruthenium complexes bridged

by a 1,2,5-oxadiazole ring were found to allow good electronic communication, as evidenced by the ΔEp values. An important electrochemical difference in some of the ruthenium complexes prepared, was the reversibility of the reductions of the heterodiazole ligands. In particular, strict irreversibility of the 1,2,5-oxadiazoles and the sometimes reversible behaviour of the 1,2,5-thiadiazoles were observed. An attempt to explain this behaviour was made by preliminary *ab initio* calculations.

Chapter 6

Conclusions and Prospects

The work described in this thesis involved previously little-studied heterocyclic systems contained in chelating multidentate ligands. The aim of this work was to gain insight into the nature of these heterocyclic systems by the preparation and study of their metal complexes. The effects of the $Ru(bpy)_2^{2+}$ unit are well understood, and this moiety was used as a template in this work, serving as a basis for comparison and examination. By the preparation of complexes with other metal ions, having different geometrical preferences, the metallosupramolecular chemistry with many ligands was also investigated.

^1H NMR spectroscopy proved a useful tool in the characterisation of the many ruthenium and palladium complexes produced in this work. The use of ^1H nOe and 1-D TOCSY experiments was crucial for determination of the structures of such complexes. From the calculation and subsequent interpretation of proton CIS values, which required unambiguous assignment of ^1H NMR spectra, the nature of the metal-ligand interaction was probed. The electronic nature of the metal-ligand interaction in the ruthenium complexes was further investigated with UV-visible spectroscopy and cyclic voltametric measurements. The technique of X-ray crystallography was able to provide direct structural assignment for twenty complexes, and was also used to study the solid state conformations of molecules containing a biheterocyclic unit or subunit.

As the heterocyclic systems investigated in Chapters 2 and 3 are sufficiently different from the heterodiazoles of Chapters 4 and 5, conclusions about them will be drawn separately. In Chapter 2, the benzo-fused benzoxazole, benzisoxazole, and benzothiazole systems were studied for a combination of new and known ligands. We felt a study of the parent biheterocyclic ligands, when chelated to $Ru(bpy)_2^{2+}$, would provide the effects due solely to the heterocyclic systems. The studies of the benzoxazole and benzothiazole biheterocycles proved successful, and the effects due to the heterocyclic systems were determined, and were found to have significantly different properties from those of bpy. This now allows ligands containing these heterocyclic systems to be designed with these properties in mind.

We were also interested in a comparison of the benzoxazole ring with the 1,2-benzisoxazole ring. Although the biheterocycle 3,3'-bi-1,2-benzisoxazole (**5**) could not be synthesised, some feeling about the nature of the isomeric ring systems was gained from the synthesis and study of 3-(2-pyridyl)-1,2-benzisoxazole (**6**). The important differences were

that the 1,2-benzisoxazole-containing ligand raised the oxidation potential of the ruthenium complex more than the benzoxazole-containing ligand and also proved to be electrochemically unstable. Notable by its absence was any investigation into the 1,2-benzisothiazole system in this study, and this area remains unexplored. Also there has been little study of ruthenium complexes involving isoxazoles or isothiazoles and together these still represent a gap in the literature.

The benzotriazole system was examined in Chapter 3, with the investigations of five 1-substituted benzotriazole-containing ligands. The main feature from this study was that the 3-position of the triazole ring was the preferred nitrogen for coordination. This disposed the ligands to act in bridging fashions, rather than the desired chelating mode. However, ligands containing the benzotriazole system were able to be forced to chelate, and the study of these complexes provided an insight into the electronic nature of the 1-substituted benzotriazole ring. Ligands containing a 2-substituted benzotriazole have received little attention. A study of such ligands would provide an interesting comparison between the 1- and 2-substituted benzotriazole ring. This is an opportune area for further study.

An interesting comparison between Chapters 2 and 3 is that of 3-(2-pyridyl)-1,2-benzisoxazole (**6**) and 1-(2-pyridyl)benzotriazole (**27**). These ligands are isoelectronic, but analysis of their respective electrochemical properties (Table 6.1) of their ruthenium complexes, **13** and **35**, (Fig. 6.1) reveals very different behaviour.

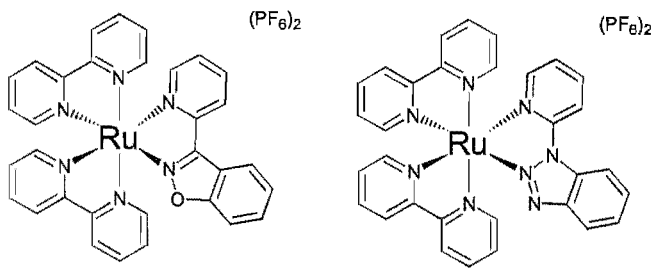

13 **35**

Fig. 6.1

Table 6.1 Redox Potentials[a] of **13** and **35**.

	E_{ox}	E_{red1}	E_{red2}	E_{red3}	$\Delta E_{ox\text{-}red1}$
$Ru(bpy)_3^{2+}$	+1.26	-1.33	-1.51	-1.75	2.59
$Ru(bpy)_2(\mathbf{6})^{2+}$ (**13**)	+1.36	-1.01[b]	-	-	2.37
$Ru(bpy)_2(\mathbf{27})^{2+}$ (**35**)	+1.53	-1.39	-1.60	-	2.92

[a] In volts *vs* SCE in acetonitrile. [b] Irreversible reduction.

The effect of both heterocyclic systems is to reduce electron density on the ruthenium atom, and therefore raise the oxidation potential of the respective complexes, relative to $Ru(bpy)_3^{2+}$. Interestingly, the triazole has done so more than the isoxazole. With regards to

the reductions of the ligands **6** and **27** in the complexes, the difference is even more pronounced. The first reduction of complex **13** is attributed to that of ligand **6**, while no reduction was attributed to the ligand **27** in complex **35**, as the two observed reductions are assigned to the bpy ligands. The combined result of these effects is manifested in the $\Delta E_{ox\text{-}red1}$ values. As the metal atom is less electron-rich and the benzotriazole-ligand harder to reduce, complex **35** has a very large $\Delta E_{ox\text{-}red1}$ value 2.92; and although the incorporation of the 1,2-benzisoxazole ring has raised the oxidation potential of the complex, the 1,2-benzisoxazole-containing ligand is much more easily reduced than bpy, giving the smaller $\Delta E_{ox\text{-}red1}$ value, relative to $Ru(bpy)_3^{2+}$, of 2.37. These examples demonstrate how one can control the physicochemical properties of such complexes.

The latter half of this work focused on two isomers of the heterodiazoles - the 1,2,4-systems and the 1,2,5-systems. The aims for these chapters were twofold; firstly, to study the effects due to the heterocyclic systems in mononuclear complexes and, secondly, to examine metal-metal interactions in dinuclear complexes containing these types of ligands. Very little previous study has been conducted on complexes with heterodiazole-containing ligands. Accordingly, they are currently not well understood.

The study of Chapter 4 found that the 1,2,4-oxadiazole ring is not robust, and is therefore not suitable for the construction of polynuclear ruthenium complexes. Indications of a preference for N4 coordination were seen for the 1,2,4-oxadiazole ring. In contrast, the 1,2,4-thiadiazole ring proved to be much more stable, and was found to impart significantly different properties to complexes relative to bpy. Thus, it is a useful component for incorporation into chelating ligands.

A complex studied in Chapter 4, $[Ru(bpy)_2(\mathbf{65})](PF_6)_2$ (**84**), can be compared to a complex studied in Chapter 5, $[Ru(bpy)_2(\mathbf{93})](PF_6)_2$ (**108**), both of these complexes are shown in Fig. 6.2, and their respective electrochemistry summarised in Table 6.2. These complexes differ only in the transposition of CH and S subunits.

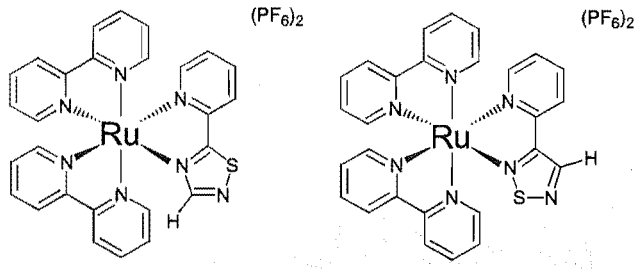

84 **108**

Fig. 6.2

Table 6.2 Redox Potentials[a] of **84** and **108**.

	E_{ox}	E_{red1}	E_{red2}	E_{red3}	$\Delta E_{ox\text{-}red1}$
$Ru(bpy)_3^{2+}$	+1.26	-1.33	-1.51	-1.75	2.59
$Ru(bpy)(\mathbf{65})^{2+}$ (**84**)	+1.29	-1.02	-1.58	-1.92	2.31
$Ru(bpy)(\mathbf{93})^{2+}$ (**108**)	+1.36	-1.19	-1.55	-	2.55

[a] In volts *vs* SCE in acetonitrile.

Clearly, the introduction of these heterocyclic systems has had a dramatic effect electrochemically. The incorporation of just one heterodiazole ring into the complexes has altered the properties of the resulting complex relative to $Ru(bpy)_3^{2+}$. The metal atoms in **84** and **108** are less electron-rich than in $Ru(bpy)_3^{2+}$, as the oxidation potential is higher in each case, and in turn, the metal atom in **108** is significantly less electron rich than in **84**. Somehow the 1,2,5-thiadiazole has reduced the electron density on the metal more than the 1,2,4-thiadiazole. At this time we suspect this effect is primarily due to the donor strength of the coordinating nitrogen, and therefore may show a correlation to pKb measurements. As reductions in such complexes have been shown to be ligand localised, this allows a comparison of the reduction potential due to the thiadiazole ligand in each complex. The reduction potentials show that it is easier to add an electron to the 1,2,4-thiadiazole ligand (-1.02 V) than it is to the 1,2,5-thiadiazole (-1.19 V). Obviously, the arrangement of the heteroatoms plays a role in determining the properties of the complex. Thus, this work has demonstrated that subtle variation in ligand structure can result in pronounced changes in physical properties of complexes. To aid the determination of factors responsible for these changes, the preparation of the $Ru(bpy)_2^{2+}$ complexes with the isomeric ligands 2-(1,2,3-thiadiazol-4-yl)pyridine[247] and 2-(1,3,4-thiadiazol-2-yl)pyridine would be valuable.

For a statistical analysis of the complexes produced in this work, a plot of $E_{ox\text{-}red1}$ *vs* λ_{max} was drawn. The values for a dataset of sixty mononuclear ruthenium complexes were taken from the literature[5,6] and a least-squares regression line fitted to this data, resulting in a modest correlation coefficient of 0.71. The 17 mononuclear complexes synthesised and studied in this work are plotted as the triangular points and were not included in the regression analysis.

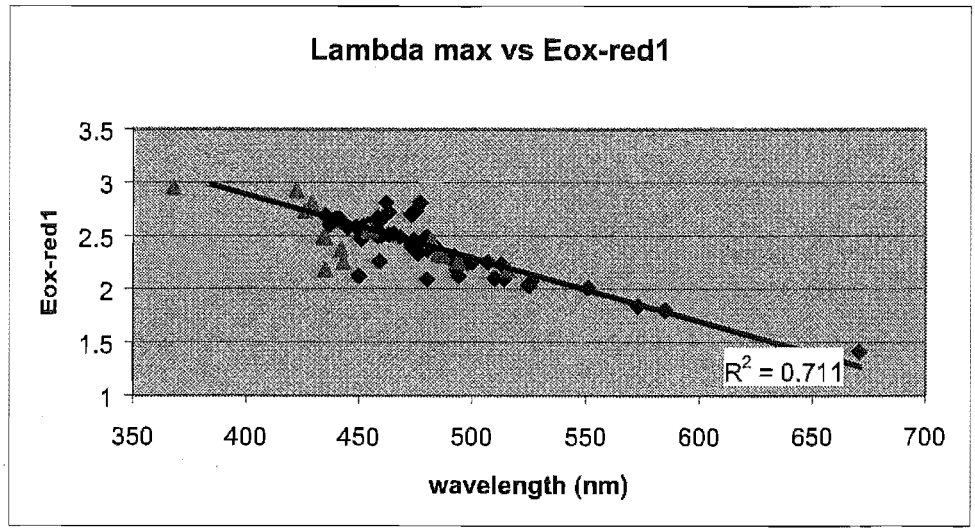

Many of the complexes produced fit nicely to the line of best fit, and inspection of these data points revealed these complexes were of the benzoxazoles and benzothiazoles of Chapter 2, the 1,2,4-thiadiazoles of Chapter 4 and the 1,2,5-thiadiazoles of Chapter 5. At shorter wavelength values (420-430 nm) are the group of three benzotriazole-containing complexes, **35**, **36** and **37**, which also conform reasonably well. The complex having the largest $E_{ox\text{-}red1}$ value is the complex **34**, which contains the chelating 1,1'-methylenebisbenzotriazole ligand, and this complex too shows a reasonable correlation to the projected line.

More interesting, however, are the points that lie well below the line. Clearly these complexes do not conform well. These five data points relate to the 1,2-benzisoxazole-containing complex, **13**, of Chapter 2, the 1,2,5-oxadiazole-containing complexes, **109** and **110**, and the pyrazolo[1,5-*a*]pyridine-containing complexes, **115** and **116**, of Chapter 5. Three of these five complexes contain a nitrogen-oxygen bond in the heterocyclic ligand and, all of these complexes have an irreversible reduction of the ligand. Obviously, the presence of this N-O moiety in the ligands changes considerably the properties of the complexes. A useful comparison would be with isoxazoles, but, as noted above, there is a complete lack of data concerning isoxazole-containing ruthenium complexes in the literature. The pyrazolo[1,5-*a*]pyridine complexes, **115** and **116**, lie farthest from the regression line, representing the largest deviation from the norm. Interestingly the two closest points to these complexes are two other complexes containing pyrazole ligands. This perhaps indicates the unique properties associated with these kinds of heterocyclic systems.

The new dinuclear complexes, **127** and **128**, produced in this work showed large metal-metal interactions, indicating efficient coupling between the metal centres. Although the 1,2,5-oxadiazole system has little aromatic character[225] it mediated strong electronic coupling (ΔEp 340 mV) in the dinuclear complex **127**. The 1,2,5-thiadiazole system also mediated electronic coupling of the metal centres, although not as well as the 1,2,5-oxadiazole

(ΔEp 260 mV for complex **128**). We postulated that the 1,2,5-thiadiazoles are more aromatic in the same way that thiophene is more aromatic than furan. This might suggest that aromaticity is not as important as previously thought. Perhaps, the oxygen and sulfur heteroatoms, in disrupting the aromaticity, enforce the bridge to behave as a diene, facilitating electronic communication *via* this pathway. From this work, it is clear that disubstituted 1,2,5-heterodiazole ligands are useful components to add to the ever-expanding pool of heterocyclic ligands.

The study of Chapter 5 could be extended to include other heterocyclic systems, which retain the desirable structural characteristics of ligands **91** and **94**. 4,5-Di(2-pyridyl)imidazole, 4,5-di(2-pyridyl)-1,2,3-triazole, and 4,5-di(2-pyridyl)-2,1,3-selenodiazole (Fig. 6.3) would be new, interesting, ligands for such a study. As the *ab initio* study by Bean[225] revealed, the incorporation of more nitrogen atoms into a five-membered ring induces more delocalisation; ie. 1,2,3-triazoles are more delocalised than pyrazoles, which is the opposite to what happens in the oxoles due to electronegativity of the oxygen atom. One might expect that the imidazole- and 1,2,3-triazole-containing ligands would show reduction at more negative potentials than the heterodiazoles examined in the present study, while the selenodiazole may be expected to exhibit redox behaviour similar to the heterodiazoles.

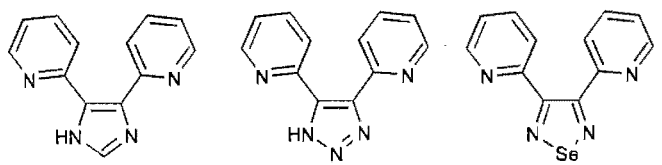

Fig. 6.3

In summary, this study has demonstrated that all the examined heterocyclic systems have imparted different properties to the $Ru(bpy)_2L^{2+}$ complexes, relative to $Ru(bpy)_3^{2+}$. Some of the examined systems seem to be unique, as they are do not conform to the $E_{ox\text{-}red1}$ *vs* λ_{max} relationship found for previously studied complexes. The reasons for this are not immediately obvious, as the heterocyclic systems investigated have had no previous study of this type and, as always in this circumstance, there is no existing model for comparison with experimental results. The use of computational methods, like those described in this work, may provide an important link for systems that are little-studied and hence not well understood.

There are a great many still unexplored heterocyclic systems, and combinations of systems, available for the type of investigation that has been conducted in this study. As the study of the more common heterocycles become exhausted, chemists will surely turn to the more exotic types of systems, similar to those examined here, in search of complexes containing new interesting properties. Thus by the compilation of data on such complexes,

chemists are offered a more diverse choice of molecular components available for incorporation into coordination complexes and supramolecular assemblies.

Chapter 7

Experimental

General Experimental

NMR spectra were recorded on Varian XL 300 or Varian Unity 300 spectrometers with a 3 mm probe and operating at 300 MHz and 75 MHz for ^{1}H and ^{13}C, respectively. ^{1}H NMR spectra recorded in $CDCl_3$ were referenced relative to the internal standard Me_4Si and those recorded in deuterated dimethyl sulfoxide and acetonitrile were referenced against the solvent signals at 2.5 and 2.0 ppm, respectively. ^{13}C NMR spectra recorded in $CDCl_3$ were referenced against the solvent signal at 77.0 ppm and those recorded in dimethyl sulfoxide and acetonitrile were referenced against the solvent signals at 36.8 and 117.7 ppm, respectively. When required, ^{1}H nOe, 1-D TOCSY, COSY, GHSQC and GHMBC experiments were performed using the standard pulse sequences available with the Unity 300 system. Unless otherwise stated the value for the chemical shift is given to the centre of the multiplet.

UV-visible spectra were recorded on a GBC spectrophotometer for *ca.* 0.1 mmol solutions in acetonitrile. Cyclic voltametric measurements were made on a PAR Model 175 Universal Programmer coupled to a PAR Model 173 potentiostat. Measurements were made of acetonitrile solutions containing *ca.* 1 mmol of complex and 0.1 M tetrabutylammonium hexafluorophosphate as the supporting electrolyte, using a scan rate of 100 mVs^{-1} and a glassy carbon electrode (area 0.07 cm^{-2}), with a platinum wire as the auxiliary electrode. Ferrocene was used as an internal standard and potentials are given *vs* the saturated calomel electrode [$E^{o}(Fc/Fc^{+}) = 0.31$ V *vs* SCE].

Mass spectra (EI and FAB) were recorded using a Kratos MS80RFA mass spectrometer with a Mach 3 data system. Electron Impact (EI) spectra were obtained at 70 eV with a source temperature of 250°C. Fast Atom Bombardment (FAB) spectra were acquired in a nitrobenzyl alcohol matrix using an Iontech ZN11NF FAB gun operated at 8 KV and 2 mA. Electrospray mass spectra were recorded using a Micromass LCT TOF mass spectrometer, with a probe operating at 3200 V and cone voltage of 30 V. Samples were dissolved in 1:1 acetonitrile/water, and spectra acquired using source and desolvation temperatures of 80°C and 150°C, respectively.

Infrared spectra were recorded as a solution in $CDCl_3$ using a Shimadzu FTIR-8201PC spectrophotometer. Melting points were determined using an Electrothermal melting point apparatus and are uncorrected. The Chemistry Department, University of Otago, Dunedin performed elemental analyses.

EHMO calculations were performed on a Power Macintosh 6100/600 personal computer with the CAChe Extended Hückel Program from the personal CAChe suite of programs, CAChe Scientific, Oxford molecular group, 1995.

Unless otherwise stated reagents were obtained from commercial sources and used as received. The following compounds were prepared using literature procedures: 3-chlorobenzisoxazole,[56] silver(II) oxide,[248] bis(2,2'-bipyridine)dichlororuthenium,[249] tetrakis(DMSO)dichlororuthenium,[250] bis(benzonitrile)dichloropalladium,[251] 2,2'-diaminoazobenzene,[99-101] 3,3'-bi-1,2,4-oxadiazole (**57**),[148] 5,5'-dimethyl-3,3'-bi-1,2,4-oxadiazole (**58**) and 5,5'-diphenyl-3,3'-bi-1,2,4-oxadiazole (**59**),[149] bis(2-pyridolyl)furoxan (**100**),[204] 2-picolylamidoxime,[147] 2-ethynylpyridine,[216] 1,2-di(2-pyridyl)ethene (**102**),[214] trithiazyl trichloride[218,219] and oxamidoxime.[146]

Preparation of Ligands

2,2'-Bibenzoxazole (1)

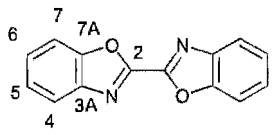

P_2O_5 (12 g) and H_3PO_4 (5 ml) were combined in a 100 ml round bottomed flask. This mixture was heated with stirring at 200°C for 30 minutes. Then resublimed 2-aminophenol (1.80 g, 17 mmol) was added in one portion. The resulting mixture turned deep blue. A reflux condenser was attached and diethyl oxalate (1.0 ml, 7 mmol) was added dropwise. After a brief period the mixture bubbled vigorously. Heating and stirring was continued for 2 hours at 220°C, during which time the colour of the solution had changed to dark orange. The mixture was cooled to *ca.* 100°C and then poured onto ice/water (100 ml). An orange precipitate formed and was collected by filtration and washed well with water. Purification by column chromatography on silica gel with chloroform as the eluant gave pure **1**. M.p. 255-256°C (lit.[44] 257-258°C); Yield 1.0 g (60%). ^{1}H NMR ($CDCl_3$) δ: H4, 7.99; H5, 7.59; H6, 7.65; H7, 7.88. ^{13}C NMR ($CDCl_3$) δ: C2, unrecorded; C3A, 149.95; C4, 120.48; C5, 124.74; C6, 126.51; C7, 110.44; C7A, 140.15.

2,2'-Bibenzothiazole (2)

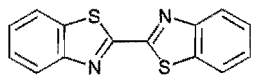

P_2O_5 (12 g) and H_3PO_4 (5 ml) were combined in a 100 ml round bottomed flask. This mixture was heated with stirring at 200°C for 30 minutes, and 2-aminothiophenol (3 ml, 28 mmol) was added in one portion. A reflux condenser was attached and diethyl oxalate (2.0 ml, 14 mmol) was added dropwise. Heating and stirring was continued for 2 hours at 220°C, during which time the colour of the solution had changed to orange. The mixture was cooled to *ca.* 100°C and then poured onto ice/water (100 ml). A light yellow precipitate formed and was collected by filtration and washed well with water. Recrystallisation from dioxane gave **2** as colourless crystals. M.p. 300-301°C (lit.[52] 300-301°C); Yield 0.3 g (8%).

2,2'-Methylenebisbenzoxazole (3)

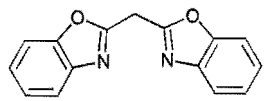

P_2O_5 (12 g) and H_3PO_4 (5 ml) were combined in a 100 ml round bottomed flask. This mixture was heated with stirring at 200°C for 30 minutes, and resublimed 2-aminophenol (1.75 g, 16 mmol) was added in one portion. The resulting mixture turned deep blue. A reflux condenser was attached and diethyl malonate (1.2 ml, 7 mmol) was added dropwise. After a brief period, the mixture bubbled vigorously. Heating and stirring was continued for 1 hour at 220°C, during which time the colour of the solution had changed to dark orange. The mixture was cooled to *ca.* 100°C and then poured onto ice/water (100 ml). A bright yellow precipitate

formed and was collected by filtration, washed well with H_2O, then recrystallised from ethanol/water. M.p. 112-113°C (lit.[53] 115-116°C); yield 0.95 g (54%).

2,2'-Methylenebisbenzothiazole (4)

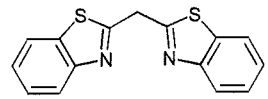

Diethyl malonate (7.5 ml, 0.05 mol) and 2-aminothiophenol (10.7 ml, 0.1 mol) were added to PPA (25 ml) at 70°C with stirring. Heating and stirring were continued for 2 hrs at 140°C, during which time the colour of the solution had changed to an orange. The mixture was cooled to *ca.* 100°C and then poured onto ice/water (200 ml). A canary-yellow precipitate formed and was collected by filtration, washed well with H_2O, then recrystallised from ethanol. M.p. 230-240°C (lit.[252] 240°C); yield 2.5 g (17%).

Attempted syntheses of 3,3'-bi-1,2-benzisoxazole *viz.* 5

***via* $Ni^{(0)}$ coupling:**

In a 50 ml two-necked round bottomed flask was placed $NiBr_2(PPh_3)_2$ (0.242 g, 0.33 mmol), zinc (0.098 g, 1.47 mmol), tetraethylammonium iodide (0.251 g, 0.98 mmol) and a magnetic spin vane. The flask was evacuated by oil pump and heated by heat gun to remove residual traces of water. This cycle was repeated three times, each time flushing the flask with argon. Under an argon atmosphere freshly distilled THF (6 ml) was added *via* syringe through a suba-seal and stirring started. The solution was left to stir for 50 minutes, at which time it was a deep red colour, before 3-chlorobenzisoxazole (0.15 g, 0.33 mmol) was added as a THF solution (2 ml). After *ca.* 5 minutes the solution had turned green. The solution was heated at 50°C and stirred for 20 hours under argon before being poured into 2 M ammonia solution (20 ml). A dark green precipitate was filtered away and a 1:1 benzene/diethyl ether solution (20 ml) added. The organic layer was separated and one more extraction with another 20 ml of benzene/diethyl ether solution was performed. The combined organic extracts were washed with water (2 x 10 ml) and brine (2 x 10 ml) before being dried over Na_2SO_4. The solvents were removed *in vacuo* and a dark brown oily residue was obtained. TLC and ^1H NMR spectra of this material gave no indication of any product that could be identified as **5**. The material was chromatographed on silica gel and the only products that came off the column were identified as PPh_3 and PPh_3O.

***via* tandem intramolecular cyclisation:**

Redistilled 2-methoxybenzaldehyde (5.0 g, 36 mmol) was added to a mixture of ethanol (6.5 ml) and water (5 ml) containing NaCN (0.5 g). The mixture was refluxed with stirring for 2 hrs. After cooling to room temperature the ethanol was removed *in vacuo*. The residue was suspended in ethyl acetate (*ca.* 100 ml), washed with water (3 x 40 ml) and dried

(Na_2SO_4). Removal of the solvent *in vacuo* gave an orange coloured oil. The starting aldehyde was distilled away under reduced pressure and the red residue chromatographed on silica gel (2 x 20 cm) with 20% ethyl acetate:pet. ether as eluent. Combining the relevant fractions and removing the solvents *in vacuo* gave a yellow oil that crystallised on standing to give 2,2'-dimethoxybenzoin. M.p. 93-98°C (EtOH); yield 1.0 g (20%). Positive-ion EI mass spectrum: Calc. *m/z* for $C_{16}H_{16}O_4$ 272.1049; found 272.1051. *m/z* 272.1 (M^+, 11%), 137.1 (MeO-C_6H_4-$CHOH^+$, 92%), 135.0 (MeO-C_6H_4-CO^+, 100%). ^1H NMR ($CDCl_3$) δ: 3.71, s, 3H; 3.72, s, 3H; 4.47, d, (5.8Hz) 1H; 6.10, d, (5.4 Hz) 1H; 6.73-6.78, m, 2H; 6.83, t, 1H; 6.92, t, 1H; 7.13-7.21, m, 2H; 7.36, t, 1H; 7.68, d, 1H.

NH_4NO_3 (0.38 g, 4.8 mmol), $Cu(OAc)_2.2H_2O$ (0.09 g, 0.5 mmol) and 2,2'-dimethoxybenzoin (1.0 g, 3.6 mmol) were placed in a 20 ml round bottomed flask. An 80% solution of aqueous acetic acid (4 ml) was added to the solids and the mixture heated at reflux with stirring for 2.5 hrs then left to cool. The reaction mixture was taken up in ethyl acetate solution (80 ml) and washed with 10% aqueous NaOH (4 x 30 ml), H_2O (1 x 20 ml) and dried (Na_2SO_4). Removal of the solvent *in vacuo* gave a light yellow solid that was recrystallised from ethanol to give pure 2,2'-dimethoxybenzil. M.p. 128-128.5°C; yield 0.94 (94%). Positive-ion EI mass spectrum: Calc. *m/z* for $C_{16}H_{16}O_4$ 270.0892; found 270.0887. *m/z* 270.1 (M^+, 8%), 135.0 (MeO-C_6H_4-CO^+, 100%), ^1H NMR ($CDCl_3$) δ: 3.60, s, 3H; 6.96, d, 1H; 7.12, t, 1H; 7.58, t, 1H; 8.08, d, 1H.

2,2'-Dimethoxybenzil (0.5 g, 1.9 mmol) was dissolved in dry CH_2Cl_2 (35 ml) and cooled to -78°C. Boron tribromide (1.4 ml, 4.0 mmol) was added in one portion to the stirred solution. Immediately, the solution turned bright red and a suspension formed. The stirred mixture was allowed to attain room temperature overnight. In the morning, ice was added to the now yellow solution, and the mixture stirred vigorously for 30 minutes before separating the organic layer, drying (Na_2SO_4), and removing the solvent *in vacuo*. The yellow oil was used immediately without further purification after a ^1H NMR spectrum showed no signal for a methoxy group. Hydroxylamine-O-sulfonic acid (0.52 g, 4.6 mmol) was dissolved in 1:1 methanol/water (4 ml) and added to yellow oil dissolved in ethanol (10 ml). After approximately 10 minutes there was a slight precipitate and the mixture was gently heated at *ca.* 50°C for 30 minutes, at which time the solution was clear. The volume of the solution was reduced by removal of *ca.* ¾ of the solvent *in vacuo* and more H_2O (5 ml) was added. A saturated aqueous solution of Na_2CO_3 was added dropwise to the vigorously stirred solution until the pH was adjusted to 8-9 and dichloromethane (10 ml) was added and the biphasic solution left to stir overnight. In the morning the dichloromethane solution was separated, dried (Na_2SO_4), and the solvent removed *in vacuo* leaving a white solid. However the desired ligand could not be identified in this product.

3-(2-Pyridyl)-1,2-benzisoxazole (6)

To an oven-dried, 25 ml, two-necked flask containing a magnetic stirring bar, was attached a suba-seal and a N_2 gas supply/vacuum line. After flushing the system, 2-bromopyridine (1.0 ml, 10.5 mmol) and dry THF (5 ml) were introduced through the seal and cooled to -78°C. n-Butyllithium (7.25 ml , 11.6 mmol) was added dropwise *via* syringe, and the deep red solution left to stir for 5 minutes. 2-Chlorobenzaldehyde (1.30 ml, 11.5 mmol) in dry THF (2 ml) was added dropwise with stirring at -78°C. The cooling bath was left to evaporate and the stirred solution attained room temperature overnight. In the morning, a saturated solution of aqueous NH_4Cl (*ca.* 10 ml) was added cautiously to the reaction mixture cooled in an ice-bath. This solution was poured into a separating funnel and CH_2Cl_2 (40 ml) added. The organic layer was separated, washed with brine (1 x 20 ml) and H_2O (1 x 20 ml) before being dried over $MgSO_4$. Removal of the solvent *in vacuo* yielded a dark coloured oil. ^1H NMR ($CDCl_3$) δ: 8.57, d, 1H; 7.60, t, 1H; 7.48 t, 2H; 7.30-7.20, m, 4H; 6.28, s, 1H.

To the brown oil thus obtained was added acetone (20 ml). Jones reagent, prepared from CrO_3 (1.59 g, mmol) in H_2O (3 ml) and H_2SO_4 (1 ml), was added dropwise with stirring, and the solution left to stir for 30 minutes. Excess reagent was quenched by the addition of isopropyl alcohol and the solvent then removed *in vacuo*. The brown residue was extracted with ether (3 x 40 ml). The extracts were combined, dried ($MgSO_4$), and then solvent removed *in vacuo* to give a dark coloured oil. Positive-ion EI mass spectrum: Calc. *m/z* for $C_{12}H_8N_2OCl$ 216.0216; found 216.0206. *m/z* 216.0 (M^+, 2.27%), 182.1 (M^+-Cl, 100%), 154.1 (M^+-COCl, 12%), 139.0 (M^+- Py, 31%), 111.0 ($C_6H_4Cl^+$, 22%). ^1H NMR ($CDCl_3$) δ: 8.70, d, 1H, H6; 8.14, d, 1H, H3; 7.90, t, 1H, H4; 7.54-7.38, m, 5H. ^{13}C NMR ($CDCl_3$) δ: 195.19; 153.71; 149.26; 138.11; 137.08; 131.90; 131.55; 129.93; 129.89; 126.98; 126.55; 123.70.

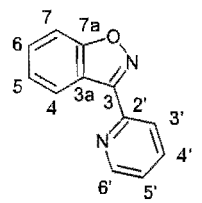

Hydroxylammonium chloride (0.32 g, 4.60 mmol) and NaOH (0.30 g, 7.50 mmol) were dissolved in 1:1 ethanol/water (2 ml) and added to the oil prepared above in a 10 ml round bottomed flask. This mixture was refluxed with stirring for 5 hrs before removing the ethanol *in vacuo,* adding KOH (0.7 g, 12.5 mmol) and more H_2O (1 ml) to the flask and returning it to reflux. After 3 days the flask was cooled to room temperature and the white solid that had formed was filtered and washed with H_2O before being recrystallised from ethanol/water. M.p. 60-62°C; yield 0.40 g (19%) (Found: C, 73.47; H, 4.04; N, 14.57. Calc. for $C_{12}H_8N_2O$: C, 73.46; H, 4.11; N, 14.27). Positive-ion EI mass spectrum: Calc. *m/z* for $C_{12}H_8N_2O$ 196.0637; found 196.0642. *m/z* 196.1 (M^+, 81%), 168.1 (M^+- CO, 64%), 78.0 (Py^+, 100%). ^1H NMR ($CDCl_3$) δ: 8.24, d, 1H, H3'; 7.83, t, 1H, H4'; 7.40, t, 1H, H5'; 8.81, d, 1H, H6'; 8.58, d, 1H, H4; 7.41, t, 1H, H5; 7.59, t, 1H, H6; 7.62, d, 1H, H7. ^{13}C NMR ($CDCl_3$) δ: C2', 156.48; C3', 122.61; C4', 136.76; C5', 124.49; C6', 149.79; C3 not found; C3a, 120.45; C4, 124.99; C5, 124.18; C6, 129.83; C7, 109.57; C7a, 164.06.

1,1'-Bibenzotriazole (23)

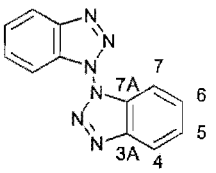

Ligand **23** was prepared from the method of Harder *et al.*[102] ^{1}H NMR ($CDCl_3$) δ: H4, 8.27; H5, 7.58; H6, 7.65; H7, 7.33. ^{13}C NMR ($CDCl_3$) δ: C3A, 144.28; C4, 121.08; C5, 125.82; C6, 130.28; C7, 108.57; C7A, 132.08.

1,1'-Methylenebisbenzotriazole (24)

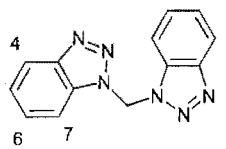

Benzotriazole (2.55 g, 21.4 mmol) and CH_2I_2 (1.70 ml, 21.1 mmol) were added along with a few drops of a saturated tetrabutylammonium hydroxide solution to 50 ml benzene and 40% aqueous NaOH (10 ml) in a 100 ml round bottomed flask. The mixture was vigorously stirred and refluxed for 15 hrs. After cooling to room temperature, 25 ml more benzene was added and the organic layer separated, washed with H_2O, dried (Na_2SO_4), and the solvent removed *in vacuo* to give a white solid. ^{1}H NMR showed that there existed a 6:4:1 ratio of isomers between **24**, 1,2'-methylenebisbenzotriazole (**25**) and 2,2'-methylenebisbenzotriazole (**26**). Recrystallisation from toluene/hexane gave pure **24**. M.p. 185-188°C (lit.[105] 188°C); yield 0.79 g (30%). ^{1}H NMR (CD_3CN) δ: H4, 8.05; H5, 7.46; H6, 7.67; H7, 8.00; CH_2, 7.43.

1-(2-Pyridyl)benzotriazole (27)

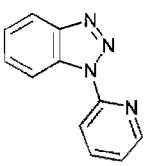

Ligand **27** was prepared following the method of Katritzky,[106] except that 2-chloropyridine was used in place of 2-bromopyridine. Benzotriazole (2.10 g, 17.5 mmol) and 2-chloropyridine (0.83 ml, 8.75 mmol) were refluxed in dry toluene (2 ml) under an atmosphere of N_2 for 19 hrs. The reaction mixture was then suspended in *ca.* 30 ml of ethyl acetate and washed with 5% aqueous KOH to remove the unreacted benzotriazole. Evaporation under reduced pressure yielded **27** as a white solid. M.p. 107-108°C (lit.[106] 110-111°C); yield 1.16 g (67%).

1-[2-Pyridyl(methyl)]benzotriazole (28)

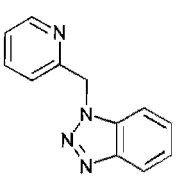

Benzotriazole (1.0 g, 8.4 mmol) and 2-picolyl chloride hydrochloride (1.0 g, 6.1 mmol) were added along with a few drops of a saturated tetrabutylammonium hydroxide solution to benzene (25 ml) and 40% aqueous NaOH (7 ml) in a 100 ml round bottomed flask. The mixture was vigorously stirred and refluxed for 15 hrs. After cooling to room temperature 25 ml more benzene was added and the organic layer separated, washed with H_2O, dried (Na_2SO_4), and the solvent removed *in vacuo* to give a white solid (0.79 g). ^{1}H NMR showed that there existed a 10:1 ratio of isomers between **28** and 2-[2-pyridyl(methyl)]benzotriazole

(**30**). Recrystallisation from toluene gave pure **28**. M.p. 101-102°C (lit.[107] 102-103°C); yield 0.50 g (45%).

1-(1-Isoquinolyl)benzotriazole (29)

Isoquinoline (2.0 g, 15.5 mmol) was added to a solution of glacial acetic acid (10 ml) with 50% H_2O_2 (2 ml). This mixture was refluxed overnight at which time the solution was brown. The glacial acetic acid was removed *in vacuo*, and H_2O (5 ml) was added to the residue. Solid K_2CO_3 was added with gentle swirling until the pH = 8, when the solution turned to solid. The solid was filtered and washed with a small amount of cold H_2O. Upon standing more crystals formed in the filtrate and these were again collected by filtration. M.p. 80-85°C (lit. 103-105°C); yield 1.7 g (76%).

The isoquinoline-N-oxide (1.7 g, 11.7 mmol) obtained was added in small portions with stirring to freshly distilled $POCl_3$ (6 ml) at ice-bath temperature. This mixture was then refluxed for 3 hrs before cooling to room temperature and pouring onto ice (15 g). The resulting solution was made alkaline with 0.880 NH_3 and extracted with CH_2Cl_2 (3 x 10 ml). The organic extracts were collected, dried (Na_2SO_4) and evaporated *in vacuo* to give a brown residue. This was passed through a small column of silica gel to produce a yellow oil that gave white crystals on standing. Yield 0.98 g (50%).

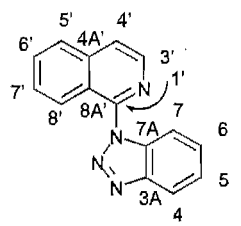

1-Chloroisoquinoline (0.42 g, 2.5 mmol) and benzotriazole (0.61 g, 5.3 mmol) were refluxed in dry toluene (2 ml) under an atmosphere of N_2 for 19 hrs. The reaction mixture was then suspended in *ca.* 30 ml of ethyl acetate and washed with 5% aqueous KOH to remove the unreacted benzotriazole. Evaporation of the solvent under reduced pressure yielded a white solid. Recrystallisation from methanol or benzene gave pure compound. M.p. 151-152°C; yield 0.44 g (70%) (Found: C, 73.07; H, 3.92; N, 22.92. Calc. for $C_{15}H_{10}N_4$: C, 73.15; H, 4.09; N, 22.75). Positive-ion EI mass spectrum: Calc. *m/z* for $C_{15}H_{10}N_4$ 246.0906; found 246.0904. *m/z* 246.1 (M^+, 23%), 218.1 (M^+- N_2, 100%), 128.1 (M^+- Bt, 53%). ^{1}H NMR ($CDCl_3$) δ: H3', 8.58; H4', 7.80; H5', 7.99; H6', 7.81; H7', 7.71; H8', 8.60; H4, 8.21; H5, 7.49; H6, 7.61; H7, 8.08. ^{13}C NMR ($CDCl_3$) δ: C1', 148.18; C3', 140.66; C4', 121.95; C4A', 138.87; C5', 126.95; C6', 131.14; C7', 128.78; C8', 126.25; C8A', 122.84; C3A, 145.93; C4, 119.87; C5, 124.88; C6, 128.86; C7, 112.89; C7A, 133.37.

Attempted synthesis of 5,5'-di(2-pyridyl)-3,3'-bi-1,2,4-oxadiazole *viz.* 60

Picolinic acid (0.50 g, 4.1 mmol) was stirred in $SOCl_2$ (5 ml) for three days at room temperature under an atmosphere of nitrogen. At this time the colour of the solution was a deep red. The excess $SOCl_2$ was removed *in vacuo* and oxamidoxime (0.15 g, 1.2 mmol) dissolved in dry THF (28 ml) was added under nitrogen. After addition the solution was refluxed for a ½ hour and the resulting insoluble product was filtered off (0.47 g). ^1H NMR (d_6-DMSO) δ: H3, 8.38; H4, 8.14; H5, 7.76; H6, 8.70; $-NH_2$, 7.2 (2H).

Polyphosphoric acid was prepared by adding P_2O_5 (12 g) to H_3PO_4 (5 ml) and heating at 200°C for 30 minutes. This solution was allowed to cool to 140°C, and the above material (0.47 g) was added as a solid. After 20 minutes the mixture was poured onto crushed ice (100 g) and made alkaline with 40% aqueous NaOH (pH=8). The aqueous solution was extracted with chloroform (6 x 50 ml), and the combined extracts were dried over Na_2SO_4. The solvent was removed under reduced pressure to yield an off-white solid (0.10 g), which was identified as the monocyclised product. ^1H NMR (d_6-DMSO) δ: H3, 8.26; H4, 8.09; H5, 7.70; H6, 8.80; N-O<u>H</u>, 10.60; -N<u>H</u>$_2$, 6.00. The FAB mass spectrum of this material showed the most intense ion at 206.0 a.m.u. ($C_9H_7N_5O_2$), with another weaker ion at 411.0 a.m.u., which was interpreted as the H-bonded dimer.

Attempted synthesis of 5,5'-bi-1,2,4-oxadiazole *viz.* 61

Formamidoxime (0.50 g, 0.83 mmol) and diethyl oxalate (0.65 ml, 0.42 mmol) were combined in a 10 ml round bottomed flask with a drop of boron trifluoride diethyl etherate. The flask was heated with stirring at 50°C for one hour. The colour of the mixture had changed to a yellow by this time. Ethanol (4 ml) was added to the syrup-like mixture, and by stirring a yellow solid was suspended. This was filtered off (0.22 g) and analysed by ^1H NMR spectroscopy and mass spectrometry. These only showed starting formamidoxime. The filtrate was reduced to an oily yellow residue and ^1H NMR showed that this was mainly diethyl oxalate. This reaction was repeated in differing solvents (toluene and dry ethanol) and with or without catalysts (BF_3 and NEt_3) all with no success.

3,3'-Di(2-pyridyl)-5,5'-bi-1,2,4-oxadiazole (62)

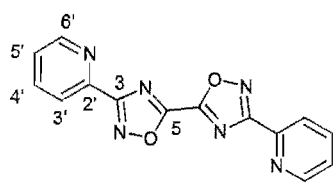

Diethyl oxalate (0.50 ml, 3.7 mmol) was heated with a couple of drops of boron trifluoride diethyl etherate to 160°C in a 5 ml round bottomed flask. 2-Picolylamidoxime (1.0 g, 7.3 mmol) was then added in small portions to the stirred solution. Heating and stirring was continued for 30 minutes at 160°C before the temperature was increased to 200°C. When a white solid started forming, the round bottomed flask was removed from the heat and allowed to cool to room temperature. The solid was rinsed onto a

filter with ethanol and then recrystallised from DMSO. M.p. 265-266°C; yield 0.28 g (26%) (Found: C, 57.80; H, 2.58; N, 28.96. Calc. for $C_{14}H_8N_6O_2$: C, 57.54; H, 2.76; N, 28.76). Positive-ion EI mass spectrum: Calc. for $C_{14}H_8N_6O_2$ 292.0709; found 292.0707. *m/z* 292.1 (M^+, 43%), 146.0 ($C_7H_4N_3O^+$, 14.8%), 104.0 ($PyCN^+$, 100%), 78.0 (Py^+, 25%). ^1H NMR (d_6-DMSO) δ: H3', 8.26; H4', 8.13; H5', 7.71; H6', 8.86.

The ethanolic washings were evaporated to dryness *in vacuo*. The resulting solid was then suspended in ethyl acetate (*ca.* 20 ml), washed with 5% aqueous NaOH (2 x 10 ml), dried (Na_2SO_4) then the solvent evaporated *in vacuo* to give 3,5-di(2-pyridyl)-1,2,4-oxadiazole (0.25 g).

2-(1,2,4-Oxadiazol-3-yl)pyridine (63)

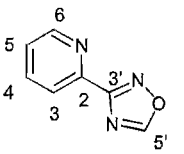

2-Picolylamidoxime (0.50 g, 3.6 mmol) was refluxed in triethyl orthoformate (1 ml) with 1 drop boron trifluoride diethyl etherate for 30 minutes. After cooling to room temperature the white crystalline solid was collected by filtration. Additional product was obtained after concentration of the filtrate. M.p. 108°C (lit.[153] 109-110°C); yield 0.44 g (82%) (Found: C, 57.31; H, 3.19; N, 28.71. Calc. for $C_7H_5N_3O$: C, 57.15; H, 3.43; N, 28.55). Positive-ion EI mass spectrum: Calc. *m/z* for $C_7H_5N_3O$ 147.0433; found 147.0433. *m/z* 147.0 (M^+, 23%), 120.0 ($PyCNO^+$, 13%), 104.0 ($PyCN^+$, 100%). ^1H NMR ($CDCl_3$) δ: H5', 8.86; H3, 8.17; H4, 7.88; H5, 7.46; H6, 8.83. ^{13}C NMR (protonated carbons only) ($CDCl_3$) δ: C5', 165.29; C3, 123.32; C4, 137.10; C5, 125.70; C6, 150.52.

Attempted synthesis of 2-(1,2,4-oxadiazol-5-yl)pyridine *viz.* 64

Picolinamide (0.50 g, 4.1 mmol) and N,N'-dimethylformamide dimethyl acetal(0.58 ml, 4.3 mmol) were combined in a 10 ml round bottomed flask and heated at 50°C for thirty minutes. Hydroxylamine hydrochloride (0.43 g, 6.2 mmol) and NaOH (0.25 g, 6.3 mmol) were dissolved in water (1 ml) and 70% aqueous acetic acid (3 ml), and this mixture added to the solution of the amide and stirred for 15 minutes at 50°C. The reaction mixture was then diluted with more water (3 ml) and left to cool in an ice-bath. The white solid that formed was collected by filtration and recrystallised from water. M.p. 154-155°C; yield 0.47 g (69%). Positive-ion EI mass spectrum: Calc. *m/z* for $C_7H_5N_3O_2$ 165.0538; found 165.0539. *m/z* 165.1 (M^+, 7%), 134.0 (M^+- NOH, 56%), 106.0 ($PyCO^+$, 14%), 78.0 (Py^+, 100%). ^1H NMR ($CDCl_3$) δ: H3, 8.25; H4, 7.92; H5, 7.44; H6, 8.66; 7.86, d, 1H; 10.7, s(br), 1H.

To the material prepared above (0.27 g, 1.6 mmol) was added acetic acid (1 ml) and dioxane (1 ml) and the mixture refluxed for 1 hour. Water (3 ml) was then added, and the mixture left to cool to room temperature overnight. In the morning, white crystals were filtered off and air-dried. The ^1H NMR spectrum of the crystals obtained was different from

that of the starting material and also was not consistent with that of the expected product. The EI mass spectrum was also different from that of the starting material. Elemental analysis of the crystals determined that the composition had not changed. M.p. 180-183°C; yield 0.14 g (51%) (Found: C, 50.66; H, 4.17; N, 25.51. Calc. for $C_7H_7N_3O_2$: C, 50.91; H, 4.27; N, 25.44). Positive-ion EI mass spectrum: *m/z* 165.1 (M^+, 10%), 149.0 (M^+-16, 80%), 122.0 ($PyCONH_2^+$, 65%), 106.0 ($PyCO^+$, 78%), 78.0 (Py^+, 100%). ^1H NMR ($CDCl_3$) δ: H3, 8.26; H4, 7.92; H5, 7.43; H6, 8.67; 10.0, s(br), 1H; 8.25, s(br), 1H; 5.5, s(br), 1H.

2-(1,2,4-Thiadiazol-5-yl)pyridine (65)

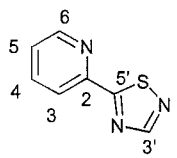

Thiopicolinamide (0.50 g, 3.6 mmol) and dimethylformamide dimethyl acetal(0.48 ml, 3.6 mmol) were combined and allowed to stand in a vial for 35 minutes. A solution made of hydroxylamine-O-sulphonic acid (0.49 g, 4.3 mmol) in methanol (3 ml) and pyridine (0.58 ml, 7.5 mmol) in ethanol (5 ml) was then added. The solution was stirred magnetically at room temperature for 5 hrs. The solvents were then removed *in vacuo* and the residue taken up in *ca.* 25 ml CH_2Cl_2. The CH_2Cl_2 solution was washed with H_2O (1 x 10 ml), 0.1 N NaOH (1 x 10 ml), and once more with H_2O (1 x 10 ml), dried over Na_2SO_4 then concentrated *in vacuo*. The residue was chromatographed on silica gel (1 x 18 cm) with 20% ethyl acetate:pet. ether and **65** (Rf 0.37) was obtained as a canary-yellow solid. M.p. 73-75°C (lit.[130] 68-69°C); yield 0.44 g (75%) (Found: C, 51.56; H, 3.08; N, 25.57; S, 19,92. Calc. for $C_7H_5N_3S$: C, 51.52; H, 3.09; N, 25.75; S, 19.65). Positive-ion EI mass spectrum: Calc. *m/z* for $C_7H_5N_3S$ 163.0204; found 163.0200. *m/z* 163.0 (M^+, 100%), 136.0 (M^+- CNH, 43%), 104.0 ($PyCN^+$, 53%), 78.0 (Py^+, 26%), 59 ($SCNH^+$, 17%). ^1H NMR ($CDCl_3$) δ: H3', 8.75; H3, 8.18; H4, 7.88; H5, 7.43; H6, 8.66. ^{13}C NMR (protonated carbons only) ($CDCl_3$) δ: C3', 163.50; C3, 120.38; C4, 137.51; C5, 126.21; C6, 149.99.

3,5-Di(2-pyridyl)-1,2,4-oxadiazole (66)

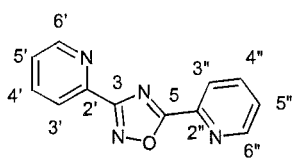

2-Picolylamidoxime (0.28 g, 1.9 mmol) was heated at 210°C for 30 minutes. After cooling, the solid was dissolved in $CHCl_3$ and washed with 5% aqueous NaOH, dried (Na_2SO_4), and the solvent removed *in vacuo* to yield a white solid. Recrystallisation from water gave pure white needles. M.p. 172-173°C (lit.[157] 173-175°C); yield 0.11 g (50%) (Found: C, 64.23; H, 3.48; N, 25.10. Calc. for $C_{12}H_8N_4O$: C, 64.28; H, 3.60; N, 24.99). Positive-ion EI mass spectrum: Calc. *m/z* for $C_{12}H_8N_4O$ 224.0698; found 224.0696. *m/z* 224.1 (M^+, 100%), 194.1 (M^+- NO, 37%), 120.0 ($PyCNO^+$, 99%), 104.0 ($PyCN^+$, 15%), 78.0 (Py^+, 83%). ^1H NMR ($CDCl_3$) δ: H3', 8.30; H4', 7.90; H5', 7.48; H6', 8.84; H3", 8.42; H4", 7.96; H5", 7.56; H6", 8.88. ^{13}C NMR ($CDCl_3$) δ: C2', 146.19; C3', 123.43; C4', 137.08; C5', 125.64; C6', 150.44; C2", 143.48, C3", 124.48; C4", 137.53; C5", 126.82; C6", 150.62; C3, 168.91; C5, 174.98.

Attempted syntheses of 3,5-di(2-pyridyl)-1,2,4-thiadiazole *viz.* 67

***Via* reaction of iodine with thiopicolinamide:**

Thiopicolinamide (0.25 g, 1.8 mmol) was dissolved in warm ethanol (9 ml) and added to I_2 (1.37 g, 5.4 mmol) dissolved in ethanol (14 ml). The temperature of the solution rose from 20°C to 30°C immediately after addition. The solution was stirred for 10 minutes then left to stand overnight. The solution was then refluxed for 30 minutes and the hot solution filtered through a glass frit. The filtrate was reduced in volume by approximately one half, and treated with a solution of aqueous $Na_2S_2O_3$ to destroy excess I_2. The solution was taken to dryness *in vacuo* and the red residue chromatographed on silica gel (1 x 20 cm) with 50% ethyl acetate:pet. ether as the eluant. M.p. 155-160°C; yield 0.11 g (59%); Positive-ion EI mass spectrum: Calc. *m/z* for $C_{18}H_{14}N_6$ 314.1281; found 314.1280. ^{1}H NMR ($CDCl_3$) δ: 9.94, d, 1H; 9.36, s(br), 1H; 8.64, m, 3H; 8.28, d, 1H; 7.99, d, 1H; 7.83, t, 1H; 7.78, t, 1H; 7.58, s(br), 1H; 7.36, t, 1H; 7.16, t, 1H; 6.87, t, 1H; 6.79, t, 1H.

***Via* reaction of hydrogen peroxide with thiopicolinamide in pyridine solution:**

Thiopicolinamide (0.52 g, 3.7 mmol) was dissolved in pyridine (3 ml) and a 50% solution of H_2O_2 (0.6 ml, 8.0 mmol) was added dropwise at such a rate to keep the solution from refluxing. The use of an ice-bath was necessary to cool the reaction flask at times during the addition. The reaction mixture was then stirred at ambient temperature for 24 hours before the reaction mixture was poured into water (20 ml). The aqueous solution was extracted with chloroform (3 x 10 ml) and the combined extracts dried over Na_2SO_4. TLC showed the presence of starting material and another component. After removing the solvent under reduced pressure, the yellow solid obtained was chromatographed on silica gel (1 x 20 cm) with ethyl acetate as the eluant. Two fractions were obtained and analysed by ^{1}H NMR spectroscopy. The first fraction was identified as starting material, and the second as a molecule containing a single pyridine ring. FAB mass spectrometry of the second fraction identified the molecular formula of $C_6H_5N_2SO$ for this product. (This was assumed to be the S-oxide product as the chemical shift of H4 changed little between starting thioamide and the resulting product.)

***Via* reaction of nitrous acid with thiopicolinamide:**

Thiopicolinamide (0.25 g, 1.7 mmol) was dissolved in 2:1 acetic acid/water (6 ml) and $NaNO_2$ (0.17 g, 2.4 mmol) dissolved in water (2 ml) was added dropwise. The mixture turned green during the addition with the evolution of brown fumes. After the addition was complete the mixture was left to stand for thirty minutes before being poured onto 50 ml ice/water. The precipitated material was collected by filtration (0.19 g). A ^{1}H NMR spectrum of this

material showed it was mostly starting thioamide. No signals were observed that were consistent with the desired product.

***Via* [3 + 2] intermolecular cycloaddition:**

5-(2-Pyridyl)-1,3,4-oxathiazol-2-one

Protected from atmospheric moisture by a $CaCl_2$ guard tube, chlorocarbonyl sulfenyl chloride (5 g, 38 mmol) was added dropwise with stirring to picolinamide (4.66 g, 38 mmol) dissolved in dry $CHCl_3$ (50 ml) at 40-50°C. The temperature was increased, and as the solution began to reflux a white solid appeared. After 1 hr, dry triethylamine (8 ml) was added dropwise, and the mixture refluxed for a further hour. The hot solution was filtered to remove picolinamide hydrochloride and the filtrate allowed to cool to room temperature. The filtrate was treated by stirring with 10% aqueous Na_2CO_3 solution (100 ml), washing with H_2O (1 x 50 ml), and drying with Na_2SO_4. Removal of the solvent *in vacuo* gave a dark solid that was chromatographed on silica gel (2 x 30 cm) with 20% ethyl acetate:pet. ether as eluant. After recrystallisation from toluene the desired compound (Rf 0.18) was obtained as small colourless blocks. M.p. 94-96°C; yield 0.80 g (12%) (Found: C, 46.79; H, 2.12; N, 15.72; S, 18.04. Calc. for $C_7H_4N_2O_2S$: C, 46.67; H, 2.24; N, 15.54; S, 17.79). Positive-ion FAB mass spectrum: Calc. for $C_7H_4N_2O_2S$ 179.9994; found 179.9993. *m/z* 180.0 (M^+, 29%), 152.0 (M^+-CO, 24%), 106.0 ($PyCO^+$, 56%), 78.0 (Py^+, 100%). ^1H NMR ($CDCl_3$) δ: H3, 8.02; H4, 7.88; H5, 7.49; H6, 8.77.

5-(2-Pyridyl)-1,3,4-oxathiazol-2-one (0.20 g, 1.1 mmol) was added in small portions to redistilled 2-cyanopyridine (*ca.* 1 ml) heated to 200°C. The colour of the resulting solution changed to green during the addition, and heating was continued for about 10 minutes after the completion of addition. The reaction mixture was allowed to cool to room temperature. TLC showed the presence of a very small component and the whole mixture was chromatographed on silica gel (2 x 20 cm) with 40% ethyl acetate:pet. ether as eluant. However, the minor component was not isolated from the column.

1-(Thiomethyl)-3-(dimethylamino)-imidazo[1,5-*a*]pyridine (72)

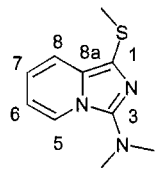

Thiopicolinamide (0.50 g, 3.6 mmol) and dimethylformamide dimethyl acetal (0.58 ml, 3.6 mmol) were combined in a 7 ml vial. The vial was capped and the mixture left to stand for 4 days. The methanol produced was removed *in vacuo*, and the residue chromatographed on silica gel (2 x 20 cm) with 25% ethyl acetate:pet. ether as eluant, after combining the relevant fractions (Rf 0.18), the title compound was obtained. M.p. 34-37°C; yield 0.40 g (54%) (Found: C, 57.72; H, 6.41; N, 20.33; S, 15.72. Calc. for $C_{10}H_{13}N_3S$: C, 57.95; H, 6.22; N, 20.26; S, 15.47). Positive-ion EI mass spectrum: Calc. *m/z* for $C_{10}H_{13}N_3S$ 207.0830; found

207.0830. *m/z* 207.1 (M^+, 100%), 192.0 (M^+-CH_2, 55%), 78.0 (Py^+, 29%). ^{1}H NMR ($CDCl_3$) δ: H5, 7.67; H6, 6.48; H7, 6.65; H8, 7.47; -SMe, 2.38; -NMe_2, 2.87. ^{13}C NMR ($CDCl_3$) δ: C1, 119.00; C3, 144.39; C5, 120.69; C6, 111.75; C7, 118.48; C8, 118.09; C8a, 129.94; -SMe, 20.10; -NMe_2, 42.18.

3,6-Di(2-pyridyl)-1,4,2,5-dioxadiazine (87)

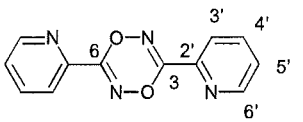

Pyridine hydroximinoylchloride hydrochloride[202] (0.51 g, 2.6 mmol) was dissolved in ethanol (25 ml). Triethylamine (0.73 ml, 5.3 mmol) and pyridine (0.64 ml, 7.9 mmol) were added and the solution swirled. The resultant solution changed to a yellow colour and a precipitate developed after *ca.* 1 minute. The reaction was left overnight. In the morning, the precipitated material was filtered off, and the filtrate taken to dryness *in vacuo*. The white solid from the filtrate was suspended in H_2O (20 ml), filtered, and recrystallised from water. M.p. 154-158°C; yield 0.18 g (59%) (Found: C, 60.05; H, 3.19; N, 23.47. Calc. for $C_{12}H_8N_4O_2$: C, 60.00; H, 3.36; N, 23.32). Positive-ion EI mass spectrum: Calc. *m/z* for $C_{12}H_8N_4O_2$ 240.0647; found 240.0648. *m/z* 240.1 (M^+, 1.8%), 120.0 ($PyCNO^+$, 20%), 104.0 ($PyCN^+$, 100%), 78.0 (Py^+, 62%). ^{1}H NMR ($CDCl_3$) δ: H3', 7.94; H4', 7.80; H5', 7.44; H6', 8.73. ^{13}C NMR ($CDCl_3$) δ: C2', 144.66; C3', 123.26; C4', 136.99; C5', 126.69; C6', 150.30; C3/C6, 160.63.

Preliminary synthetic steps to **2-(1,2,5-oxadiazol-3-yl)pyridine (90)**

A solution of sodium ethoxide was prepared by adding sodium metal (0.22 g, 9.6 mmol) to ethanol (25 ml). After all sodium had dissolved, 2-acetylpyridine (1 ml, 8.9 mmol) was added and the resultant solution left to stir for 5 minutes. Amyl nitrite (1.2 ml, 8.9 mmol) was added dropwise to the stirred mixture. After stirring for one hour the solution was refluxed for a further 4 hours. After cooling to room temperature, HCl was added to pH=5 and the solvent removed *in vacuo* to give an oily residue. This material was used without purification for the next step. The residue was dissolved in ethanol (5 ml) and a solution made of hydroxylamine hydrochloride (0.65 g, 9.3 mmol) and sodium acetate (0.80 g, 9.7 mmol) in water (3 ml) was added. The mixture was refluxed for four hours and was then allowed to cool. Evaporation of the solvent *in vacuo* left a white solid, which was identified as a mixture of the monoxime and glyoxime. Chromatography on silica gel (2 x 20 cm) with 40% ethyl acetate:pet. ether gave pure dioxime as a colourless solid, 0.22 g (17%.)

3,4-Di(2-pyridyl)-1,2,5-oxadiazole (91)

2,2'-Pyridil (0.50 g, 2.4 mmol), hydroxylammonium chloride (0.65 g, 9.4 mmol) and NaOH (2 g) were contained in a 20 ml vial with a magnetic stirring bar. H_2O (10 ml) was added and the solution stirred for 36 hrs. The solution was cooled in an ice-bath and

concentrated HCl was added dropwise until a flocculent precipitate developed. The solid was collected by filtration and washed with a small amount of cold water. M.p. 243-244°C; yield 0.24 g (42%). Positive-ion EI mass spectrum: Calc. *m/z* for $C_{12}H_{10}N_4O_2$ 240.0647; found 240.0633; *m/z* 240.0 (M^+, 2.61%), 224.0 (M^+- H_2O, 61%), 207.1 (M^+- $2H_2O$, 87%), 104.0 ($PyCN^+$, 100%), 78.0 (Py^+, 62%). ^1H NMR (d_6-DMSO) δ: H3', 7.49; H4', 7.85; H5', 7.35; H6', 8.60; N-OH, 11.72. ^{13}C NMR (d_6-DMSO) δ: C2', 154.56; C3', 126.26; C4', 136.15; C5', 124.77; C6', 149.14; C1/C2, 152.04.

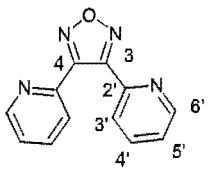

The above dioxime (0.70 g, 2.89 mmol) and H_2O (1 ml) were placed in a tube of dimensions; 33 mm I.D., 41 mm O.D., vol. 85ml, and the tube sealed. This was placed in an oven and heated at 185°C for 7 hrs. The tube was then allowed to come to room temperature and the contents rinsed out with methanol. The washings were collected and the solvent removed *in vacuo* to give a red residue. Chromatography on silica gel successfully separated **91**, which was then recrystallised from acetone/water. M.p. 121-125°C; yield 0.22 g (33%) (Found: C, 64.13; H, 3.29; N, 25.10. Calc. for $C_{12}H_8N_4O$: C, 64.28; H, 3.60; N, 24.99). Positive-ion EI mass spectrum: Calc. *m/z* for $C_{12}H_8N_4O$ 224.0698; found 224.0701. *m/z* 224.1 (M^+, 23%), 104.0 ($PyCN^+$, 21%), 78.0 (Py^+, 100%). ^1H NMR ($CDCl_3$) δ: H3', 7.92; H4', 7.84; H5', 7.40; H6', 8.60. ^{13}C NMR ($CDCl_3$) δ: C2', 146.23; C3', 124.74/124.67; C4', 136.76; C5', 124.67/124.74; C6', 149.69; C3 and C4, 153.34.

Attempted syntheses of 4,4'-di(2-pyridyl)-3,3'-bi-1,2,5-oxadiazole *viz.* 92

***Via* tin reduction of bis(2-pyridoyl)furoxan:**

Bis(2-pyridoyl)furoxan[204] (0.20 g, 0.68 mmol) and $SnCl_2.2H_2O$ (0.60, 2.68 mmol) were combined in a 10 ml round bottomed flask. Acetic acid (2 ml) and concentrated aqueous HCl (5 drops) were added to the solids and the mixture heated at 30°C for one week. At this time there was a little solid on the bottom of the flask. This solid was filtered off and a ^1H NMR spectrum and melting point of this material was recorded. By comparison, this was assigned as picolinic acid. The filtrate was poured onto water (30 ml) and extracted with chloroform (3 x 30 ml). The combined extracts were dried (Na_2SO_4) and the solvent removed under reduced pressure leaving a small residue. The aqueous solution was then adjusted to pH = 7 by the addition of a 40% aqueous solution of NaOH and again extracted with chloroform in the same manner as above. However, after treating the combined extracts as above nothing was obtained after removal of the solvent *in vacuo*.

***Via* deoxygenation using triethylphoshite:**

All operations were performed under an atmosphere of nitrogen. Bis(2-pyridoyl)furoxan (0.50 g, 1.7 mmol) was placed in a 50 ml two-necked round bottomed flask

with a magnetic spin vane. Dry benzene (25 ml) was added via syringe and stirring was started. After all the solid had dissolved freshly distilled $P(OEt)_3$ (0.30 ml, 1.8 mmol) was added and the mixture gradually turned dark. The mixture was stirred magnetically at room temperature overnight. In the morning, TLC still showed the presence of only the starting material, and so the mixture was set to reflux. However, after 5 hours TLC of the reaction mixture still showed no change. The experiment was repeated using the same quantities, this time with reflux started immediately. This did not seem to effect deoxygenation either as only starting material was recovered from the reaction.

All operations were performed under an atmosphere of nitrogen. Bis(2-pyridoyl)furoxan (0.44 g, 1.5 mmol) was placed in a 25 ml two-necked round bottomed flask with a magnetic spin vane. Freshly distilled $P(OEt)_3$ was added (3 ml) and the mixture immediately turned dark. The mixture was stirred magnetically while being heated at reflux. After 20 hours the reaction mixture was poured into water (50 ml) containing a few drops of concentrated aqueous HCl. After a few days a brown powder had deposited and was collected by filtration. However, none of the desired product could be identified in ^1H NMR spectra or seen in TLC.

2-(1,2,5-Thiadiazol-3-yl)pyridine (93)

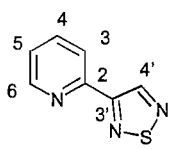

2-Vinylpyridine (0.26 ml, 2.4 mmol) was dissolved in a mixture of dry toluene (3 ml) and dry pyridine (3 ml). Trithiazyl trichloride ($S_3N_3Cl_3$) (0.90 g, 3.5 mmol) dissolved in dry toluene (10 ml) was added dropwise with stirring at room temperature. The clear solution immediately turned dark red. The mixture was set to reflux with stirring for 4 hrs before being allowed to cool to room temperature. The solution was decanted into a separating funnel leaving a large dark solid. The solution was washed with saturated aqueous $NaHCO_3$ (3 x 20 ml), then with H_2O (1 x 20 ml). To the solid was added *ca.* 30 ml water, then solid $NaHCO_3$ with swirling until pH = 8. This solution was then extracted with CH_2Cl_2 (3 x 10 ml). The organic fractions were combined, dried (Na_2SO_4), then the solvent removed *in vacuo*. Chromatography on silica gel (2 x 20 cm) with 30% ethyl acetate: pet. ether as the eluant separated the compounds. Pure **93** (Rf 0.51) was obtained after recrystallisation from ethanol/water. M.p. 43-48°C; yield 0.17 g (43%) (Found: C, 51.22; H, 3.18; N, 25.90; S, 19.92. Calc. for $C_7H_5N_3S$: C, 51.52; H, 3.09; N, 25.75; S, 19.65). ^1H NMR ($CDCl_3$) δ: H4', 9.32; H3, 8.17; H4, 7.84; H5, 7.36; H6, 8.70. ^{13}C NMR (protonated carbons only) ($CDCl_3$) δ: C4', 149.69/149.61; C3, 122.35; C4, 137.15; C5, 124.42; C6, 149.61/149.69.

3,4-Di(2-pyridyl)-1,2,5-thiadiazole (94)

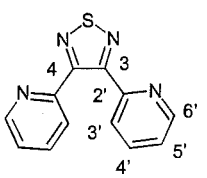

1,2-Di(2-pyridyl)ethene (0.59 g, 3.3 mmol) was dissolved in a mixture of dry toluene (5 ml) and dry pyridine (2 ml). Trithiazyl

trichloride ($S_3N_3Cl_3$) (0.83 g, 3.4 mmol) dissolved in dry toluene (15 ml) was added dropwise with stirring at room temperature. The clear solution became green and a precipitate developed. The mixture was set to reflux with stirring for 18 hrs. At this time the solution was a clear red with a small brown precipitate. After cooling, the solution was decanted into a separating funnel and more toluene (20 ml) added. The solution was washed with saturated aqueous $NaHCO_3$ (3 x 20 ml), then with H_2O (1 x 20 ml). To the solid was added *ca.* 30 ml H_2O, then solid $NaHCO_3$ with swirling until pH = 8. This solution was then extracted with toluene (3 x 10 ml). The organic fractions were combined, dried (Na_2SO_4), then the solvent removed *in vacuo*. Chromatography on silica gel (2 x 30 cm) with ethyl acetate as the eluant separated **94** (Rf 0.61), which was recrystallised from ethanol/water. M.p. 63-69°C; yield 0.39 g (49%) (Found: C, 60.24; H, 3.38; N, 23.09; S, 13.06. Calc. for $C_{12}H_8N_4S$: C, 59.99; H, 3.36; N, 23.31; S, 13.34). Positive-ion EI mass spectrum: Calc. *m/z* for $C_{12}H_8N_4S$ 240.0470; found 240.0391. *m/z* 240.0 (M^+, 89%). ^1H NMR ($CDCl_3$) δ: H3', 7.78; H4', 7.78; H5', 7.30; H6', 8.50. ^{13}C NMR (protonated carbons only) ($CDCl_3$) δ: C3', 124.20; C4', 136.45; C5', 123.73; C6', 149.11.

4,4'-Di(2-pyridyl)-3,3'-bi-1,2,5-thiadiazole (95)

In freshly distilled acetone (20 ml) was placed a magnetic stirring bar, CuCl (75 mg) and TMEDA (0.10 ml). Stirring was started and O_2 was introduced through a small fritted bubbler for 5 minutes before adding 2-ethynylpyridine (1 ml, 15 mmol). Bubbling and stirring was continued for 30 minutes. The acetone was then removed *in vacuo,* and the residue taken up in the minimum of $CHCl_3$, and passed through a small column of alumina. Removal of the $CHCl_3$ *in vacuo* gave a tan solid, which was recrystallised from cyclohexane to give pure 1,4-di(2-pyridyl)buta-1,3-diyne. M.p. 121-122°C (lit.[215] 122-123); yield 1.0 g (66%).

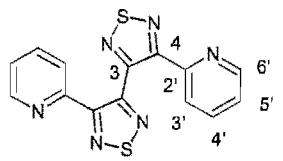

1,4-Di(2-pyridyl)buta-1,3-diyne (0.37 g, 1.8 mmol) was dissolved in dry toluene (3 ml) and dry pyridine (3 ml). Trithiazyl trichloride ($S_3N_3Cl_3$) (1.0 g, 4.1 mmol) dissolved in dry toluene (10 ml) was added dropwise with stirring at room temperature. The clear solution became green and a precipitate developed. The mixture was set to reflux with stirring for 7 hrs. The mixture was then allowed to cool to room temperature and the solution was decanted into a separating funnel leaving a large dark solid. The solid was washed with more toluene (1 x 20 ml), and this was added to the decanted solution. The combined toluene solution was washed with saturated aqueous $NaHCO_3$ (3 x 20 ml), then with H_2O (1 x 20 ml). To the solid was added *ca.* 30 ml H_2O, then solid $NaHCO_3$ with swirling until pH = 8. This solution was then extracted with CH_2Cl_2 (3 x 10 ml). The organic fractions were combined, dried (Na_2SO_4), then the solvent removed *in vacuo*. Chromatography on silica gel (2 x 20 cm) with 40% ethyl acetate:pet. ether as the eluent separated **95** (Rf 0.41) which was recrystallised from ethanol/water to get canary-yellow needles. M.p. 128-129°C; yield 0.10 g

(17%) (Found: C, 51.92; H, 2.16; N, 25.94; S, 19.68. Calc. for $C_{14}H_8N_6S_2$: C, 51.85; H, 2.49; N, 25.90; S, 19.77). Positive-ion EI mass spectrum: Calc. *m/z* for $C_{14}H_8N_6S_2$ 324.0252; found 324.0257. *m/z* 324.0 (M^+, 9%), 246.0 (M^+- Py, 100%). ^1H NMR ($CDCl_3$) δ: H3', 7.91; H4', 7.58; H5', 7.02; H6', 8.07. ^{13}C NMR (protonated carbons only) ($CDCl_3$) δ: C3', 123.58; C4', 136.43; C5', 122.72; C6', 148.61.

Synthesis of Complexes

Bis(2,2'-bipyridine)(2,2'-bibenzoxazolyl)chlororuthenium(II) hexafluorophosphate (8) and bis(2,2'-bipyridine)(2,2'-bibenzoxazolyl)ruthenium(II) bis(hexafluorophosphate) (7)

Ligand **1** (14 mg, 0.06 mmol) and $Ru(bpy)_2Cl_2.2H_2O$ (30 mg, 0.06 mmol) in 3:1 $EtOH/H_2O$ (16 ml) were refluxed for 2 days. After cooling, the reaction mixture was concentrated to dryness *in vacuo*. The residue was redissolved in the minimum of water, filtered to remove unreacted ligand, and the products precipitated out by the addition of an aqueous solution of NH_4PF_6. Chromatography on alumina (1 x 7 cm) with 100:1 CH_2Cl_2/MeOH as eluant, cleanly separated a dark red fraction then an orange fraction. ^1H NMR spectra and FAB mass spectrometry helped identify the fractions as the above mentioned complexes, respectively.

Bis(2,2'-bipyridine)(2,2'-bibenzoxazolyl)chlororuthenium(II)-(hexafluorophosphate) (**8**)

Yield 10.3 mg (20%). ^1H NMR (CD_3CN) δ: 5.95, d, 1H, H4; 6.19, t, 1H; 6.25, d, 1H; 6.60, d, 1H; 6.80, t, 1H; 7.18, t, 1H, bpy H5; 7.25, t, 1H, H5; 7.38, t, 1H, bpy H5; 7.48, m, 2H, bpy H5 and ; 7.55, d, 1H, H6; 7.62; 7.68, t, 1H, bpy H5; 7.75, t, 1H, bpy H4; 7.87, d, 1H, H7; 8.07, m, 2H, bpy H4's; 8.09, t, 1H, bpy H4; 8.11, d, 1H, bpy H3; 8.25, d, 2H, bpy H3 and bpy H6; 8.50, d, 1H, bpy H3; 8.53, d, 1H, bpy H3; 9.30, d, 1H, bpy H6.

Bis(2,2'-bipyridine)(2,2'-bibenzoxazolyl)ruthenium(II) bis(hexafluorophosphate) (7)

Yield 28.1 mg (50%) (Found: C, 43.68; H, 2.58; N, 8.85. Calc. for $C_{34}H_{24}N_8F_{12}O_2P_2Ru$: C, 43.46; H, 2.57; N, 8.94). Positive-ion FAB mass spectrum: Calc. *m/z* for $C_{34}H_{24}N_8F_6O_2PRu^+$ ($[(bpy)_2Ru(1)](PF_6)^+$) 795.0651; found 795.0646. λ_{max} (CH_3CN) 485 nm, ε 7300 $M^{-1}cm^{-1}$. E^o (CH_3CN) Ru^{2+}/Ru^{3+} 1.36 V, $E^{1/2}$ 60 mV; E^o_{red} -0.97 V, $E^{1/2}$ 60 mV; E^o_{red} -1.55 V, $E^{1/2}$ 60 mV; E^o_{red} -1.77 V, $E^{1/2}$ 60 mV. ^1H NMR (CD_3CN) δ: 8.60, d, 2H, bpy H3; 8.25, t, 2H, bpy H4; 7.55, t, 2H, bpy H5; 8.00, d, 2H, bpy H6; 8.55, d, 2H, bpy H3'; 8.08, t, 2H, bpy H4'; 7.45, t, 2H, bpy H5'; 8.10, d, 2H bpy, H6'; 6.03, d, 2H, H4; 7.43, t, 2H, H5; 7.75, t, 2H, H6; 8.01, d, 2H, H7. ^{13}C NMR (CD_3CN) δ: 113.79; 124.31; 124.63; 127.80; 128.43; 130.62; 138.513; 139.02; 153.32; 154.49.

Alternatively, **7** was prepared *via* the silver method as follows: $AgClO_4$ (20 mg, 0.09 mmol) and $Ru(bpy)_2Cl_2.2H_2O$ (15 mg, 0.03 mmol) were stirred in 1:1 deaerated acetone:ethanol (10 ml) for 2 hrs. The AgCl formed was filtered off and ligand **1** (10 mg, mmol) was added and the solution again dearated by N_2 bubbling before refluxing for 4 hrs. After cooling, the reaction mixture was concentrated to dryness *in vacuo*. The resulting was suspended in water (10 ml) and a large excess of NH_4PF_6 added and stirred for 12 hours before the solid was collected by filtration and purified by chromatography. Yield 17 mg (64%).

Bis(2,2'-bipyridine)(2,2'-bibenzothiazolyl)ruthenium(II) bis(hexafluorophosphate) (9)

$Ru(bpy)_2Cl_2.2H_2O$ (60 mg, 0.12 mmol) in 3:1 $EtOH/H_2O$ (24 ml) was refluxed for 1 hr before the addition of ligand **2** (31 mg, 0.12 mmol) as a solid. Reflux was continued for another 3 days. After cooling, the reaction mixture was concentrated to dryness *in vacuo*. The residue was redissolved in the minimum of water, filtered to remove unreacted ligand, and the product precipitated out by the addition of an aqueous solution of NH_4PF_6. Yield 74 mg (66%) (Found: C, 42.63; H, 2.71; N, 8.57. Calc. for $C_{34}H_{24}N_6F_{12}P_2RuS_2$: C, 42.03; H, 2.49; N, 8.65). Positive-ion FAB mass spectrum: Calc. *m/z* for $C_{34}H_{24}N_6F_6PRuS_2^+$ ($[(bpy)_2Ru(2)](PF_6)^+$) 827.0214; found 827.0189. λ_{max} (CH_3CN) 516 nm, ε 8500 $M^{-1}cm^{-1}$. E^o (CH_3CN) Ru^{2+}/Ru^{3+} 1.32 V, $E^{1/2}$ 60 mV; E^o_{red} -0.86 V, $E^{1/2}$ 60 mV; E^o_{red} -1.46 V, $E^{1/2}$ 60 mV; E^o_{red} -1.73 V, $E^{1/2}$ 60 mV. ^1H NMR (CD_3CN) δ: 8.60, d, 2H, bpy H3; 8.24, t, 2H, bpy H4; 7.54, t, 2H, bpy H5; 7.92, d, 2H, bpy H6; 8.55, d, 2H, bpy H3'; 8.08, t, 2H, bpy H4'; 7.40, t, 2H, bpy H5'; 7.82, d, 2H, bpy H6'; 6.28, d, 2H, H4; 7.36, t, 2H, H5; 7.68, t, 2H, H6; 8.32, d, 2H, H7. ^{13}C NMR (CD_3CN) δ: bpy C2, 157.24; bpy C3, 125.04; bpy C4, 139.18; bpy C5, 128.38/128.33; bpy C6, 152.74; bpy C2', 158.47; bpy C3', 124.64; bpy C4', 138.45; bpy C5', 128.33/128.38; bpy C6', 153.60; C2, not recorded; C3a, 151.87; C4, 120.45; C5, 129.55; C6, 129.26; C7, 124.91; C7a, 135.87.

Bis(2,2'-bipyridine)(bis[2-benzoxazolyl]methine)ruthenium(II)-(hexafluorophosphate) (11)

Ligand **3** (49 mg, 0.20 mmol) and $Ru(bpy)_2Cl_2.2H_2O$ (85 mg, 0.16 mmol) in 3:1 $EtOH/H_2O$ (8 ml) were refluxed for 24 hrs. After cooling, the reaction mixture was concentrated to dryness *in vacuo*. The residue was redissolved in the minimum of water, filtered to remove unreacted ligand, and the product precipitated out by the addition of an aqueous solution of NH_4PF_6. Chromatography on alumina (1 x 10 cm) with 200:1 CH_2Cl_2:MeOH separated a small green head band that was identified as the title compound. Yield 15 mg (11%). Positive-ion FAB mass spectrum: Calc. *m/z* for $C_{35}H_{25}N_6O_2Ru^+$ ($[(bpy)_2Ru(3\text{-}H)]^+$) 663.1090; found 663.1083. λ_{max} (CH_3CN) 405 nm, ε 17 600 $M^{-1}cm^{-1}$. E^o (CH_3CN) Ru^{2+}/Ru^{3+} 1.39 V, $E^{1/2}$ 60 mV; E_{red} -1.04 V (irreversible). ^1H NMR (CD_3CN) δ: 8.52, d, 2H, bpy H3; 8.09, t, 2H, bpy H4; 7.57, t, 2H, bpy H5; 8.83, d, 2H, bpy H6; 8.49, d,

2H, bpy H3'; 8.05, t, 2H, bpy H4'; 7.36, t, 2H, bpy H5'; 8.00, d, 2H, bpy H6'; 5.20, d, 2H, H4; 6.65, t, 2H, H5; 6.96, t, 2H, H6; 7.28, d, 2H, H7; 5.20, s, 1H, -CH-. ^{13}C NMR (CD_3CN) δ: 59.99; 109.13; 112.25; 120.99; 123.80; 124.30; 126.78; 127.10; 136.77; 136.95; 152.74; 153.05.

Alternatively, **11** (as the BF_4 salt) was synthesised by the silver method as follows: $Ru(bpy)_2Cl_2.2H_2O$ (24.8 mg, 0.05 mmol) and $AgBF_4$ (32.5 mg, 0.11 mmol) were stirred in deaerated 1:1 acetone/EtOH (8 ml) at ambient temperature for 90 minutes. The solution was filtered to remove precipitated AgCl, and flushed with argon before ligand **3** (12 mg, 0.05 mmol) was added as a solid. The reaction solution was heated at 40°C for two hours before being filtered and the solvent removed *in vacuo*. The residue was chromatographed on alumina (1 x 5 cm) and one green fraction was collected and identified as **11**. Yield 20 mg (50%)

Bis(2,2'-bipyridine)(3-[2-pyridyl]-1,2-benzisoxazolyl)ruthenium(II) bis(hexafluorophosphate) (13)

Ligand **6** (18.8 mg, 0.10 mmol) and $Ru(bpy)_2Cl_2.2H_2O$ (50.0 mg, 0.10 mmol) in 3:1 $EtOH/H_2O$ (8 ml) were refluxed for 15 hrs. After cooling, the reaction mixture was concentrated to dryness *in vacuo*. The residue was redissolved in the minimum of water, filtered to remove unreacted ligand, and the product precipitated out by the addition of an aqueous solution of NH_4PF_6. Yield 80 mg (94%) (Found: C, 42.92; H, 2.94; N, 9.15. Calc. for $C_{32}H_{24}N_6F_{12}OP_2Ru$: C, 42.73; H, 2.69; N, 9.34). Positive-ion FAB mass spectrum: Calc. *m/z* for $C_{32}H_{24}N_6F_6OPRu^+$ ($[(bpy)_2Ru(\mathbf{6})](PF_6)^+$) 755.0668; found 755.0697. λ_{max} (CH_3CN) 442 nm, ε 18 200 $M^{-1}cm^{-1}$. E^o (CH_3CN) Ru^{2+}/Ru^{3+} 1.36 V, $E^{1/2}$ 60 mV; E^o_{red} -1.01 V (irreversible), E^o_{red} -1.72 V (irreversible), E^o_{red} -1.98 V (irreversible). ^{1}H NMR (CD_3CN) δ: 7.49, m, 3H, 3 x bpy H5's; 7.57, t, 1H, bpy H5; 7.59, t, 1H, H5'; 7.67, d, 1H, H7; 7.73, t, 1H, H5; 7.83, m, 3H, H6 and 2 x bpy H6's; 7.86, m, 2H, H6' and bpy H6; 8.02, d, 1H, bpy H6; 8.14, m, 3H, 3 x bpy H4's; 8.21, t, 1H, bpy H4; 8.27, t, 1H, H4'; 8.42, d, 1H, H4; 8.58, m, 4H, 4 x bpy H3's; 8.79, d, 1H, H3'.

(2,2'-Bibenzoxazolyl)dichloropalladium (14)

A methanolic solution of 0.0904M Li_2PdCl_4 (2.5 ml, 0.23 mmol) was added to a stirred solution of ligand **1** (50 mg, 0.21 mmol) dissolved in boiling MeOH (25 ml). The tan precipitate that formed was collected by filtration and recrystallised from $MeNO_2$. M.p. >300°C; yield 74 mg (82%) (Found: C, 40.36; H, 2.02; N, 6.82; Cl, 16.98. Calc. for $C_{14}H_8N_2Cl_2O_2Pd$: C, 40.66; H, 1.95; N, 6.77; Cl, 17.15). Positive-ion FAB mass spectrum: Calc. *m/z* for $C_{14}H_8N_2O_2Pd^+$ [(**1**)Pd^+, 100%] 343.9619; found 343.9618.

(2,2'-Methylenebisbenzoxazolyl)dichloropalladium.hemihydrate (15)

A methanolic solution of 0.0363M Li_2PdCl_4 (4.5 ml, 0.16 mmol) was added to a stirred solution of ligand **3** (38.8 mg, 0.16 mmol) in MeOH (3 ml). After a few seconds a precipitate developed and was filtered off (37.9 mg). The solution was then reduced in volume by removal of *ca.* half the solvent *in vacuo* and was then diluted with water (5 ml) and an orange precipitate formed and was again collected by filtration (15.4 mg). M.p. 288-291°C; yield 53.3 mg (78%) (Found: C, 41.62; H, 2.23; N, 6.31; Cl, 16.32. Calc. for $C_{15}H_{10}N_2Cl_2O_2Pd.½H_2O$: C, 41.27; H, 2.54; N, 6.41; Cl, 16.24). Positive-ion FAB mass spectrum: Calc. *m/z* for $C_{15}H_{10}N_2ClO_2Pd^+$ [(**3**)$PdCl^+$, 100%] 392.9464; found 392.9470. ^1H NMR ($CDCl_3$) δ: 8.56, d, 2H, H4; 7.49, t, 2H, H5; 7.53, t, 2H, H6; 7.58, d, 2H, H7; 5.16, s, 2H, CH_2.

(2,2'-Methylenebisbenzothiazolyl)dichloropalladium.hemihydrate (16)

A methanolic solution of 0.0904M Li_2PdCl_4 (1.2 ml, 0.11 mmol) was added to a stirred solution of ligand **4** (30 mg, 0.11 mmol) in boiling MeOH (25 ml). After a few seconds small golden flakes fell out of solution. After cooling to room temperature, the flakes were collected by filtration. The solution was then reduced in volume by removal of *ca.* half the solvent *in vacuo*, and upon standing more golden flakes formed and were collected by filtration. M.p. 278-280°C; yield 40 mg (82%) (Found: C, 38.67; H, 2.31; N, 6.00; S, 15.10. Calc. for $C_{15}H_{10}N_2Cl_2S_2Pd.½H_2O$: C, 38.44; H, 2.37; N, 5.97; S, 15.12). Positive-ion FAB mass spectrum: Calc. *m/z* for $C_{15}H_{10}N_2ClS_2Pd^+$ [(**4**)$PdCl^+$, 100%] 424.9015; found 424.9013. ^1H NMR (d_6-DMSO) δ: 8.65, d, 2H, H4; 7.65, t, 2H, H5; 7.58, t, 2H, H6; 7.18, d, 2H, H7; 5.90, s, 2H, CH_2.

[3-(2-Pyridyl)-1,2-benzisoxazolyl]dichloropalladium (17)

Ligand **6** (29.3 mg, 0.13 mmol) was dissolved in MeOH (2 ml) and added to a methanolic solution of 0.0363M Li_2PdCl_4 (4.2 mls, 0.15 mmol). The yellow precipitate that formed was collected by filtration and washed well with MeOH. M.p. >300°C; yield 52.4 mg (94%) (Found: C, 38.67; H, 2.20; N, 7.75; Cl, 19.22. Calc. for $C_{12}H_8N_2OCl_2Pd$: C, 38.56; H, 2.16; N, 7.50; Cl, 18.98). ^1H NMR (d_6-DMSO) δ: 8.66, d, 1H, H4; 7.73, t, 1H, H5; 7.85, t, 1H, H6; 8.11, d, 1H, H7; 8.83, d, 1H, H3'; 8.49, t, 1H, H4'; 7.95, t, 1H, H5'; 9.11, d, 1H, H6'.

(2,2'-Bibenzoxazolyl)dinitratodisilver (18)

Ligand **1** (41 mg, 0.17 mmol) dissolved in chloroform (4 ml) was poured into a vial containing $AgNO_3$ (30 mg 0.18 mmol) dissolved in hot 2:1 methanol/chloroform (6 ml). The solution immediately turned pink. The precipitated material was filtered after one day. M.p.

249-250°C; yield 43 mg (84%) (Found: C, 29.38; H, 0.94; N, 9.44. Calc for $C_{14}H_8N_4O_6Ag_2$: C, 29.19; H, 1.40; N, 9.72).

Reaction of 2,2'-methylenebisbenzoxazole with silver nitrate, *viz* 1,1',2,2'-tetrabenzoxazol-2-yl ethene (19)

Ligand **3** (46.5 mg, 0.186 mmol) dissolved in methanol (4 ml) was added to $AgNO_3$ (33.4 mg, 0.196 mmol) dissolved in 1:1 methanol/water (2 ml). The solution darkened upon the addition. After one day metallic silver had deposited around the sides of the vial and the solution was filtered to remove this everyday thereafter until no more precipitated (*ca.* 4 days). The solution was then reduced to dryness *in vacuo* and the material analysed by ^1H NMR spectroscopy and TLC. The spectrum showed signals due to the starting material and another component. By GCMS this component was identified as **19**. No attempt at separation of the components was made.

(2,2'-Methylenebisbenzothiazolyl)nitratosilver (20)

$AgNO_3$ (21 mg, 0.12 mmol) dissolved in hot MeOH (2 ml) was added to a stirred solution of ligand **4** (35 mg, 0.12 mmol) dissolved in boiling MeOH (20 ml). The solution darkened upon the addition. After evaporation of the solution, long crystals and some powdery material was left. The crystals were collected. M.p. 265-268°C; yield 30 mg (55%) (Found: C, 39.56; H, 2.28; N, 9.37; S, 14.00. Calc. for $C_{15}H_{10}N_3O_3S_2Ag$: C, 39.83; H, 2.23; N, 9.29; S, 14.20).

Bis(N3-[2,2'-bibenzoxazolyl])dichlorocopper (21)

$CuCl_2.2H_2O$ (36 mg, 0.21 mmol) dissolved in MeOH (1/2 ml) was added to ligand **1** (50 mg, 0.21 mmol) dissolved in $CHCl_3$ (4 ml). The resulting solution turned dark purple. After complete evaporation of the solvent there remained purple cubes and blue needles. These were both collected and by washing with a small amount of ethanol the blue needles dissolved. M.p. 217-222°C; yield 30 mg (47%). Positive-ion FAB mass spectrum: Calc. *m/z* for $C_{28}H_{16}N_4O_4Cu^+$ [$(\mathbf{1})_2Cu^+$, 100%] 535.0480; found 535.0470.

Bis[3-(2-pyridyl)-1,2-benzisoxazolyl]dinitratocopper (22)

Ligand **6** (23.0 mg, 0.117 mmol) in MeOH (2 ml) was added to $Cu(NO_3)_2.3H_2O$ (28.3 mg, 0.117 mmol) in MeOH (1 ml) and left to stand. Large green crystals formed overnight and were collected by filtration. More green crystals grew upon more evaporation of the solution and these were also collected. M.p. 242-243°C; yield 26.0 mg (76%) (Found: C, 49.71; H, 2.51; N, 14.22. Calc. for $C_{24}H_{16}N_6O_8Cu$: C, 49.71; H, 2.78; N, 14.49). Positive-ion

FAB mass spectrum: Calc. *m/z* for $C_{24}H_{16}N_4O_2Cu^+$ [(**6**)$_2$Cu$^+$, 100%] 455.0584; found 455.0571.

Bis(2,2'-bipyridine)[N3-(1,1'-bibenzotriazolyl)]chlororuthenium(II)-(hexafluorophosphate) (31)

Ligand **23** (24.0 mg, 0.10 mmol) and $Ru(bpy)_2Cl_2.2H_2O$ (52.9 mg, 0.10 mmol) were refluxed in 3:1 EtOH/H_2O (8 ml) for 48 hrs. After cooling, the reaction mixture was concentrated to dryness *in vacuo*. The residue was redissolved in the minimum of water, filtered to remove unreacted ligand, and the product precipitated out by the addition of an aqueous solution of NH_4PF_6. Yield 69.6 mg (82%) (Found: C, 44.86; H, 3.05; N, 16.39. Calc. for $C_{32}H_{24}N_{10}ClF_6PRu.1½H_2O$: C, 44.84; H, 3.00; N, 16.33). Positive-ion FAB mass spectrum: Calc. *m/z* for $C_{32}H_{24}N_{10}ClRu^+$ ([(bpy)$_2$Ru(**23**)Cl]$^+$) 685.0908; found 685.0917. λ_{max} (CH_3CN) 479 nm, ε 8650 $M^{-1}cm^{-1}$.

^{1}H NMR (CD_3CN) δ:
bpy H3, 8.35; bpy H4, 8.12; bpy H5, 7.80; bpy H6, 10.18.
bpy H3, 8.21; bpy H4, 7.75; bpy H5, 7.08; bpy H6, 7.87
bpy H3, 8.45; bpy H4, 7.80; bpy H5, 7.30; bpy H6, 7.77.
bpy H3, 8.58; bpy H4, 8.16; bpy H5, 7.63; bpy H6, 9.04.
Bt H4, 9.12; Bt H5, 7.65; Bt H6, 7.78; Bt H7, 7.57.
Bt H4', 8.36; Bt H5', 7.70; Bt H6', 7.80; Bt H7', 7.53.

Bis(2,2'-bipyridine)[N3-(1,1'-bisbenzotriazolyl)methane)]chlororuthenium(II)-(hexafluorophosphate) (32)

Ligand **24** (17.0 mg, 0.11 mmol) and $Ru(bpy)_2Cl_2.2H_2O$ (32.1 mg, 0.11 mmol) were refluxed in 3:1 EtOH/H_2O (8 ml) for 6 hrs. After cooling, the reaction mixture was concentrated to dryness *in vacuo*. The residue was redissolved in the minimum of water, filtered to remove unreacted ligand, and the product precipitated out by the addition of an aqueous solution of NH_4PF_6. Yield 44.0 mg (82%) (Found: C, 45.90; H, 2.93; N, 15.93. Calc. for $C_{33}H_{26}N_{10}ClF_6PRu.H_2O$: C, 45.98; H, 3.27; N, 16.24). Positive-ion FAB mass spectrum: Calc. *m/z* for $C_{33}H_{26}N_{10}ClRu^+$ ([(bpy)$_2$Ru(**24**)Cl]$^+$) 699.1056; found 699.1074. λ_{max} (CH_3CN) 471 nm, ε 7000 $M^{-1}cm^{-1}$.

^{1}H NMR (CD_3CN) δ:
bpy H3, 8.34; bpy H4, 8.04; bpy H5, 7.67; bpy H6, 10.07.
bpy H3, 8.24; bpy H4, 7.84; bpy H5, 7.19; bpy, H6 7.86.
bpy H3, 8.41; bpy H4, 7.88; bpy H5, 7.24; bpy, H6 7.71.
bpy H3, 8.53; bpy H4, 8.10; bpy H5, 7.41; bpy, H6 8.67.
Bt H4, 8.88; Bt H5, 7.46; Bt H6, 7.71; Bt H7, 8.07.

Bt H4', 8.10; Bt H5', 7.68; Bt H6', 7.45; Bt H7', 7.78; CH_2 7.57.

Bis(2,2'-bipyridine)[N2,N2'-(1,1'-bisbenzotriazolyl)methane]-ruthenium(II) bis(hexafluorophosphate) (34)

$AgBF_4$ (34.1 mg, 0.175 mmol) and $Ru(bpy)_2Cl_2.2H_2O$ (45.1 mg, 0.087 mmol) in deaerated 1:1 ethanol/acetone (12 ml) was stirred at 35-40°C for 90 minutes. After filtering to remove precipitated AgCl, ligand **24** (25.0 mg, 0.10 mmol) was added as a solid, the solution was again deaerated by bubbling argon through the solution and the mixture stirred at 40°C for 5 hrs. The resulting solution was concentrated to dryness *in vacuo*, and the residue was chromatographed on alumina. Yield 31 mg (47%) (Found: C, 47.63; H, 3.17; N, 16.56. Calc. for $C_{33}H_{26}N_{10}B_2F_8Ru$: C, 47.34; H, 3.13; N, 16.72). Positive-ion FAB mass spectrum: Calc. *m/z* for $C_{33}H_{26}N_{10}BF_4Ru^+$ ($[(bpy)_2Ru(\mathbf{24})](BF_4)^+$) 751.1442; found 751.1415. λ_{max} (CH_3CN) 368 nm, ε 9 800 $M^{-1}cm^{-1}$. E^o (CH_2Cl_2) Ru^{2+}/Ru^{3+} 1.50 V, $E^{1/2}$ 60 mV; E^o_{red} -1.45 V, $E^{1/2}$ 60 mV; E^o_{red} -1.60 V; $E^{1/2}$ 70 mV. ^1H NMR (CD_2Cl_2) δ: 8.48, d, 2H, bpy H3; 8.17, t, 2H, bpy H4; 7.57, t, 2H, bpy H5; 8.27, d, 2H, bpy H6; 8.43, d, 2H, bpy H3'; 8.12, t, 2H, bpy H4'; 7.49, t, 2H, bpy H5'; 7.84, d, 2H, bpy H6'; 7.84, d, 2H, H4; 7.51, t, 2H, H5; 7.76, t, 2H, H6; 8.04, d, 2H, H7; 7.31 7.43, dd, 2H, CH_2.

Bis(2,2'-bipyridine)(1-(2-pyridyl)benzotriazolyl)ruthenium(II) bis(hexafluorophosphate) (35)

Ligand **27** (11.4 mg, 0.06 mmol) and $Ru(bpy)_2Cl_2.2H_2O$ (30.2 mg, 0.06 mmol) in 3:1 $EtOH/H_2O$ (8 ml) were refluxed for 4 hrs. After cooling, the reaction mixture was concentrated to dryness *in vacuo*. The residue was redissolved in the minimum of water, filtered to remove unreacted ligand, and the product precipitated out by the addition of an aqueous solution of NH_4PF_6. Yield 46.1 mg (88%) (Found: C, 41.30; H, 2.70; N, 12.40. Calc. for $C_{31}H_{24}N_8F_{12}P_2Ru$: C, 41.39; H, 2.69; N, 12.46). Positive-ion FAB mass spectrum: Calc. *m/z* for $C_{31}H_{24}N_8F_6PRu^+$ ($[(bpy)_2Ru(\mathbf{27})](PF_6)^+$) 755.0818; found 755.0809. λ_{max} (CH_3CN) 423 nm, ε 16 300 $M^{-1}cm^{-1}$. E^o (CH_3CN) Ru^{2+}/Ru^{3+} 1.53 V, $E^{1/2}$ 75 mV; E^o_{red} -1.39 V, $E^{1/2}$ 80 mV; E^o_{red} -1.60 V; $E^{1/2}$ 95 mV. ^1H NMR (CD_3CN) δ: 7.43, t, 1H, bpy H5; 7.48, m, 3H, H5' and 2 x bpy H5; 7.55, t, 1H, bpy H5; 7.71, t, 1H, H5; 7.83, m, 2H, H6' and bpy H6; 7.90, m, 4H, H6 3 x bpy H6; 8.05, d, 1H, H4; 8.16, m, 3H, 3 x bpy H4; 8.21, t, 1H, bpy H4; 8.32, t, 1H, H4'; 8.40, d, 1H, H7; 8.57, m, 3H, H3' and 2 x bpy H3; 8.59, d, 1H, bpy H3; 8.62, d, 1H, bpy H3.

Bis(2,2'-bipyridine)(N3-(1-[(2-pyridyl)methyl]benzotriazolyl))chlororuthenium(II)-(hexafluorophosphate) (38) and bis(2,2'-bipyridine)(1-[(2-pyridyl)methyl]benzotriazolyl)ruthenium(II) bis(hexafluorophosphate) (36)

Ligand **28** (13.0 mg, 0.062 mmol) and $Ru(bpy)_2Cl_2.2H_2O$ (32.1 mg, 0.062 mmol) in 3:1 $EtOH/H_2O$ (8 ml) were refluxed for 5 hrs. After cooling, the reaction mixture was concentrated to dryness *in vacuo*. The residue was redissolved in the minimum of water, filtered to remove unreacted ligand, and the product precipitated out by the addition of an aqueous solution of NH_4PF_6. Chromatography on alumina (1 x 7 cm) with 100:1 CH_2Cl_2:MeOH as eluant, cleanly separated a small dark red fraction then a larger orange fraction. ^1H NMR, UV-visible spectroscopy, FABMS and elemental analysis identified the fractions as the above mentioned complexes respectively.

Bis(2,2'-bipyridine)(N3-(1-[(2-pyridyl)methyl]benzotriazolyl))chlororuthenium(II)-(hexafluorophosphate) (**38**)

Yield 7.2 mg (14%) (Found: C, 47.97; H, 3.21; N, 14.04. Calc. for $C_{32}H_{26}N_8ClF_6PRu$: C, 47.80; H, 3.26; N, 13.93). Positive-ion FAB mass spectrum: Calc. *m/z* for $C_{32}H_{26}N_8ClRu^+$ ($[(bpy)_2Ru(\mathbf{28})Cl]^+$ 659.1028; found 659.1012. λ_{max} (CH_3CN) 494 nm, ε 5600 $M^{-1}cm^{-1}$.

^1H NMR (CD_3CN) δ:
bpy H3, 8.28; bpy H4, 8.01; bpy H5, 7.71; bpy H6, 10.19.
bpy H3, 8.14; bpy H4, 7.72; bpy H5, 7.11; bpy H6, 7.87.
bpy H3, 8.42; bpy H4, 7.86; bpy H5, 7.23; bpy H6, 7.79.
bpy H3, 8.53; bpy H4, 8.09; bpy H5, 7.56; bpy H6, 8.90.
bpy H3', 6.97; bpy H4', 7.72; bpy H5', 7.32; bpy H6', 8.42.
Bt H4, 8.84; Bt H5, 7.40; Bt H6, 7.57; Bt H7, 7.72; CH_2, 5.72.

Bis(2,2'-bipyridine)(1-[(2-pyridyl)methyl]benzotriazolyl)ruthenium(II) bis(hexafluorophosphate) (**36**)

Yield 44 mg (77%) (Found: C, 41.21; H, 2.93; N, 12.09. Calc. for $C_{32}H_{26}N_8F_{12}P_2Ru.H_2O$: C, 41.30; H, 3.03; N, 12.04). Positive-ion FAB mass spectrum: Calc. *m/z* for $C_{32}H_{26}N_8F_6PRu^+$ ($[(bpy)_2Ru(\mathbf{28})](PF_6)^+$) 769.0967; found 769.0957. λ_{max} (CH_3CN) 426 nm, ε 11 300 $M^{-1}cm^{-1}$. E^o (CH_3CN) Ru^{2+}/Ru^{3+} 1.30 V, $E^{1/2}$ 75 mV; E^o_{red} -1.43 V, $E^{1/2}$ 70 mV; E^o_{red} -1.64 V; $E^{1/2}$ 70 mV.

^1H NMR (CD_3CN) δ:
bpy H3, 8.50; bpy H4, 8.19; bpy H5 7.64; bpy H6, 8.58.
bpy H3, 8.40; bpy H4, 8.05; bpy H5 7.43; bpy H6, 7.77.
bpy H3, 8.66; bpy H4, 8.20; bpy H5 7.49; bpy H6, 7.96.

bpy H3, 8.62; bpy H4, 8.13; bpy H5 7.46; bpy H6, 7.81.
bpy H3', 8.00; bpy H4', 7.97; bpy H5', 7.25; bpy H6', 7.70.
Bt H4 7.80; Bt H5, 7.51; Bt H6, 7.71; Bt H7, 8.00; CH_2, H_{eq} 6.13, H_{ax} 5.91.

Bis(2,2'-bipyridine)(1-[1-isoquinolyl]benzotriazolyl)ruthenium(II) bis(hexafluorophosphate) (37)

Ligand **29** (20.0 mg, 0.06 mmol) and $Ru(bpy)_2Cl_2.2H_2O$ (42.0 mg, 0.06 mmol) in 3:1 $EtOH/H_2O$ (8 ml) were refluxed for 15 hrs. After cooling, the reaction mixture was concentrated to dryness *in vacuo*. The residue was redissolved in the minimum of water, filtered to remove unreacted ligand, and the product precipitated out by the addition of an aqueous solution of NH_4PF_6. Yield 67.0 mg (87%) (Found: C, 44.12; H, 2.49; N, 11.59. Calc. for $C_{35}H_{26}N_8F_{12}P_2Ru$: C, 44.27; H, 2.76; N, 11.80). Positive-ion FAB mass spectrum: Calc. *m/z* for $C_{35}H_{26}N_8F_6PRu^+$ ($[(bpy)_2Ru(\mathbf{29})](PF_6)^+$) 805.0975; found 805.0966. λ_{max} (CH_3CN) 429 nm, ε 16 200 $M^{-1}cm^{-1}$. E^o (CH_3CN) Ru^{2+}/Ru^{3+} 1.47 V, $E^{1/2}$ 80 mV; E^o_{red} -1.34 V, $E^{1/2}$ 80 mV; E^o_{red} -1.72 V (irreversible); E^o_{red} -1.93 V (irreversible). ^{13}C NMR (CD_3CN) δ: 113.90; 119.42; 124.30; 124.67; 124.71; 124.96; 127.26; 127.56; 127.84; 128.20; 128.25; 129.88; 130.24; 133.73; 138.90; 138.98; 139.16; 141.25; 152.31; 152.58; 152.87; 153.10.

^1H NMR (CD_3CN) δ:
bpy H3, 8.57; bpy H4, 8.12; bpy H5, 7.34; bpy H6, 7.90.
bpy H3, 8.56; bpy H4, 8.10; bpy H5, 7.37; bpy H6, 8.03.
bpy H3, 8.58; bpy H4, 8.19; bpy H5, 7.50; bpy H6, 7.82.
bpy H3, 8.62; bpy H4, 8.22; bpy H5, 7.55; bpy H6, 7.88.
isq H3', 7.60; isq H4', 7.94; isq H5', 8.25; isq H6', 8.10; isq H7', 8.08; isq H8', 8.58.
Bt H4, 8.04; Bt H5, 7.70; Bt H6, 7.81; Bt H7, 8.07.

(1,1'-Bibenzotriazole)diaquadichlorocopper(39)

Ligand **23** (30 mg, 0.13 mmol) in $CHCl_3$ (3 ml) was added to $CuCl_2.2H_2O$ (22 mg, 0.13 mmol) dissolved in 1:1 $MeOH/CHCl_3$ (1 ml). After several hours a light green solid had formed and was collected by filtration. M.p. 240-244°C; yield 20 mg (47%) (Found: C, 35.45; H, 2.16; N, 20.86. Calc, for $C_{12}H_8N_6Cl_2Cu.2H_2O$: C, 35.43; H, 2.97; N, 20.66).

(1,1'-Bibenzotriazolyl)tetrafluoroboratosilver (40)

Ligand **23** (57 mg, 0.23 mmol) dissolved in CH_2Cl_2 (3 ml) was added to $AgBF_4$ (47 mg, 0.23 mmol) dissolved in 1:1 $MeOH/CH_2Cl_2$ (1 ml). A white solid formed immediately and was collected by filtration. M.p. 245-246°C; yield 100 mg (97%) (Found: C, 33.63; H, 1.60; N, 19.74. Calc, for $C_{12}H_8N_6BF_4Ag$: C, 33.45; H, 1.87; N, 19.50).

(1,1'-Bibenzotriazolyl)dichloropalladium (41)

Ligand **23** (40 mg, 0.17 mmol) dissolved in warm MeOH (10 ml) was added to $PdCl_2$ (30 mg, 0.17 mmol) dissolved in hot aqueous 2M HCl (2 ml). A yellow solid precipitated immediately and was collected by filtration. M.p. >300°C; yield 52.5 mg (75%) (Found: C, 34.41; H, 1.97; N, 20.25; Cl, 17.05. Calc. for $C_{12}H_8N_6Cl_2Pd$: C, 34.85; H, 1.95; N, 20.32; Cl, 17.15).

[(1,1'-Methylenebisbenzotriazolyl)dichlorocopper]$_n$ (42)

Ligand **24** (50 mg, 0.20 mmol) dissolved in warm MeOH (3 ml) was added to $CuCl_2.2H_2O$ (28 mg, 0.20 mmol) dissolved in MeOH (1 ml). Green crystals suitable for structure determination grew from slow evaporation of this solution. M.p. 240-250°C; yield 60 mg (86%) (Found: C, 40.90; H, 2.52; N, 21.93; Cl, 18.34. Calc. for $C_{13}H_{10}N_6Cl_2Cu$: C, 40.59; H, 2.62; N, 21.84; Cl, 18.43).

[(N3-1,1'-Methylenebisbenzotriazolyl)nitratosilver. acetonitrile solvate]$_n$ (43)

Ligand **24** (35 mg, 0.14 mmol) dissolved in warm MeOH (3 ml) was added to $AgNO_3$ (24 mg, 0.14 mmol) dissolved in warm MeOH (3 ml). A white solid formed immediately and was collected by filtration. Recrystallisation from acetonitrile gave colourless crystals suitable for structure determination. M.p. 253-255°C; yield 48.4 mg (84%) (Found: C, 39.19; H, 2.57; N, 24.22. Calc. for $C_{13}H_{10}N_7O_3Ag.MeCN$: C, 39.07; H, 2.84; N, 24.30).

(1,1'-Methylenebisbenzotriazolyl)dichloropalladium (44)

Ligand **24** (25 mg, 0.10 mmol) dissolved in 2 ml warm MeOH was added to $PdCl_2$ (18 mg, 0.10 mmol) dissolved in hot aqueous 2M HCl (1 ml). A yellow solid precipitated immediately and was collected by filtration. M.p. >300°C; yield 40 mg (93%) (Found: C, 36.55; H, 2.74; N, 19.41. Calc. for $C_{13}H_{10}N_6Cl_2Pd$: C, 36.52; H, 2.36; N, 19.66).

Bis[1-(2-pyridyl)benzotriazole]dinitratocopper.hydrate.methanol solvate (45)

Ligand **27** (40 mg, 0.20 mmol) dissolved in MeOH (2 ml) was added to $Cu(NO_3)_2.3H_2O$ (49 mg, 0.20 mmol) dissolved in MeOH (1 ml). Green crystals suitable for structure determination grew from slow evaporation of this solution. M.p. 223-225°C; yield 65 mg (60%) (Found: C, 44.01; H, 3.38; N, 22.32. Calc. for $C_{22}H_{16}N_{10}O_6Cu.MeOH.H_2O$: C, 43.85; H, 3.52; N, 22.23). Positive-ion FAB mass spectrum: Calc. *m/z* for $C_{22}H_{16}N_8Cu^+$ [$(\mathbf{27})_2Cu^+$, 100%] 455.0802; found 455.0796.

μ-Bis[1-(2-pyridyl)benzotriazolyl]dinitratodisilver (46)

Ligand **27** (40 mg, 0.20 mmol) dissolved in MeOH (3 ml) was added to $AgNO_3$ (35 mg, 0.20 mmol) dissolved in hot MeOH (2 ml). Colourless crystals suitable for structure determination grew from slow evaporation of this solution. M.p. 228-229°C; yield 57 mg (77%) (Found: C, 36.13; H, 1.99; N, 19.23. Calc. for $C_{22}H_{16}N_{10}O_6Ag_2$: C, 36.09; H, 2.20; N, 19.13).

[1-(2-Pyridyl)benzotriazolyl]dichloropalladium.hemihydrate (47)

Ligand **27** (40 mg, 0.20 mmol) dissolved in MeOH (2 ml) was added to $PdCl_2$ (35 mg, 0.20 mmol) dissolved in hot aqueous 2M HCl (2 ml). A yellow solid precipitated immediately and was collected by filtration and recrystallised from $MeNO_2$. M.p. >300°C; yield 70 mg (93%) (Found: C, 34.38; H, 2.47; N, 14.80. Calc. for $C_{11}H_8N_4Cl_2Pd.½H_2O$: C, 34.53; H, 2.11; N, 14.64).

Bis[1-([2-pyridyl]methyl)benzotriazole]diperchloratocopper (48)

Ligand **28** (57 mg, 0.27 mmol) dissolved in MeOH (2 ml) was added to $Cu(ClO_4)_2.6H_2O$ (100 mg, 0.27 mmol) dissolved in MeOH (1 ml). Blue plates grew from slow evaporation of this solution. M.p. 190°C; yield 80 mg (76%) (Found: C, 36.84; H, 2.42; N, 14.23. Calc. for $C_{36}H_{30}N_{12}Cl_4O_{16}Cu_2.H_2O$: C, 36.84; H, 2.75; N, 14.32). Positive-ion FAB mass spectrum: Calc. *m/z* for $C_{24}H_{20}N_8ClO_4Cu_2^+$ [(**28**)$_2$$Cu_2(ClO_4)^+$, 50%], 646.9860; found 646.9872. Calc. *m/z* for $C_{24}H_{20}N_8ClO_4Cu^+$ [(**28**)$_2$$Cu(ClO_4)^+$, 50%] 582.0601; found 582.0594. Fractional recrystallisation of this mixture from DMF afforded pure **48**.

μ-Bis[1-([2-pyridyl]methyl)benzotriazole]dinitratodisilver (49)

Ligand **28** (48 mg, 0.23 mmol) dissolved in MeOH (2 ml) was added to $AgNO_3$ (39 mg, 0.23 mmol) dissolved in hot MeOH (2 ml). A white solid precipitated immediately and was collected by filtration. Recrystallisation from MeCN gave colourless crystals suitable for structure determination. M.p. 225-227°C; yield 64 mg (73%) (Found: C, 38.10; H, 2.84; N, 18.28. Calc. for $C_{24}H_{20}N_{10}O_6Ag_2$: C, 37.91; H, 2.65; N, 18.42).

μ-Bis[(1-[2-pyridyl]methyl)benzotriazolyl]tetrachlorodipalladium.methanol solvate (50)

Ligand **28** (52 mg, 0.25 mmol) dissolved in MeOH (2 ml) was added to $PdCl_2$ (44 mg, 0.25 mmol) dissolved in hot aqueous 2M HCl (3 ml). A yellow solid precipitated immediately and was collected by filtration and recrystallised from $MeNO_2$. Crystals suitable for structure determination were grown from vapour diffusion of MeOH into a DMF solution of the complex. M.p. 250-260°C; yield 94 mg (98%) (Found: C, 37.15; H, 3.29; N, 13.82; Cl,

17.27. Calc. for $C_{24}H_{20}N_8Cl_4Pd_2$.MeOH: C, 37.20; H, 3.00; N, 13.88; Cl, 17.57). Positive-ion FAB mass spectrum: Calc. *m/z* for $C_{24}H_{20}N_8Cl_3Pd_2^+$ [(**28**)$_2$$Pd_2Cl_3^+$, 100%] 738.8965; found 738.8947.

Hexakis(μ-2-chloro)(μ-4-oxo)-tetrakis[1-(1-isoquinolyl)benzotriazole-copper(II)] (51)

$CuCl_2.2H_2O$ (22.9 mg, 0.13 mmol) dissolved in 1:1 chloroform/methanol (1 ml) was added to ligand **29** (33.0 mg, 0.13 mmol) dissolved in chloroform (2 ml) and the resulting solution swirled. After 1 day a yellow solid had formed and this was filtered off. Vapour diffusion of ether into the filtrate precipitated more tan solid. Yield 45.4 mg (89%) (Found: C, 47.05; H, 2.58; N, 14.61; Cl, 18.47. Calc. for $C_{15}H_{10}N_4Cl_2Cu$: C, 47.32; H, 2.65; N, 14.71; Cl, 18.63). This material was recrystallised from nitromethane to give thin orange plate-like crystals of **51**.

[1-(1-Isoquinolyl)benzotriazolyl]tetrafluoroboratosilver.hemihydrate (52)

$AgBF_4$ (33.5 mg, 0.17 mmol) dissolved in 1:1 chloroform/methanol (1 ml) was added to **29** (41 mg, 0.17 mmol) dissolved in chloroform (2 ml). The reaction mixture was kept in the dark and a white solid developed over several days. The solid was filtered off and washed with chloroform. Yield 62 mg (83%) (Found: C, 39.93; H, 2.13; N, 12.43. Calc. for $C_{15}H_{10}N_4BF_4Ag.½H_2O$: C, 40.04; H, 2.46; N, 12.44).

μ-Bis[1-(1-isoquinolyl)benzotriazole]tetrachlorodipalladium (53)

A solution of 0.0363M Li_2PdCl_4 (5.70 ml, 0.21 mmol) in methanol was added to **29** (50.3 mg, 0.21 mmol) dissolved in 25 ml refluxing MeOH. A yellow solid, which precipitated immediately, was collected by filtration and recrystallised from $MeNO_2$. M.p. 255-260°C; yield 71.1 mg. Positive-ion FAB mass spectrum: Calc. *m/z* for $C_{30}H_{20}N_8Cl_3Pd_2$ [(**29**)$_2$$Pd_2Cl_3^+$, 100%] 810.8956; found 810.8947.

[N4,N4'-(3,3'-Bi-1,2,4-oxadiazolyl)]dichloropalladium (75)

Ligand **57** (66 mg, 0.48 mmol) dissolved in MeOH (2.5 ml) was added to a methanolic solution of 0.0942M Li_2PdCl_4 (5.2 ml, 0.49 mmol). After evaporation of *ca.* half the solution, orange plates had formed and these were collected by filtration (35 mg). A yellow solid was obtained after more evaporation of the filtrate and this too was collected by filtration (60 mg). M.p. >300°C; yield 95 mg (63%) (Found: C, 15.15; H, 0.46; N, 17.96; Cl, 23.06. Calc. for $C_4H_2N_4Cl_2O_2Pd$: C, 15.23; H, 0.62; N, 17.76; Cl, 22.48).

[N4-(3,3'-Bi-1,2,4-oxadiazolyl)nitratosilver]$_n$ (76)

Ligand **57** (20 mg, 0.15 mmol) dissolved in MeOH (1 ml) was added to $AgNO_3$ (31 mg, 0.15 mmol) dissolved in MeOH (1 ml) and H_2O (3-4 drops). A white solid formed immediately and was collected by filtration. Recrystallisation from acetonitrile produced crystals suitable for X-ray diffraction. M.p. 141-145°C; yield 35 mg (69%) (Found: C, 15.70; H, 0.39; N, 22.69. Calc. for $C_4H_2N_5O_5Ag$: C, 15.60; H, 0.65; N, 22.74).

(5,5'-Dimethyl-3,3'-bi-1,2,4-oxadiazolyl)dichloropalladium (77)

$PdCl_2$ (44 mg, 0.25 mmol) dissolved in hot aqueous 2M HCl (3 ml) was added to ligand **58** (40 mg, 0.25 mmol) dissolved in warm MeOH (4 ml). After standing for several days thin orange rods had formed and these were collected by filtration. M.p. >300°C; yield 50 mg (60%) (Found: C, 21.05; H, 1.90; N, 16.20; Cl, 20.86. Calc. for $C_6H_6N_4Cl_2O_2Pd$: C, 20.98; H, 1.76; N, 16.31; Cl, 20.65).

[2-(1,2,4-Oxadiazol-3-yl)pyridine]dichloropalladium (78)

A methanolic solution of 0.0942M Li_2PdCl_4 (3 ml, 0.28 mmol) was added to a stirred solution of ligand **63** (40 mg, 0.27 mmol) dissolved in MeOH (3 ml). The yellow precipitate that formed was collected by filtration and recrystallised from $MeNO_2$. M.p. >300°C; yield 84 mg (95%) (Found: C, 26.04; H, 1.31; N, 12.95; Cl, 21.56. Calc. for $C_7H_5N_3Cl_2OPd$: C, 25.95; H, 1.55; N, 12.95; Cl, 21.85). ^{1}H NMR (d_6-DMSO) δ: 8.41, d, 1H, H3; 8.41, t, 1H, H4; 7.96, t, 1H, H5; 9.08, d, 1H, H6; 10.73, s, 1H, H5'.

Bis[methyl picolinimidate]dinitratodiaquacopper (79)

Ligand **63** (35.0 mg, 0.238 mmol) dissolved in methanol (3 ml) was added to $Cu(NO_3)_2.3H_2O$ (31.1 mg, 0.129 mmol) dissolved in methanol (2 ml). After several days sky blue crystals had formed and these were collected by filtration. M.p. 185-187°C; yield 39.2 mg (61%) (Found: C, 34.11; H, 4.05; N, 16.86. Calc for $C_{14}H_{20}N_6O_{10}Cu$: C, 33.91; H, 4.07; N, 16.94).

[2-(1,2,4-Oxadiazol-3-yl)pyridine]dichlorocopper (80)

Ligand **63** (46.3 mg, 0.31 mmol) dissolved in MeOH (2 ml) was added to $CuCl_2.2H_2O$ (54.0 mg, 0.32 mmol) dissolved in MeOH (1 ml). The lime precipitate that formed was collected by filtration. M.p. >300°C; yield 88 mg (99%) (Found: C, 29.98; H, 1.59; N, 14.83; Cl, 25.08. Calc for $C_7H_5N_3Cl_2OCu$: C, 29.86; H, 1.79; N, 14.92; Cl, 25.18).

[N1,N4'-2-(1,2,4-Thiadiazol-5-yl)pyridine]dichloropalladium (81)

Ligand **65** (53 mg, 0.33 mmol) dissolved in MeOH (3 ml) was added to a methanolic solution of 0.0363M Li_2PdCl_4 (9 ml, 0.33 mmol) and the resulting solution swirled. The voluminous yellow precipitate that formed was collected by filtration and recrystallised from $MeNO_2$. M.p. >300°C; yield 94 mg (85%) (Found: C, 24.80; H, 1.48; N, 12.53; Cl, 20.90. Calc. for $C_7H_5N_3Cl_2SPd$: C, 24.69; H, 1.48; N, 12.34; Cl, 20.82). ^1H NMR (d_6-DMSO) δ: 8.78, d, 1H, H3; 8.43, t, 1H, H4; 7.95, t, 1H, H5; 9.03, d, 1H, H6; 9.14, s, 1H, H3'.

[N1,N4'-2-(1,2,4-Thiadiazol-5-yl)pyridine]dichlorocopper (82)

Ligand **65** (55 mg, 0.34 mmol) dissolved in MeOH (3 ml) was added to $CuCl_2.2H_2O$ (53 mg, 0.34 mmol) dissolved in MeOH (1 ml) and the resulting solution swirled. The light lime precipitate that formed was collected by filtration. M.p. >300°C; yield 94 mg (98%) (Found: C, 28.31; H, 1.67; N, 14.00; Cl, 23.83. Calc. for $C_7H_5N_3Cl_2SCu$: C, 28.25; H, 1.69; N, 14.11; Cl, 23.82). Positive-ion FAB mass spectrum: Calc. *m/z* for $C_7H_5N_3ClSCu^+$ [(**65**)$CuCl^+$, 100%] 260.9192; found 260.9191.

Bis(4,4'-dimethyl-2,2'-bipyridine)(N1,N4'-[2-(1,2,4-thiadiazol-5-yl)pyridine])ruthenium(II) bis(hexafluorophosphate) (83)

Ligand **65** (12.0 mg, 0.074 mmol) and $Ru(dmb)_2Cl_2.2H_2O$ (40.0 mg, 0.069 mmol) in 3:1 EtOH/H_2O (8 ml) were refluxed for 15 hrs. After cooling, the reaction mixture was concentrated to dryness *in vacuo*. The residue was redissolved in the minimum of water, filtered to remove unreacted ligand, and the product precipitated out by the addition of an aqueous solution of NH_4PF_6. Yield 61 mg (96%) (Found: C, 40.10; H, 3.06; N, 10.59. Calc. for $C_{31}H_{29}N_7F_{12}P_2RuS$: C, 40.35; H, 3.17; N, 10.63). Positive-ion FAB mass spectrum: Calc. *m/z* for $C_{31}H_{29}N_7F_6PRuS^+$ ([(dmb)$_2$Ru(**65**)](PF$_6$)$^+$) 778.0910; found 778.0891. λ_{max} (CH_3CN) 487 nm, ε 9400 $M^{-1}cm^{-1}$. E^o (CH_3CN) Ru^{2+}/Ru^{3+} 1.18 V, $E^{1/2}$ 75 mV; E^o_{red} -1.08 V, $E^{1/2}$ 60 mV; E^o_{red} -1.69 V, $E^{1/2}$ 80 mV; E^o_{red} -1.88 V, $E^{1/2}$ 60 mV. ^1H NMR (CD_3CN) δ: 2.59, s, 12H, dmb4-CH3's; 7.29, m, 4H, dmb H5's; 7.56, m, 3H, H5 and 2 x dmb H6's; 7.65, m, 2H, 2 x dmb H6's; 7.85, d, 1H, H6; 8.15, t, 1H, H4; 8.28, s, 1H, H3'; 8.39, m, 4H, dmb H3's; 8.59, d, 1H, H3.

Bis(2,2'-bipyridine)(N1,N4'-[2-(1,2,4-thiadiazol-5-yl)pyridine])ruthenium(II) bis(hexafluorophosphate) (84)

Ligand **65** (16.0 mg, 0.098 mmol) and $Ru(bpy)_2Cl_2.2H_2O$ (51.0 mg, 0.098 mmol) in 3:1 EtOH/H_2O (8 ml) were refluxed for 4 hrs. After cooling, the reaction mixture was concentrated to dryness *in vacuo*. The residue was redissolved in the minimum of water, filtered to remove unreacted ligand, and the product precipitated out by the addition of an

aqueous solution of NH_4PF_6. Yield 65.1 mg (77%) (Found: C, 37.64; H, 2.57; N, 11.04. Calc. for $C_{27}H_{21}N_7F_{12}P_2RuS$: C, 37.42; H, 2.44; N, 11.31). Positive-ion FAB mass spectrum: Calc. *m/z* for $C_{27}H_{21}N_7F_6PRuS^+$ ($[(bpy)_2Ru(L)](PF_6)^+$) 722.0280; found 722.0265. λ_{max} (CH_3CN) 487 nm, ε 9400 $M^{-1}cm^{-1}$. E^o (CH_3CN) Ru^{2+}/Ru^{3+} 1.29 V, $E^{1/2}$ 60 mV; E^o_{red} -1.02 V, $E^{1/2}$ 60 mV; E^o_{red} -1.58 V, $E^{1/2}$ 60 mV; E^o_{red} -1.92 V, $E^{1/2}$ 70 mV. ^1H NMR (CD_3CN) δ: 7.48, m, 4H, H5 and 3 x bpy H5; 7.58, t, 1H, bpy H5; 7.75, d, 1H, bpy H6; 7.79, d, 1H, bpy H6; 7.86, m, 3H, 3 x bpy H6; 8.15, m, 5H, H4 and 4 x bpy H4; 8.31, s, 1H, H3'; 8.56, m, 4H, H3 and 3 x bpy H3; 8.62, d, 1H, bpy H3.

[3,6-Di(2-pyridyl)-1,4,2,5-dioxadiazine]nitratosilver (88)

$AgNO_3$ (22.4 mg, 0.13 mmol) dissolved in hot MeOH (3 ml) was added to ligand **87** (31.3 mg, 0.13 mmol) in warm MeOH (2 ml). A colourless precipitate formed immediately and was collected by filtration. Yield 51.4 mg (96%) (Found: C, 34.94; H, 1.79; N, 16.80. Calc. for $C_{12}H_8N_5O_5Ag$: C, 35.15; H, 1.97; N, 17.07).

[1,4-Bis(2-pyridyl)buta-1,3-diyne]nitratosilver (104)

$AgNO_3$ (46 mg, 0.27 mmol) dissolved in hot MeOH (2 ml) was added to **103** (50 mg, 0.24 mmol) dissolved in MeOH (1 ml). The fawn precipitate that formed was collected by filtration. Crystals suitable for X-ray analysis were grown from slow evaporation of a CH_3CN solution of the complex. M.p. >179°C; yield 83 mg (86%) (Found: C, 44.60; H, 2.05; N, 11.13. Calc. for $C_{14}H_8N_3O_3Ag$: C, 44.95; H, 2.16; N, 11.23).

Bis(2,2'-bipyridine)(2-[N5-1,2,5-thiadiazol-3-yl]pyridine)chlororuthenium(II)-hexafluorophosphate (107) and bis(2,2'-bipyridine)(2-[N2-1,2,5-thiadiazol-3-yl]pyridine)ruthenium(II) bis(hexafluorophosphate) (108)

$Ru(bpy)_2Cl_2.2H_2O$ (64.0 mg, 0.122 mmol) in 3:1 $EtOH/H_2O$ (8 ml) was refluxed for 1 hr before the addition of ligand **93** (20.0 mg, 0.123 mmol) as a solid. Reflux was continued for another 2 hrs. After cooling, the reaction mixture was concentrated to dryness *in vacuo*. The residue was redissolved in the minimum of water, filtered to remove unreacted ligand, and the product precipitated out by the addition of an aqueous solution of NH_4PF_6. Chromatography on alumina (1 x 7 cm) with 100:1 CH_2Cl_2/MeOH as eluent, cleanly separated a small dark red fraction, then a larger orange fraction. ^1H NMR, UV-visible spectroscopy, FAB mass spectrometry and elemental analysis identified the fractions as the above mentioned complexes respectively.

Bis(2,2'-bipyridine)(2-[N5-1,2,5-thiadiazol-3-yl]pyridine)chlororuthenium(II)-hexafluorophosphate (**107**)

Yield 5.5 mg (8%). Positive-ion FAB mass spectrum: Calc. *m/z* for $C_{27}H_{21}N_7ClRuS^+$ ($[(bpy)_2Ru(\mathbf{93})Cl]^+$) 612.0321; found 612.0311.

Bis(2,2'-bipyridine)(N1,N2'-[2-(1,2,5-thiadiazol-3-yl)pyridine])ruthenium(II) bis(hexafluorophosphate) (**108**)

Yield 77.7 mg (73%) (Found: C, 37.70; H, 2.23; N, 11.14. Calc. for $C_{27}H_{21}N_7F_{12}P_2RuS$: C, 37.42; H, 2.44; N, 11.31). Positive-ion FAB mass spectrum: Calc. *m/z* for $C_{27}H_{21}N_7F_6PRuS^+$ ($[(bpy)_2Ru(\mathbf{93})](PF_6)^+$) 722.0278; found 722.0265. λ_{max} (CH_3CN) 450 nm, ε 11 600 $M^{-1}cm^{-1}$. E^o (CH_3CN) Ru^{2+}/Ru^{3+} +1.36 V, $E^{1/2}$ 65 mV; E^o_{red} -1.19 V, $E^{1/2}$ 70 mV; E^o_{red} -1.55 V (irreversible). ^1H NMR (CD_3CN) δ: 7.55, m, 5H, H5 and 4 x bpy H5's; 7.64, d, 1H, bpy H6; 7.80, m, 3H, 3 x bpy H6's; 7.86, d, 1H, bpy H6; 8.18, m, 5H, H4 and 4 x bpy H4's; 8.60, 5H, H6 and 4 x bpy H6; 9.55, s, 1H, H4'.

Bis(2,2'-bipyridine)(N2,N1'-[3,4-di(2-pyridyl)-1,2,5-oxadiazolyl])ruthenium(II) bis(hexafluorophosphate) (109)

Ligand **91** (15.0 mg, 0.067 mmol) and $Ru(bpy)_2Cl_2.2H_2O$ (34.8 mg, 0.067 mmol) in 3:1 $EtOH/H_2O$ (8 ml) were refluxed for 4 hrs. After cooling, the reaction mixture was concentrated to dryness *in vacuo*. The residue was redissolved in the minimum of water, filtered to remove unreacted ligand, and the product precipitated out by the addition of an aqueous solution of NH_4PF_6. Yield 56.0 mg (92%) (Found: C, 41.50; H, 2.48; N, 12.06. Calc. for $C_{32}H_{24}N_8F_{12}OP_2Ru$: C, 41.44; H, 2.61; N, 12.08). Positive-ion FAB mass spectrum: Calc. *m/z* for $C_{32}H_{24}N_8F_6OPRu^+$ ($[(bpy)_2Ru(\mathbf{91})](PF_6)^+$) 783.0773; found 783.0758. λ_{max} (CH_3CN) 435 nm, ε 13 400 $M^{-1}cm^{-1}$. E^o (CH_3CN) Ru^{2+}/Ru^{3+} 1.51 V, $E^{1/2}$ 60 mV; E^o_{red} -0.97 V (irreversible).

^1H NMR (CD_3CN) δ:
bpy H3, 8.59; bpy H4, 8.18; bpy H5, 7.53; bpy H6, 8.03.
bpy H3, 8.56; bpy H4, 8.17; bpy H5, 7.50; bpy H6, 7.86.
bpy H3, 8.58; bpy H4, 8.16; bpy H5, 7.54; bpy H6, 7.74.
bpy H3, 8.63; bpy H4, 8.23; bpy H5, 7.57; bpy H6, 7.79.
H3, 9.86; H4, 8.22; H5, 7.59; H6, 7.88.
H3', 8.27; H4', 8.16; H5', 7.77; H6', 9.03.

Bis(4,4'-dimethyl-2,2'-bipyridine)(N2,N1'-[3,4-di(2-pyridyl)-1,2,5-oxadiazolyl])ruthenium(II) bis(hexafluorophosphate) (110)

Ligand **91** (10.0 mg, 0.045 mmol) and $Ru(dmb)_2Cl_2.2H_2O$ (25.8 mg, 0.045 mmol) in 3:1 $EtOH/H_2O$ (8 ml) were refluxed for 4 hrs. After cooling, the reaction mixture was concentrated to dryness *in vacuo*. The residue was redissolved in the minimum of water,

filtered to remove unreacted ligand and the product precipitated out by the addition of an aqueous solution of NH_4PF_6. Yield 19.1 mg (89%) (Found: C, 43.77; H, 3.41; N, 11.12. Calc. for $C_{36}H_{32}N_8F_{12}OP_2Ru$: C, 43.96; H, 3.28; N, 11.39). Positive-ion FAB mass spectrum: Calc. *m/z* for $C_{32}H_{24}N_8F_6OPRu^+$ ([(dmb)$_2$Ru(**91**)](PF$_6$)$^+$) 778.0910 found 778.0891. λ_{max} (CH_3CN) 441nm, ε 23 500 $M^{-1}cm^{-1}$. E^o (CH_3CN) Ru^{2+}/Ru^{3+} +1.40 V, $E^{1/2}$ 60 mV; E^o_{red} -1.08 V (irreversible). ^1H NMR (CD_3CN) δ: 2.60, s, 3H, dmb4-CH3; 2.62, s, 6H, dmb4-CH3; 2.64, s, 3H, dmb4-CH3; 7.35, m, 3H, 3 x dmb H5; 7.40, d, 1H, dmb H5; 7.52, d, 1H, dmb H6; 7.56, t, 1H, H5; 7.59, d, 1H, dmb H6; 7.67, d, 1H, dmb H6; 7.76, t, 1H, H5'; 7.82, d, 1H, dmb H6; 7.85, d, 1H, H6; 8.17, t, 1H, H5; 8.18, t, 1H, H5'; 8.25, d, 1H, H3'; 8.42, s, 1H, dmb H3; 8.43, s, 2H, 2 x dmb H3; 8.48, s, 1H, dmb H3; 9.02, d, 1H, H6'; 9.80, d, 1H, H3.

Bis(2,2'-bipyridine)(N2,N1'-[3,4-di(2-pyridyl)-1,2,5-thiadiazolyl])ruthenium(II) bis(hexafluorophosphate) (111)

Ligand **94** (45 mg, 0.19 mmol) and Ru(bpy)$_2$Cl$_2$.2H$_2$O (105 mg, 0.20 mmol) in 3:1 EtOH/H$_2$O (8 ml) were refluxed for 5 hrs. After cooling, the reaction mixture was concentrated to dryness *in vacuo*. The residue was redissolved in the minimum of water, filtered to remove unreacted ligand, and the product precipitated out by the addition of an aqueous solution of NH_4PF_6. Chromatography on alumina separated a small amount of the dinuclear complex from the desired mononuclear complex. Yield 153 mg (87%) (Found: C, 40.45; H, 2.46; N, 11.62. Calc. for $C_{32}H_{24}N_8F_{12}P_2RuS$: C, 40.73; H, 2.56; N, 11.87). Positive-ion FAB mass spectrum: Calc. *m/z* for $C_{32}H_{24}N_8F_6PRuS^+$ ([(bpy)$_2$Ru(**94**)](PF$_6$)$^+$) 759.0540; found 759.0537. λ_{max} (CH_3CN) 454 nm, ε 15 000 $M^{-1}cm^{-1}$. E^o (CH_3CN) Ru^{2+}/Ru^{3+} +1.37 V, $E^{1/2}$ 65 mV; E^o_{red} -1.18 V, $E^{1/2}$ 65 mV; E^o_{red} - 1.53 V (irreversible).

^1H NMR (CD_3CN) δ:
bpy H3, 8.59; bpy H4, 8.16; bpy H5, 7.51; bpy H6, 7.92.
bpy H3, 8.61; bpy H4, 8.18; bpy H5, 7.52; bpy H6, 7.81.
bpy H3, 8.59; bpy H4, 8.18; bpy H5, 7.52; bpy H6, 7.77.
bpy H3, 8.60; bpy H4, 8.20; bpy H5, 7.50; bpy H6, 7.88.
H3, 9.02; H4, 8.03; H5, 7.49; H6, 7.86.
H3', 8.09; H4', 8.12; H5', 7.74; H6', 8.90.

Tris(N2,N1'-[3,4-di(2-pyridyl)-1,2,5-thiadiazolyl])ruthenium(II) bis(hexafluorophosphate) (112)

Ligand **94** (0.1056 g, 0.44 mmol) and Ru(DMSO)$_4$Cl$_2$ (0.0630 g, 0.13 mmol) in 3:1 ethanol/water (8 ml) were refluxed for 24 hours. After cooling, the reaction mixture was concentrated to dryness *in vacuo*. The residue was redissolved in the minimum of water, filtered to remove unreacted ligand, and the product precipitated out by the addition of an aqueous solution of NH_4PF_6 and purified by chromatography on alumina (1 x 5 cm) with

200:1 dichloromethane/methanol. Yield 113 mg (78%) (Found: C, 38.44; H, 2.36; N, 14.56; S, 8.58. Calc. for $C_{36}H_{24}N_{12}F_{12}P_2RuS_3.H_2O$: C, 38.27; H, 2.32; N, 14.87; S, 8.51). Positive-ion FAB mass spectrum: Calc. *m/z* for $C_{36}H_{24}N_{12}F_6PRuS_3^+$ ($[(\mathbf{94})_3Ru](PF_6)^+$) ; found . λ_{max} (CH_3CN) 435 nm, ε 18 900 $M^{-1}cm^{-1}$. E^o_{red} (CH_3CN) - 0.73 V (irreversible).

Tris(N2,N1'-[3,4-di(2-pyridyl)-1,2,5-oxadiazolyl])ruthenium(II) bis(hexafluorophosphate) (113)

Ligand **91** (31.6 mg, 0.14 mmol) and $Ru(DMSO)_4Cl_2$ (19.5 mg, 0.04 mmol) in 3:1 ethanol/water (6 ml) were refluxed for 5 hours. After cooling, the reaction mixture was concentrated to dryness *in vacuo*. The residue was redissolved in the minimum of water, filtered to remove unreacted ligand, and the product precipitated out by the addition of an aqueous solution of NH_4PF_6 and purified by chromatography on alumina (1 x 4 cm) with 200:1 dichloromethane/methanol. Yield 19 mg (45%). Positive-ion FAB mass spectrum: Calc. *m/z* for $C_{36}H_{24}N_{12}F_6O_3PRu^+$ ($[(\mathbf{91})_3Ru](PF_6)^+$) 919.0810; found 919.0780. λ_{max} (CH_3CN) 401 nm, ε 16 900 $M^{-1}cm^{-1}$. E^o_{red} (CH_3CN) - 0.41 V (irreversible).

Bis(2,2'-bipyridine)[2-(2-pyridyl)-3-nitro-pyrazolo[1,5-*a*]pyridine]-ruthenium(II) bis(hexafluorophosphate) (115)

Ligand **99** (17.0 mg, 0.058 mmol) and $Ru(bpy)_2Cl_2.2H_2O$ (30.0 mg, 0.058 mmol) in 3:1 $EtOH/H_2O$ (8 ml) were refluxed for 4 hrs. After cooling, the reaction mixture was concentrated to dryness *in vacuo*. The residue was redissolved in the minimum of water, filtered to remove unreacted ligand, and the product precipitated out by the addition of an aqueous solution of NH_4PF_6. Yield 59.1 mg (90%) (Found: C, 40.97; H, 2.31; N, 11.68. Calc. for $C_{31}H_{24}N_8F_{12}P_2Ru$: C, 40.74; H, 2.56; N, 11.87). Positive-ion FAB mass spectrum: Calc. *m/z* for $C_{31}H_{24}N_8F_6PRu^+$ ($[(bpy)_2Ru(\mathbf{L})](PF_6)^+$) 799.0722; found 799.0708. λ_{max} (CH_3CN) 443 nm, ε 15 900 $M^{-1}cm^{-1}$. E^o (CH_3CN) Ru^{2+}/Ru^{3+} +1.28 V, $E^{1/2}$ 65 mV; E^o_{red} -0.97 V, $E^{1/2}$ 65mV.

^1H NMR (CD_3CN) δ:
bpy H3, 8.53; bpy H4, 8.10; bpy H5, 7.47; bpy H6, 7.70.
bpy H3, 8.56; bpy H4, 8.15; bpy H5, 7.45; bpy H6, 7.60.
bpy H3, 8.58; bpy H4, 8.14; bpy H5, 7.42; bpy H6, 7.97.
bpy H3, 8.59; bpy H4, 8.18; bpy H5, 7.54; bpy H6, 7.96.
H3, 9.55; H4, 8.23; H5, 7.50; H6, 7.84.
H4', 8.57; H5', 7.91; H6', 7.16; H7', 7.34.

Bis(4,4'-dimethyl-2,2'-bipyridine)[2-(2-pyridyl)-3-nitro-pyrazolo[1,5-*a*]pyridine]-ruthenium(II) bis(hexafluorophosphate) (116)

Ligand **99** (14.6 mg, 0.061 mmol) and $Ru(dmb)_2Cl_2.2H_2O$ (35.1 mg, 0.061 mmol) in 3:1 $EtOH/H_2O$ (8 ml) were refluxed for 4 hrs. After cooling, the reaction mixture was concentrated to dryness *in vacuo*. The residue was redissolved in the minimum of water, filtered to remove unreacted ligand, and the product precipitated out by the addition of an aqueous solution of NH_4PF_6. The dark red salt was recrystallised by vapour diffusion of diethylether into an acetonitrile solution of the complex. Yield 55.0 mg (90%) (Found: C, 43.75; H, 3.10; N, 11.64. Calc. for $C_{36}H_{32}N_8F_{12}O_2P_2Ru.½CH_3CN$: C, 43.56; H, 3.30; N, 11.66). Positive-ion FAB mass spectrum: Calc. *m/z* for $C_{36}H_{32}N_8F_6O_2PRu^+$ ($[(dmb)_2Ru(\mathbf{L})](PF_6)^+$) 855.1340; found 855.1334. λ_{max} (CH_3CN) 438 nm, ε 15 500 $M^{-1}cm^{-1}$. E^o (CH_3CN) Ru^{2+}/Ru^{3+} 1.18 V, $E^{1/2}$ 70 mV; E^o_{red} -1.00 V, $E^{1/2}$ 60 mV. ^1H NMR (CD_3CN) δ: 2.56, s, 3H, dmb4-CH3; 2.58, s, 3H, dmb4-CH3; 2.59, 3H, dmb4-CH3; 2.62, 3H, dmb4-CH3; 7.18, t, 1H, H6'; 7.23, t, 1H, dmb H5; 7.29, m, 2H, dmb H5's; 7.37, d, 2H, H7' and dmb H5; 7.40, d, 1H, dmb H6; 7.48, t, 1H, H5; 7.50, d, 1H, dmb H6, 7.76, d, 2H, dmb H6's; 7.83, d, 1H, H6; 7.91, t, 1H, H5'; 8.20, t, 1H, H4; 8.37, s, 1H, dmb H3; 8.41, s, 2H, dmb H3; 8.44, s, 1H, dmb H3; 8.57, d, 1H, H4'; 9.53, d, 1H, H3.

[N1',N1''-3,4-Di(2-pyridyl)-1,2,5-oxadiazolyl-2-oxide]dichloropalladium (117)

A methanolic solution of 0.0363M Li_2PdCl_4 (2.1 ml, 0.075 mmol) was added to a stirred solution of ligand **99** (18.2 mg, 0.075 mmol) dissolved in MeOH (2 ml). After a few seconds a yellow precipitate formed and was then collected by filtration. M.p. >300°C; yield 30 mg (97%) (Found: C, 34.65; H, 1.79; N, 13.45; Cl, 16.93. Calc for $C_{12}H_8N_4Cl_2O_2Pd$: C, 34.52; H, 1.93; N, 13.41; Cl, 16.98). Positive-ion FAB mass spectrum: Calc. *m/z* for $C_{12}H_8N_4ClO_2Pd^+$ [(**99**)$PdCl^+$, 100%] 380.9361; found 380.9368. ^1H NMR (d_6-DMSO) δ: 8.03, d, 1H, H3; 8.27, t, 1H, H4; 7.82, t, 1H, H5; 9.14, d, 1H, H6; 8.07, d, 1h, H3', 8.28, t, 1H, H4'; 7.90, t, 1H, H5'; 9.18, d, 1H, H6'.

Bis[N1',N1''-3,4-di(2-pyridyl)-1,2,5-oxadiazolyl-2-oxide]tetrachlorodicopper (118)

Ligand **99** (15.8 mg, 0.09 mmol) dissolved in MeOH (2 ml) was added with stirring to $CuCl_2.2H_2O$ (22.2 mg, 0.09 mmol) dissolved in MeOH (1 ml). Green crystals started forming after several minutes. The solution was left to stand overnight and the crystals were then collected by filtration. M.p. 284-287°C; yield 32 mg (92%) (Found: C, 38.67; H, 1.95; N, 15.05; Cl, 18.97. Calc for $C_{24}H_{16}N_8Cl_4O_4Cu_2$: C, 38.47; H, 2.15; N, 14.95; Cl, 18.93).

[3,4-Di(2-pyridyl)-1,2,5-oxadiazolyl-2-oxide]nitratosilver (119)

Ligand **99** (21 mg, 0.09 mmol) dissolved in MeOH (2 ml) was added with stirring to $AgNO_3$ (15 mg, 0.09 mmol) dissolved in MeOH (1 ml). A white precipitate developed and was collected by filtration. Yield 31 mg (86%) (Found: C, 35.18; H, 1.74; N, 17.28. Calc. for $C_{12}H_8N_5O_5Ag$: C, 35.23; H, 1.97; N, 17.11).

[N1,N2'-2-(1,2,5-thiadiazol-3-yl)pyridine]dichloropalladium (120)

A methanolic solution of 0.0904M Li_2PdCl_4 (2.5 ml, 0.23 mmol) was added to ligand **93** (34.3 mg, 0.21 mmol) dissolved in methanol (2 ml). The yellow precipitate that formed was collected by filtration. M.p. >300°C; yield 65.1 mg (91%) (Found: C, 24.71; H, 1.39; N, 12.50; S, 9.18. Calc. for $C_7H_5N_3SCl_2Pd$: C, 24.69; H, 1.48; N 12.34; S, 9.42). ^1H NMR (d_6-DMSO) δ: 8.57, d, 1H, H3; 8.44, t, 1H, H4; 7.88, t, 1H, H5; 8.93, d, 1H, H6; 9.76, s, 1H, H4'.

[N1',N1"-3,4-di(2-pyridyl)-1,2,5-oxadiazolyl]dichloropalladium (121)

An excess of 0.0904M Li_2PdCl_4 was added to ligand **91** (6.5 mg, 0.029 mmol) dissolved in methanol (1 ml). The fine yellow precipitate that developed was collected by filtration. M.p. >300°C; yield 11.1 mg (95%) (Found: C, 35.71; H, 2.04; N, 13.38; Cl, 17.43. Calc. for $C_{12}H_8N_4Cl_2OPd$: C, 35.88; H, 2.01; N, 13.95; Cl, 17.66). ^1H NMR (d_6-DMSO) δ: 8.05, d, 2H, H3; 8.26, t, 2H, H4; 7.86, t, 2H, H5; 9.15, d, 2H, H6.

[N1,N1"-3,4-di(2-pyridyl)-1,2,5-thiadiazolyl]dichloropalladium (122)

An excess of 0.0904M Li_2PdCl_4 was added to ligand **94** (19.4 mg, 0.081 mmol) dissolved in methanol (2 ml). The yellow precipitate that formed was collected by filtration and washed with methanol. M.p. >300°C; yield 30.3 mg (90%) (Found: C, 34.55; H, 2.02; N, 13.04; S, 7.68. Calc. for $C_{12}H_8N_4Cl_2PdS$: C, 34.52; H, 1.93; N, 13.41; S, 7.68). ^1H NMR (d_6-DMSO) δ: 8.93, d, 2H, H3; 8.19, t, 2H, H4; 7.79, t, 2H, H5; 9.08, d, 2H, H6.

[3,4-Di(2-pyridyl)-1,2,5-thiadiazolyl]dichloroplatinum (123)

Ligand **94** (37.5 mg, 0.155 mmol) dissolved in nitromethane (2 ml) was added to $(DMSO)_2PtCl_2$ (66.5 mg, 0.158 mmol) dissolved in nitromethane (3 ml), and the clear solution left overnight. In the morning the resulting yellow microcrystals were filtered off. M.p. >300°C; yield 71.2 mg (91%) (Found: C, 28.49; H, 1.67; N, 10.85; Cl, 13.91; S, 6.13. Calc. for $C_{12}H_8N_4Cl_2PtS$: C, 28.45; H, 1.60; N, 10.77; Cl, 13.99; S, 6.19). Electrospray MS: Calc. for $C_{12}H_8N_4ClPtS^+$: 469.9806; found 469.9788.

[N1,N1"-3,4-di(2-pyridyl)-1,2,5-thiadiazolyl]dinitratocopper (124)

Ligand **94** (39.5 mg, 0.160 mmol) dissolved in methanol (2.5 ml) was added to $Cu(NO_3)_2.3H_2O$ (85.0 mg, 0.350 mmol) dissolved in methanol (2.5 ml). After several days the sky blue crystals that had formed were collected by filtration. M.p. 190-200°C; yield 41.1 mg (58%) (Found: C, 33.80; H, 1.84; N, 19.32. Calc. for $C_{12}H_8N_6O_6CuS$: C, 33.69; H, 1.88; N, 19.64).

[N1,N1"-3,4-di(2-pyridyl)-1,2,5-thiadiazole silver nitrate]$_n$ (125)

$AgNO_3$ (26.3 mg 0.154 mmol) dissolved in hot methanol (2.5 ml) was added to ligand **94** (37.9 mg, 0.158 mmol) dissolved in methanol (3 ml). After several days a powder had formed, and the methanolic solution was withdrawn. The remaining solid was recrystallised from acetonitrile. Yield 56 mg (88%) (Found: C, 35.23; H, 1.85; N, 17.20. Calc. for $C_{12}H_8N_4O_3AgS$: C, 35.14; H, 1.97; N, 17.07).

Tetrakis(4,4'-dimethyl-2,2'-bipyridine)-μ-[3,4-di(2-pyridyl)-1,2,5-oxadiazolyl]-diruthenium(II)-tetrakis(hexafluorophosphate) (126)

Ligand **91** (15.5 mg, 0.069 mmol) and $Ru(dmb)_2Cl_2.2H_2O$ (80 mg, 0.138 mmol) in 3:1 $EtOH/H_2O$ (16 ml) were refluxed for 24 hrs. After cooling, the reaction mixture was concentrated to dryness *in vacuo*. The residue was redissolved in the minimum of water, filtered to remove unreacted ligand, and the product precipitated out by the addition of an aqueous solution of NH_4BF_4. Additional product was obtained by extraction of the aqueous solution with dichloromethane. Chromatography on alumina separated the mononuclear complex from the dinuclear complex. The ^1H NMR spectrum of **126** showed the presence of two diastereoisomers in a ratio of 5:6. The isomers were not assigned to the meso or the racemic forms. Yield 42 mg (35%) (Found: C, 44.55; H, 3.71; N, 9.01. Calc. for $C_{60}H_{56}N_{12}F_{24}OP_4Ru_2$: C, 41.35; H, 3.24; N, 9.64). Positive-ion FAB mass spectrum: Calc. *m/z* for $C_{60}H_{56}N_{12}F_{18}OP_3Ru_2^+$ ([(dmb)$_2$Ru(**91**)Ru(dmb)$_2$](PF$_6$)$_3^+$) 1599.1727; found 1599.1713. λ_{max} (CH_3CN) 497 nm, ε 15 000 $M^{-1}cm^{-1}$. E^o_{ox1} (CH_3CN) +1.42 V, $E^{1/2}$ 60 mV; E^o_{ox2} +1.80 V, $E^{1/2}$ 60 mV; E^o_{red1} -0.58 V (irreversible). ^1H NMR (CD_3CN) δ: 2.54, 6H, dmb4-CH3; 2.56, 6H, dmb4-CH3; 2.57, 6H, dmb4-CH3; 2.61, 6H, dmb4-CH3; 2.62, 12H, dmb4-CH3; 2.64, 6H, dmb4-CH3; 2.71, 6H, dmb4-CH3; 6.96, m, 4H, dmb H5's; 7.14, m, 6H, dmb H5's; 7.26, d, 2H, dmb H6; 7.30, d, 2H, dmb H6; 7.42, m, 2H, dmb H5; 7.45, d, 4H, dmb H6's; 7.53, m, 4H, dmb H6 and dmb H5; 7.66, m, 4H, H5's; 7.73, d, 2H, dmb H6; 7.90, d, 2H, H6; 7.98, d, 2H, H6; 8.04, d, 2H, dmb H6; 8.19, s, 2H, dmb H3; 8.22, s, 2H, dmb H3; 8.24, s, 2H, dmb H3; 8.33, t, 4H, H4's; 8.39, s, 4H, dmb H3's; 8.44, s, 4H, dmb H3's; 8.47, s, 4H, dmb H3's; 8.96, d, 4H, H3's.

Tetrakis(2,2'-bipyridine)-μ-[3,4-di(2-pyridyl)-1,2,5-oxadiazolyl]-diruthenium(II)-tetrakis(tetrafluoroborate) (127)

Ligand **91** (36.6 mg, 0.16 mmol) and $Ru(bpy)_2Cl_2.2H_2O$ (144.1 mg, 0.27 mmol) in 3:1 $EtOH/H_2O$ (16 ml) were refluxed for 24 hrs. After cooling, the reaction mixture was concentrated to dryness *in vacuo*. The residue was redissolved in the minimum of water, filtered to remove unreacted ligand, and the product precipitated out by the addition of an aqueous solution of NH_4BF_4. Chromatography on alumina separated the mononuclear

complex from the dinuclear complex. The ^{1}H NMR spectrum of **127** showed the presence of two diastereoisomers, in a ratio of 5:6. The isomers could not be assigned to either the meso or the racemic forms. Yield 53.7 mg (31%) (Found: C, 44.06; H, 2.94; N, 11.93. Calc. for $C_{52}H_{40}N_{12}B_4F_{16}ORu_2.H_2O$: C, 44.10; H, 2.99; N, 11.86). Positive-ion FAB mass spectrum: Calc. *m/z* for $C_{52}H_{40}N_{12}F_{12}OB_3Ru_2^+$ ([(bpy)$_2$Ru(**91**)Ru(bpy)$_2$](BF$_4$)$_3^+$) 1312.1631; found 1312.1635. λ_{max} (CH_3CN) 497 nm, ε 11 600 $M^{-1}cm^{-1}$. E^o_{ox1} (CH_3CN) +1.48 V, $E^{1/2}$ 60 mV; E^o_{ox2} +1.82 V, $E^{1/2}$ 60 mV; E^o_{red1} -0.53 V (irreversible); E^o_{red2} -1.70 V (2e$^-$), $E^{1/2}$ 80 mV.

Tetrakis(2,2'-bipyridine)-μ-[3,4-di(2-pyridyl)-1,2,5-thiadiazolyl]-diruthenium(II)-tetrakis(hexafluorophosphate) (128)

Ligand **94** (30 mg, 0.125 mmol) and Ru(bpy)$_2$Cl$_2$.2H$_2$O (130 mg, 0.250 mmol) in 3:1 EtOH/H$_2$O (16 ml) were refluxed for 24 hrs. After cooling, the reaction mixture was concentrated to dryness *in vacuo*. The residue was redissolved in the minimum of water, filtered to remove unreacted ligand, and the product precipitated out by the addition of an aqueous solution of NH_4PF_6. Chromatography on alumina separated the mononuclear complex from the dinuclear complex. The ^{1}H NMR spectrum of **128** showed the presence of two diastereoisomers, **128a** and **128b**, in a ratio of 3:1. The isomers could not be assigned to the meso or the racemic forms. However, because of the large diastereoisomeric excess, they could be assigned to the major component (**128a**) or the minor component (**128b**). Yield 97 mg (47%) (Found: C, 37.63; H, 2.35; N, 10.06. Calc. for $C_{52}H_{40}N_{12}F_{24}P_4Ru_2S$: C, 37.92; H, 2.45; N, 10.20). Positive-ion FAB mass spectrum: Calc. *m/z* for $C_{52}H_{40}N_{12}F_{18}P_3Ru_2S^+$ ([(bpy)$_2$Ru(**94**)Ru(bpy)$_2$](PF$_6$)$_3^+$) 1503.0272; found 1503.0253. λ_{max} (CH_3CN) 531 nm, ε 16 000 $M^{-1}cm^{-1}$. E_{ox1} (CH_3CN) +1.41 V, $E^{1/2}$ 60 mV; E_{ox2} +1.67 V, $E^{1/2}$ 60 mV; E_{red1} -0. 62V; $E^{1/2}$ 60 mV; E_{red2} -1.08 V (irreversible); E_{red3} -1.60 V (2e$^-$); E_{red4} -1.86 V (2e$^-$).

^{1}H NMR (**128a**) (CD_3CN) δ:
bpy H3, 8.42; bpy H4, 8.10; bpy H5, 7.41; bpy H6, 7.53.
bpy H3, 8.42; bpy H4, 8.05; bpy H5, 7.37; bpy H6, 7.71.
bpy H3, 8.62; bpy H4, 8.19; bpy H5, 7.49; bpy H6, 7.60.
bpy H3, 8.62; bpy H4, 8.24; bpy H5, 7.66; bpy H6, 8.08.
H3, 9.00; H4, 8.30; H5, 7.66; H6, 7.95.

^{1}H NMR (**128b**) (CD_3CN) δ:
bpy H3, 8.59; bpy H4, ; bpy H5, ; bpy H6, 7.69.
bpy H3, 8.49; bpy H4, 8.05; bpy H5, 7.32; bpy H6, 7.55.
bpy H3, 8.56; bpy H4, 8.14; bpy H5, 7.24; bpy H6, 7.32.
bpy H3, 8.60; bpy H4, 8.31; bpy H5, 7.65; bpy H6, 8.03.
H3, 8.98; H4, 8.27; H5, 7.62; H6, 7.92.

Tetrakis(4,4'-dimethyl-2,2'-bipyridine)-μ-[4,4'-di(2-pyridyl)-3,3'-bi-1,2,5-thiadiazolyl]-diruthenium(II)-tetrakis(hexafluorophosphate) (129)

Ligand **95** (8.1 mg, 0.025 mmol) and $Ru(dmb)_2Cl_2.2H_2O$ (37.8 mg, 0.066 mmol) in 3:1 $EtOH/H_2O$ (8 ml) were refluxed for 42 hrs. After cooling, the reaction mixture was concentrated to dryness *in vacuo*. The residue was redissolved in the minimum of water, filtered to remove unreacted ligand, and the product precipitated out by the addition of an aqueous solution of NH_4PF_6. Chromatography on alumina separated a small amount of the mononuclear complex from the dinuclear complex. Yield 43.2 mg (95%) (Found: C, 41.32; H, 3.04; N, 10.41. Calc. for $C_{62}H_{56}N_{14}F_{24}P_4Ru_2S$: C, 40.40; H, 3.06; N, 10.63). Positive-ion FAB mass spectrum: Calc. *m/z* for $C_{62}H_{56}N_{14}F_{18}P_3Ru_2S^+$ ($[(bpy)_2Ru(\mathbf{95})Ru(bpy)_2](PF_6)_3^+$) 1699.1292; found 1699.1266. λ_{max} (CH_3CN) 481 nm, ε 24 800 $M^{-1}cm^{-1}$. E^o_{ox1} (CH_3CN) +1.31 V ($2e^-$), $E^{1/2}$ 70 mV; E^o_{red1} -1.02 V, $E^{1/2}$ 65 mV; E^o_{red2} -1.14 V, $E^{1/2}$ 65 mV. ^1H NMR (CD_3CN) δ: 2.60, s, 6H, dmb4-CH3; 2.61, s, 6H, dmb4-CH3; 2.63, s, 24H, dmb4-CH3; 2.64, s, 12H, dmb4-CH3; 7.35, m, 16H, dmb H5; 7.51, m, 6H, H5 and dmb H6; 7.57, d, 6H, dmb H6; 7.71, m, 4H, dmb H6; 7.79, d, 4H, dmb H6; 7.86, d, 4H, H6; 7.91, t, 4H, H4; 8.12, d, 4H, H3; 8.45, s, 4H, dmb H3; 8.48, s, 12H, dmb H3.

Tetrakis(2,2'-bipyridine)-μ-[4,4'-di(2-pyridyl)-3,3'-bi-1,2,5-thiadiazolyl]-diruthenium(II)-tetrakis(hexafluorophosphate) (130)

Ligand **95** (16.5 mg, 0.051 mmol) and $Ru(bpy)_2Cl_2.2H_2O$ (68.0 mg, 0.130 mmol) in 3:1 $EtOH/H_2O$ (16 ml) were refluxed for 24 hrs. After cooling, the reaction mixture was concentrated to dryness *in vacuo*. The residue was redissolved in the minimum of water, filtered to remove any unreacted ligand, and the product precipitated out by the addition of an aqueous solution of NH_4PF_6. Yield 86 mg (96%) (Found: C, 37.16; H, 2.45; N, 11.61. Calc. for $C_{52}H_{40}N_{12}F_{24}P_4Ru_2S_2$: C, 37.47; H, 2.33; N, 11.32). Positive-ion FAB mass spectrum: Calc. *m/z* for $C_{52}H_{40}N_{12}F_{18}P_3Ru_2S_2^+$ ($[(bpy)_2Ru(\mathbf{95})Ru(bpy)_2](PF_6)_3^+$) 1587.0058; found 1587.0014. λ_{max} (CH_3CN) 471 nm, ε 25 500 $M^{-1}cm^{-1}$. E^o_{ox1} (CH_3CN) +1.41 V ($2e^-$), $E^{1/2}$ 70 mV; E^o_{red1} -0.98 V, $E^{1/2}$ 60 mV; E^o_{red2} -1.10 V, $E^{1/2}$ 60 mV. ^1H NMR (CD_3CN) δ: 7.49-7.58, m, 20H, H5's; 7.74-7.82, m, 6H, H6's; 7.86-8.02, m, 14H, H6's; 8.12-8.26, m, 20H, H4's; 8.58-8.68, m, 20H, H3's.

Bis(2,2'-bipyridine)(dichloropalladium(II)-μ-[3,4-di(2-pyridyl)-1,2,5-thiadiazolyl]-ruthenium(II) bis(chloride) (131)

A methanolic solution of 0.1140M Li_2PdCl_4 (0.45 ml, 0.051 mmol) was added to **111** (44.0 mg, 0.047 mmol) dissolved in refluxing 3:1 ethanol/acetone (8 ml). A precipitate formed immediately. Refluxing was continued for 5 minutes and then the reaction mixture allowed to cool to room temperature and the dark red precipitate collected by filtration and washed with ethanol. Yield 44.7 mg (100%). λ_{max} (CH_3CN) 456 nm, ε 12 000 $M^{-1}cm^{-1}$. ^1H

NMR (CD_3CN) δ: 7.51, m, 5H, H5 and 4 x bpy H5; 7.68, d, 1H, H3; 7.86, m, 7H, H4, H6, H3', H5' and 3 x bpy H6; 8.17, m, 5H, H4'; 8.38, d, 1H, bpy H6; 8.60, m, 4H, 4 x bpy H3; 9.35, d, 1H, H6'.

Bis(4,4'-dimethyl-2,2'-bipyridine)(dichloropalladium(II)-μ-[3,4-di(2-pyridyl)-1,2,5-oxadiazolyl]-ruthenium(II) bis(chloride) (132)

A methanolic solution of 0.0904M Li_2PdCl_4 (0.5 ml, 0.057 mmol) was added to **110** (22.3 mg, 0.024 mmol) dissolved in refluxing 3:1 ethanol/acetone (8 ml). A precipitate formed immediately. Refluxing was continued for 5 minutes and then the reaction mixture allowed to cool to room temperature and the orange precipitate collected by filtration and washed with ethanol. Yield 22.8 mg (100%). ^{1}H NMR (CD_3CN) δ: 2.56, s, 3H, dmb4-CH3; 2.60, s, 3H, dmb4-CH3; 2.61, s, 3H, dmb4-CH3; 2.63, s, 3H, dmb4-CH3; 7.38, m, 4H, 4 x dmb H5; 7.52, t, 1H, H5; 7.56, m, 1H; 7.61, d, 1H, dmb H6; 7.69, d, 1H, dmb H6; 7.71, d, 1H, dmb H6; 7.85, m, 3H, H3, H5' and dmb H6; 7.93, t, 1H, H4; 8.06, d, 1H, H3'; 8.26, t, 1H; H4'; 8.40, s, 1H, dmb H3; 8.45, s, 3H, 3 x dmb H3; 9.33, d, 1H, H6'.

Dichloro(benzonitrile)-palladium(II)-bis(2,2'-bipyridine)-μ-[3,4-di(2-pyridyl)-1,2,5-thiadiazolyl]-ruthenium(II) bis(hexafluorophosphate) (133)

$(PhCN)_2PdCl_2$ (12.7 mg, 0.034 mmol) dissolved in $CHCl_3$ (0.5 ml) was added to **111** (32.2 mg, 0.034 mmol) dissolved in CH_2Cl_2 (1 ml). A precipitate formed immediately and was collected by filtration and washed with $CHCl_3$. Yield 37.8 mg (91%). Positive-ion FAB mass spectrum: Calc. *m/z* for $C_{39}H_{30}N_9ClF_6PPdRuS^+$ ([(bpy)$_2$Ru(**94**)PdCl(NCPh)](PF$_6$)$^+$) 1045.9730; found 1045.9758. λ_{max} (CH_3CN) 455 nm, ε 13 700 $M^{-1}cm^{-1}$.

Bis(2,2'-bipyridine)(dichloropalladium(II)-μ-[3,4-di(2-pyridyl)-1,2,5-thiadiazolyl]-ruthenium(II) bis(hexafluorophosphate) (134)

(Found: C, 34.22; H, 1.97; N, 9.74. Calc. for $C_{32}H_{24}N_8Cl_2F_{12}P_2PdRuS$: C, 34.29; H, 2.16; N, 9.99).

(Dimethyl sulfoxide)(dichloroplatinum(II)-μ-[3,4-di(2-pyridyl)-1,2,5-thiadiazolyl]-bis(2,2'-bipyridine)ruthenium(II) bis(hexafluorophosphate) (136)

Complex **111** (42.3 mg, 0.045 mmol) dissolved in 1:1 acetone/ethanol (2 ml) was added to $(DMSO)_2PtCl_2$ (19.5 mg, 0.046 mmol) dissolved in nitromethane (½ ml), and the resultant solution left overnight. The reaction mixture was then concentrated to dryness *in vacuo*. The residue was redissolved in acetone (*ca.* 1 ml) and was filtered through a small plug of celite into a small vial. Vapour diffusion of diethyl ether into this solution

precipitated a red powder (53 mg). A sample was examined by positive-ion FAB mass spectrometry: Calc. *m/z* for $C_{39}H_{30}N_9ClF_6PPdRuS^+$ ([(bpy)$_2$Ru(**94**)PtCl$_2$(DMSO)](PF$_6$)$^+$) 1142.9693; found 1142.9696. All the remaining material was redissolved in 1:1 ethanol/nitromethane (4 ml) and refluxed for 8 hours. After cooling the same workup procedure was followed. Yield 51 mg (88%) (Found: C, 31.85; H, 2.24; N, 8.87. Calc. for $C_{52}H_{40}N_{12}F_{24}P_4Ru_2S_2$: C, 31.71; H, 2.35; N, 8.70). λ_{max} (CH_3CN) 514 nm, ε 7000 $M^{-1}cm^{-1}$, λ_2 458 nm, ε 11 300 $M^{-1}cm^{-1}$; λ_3 423 nm, ε 11 500 $M^{-1}cm^{-1}$. E^o_{ox1} (CH_3CN) +1.41 V ($2e^-$), $E^{1/2}$ 65 mV; E^o_{ox2} +1.67 V, $E^{1/2}$ 70 mV; E^o_{red1} -0.60 V (irreversible). ^{1}H NMR (CD_3CN) δ: 2.61, s, 6H, DMSO; 7.50, m, 4H, 4 x bpy H6; 7.62, t, 1H, H5; 7.71, d, 1H, bpy H6; 7.74, d, 1H, bpy H6; 7.86, m, 3H, ; 7.95, d, 1H, H6; 8.19, m, 5H, 4 x bpy H4 + H4; 8.50, t, 1H, H4'; 8.60, m, 4H, 4 x bpy H6; 8.76, d, 1H, H3'; 8.86, d, 1H, H3; 9.07, d, 1H, H6'.

Crystallography

Tables C1-C5 list crystal data and X-ray experimental details for the structures determined. Selected bond lengths and angles are listed in the discussion of the structures and the remaining distances and angles, as well as atom coordinates, anisotropic displacement parameters and hydrogen atom coordinates, are available from the Chemistry Department, University of Canterbury.

Intensity data were collected with:

(I) a Siemens P4s four-circle diffractometer using monochromatised Mo Kα radiation. Cell parameters were determined by least-squares refinement of at least 25 accurately centred reflections ($2\theta > 20°$). Throughout the data collections the intensities of three standard reflections were monitored at regular intervals, and this showed no significant crystal decomposition.

(II) a Siemens SMART CCD area detector using monochromatised Mo Kα radiation, and the standard software SMART and SAINT. Intensities were corrected for Lorentz, polarisation and absorption effects.

The structures were solved by direct methods using SHELXS[253] and refined, using SHELXL,[254] on F^2 using all data. The functions minimised were $\Sigma w(F_o^2 - F_c^2)$, with $w = [\sigma^2(F_o^2) + aP^2 + bP]^{-1}$ where $P = [\max(F_o^2 + 2F_c^2)]/3$. The hydrogens were included in calculated positions and assigned isotropic displacement parameters 1.3 times the isotropic equivalent of their carrier atoms. In all cases the final Fourier synthesis did not show any significant residual electron density in chemically sensible locations.

Table C1 Crystal Data and X-ray Experimental Details for **1**, **2**, **7**, **21** and **22**.

Compound	**1**	**2**	**7**	**21**	**22**
Data collection device	P4s	P4s	CCD	CCD	CCD
Empirical formula	$C_{14}H_8N_2O_2$	$C_{14}H_8N_2S_2$	$C_{35}H_{26}Cl_2F_{12}N_6O_2P_2Ru$	$C_{28}H_{16}Cu_1N_4Cl_4O_4$	$C_{24}H_{16}CuN_6O_8$
Formula weight	236.22	268.34	1024.53	606.88	289.99
Temperature (K)	163(2)	163(2)	168(2)	153(2)	168(2)
Crystal system	Monoclinic	Monoclinic	Triclinic	Monoclinic	Triclinic
Space group	$P2_1/n$	$P2_1/c$	P-1	$P2_1/c$	P-1
Unit cell dimensions: a (Å)	4.627(1)	8.993(1)	10.724(3)	9.980(1)	7.031(2)
b (Å)	16.480(2)	5.998(1)	11.124(4)	14.426(2)	9.060(2)
c (Å)	7.004(1)	11.445(2)	18.866(6)	9.472(1)	9.894(3)
α (°)	90	90	101.652(4)	90	77.568(3)
β (°)	94.34(1)	110.870(10)	91.649(4)	117.422(3)	76.300(4)
γ (°)	90	90	110.354(4)	90	68.521(3)
Volume ($Å^3$)	535.5(2)	575.9(2)	2054.7(12)	1210.5(3)	564.0(3)
Z	2	2	2	2	1
Density (calculated) (Mg/m^3)	1.473	1.548	1.656	1.665	1.708
Absorption coefficient (mm^{-1})	0.101	0.441	0.685	1.169	1.036
F(000)	244	276	1020	614	295
Crystal size (mm^3)	0.34 x 0.22 x 0.18	0.77 x 0.21 x 0.13	0.38 x 0.19 x 0.04	0.23 x 0.19 x 0.17	0.80 x 0.40 x 0.37
Theta range for data collection (°)	2.47 to 26.00	2.42 to 26.99	2.06 to 22.50	2.30 to 23.22	2.14 to 27.73
Reflections collected	1733	1619	19597	1549	7402
Independent reflections [R(int)]	1044 [0.0354]	1262 [0.0265]	5373 [0.0968]	1197 [0.0275]	2415 [0.0311]
Observed reflections [$I>2\sigma(I)$]	741	964	3444	1024	2233
Data / restraints / parameters	1044 / 0 / 82	1261 / 0 / 82	5373 / 0 / 541	1197 / 0 / 178	2415 / 0 / 178
Goodness-of-fit on F^2	0.920	0.931	1.024	1.071	1.081
R_1 [$I>2\sigma(I)$]	0.0413	0.0342	0.0509	0.0497	0.0324
wR_2 (all data)	0.1127	0.1068	0.1248	0.1884	0.0899

Table C5 Crystal data and X-ray Experimental Details for **104**, **115**, **118**, **124** and **125**.

Compound	**104**	**115**	**118**	**124**	**125**
Data collection device	CCD	CCD	CCD	CCD	CCD
Empirical formula	$C_{14}H_8AgN_3O_3$	$C_{32.50}H_{25}ClF_{12}N_8O_{2.50}P_2Ru$	$C_{12}H_8Cl_2CuN_4O_2$	$C_{12}H_8CuN_6O_6S$	$C_{12}H_8AgN_5O_3S$
Formula weight	374.10	994.07	374.66	427.84	410.16
Temperature (K)	158(2)	168(2)	168(2)	168(2)	168(2)
Crystal system	Triclinic	Monoclinic	Monoclinic	Triclinic	Monoclinic
Space group	P-1	C2/c	$P2_1/n$	P-1	$P2_1/n$
Unit cell dimensions: a (Å)	8.6182(8)	21.86(8)	9.711(4)	7.737(2)	7.054(2)
b (Å)	9.3085(9)	13.81(5)	9.571(4)	8.108(2)	14.793(4)
c (Å)	9.7959(9)	24.70(7)	15.080(6)	12.933(3)	13.249(4)
α (°)	90.059(1)	90	90	96.838(3)	90
β (°)	112.297(1)	96.16	92.877(6)	100.565(3)	101.286(3)
γ (°)	115.467(1)	90	90	102.623(3)	90
Volume ($Å^3$)	643.64(10)	7415(42)	1399.9(9)	767.5(3)	1355.7(7)
Z	2	8	4	2	4
Density (calculated) (Mg/m^3)	1.930	1.781	1.778	1.851	2.010
Absorption coefficient (mm^{-1})	1.579	0.698	1.949	1.607	1.661
F(000)	368	3960	748	430	808
Crystal size (mm^3)	0.62 x 0.44 x 0.10	0.16 x 0.13 x 0.08	0.35 x 0.13 x 0.06	0.56 x 0.46 x 0.07	0.45 x 0.41 x 0.21
Theta range for data collection (°)	2.79 to 26.35	2.34 to 24.00	2.44 to 26.40	2.61 to 26.43	2.09 to 26.40
Reflections collected	7309	13551	9273	9879	17123
Independent reflections [R(int)]	2462 [0.0189]	5558 [0.2323]	2830 [0.0513]	3113 [0.0202]	2764 [0.0374]
Observed reflections [$I>2\sigma(I)$]	2285	1561	1603	2799	2584
Data / restraints / parameters	2462 / 0 / 190	5558 / 0 / 543	2830 / 1 / 200	3113 / 0 / 235	2764 / 0 / 199
Goodness-of-fit on F^2	1.030	0.801	0.801	1.059	1.169
R_1 [$I>2\sigma(I)$]	0.0205	0.0742	0.0337	0.0247	0.0318
wR_2 (all data)	0.0559	0.2006	0.0550	0.0654	0.0778

Table C4 Crystal Data and X-ray Experimental Details for **75**, **76**, **79**, **82** and **95**.

Compound	**75**	**76**	**79**	**82**	**95**
Data collection device	CCD	P4s	CCD	CCD	CCD
Empirical formula	$C_4H_2Cl_2N_4O_2Pd$	$C_4H_2AgN_5O_5$	$C_{14}H_{20}CuN_6O_{10}$	$C_7H_5Cl_2CuN_3O_{0.25}S$	$C_{14}H_8N_6S_2$
Formula weight	315.40	307.98	495.90	301.64	324.38
Temperature (K)	153(2)	153(2)	168(2)	168(2)	168(2)
Crystal system	Orthorhombic	Orthorhombic	Triclinic	Monoclinic	Triclinic
Space group	Pbca	Pnma	P-1	C2/c	P-1
Unit cell dimensions: a (Å)	7.7176(4)	10.0248(10)	7.525(2)	17.652(7)	6.354(2)
b (Å)	13.1725(6)	14.7795(11)	8.121(2)	17.215(7)	9.030(3)
c (Å)	16.5280(8)	5.3288(5)	8.146(2)	7.149(3)	12.241(4)
α (°)	90	90	84.167(4)	90	84.602(5)
β (°)	90	90	78.256(3)	91.172(5)	85.788(5)
γ (°)	90	90	84.969(4)	90	78.885(4)
Volume ($Å^3$)	1680.24(14)	789.52(12)	483.7(2)	2171.9(15)	685.1(4)
Z	8	4	1	8	2
Density (calculated) (Mg/m^3)	2.494	2.591	1.703	1.845	1.573
Absorption coefficient (mm^{-1})	2.812	2.567	1.198	2.659	0.393
F(000)	1200	592	255	1192	332
Crystal size (mm^3)	0.40 x 0.21 x 0.04	0.78 x 0.42 x 0.21	0.47 x 0.25 x 0.07	0.34 x 0.11 x 0.08	0.55 x 0.25 x 0.15
Theta range for data collection (°)	2.46 to 23.32	2.76 to 27.00	2.53 to 26.39	2.31 to 26.32	2.31 to 23.00
Reflections collected	4956	1198	5934	13724	6864
Independent reflections [R(int)]	1212 [0.0491]	895 [0.0458]	1952 [0.0363]	2205 [0.0818]	1890 [0.0638]
Observed reflections [I>2σ(I)]	4129	854	1843	1691	1707
Data / restraints / parameters	1212 / 0 / 120	895 / 0 / 77	1952 / 0 / 146	2205 / 0 / 170	1890 / 0 / 199
Goodness-of-fit on F^2	0.991	1.064	1.120	1.220	1.312
R_1 [I>2σ(I)]	0.0245	0.0262	0.0350	0.0854	0.1052
wR_2 (all data)	0.0492	0.0684	0.0887	0.1670	0.2240

Table C3 Crystal Data and X-ray Experimental Details for **48**, **49**, **50**, **51**and **59**.

Compound	**48**	**49**	**50**	**51**	**59**
Data collection device	P4s	P4s	P4s	CCD	CCD
Empirical formula	$C_{30}H_{36}Cl_2CuN_{10}O$	$C_{12}H_{10}AgN_5O_3$	$C_{12.50}H_{12}Cl_2N_4O_{0.50}Pd$	$C_{40}H_{40}Cl_8Cu_4N_{16}O_1$	$C_{16}H_{10}N_4O_2$
Formula weight	431.56	380.12	403.56	1298.64	290.28
Temperature (K)	163(2)	168(2)	153(2)	168(2)	150(2)
Crystal system	Triclinic	Monoclinic	Monoclinic	Monoclinic	Monoclinic
Space group	P-1	C2/c	$P2_1/c$	C2/c	$P2_1/c$
Unit cell dimensions: a (Å)	8.277	16.252(2)	10.820(2)	42.568(11)	8.5243(5)
b (Å)	10.216	11.020(2)	15.273(2)	13.657(3)	5.6457(3)
c (Å)	12.594	14.709(2)	17.715(3)	24.603(7)	13.7393(8)
α (°)	99.11(1)	90	90	90	90
β (°)	108.43(1)	96.98(1)	97.21(1)	109.474(4)	91.742(2)
γ (°)	108.96(1)	90	90	90	90
Volume ($Å^3$)	914.15	2614.8(7)	2904.3(8)	13484(6)	660.91(6)
Z	2	8	8	8	2
Density (calculated) (Mg/m^3)	1.568	1.931	1.846	1.279	1.459
Absorption coefficient (mm^{-1})	0.821	1.560	1.642	1.600	0.101
F(000)	445	1504	1592	5216	300
Crystal size (mm^3)	0.54 x 0.30 x 0.27	0.55 x 0.34 x 0.25	0.69 x 0.05 x 0.03	0.40 x 0.21 x 0.06	0.52 x 0.26 x 0.15
Theta range for data collection (°)	2.20 to 25.00	2.24 to 27.00	2.32 to 25.03	2.03 to 22.50	2.97 to 25.99
Reflections collected	4835	2963	5828	62461	2201
Independent reflections [R(int)]	3186 [0.0382]	2865 [0.0209]	5115 [0.2082]	8814 [0.2038]	1027 [0.0706]
Observed reflections [$I>2\sigma(I)$]	2791	2365	2193	6267	871
Data / restraints / parameters	3186 / 0 / 254	2865 / 0 / 190	5115 / 0 / 361	8814 / 25 / 792	1027 / 0 / 100
Goodness-of-fit on F^2	1.350	0.981	0.662	1.217	1.170
R_1 [$I>2\sigma(I)$]	0.0769	0.0250	0.0462	0.1367	0.0495
wR_2 (all data)	0.2124	0.0609	0.0826	0.3202	0.1160

Table C2 Crystal Data and X-ray Experimental Details for **23**, **42**, **43**, **45** and **46**.

Compound	**23**	**42**	**43**	**45**	**46**
Data collection device	CCD	P4s	P4s	P4s	CCD
Empirical formula	$C_{12}H_8N_6$	$C_{13}H_{10}Cl_2CuN_6$	$C_{15}H_{13}AgN_8O_3$	$C_{24}H_{24}CuN_{10}O_8$	$C_{11}H_8AgN_5O_3$
Formula weight	236.24	384.71	461.20	644.07	366.09
Temperature (K)	168(2)	163(2)	163(2)	153(2)	168(2)
Crystal system	Orthorhombic	Triclinic	Triclinic	Monoclinic	Triclinic
Space group	$P2_12_12_1$	P-1	P-1	$P2_1/n$	P-1
Unit cell dimensions: a (Å)	7.277(3)	8.554(1)	9.212(1)	7.720(1)	8.308(2)
b (Å)	7.639(3)	9.250(1)	9.307(1)	12.016(1)	8.675(2)
c (Å)	19.940(8)	10.322(1)	11.849(1)	14.921(2)	9.664(3)
α (°)	90	88.79(1)	92.28(1)	90	102.377(4)
β (°)	90	72.78(1)	105.92(1)	103.14(1)	109.288(3)
γ (°)	90	65.83	115.69(1)	90	107.132(3)
Volume ($Å^3$)	1108.5(7)	707.01(13)	865.5(2)	1347.9(3)	589.5(3)
Z	4	2	2	4	2
Density (calculated) (Mg/m^3)	1.416	1.807	1.770	1.587	2.063
Absorption coefficient (mm^{-1})	0.094	1.926	1.082	0.879	1.726
F(000)	488	386	460	662	360
Crystal size (mm^3)	0.51 x 0.25 x 0.16	0.41 x 0.33 x 0.14	0.74 x 0.27 x 0.11	0.62 x 0.44 x 0.31	0.55 x 0.25 x 0.11
Theta range for data collection (°)	2.86 to 23.00	2.08 to 26.00	2.47 to 28.00	2.20 to 27.00	2.36 to 26.48
Reflections collected	11015	3558	4400	3157	7588
Independent reflections [R(int)]	1544 [0.0809]	2719 [0.0209]	4150 [0.0171]	2941 [0.0240]	2387 [0.0245]
Observed reflections [$I>2\sigma(I)$]	1248	2010	3561	2007	2206
Data / restraints / parameters	1544 / 0 / 163	2719 / 0 / 199	4150 / 0 / 245	2941 / 0 / 200	2387 / 0 / 181
Goodness-of-fit on F^2	1.103	0.899	1.003	0.919	1.052
R_1 [$I>2\sigma(I)$]	0.0509	0.0330	0.0281	0.0373	0.0222
wR_2 (all data)	0.1184	0.0770	0.0693	0.0893	0.0562

References

[1] F. Blau, *Chem. Ber.*, **1888**, *21*, 1077.

[2] E. C. Constable, *Adv. Inorg. Chem.*, **1989**, *34*, 1.

[3] F. H. Burstall, *J. Chem. Soc.*, **1936**, 173.

[4] J. P. Paris and W. W. Brandt, *J. Am. Chem. Soc.*, **1959**, *81*, 5001.

[5] M. Schröder and T. A. Stephenson in G. Wilkinson, R. D. Gillard and J. A. McCleverty (Eds.), *Comprehensive Coordination Chemistry*, Pergamon, Oxford, **1987**, *4*, 277 and references therein.

[6] A. Juris, V. Balzani, F. Barigelletti, S. Campagna, P. Belser and A. von Zelewsky, *Coord. Chem. Rev.*, **1988**, *84*, 85 and references therein.

[7] E. C. Constable and P. J. Steel, *Coord. Chem. Rev.*, **1989**, *93*, 205.

[8] P. J. Steel, F. Lahousse, D. Lerner and C. Marzin, *Inorg. Chem.*, **1983**, *22*, 1488.

[9] A. J. Downard, P. J. Steel and J. Steenwijk, *Aust. J. Chem.*, **1995**, *48*, 1625.

[10] V. Balzani, A. Juris, M. Venturi, S. Campagna and S. Serroni, *Chem. Rev.*, **1996**, *96*, 759 and references therein.

[11] M. Fujita, *Chem. Soc. Rev.*, **1998**, *27*, 417.

[12] A. M. Garcia, F. T. Romero-Salguero, D. M. Bassani, J.-M. Lehn, G. Baum and D. Fenske, *Chem. Eur. J.*, **1999**, *5*, 1803.

[13] A. M. Garcia, D. M. Bassani, J.-M. Lehn, G. Baum and D. Fenske, *Chem. Eur. J.*, **1999**, *5*, 1234.

[14] P. W. N. Baxter, J.-M. Lehn, G. Baum and D. Fenske, *Chem. Eur. J.*, **1999**, *5*, 102

[15] G. Baum, E. C. Constable, D. Fenske, C. E. Housecroft and T. Kulke, *Chem. Eur. J.*, **1999**, *5*, 1862.

[16] G. Baum, E. C. Constable, D. Fenske, C. E. Housecroft and T. Kulke, *Chem. Commun.*, **1997**, 195.

[17] R. Chatolia, E. C. Constable, M. Nueberger, D. R. Smith and M. Zehnder, *J. Chem. Soc., Dalton Trans.*, **1996**, 4207.

[18] A. Marquisrigault, A. Dupontgervias, P. W. N. Baxter, A. Vandersselaer and J.-M. Lehn, *Inorg. Chem.*, **1996**, *35*, 2307.

[19] S. Roche, C. Haslam, H. Adams, S. L. Heath, J. A. Thomas, *Chem. Commun.*, **1998**, 1681.

[20] S. R. Batten and R. Robson, *Angew. Chem. Int. Ed. Eng.*, **1998**, *37*, 1461.

[21] J. D. Peterson, W. R. Murphy, R. Sahai, K. J. Brewer, and R. R. Rumininski, *Coord. Chem. Rev.*, **1985**, *64*, 261.

[22] F. M. Macdonnell, M. J. Kim and S. Brodige, *Coord. Chem. Rev.*, **1999**, *186*, 535.

[23] M. Plevoets, F. Vogtle, L. Decola and V. Balzani, *New J. Chem.*, **1999**, *23*, 63.

[24] E. C. Constable and P. Harverson, *Inorg. Chim. Acta*, 1996, 252, 9.

[25] E. C. Constable, P. Harverson and M. Oberholzer, *Chem. Commun.*, **1996**, 1821.

[26] E. C. Constable, *Chem. Commun.*, **1997**, 1073.

[27] S. Campagna, G. Denti, S. Serroni, A. Juris, M. Venturi, M. Ricevuto and V. Balzani, *Chem. Eur. J.*, **1995**, *1*, 211.

[28] F. R. Keene, *Coord. Chem. Rev.*, **1997**, *166*, 121.

[29] F. R. Keene, *Chem. Soc. Rev.*, **1998**, *27*, 185.

[30] P. Hayoz, A. Von Zelewsky, *Tet. Lett.*, **1992**, *33*, 5165.

[31] H. Murner, A. Von Zelewsky and H. Stoecklievans, *Inorg. Chem.*, **1996**, *13*, 3931.

[32] N. C. Fletcher, F. R. Keene, M. Ziegler, H. Stoecklievans, H. Viebrock and A. Von Zelewsky, *Helv. Chim. Acta*, **1996**, *79*, 1192.

[33] N. C. Fletcher, F. R. Keene, H. Viebrock and A. Von Zelewsky, *Inorg. Chem.*, **1997**, *36*, 113.

[34] H. Murner, P. Belser and A. Von Zelewsky, *J. Am. Chem. Soc.*, **1996**, *118*, 7989.

[35] P. Hayoz, A. Von Zelewsky and H. Stoecklievans, *J. Am. Chem. Soc.*, **1993**, *115*, 5111.

[36] A. A. Watson, D. A. House and P. J. Steel, *Aust. J. Chem.*, **1995**, *48*, 1549.

[37] A. A. Watson, D. A. House and P. J. Steel, *J. Org. Chem.*, **1991**, *56*, 4072.

[38] E. C. Constable, T. Kulke, M. Nueburger and M. Zehnder, *New J. Chem.*, **1997** *21*, 633 and **1997**, *21*, 1091.

[39] X. Chi, A. J. Guerin, R. A. Haycock, C. A. Hunter and L. D. Sarson, *J. Chem. Soc., Chem. Commun.*, **1995**, 2563.

[40] P. J. Stang, B. Olenyuk, D. C. Muddiman and R. D. Smith, *Organometallics*, **1997**, *16*, 3094.

[41] P.W. N. Baxter, J.-M. Lehn, G. Baum and D. Fenske, *Chem. Eur. J.*, **1999**, *5*, 102.

[42] M. Munakata, L. P. Wu and T. Kuroda-Sowa, *Adv. Inorg. Chem.*, **1999**, *46*, 173.

[43] A. W. Hofmann, *Chem. Ber.*, **1880**, *13*, 1223.

[44] F. Kehrmann and C. Bener, *Helv. Chim. Acta*, **1925**, *8*, 16.

[45] M. Haga, Md. M. Ali, S. Koseki, A. Yoshimura, K. Nozaki and T. Ohno, *Inorg. Chim. Acta*, **1994**, *226*, 17.

[46] M. R. Mcdevitt, Y. Ru and A. W. Addison, *Transition Metal Chem.*, **1993**, *18*, 197.

[47] S. Baitalik, U. Florke and K. Nag, *J. Chem. Soc., Dalton Trans.*, **1999**, 719.

[48] Y. Zhou, X. Xia and Z. Gao, *Gaodeng Xuexiao Huaxue Xuebao*, **1991**, *12*, 189.

[49] V. Tralic-Kulenovic and L. Fiser-Jakic, *Spectrosc. Lett.*, **1993**, *26*, 1771.

[50] a) A. Abbotto, V. Alanzo, S. Bradamante, G. A. Pagani, C. Rizzoli and G. Calestani, *Gazz. Chim. Ital.*, **1991**, *121*, 365. b) F. Ragaini, M. Pizzotti, S. Cenini, A. Abbotto, G. Pagani and F. Denati, *J. Organomet. Chem.*, **1995**, *489*, 107. c) S. Bradamante, A. Facchetti and G. A. Pagani, *Gazz. Chim. Ital.*, **1996**, *126*, 329. d) A. Abbotto, S. Bradamante and G. A. Pagani, *J. Org. Chem.*, **1996**, *61*, 1761. e) A. Abbotto, S. Bradamante, N. Capri, H. Rzepa, D. A. Williams and A. White, *J. Org. Chem.*, **1996**, *61*, 1770.

[51] M. S. Munsey and N. R. Natale, *Coord. Chem. Rev.*, **1991**, *109*, 251.

[52] C. Rai and J. B. Braunworth, *J. Org. Chem.*, **1961**, *26*, 3434.

[53] C. Rai and J. B. Braunworth, U.S. Patent 3,250,780; *Chem. Abstr.*, **1966**, *65*, 7180g.

[54] M. H. Chisholm, J. C. Huffman, I. P. Rothwell, P. G. Bradley, N. Kress and W. H. Woodruff, *J. Am. Chem. Soc.*, **1981**, *103*, 4945.

[55] F. E. Hahn, L. Imhof and T. Lügger, *Acta Crystallogr., Sect. C*, **1998**, *54*, 668.

[56] H. Boshagen, *Chem. Ber.*, **1967**, *100*, 954 and 3326.

[57] M. Iyoda, H. Otsuka, K. Sato, N. Nisato and M. Oda, *Bull. Chem. Soc. Jpn.*, **1990**, *63*, 80.

[58] D. J. de Geest, Ph.D. Thesis, University of Canterbury, **1997**.

[59] D. S. Kemp and R. B. Woodward, *Tetrahedron*, **1965**, *21*, 3019.

[60] E. P. Kohler and W. F. Bruce, *J. Am. Chem. Soc.*, **1931**, *53*, 646.

[61] P. J. Steel and E. C. Constable, *J. Chem. Soc., Dalton Trans.*, **1990**, 1389.

[62] A. J. Downard, G. E. Honey and P. J. Steel, *Inorg. Chem.*, **1991**, *30*, 3733.

[63] G. Orellana, C. A. Ibarra and J. Santoro, *Inorg. Chem.*, **1988**, *27*, 1025.

[64] L. Braunschweiler and R. R. Ernst, *J. Magn. Reson.*, **1983**, *53*, 521.

[65] D. G. Davis and A. Bax, *J. Am. Chem. Soc.*, **1987**, *107*, 7197.

[66] T. Kantthimathi, Y. V. S. Narayana Moorthy, S. Subramanian and C. N. Pillia, *Magn. Reson. Chem.*, **1994**, *32*, 452.

[67] M. J. Heeg, R. Kroener and E. Deutsch, *Acta Crystallogr., Sect. C*, **1985**, *41*, 684.

[68] R. Hage, J. P. Turkennburg, R. A. G. de Graff, J. G. Haasnoot, J. Reedijk and J. G. Vos, *Acta Crystallogr., Sect. C*, **1989**, *45*, 381.

[69] A. G. Orpen, L. Brammer, F. H. Allen, O. Kennard, P. G. Watson and R. Taylor, *J. Chem. Soc., Dalton Trans.*, **1989**, S1.

[70] R. J. Forster, A. Boyle, J. G. Vos, R. Hage, A. H. J. Dijkhuis, R. A. G. de Graff, J. G. Haasnoot, R. Prins and J. Reedijk, *J. Chem. Soc., Dalton Trans.*, **1990**, 121.

[71] L. Stefaniak, *Org. Magn. Reson.*, **1978**, *11*, 385.

[72] P. Belser and A. von Zelewsky, *Helv. Chim. Acta*, **1980**, *63*, 1675.

[73] D. C. Craig, H. A. Goodwin, D. Onggo and A. D. Rae, *Aust. J. Chem.*, **1988**, *41*, 1625.

[74] G. Orellana, M. L. Quiroga and A. M. Braun, *Helv. Chim. Acta*, **1987**, *70*, 2073.

[75] P. J. Steel, *Adv. Heterocycl. Chem.*, **1997**, *67*, 1.

[76] I. G. Phillips, Ph.D. Thesis, University of Canterbury, **1995**.

[77] V. S. Joshi, A. Sarker and P. R. Rajamohanan, *J. Organomet. Chem.*, **1991**, *409*, 341 and references therein.

[78] K.-B. Shiu, K.-S. Liou, Y. Wang, M.-C. Cheng and G.-H. Lee, *J. Organomet. Chem.*, **1993**, *433*, 201.

[79] H. Nagao, H. Nishimura, H. Funati, Y. Ichikawa, F. S. Howell, M. Mukaida and H. Kakihana, *Inorg. Chem.*, **1989**, *28*, 3955.

[80] B. Durham, S. R. Wilson, D. J. Hodgson and T. J. Meyer, *J. Am. Chem. Soc.*, **1980**, *102*, 600.

[81] L. P. Battaglia, M. Carcelli, F. Ferraro, L. Mavilla, C. Pelizzi and G. Pelizzi, *J. Chem. Soc., Dalton Trans.*, **1994**, 2651.

[82] H. Chao, B.-H. Ye, Q.-L. Zhang and L.-N. Ji, *Inorg. Chem. Commun.*, **1999**, *2*, 338.

[83] R. Hage, J. G. Haasnoot, H. A. Niewenhuis, J. Reedijk, R. Wang and J. G. Vos, *J. Chem. Soc., Dalton Trans.*, **1991**, 3271.

[84] B. E. Buchanan, P. Degn, J. M. P. Velasio, J. G. Haasnoot and J. Reedijk, *J. Chem. Soc., Dalton Trans.*, **1992**, 1177.

[85] D. S. Moore and S. D. Robinson, *Adv. Inorg. Chem.*, **1988**, *32*, 194 and references therein.

[86] a) S. Zanias, C. P. Raptopoulou, A. Terzis and T. F. Zafiropoulos, *Inorg. Chem. Commun.*, **1999**, *2*, 48. b) V. Tangoulis, C. P. Raptopoulou, A. Terzis, E. G. Bakalbassis, E. Diamantopoulou and S. P. Perlepes, *Inorg. Chem.*, **1998**, *37*, 3142. c) K. Skorda, E. G. Bakalbassis, J. Mrozinski, S. P. Perlepes, C. P. Raptopoulou and A. Terzis, *J. Chem. Soc., Dalton Trans.*, **1995**, 2317. d) J. C. Plakatouras, T. Bakas, C. J. Huffman, J. C. Huffman, V. Papaefthymiou and S. P. Perlepes, *J. Chem. Soc., Dalton Trans.*, **1994**, 2737. e) E. Diamantopoulou, T. F. Zafiropoulos, S. P. Perlepes, C. P. Raptopoulou and A. Terzis, *Polyhedron*, **1994**, *13*, 1593.

[87] H. E. Toma, E. Geisbrecht and R. L. E. Rojas, *J. Chem. Soc., Dalton Trans.*, **1985**, 2469.

[88] H. E. Toma, E. Geisbrecht and R. L. E. Rojas, *Can. J. Chem.*, **1983**, *61*, 2520.

[89] R. C. Rocha, K. Araki and H. E. Toma, *Transition Metal Chem.*, **1998**, *23*, 13.

[90] R. C. Rocha, K. Araki and H. E. Toma, *Inorg. Chim. Acta,* **1999**, *285*, 197.

[91] K.-B. Shiu, F.-M. Shen, S.-L. Wang and S.-C. Wei, *J. Organomet. Chem.*, **1989**, *372*, 251.

[92] J. Cartwright, A. Harman and A. F. Hill, *J. Organomet. Chem.* **1990**, *396*, C31.

[93] S. Anderson, A. Harman and A. F. Hill, *J. Organomet. Chem.*, **1995**, *498*, 251.

[94] L. K. Cheng, K. S. Yeung, C.-M. Che, M. C. Cheng and Y. Wang, *Polyhedron*, **1993**, *12*, 1201.

[95] W.-Y. Yu, W.-C. Cheng, C.-M Che and Y. Wang, *Polyhedron*, **1994**, *13*, 2963.

[96] M. T. Ashby, G. N. Govindan and A. K. Grafton, *Inorg. Chem.*, **1993**, *32*, 3803.

[97] M. T. Ashby, G. N. Govindan and A. K. Grafton, *J. Am. Chem. Soc.*, **1994**, *116*, 4801.

[98] M. T. Ashby, *J. Am. Chem. Soc.*, **1995**, *117*, 2000.

[99] R. A. Carboni, J. C. Krauer, J. E. Castle and H. E. Simmons, *J. Am. Chem. Soc.*, **1967**, *89*, 2618.

[100] B. Ortiz, P. Villanueva and F. Walls, *J. Org. Chem.*, **1972**, *37*, 2748.

[101] P. Skrabal and M. Hohl-Blummer, *Helv. Chim. Acta*, **1976**, *59*, 2906.

[102] R. J. Harder, R. A. Carboni and J. E. Castle, *J. Am. Chem. Soc.*, **1967**, *89*, 2643.

[103] A. R. Katritzky, F.-B. Ji, W.-Q. Fan, J. K. Gallas, J. V. Greenhill, R. W. King and P. J. Steel, *J. Org. Chem.*, **1992**, *57*, 190.

[104] A. R. Katritzky, M. F. Gordeev, J. V. Greenhill and P. J. Steel, *J. Chem. Soc., Perkin Trans. 1*, **1992**, 1111.

[105] L. Avila, J. Elguero, S. Julia and J. M. del Mazo, *Heterocycles*, **1983**, *20*, 1787.

[106] A. R. Katritzky and J. Wu, *Synthesis*, **1994**, 597.

[107] A. R. Katritzky, G. Yao and S. J. Rachwal, *J. Heterocycl. Chem.*, **1994**, *31*, 757.

[108] C. J. Pouchert and J. Behnke, The Aldrich Library of ^{13}C and ^{1}H FT NMR spectra, **1993**, *3*, 456.

[109] R. Yang and L. Dia, *Chin. Chem. Lett.*, **1993**, *4*, 1621.

[110] W. Hiller, A. Zinn and K. Dehnicke, *Z. Naturforsch., Teil B*, **1990**, *45*, 1593.

[111] O. S. Filipenko, V. I. Ponomarev and L. O. Atovmyan, *Koord. Khim.*, **1986**, *12*, 991.

[112] S. Brownstein, N. F. Han, E. Gabe and F. Lee, *Can. J. Chem.*, **1989**, *67*, 551.

[113] B. T. Kilbourn and J. D. Dunitz, *Inorg. Chim. Acta*, **1967**, *1*, 209.

[114] M. R. Churchill, B. G. DeBoer and S. J. Mendak, *Inorg. Chem.*, **1975**, *14*, 2496.

[115] A. Tosik, M. Bukowska-Strzyzewska and J. Mrozinski, *J. Coord. Chem.*, **1991**, *24*, 113.

[116] See L. B. Clapp in A. R. Katritzky and C. W. Rees (Eds.), *Comprehensive Heterocyclic Chemistry*, Pergamon, Oxford, **1991**, *6*, 365.

[117] C. D. Hurd and R. I. Mori, *J. Am. Chem. Soc.*, **1955**, *77*, 5359.

[118] N. P. Peet and S. Sunder, *J. Heterocycl. Chem.*, **1975**, *12*, 1191.

[119] M. Al-Smadi, N. Hanold and H. Meier , *J. Heterocycl. Chem.*, **1997**, *34*, 605.

[120] V. Batzel and R. Boese, *Z. Naturforsch., Teil B*, **1981**, *36*, 172.

[121] F. Zamora, S. Rico and P. Amo-Ochoa, *J. Inorg. Biochem.*, **1997**, 257.

[122] M. Maekawa, M. Munakata, T. Kuroda-Sowa, Y. Suenaga and K. Sugimoto, *Inorg. Chim. Acta*, **1999**, *290*, 153.

[123] T. Sudershan, C. Tirupataiah, D. Radharamana and S. Srihari, *J. Indian Chem. Soc.*, **1995**, *72*, 307.

[124] J. P. Wignacourt, S. Sueur and M. L. Lagrenee, *Acta Crystallogr., Sect. C*, **1990**, *49*, 394.

[125] J. Preston, *J. Heterocycl. Chem.*, **1965**, 2, 447.

[126] A. E. Siegrist, E. Maeder, M. Duennenberger and P. Liechti, *Chem. Abstr.*, **1968**, *68*, 69002y.

[127] B. D. J. R. Fennema, F. A. G. de Graff, R. Hage, J. G. Haasnoot, J. Reedijk and J. G. Vos, *J. Chem. Soc., Dalton Trans.*, **1991**, 1043.

[128] D. P. Rillema, R. Sahai, F. Matthews, H. K. Edwards, R. J. Shaver and L. Morgan, *Inorg. Chem.*, **1990**, *29*, 167.

[129] L. Prasad, Y. Le Page and F. E. Smith, *Acta Crystallogr., Sect. B*, **1982**, *38*, 2890.

[130] G. Orellana, C. Alvarez-Ibarra and M. L. Quiroga, *Bull. Soc. Chim. Belg.*, **1988**, *97*, 731.

[131] G. Orellana, M. L. Quiroga and A. M. Braun, *Helv. Chim. Acta*, **1987**, *70*, 2073.

[132] J. C. Liu, Y. Song, Z. Yu, J. Z. Zhuang, X. Y. Huang and X. Z. You, *Polyhedron*, **1999**, *18*, 1491.

[133] B. L. Li, J. Z. Zou, C. Y. Duan, Y. J. Liu, X. W. Wei and Z. Xu, *Acta Crystallogr., Sect C*, **1999**, *55*, 165.

[134] C. L. Zilerentant, W. L. Driessen, J. G. Haasnoot, J. J. A. Kolnaar and J. Reedijk, *Inorg. Chim. Acta*, **1998**, *282*, 257.

[135] R. Hage, H. E. B. Lempers, J. G. Haasnoot, J. Reedijk, F. M. Weldon and J. G. Vos, *Inorg. Chem.*, **1997**, *36*, 3139.

[136] H. P. Hughes and J. G. Vos, *Inorg. Chem.*, **1995**, *34*, 4001.

[137] H. P. Hughes, S. Bell, D. Martin, J. J. McGarvey and J. G. Vos, *Inorg. Chem.*, **1993**, *32*, 4402.

[138] S. Serroni, S. Campagna, G. Denti, T. E. Keyes and J. G. Vos, *Inorg. Chem.*, **1996**, *35*, 4513.

[139] J. H. van Dieman, R. Hage, J. G. Haasnoot, H. E. B. Lempers, J. Reedijk, J. G. Vos, L. De Cola, F. Barigelletti and V. Balzani, *Inorg. Chem.*, **1992**, *32*, 3518.

[140] M. Martin, M. P. Garcia and L. A. Oro, *Inorg. Chim. Acta*, **1992**, *191*, 221.

[141] F. Barigelletti, L. De Cola, V. Balzani, R. Hage, J. G. Haasnoot, J. Reedijk and J. G. Vos, *Inorg. Chem.*, **1991**, *30*, 641.

[142] F. Barigelletti, L. De Cola, V. Balzani, R. Hage, J. G. Haasnoot, J. Reedijk and J. G. Vos, *Inorg. Chem.*, **1989**, *28*, 4344.

[143] R. Hage, J. G. Haasnoot, D. J. Stufkins, T. L. Snoek, J. G. Vos and J. Reedijk, *Inorg. Chem.*, **1989**, *28*, 1413.

[144] R. Hage, A. H. J. Dijkhuis, J. G. Haasnoot, R. Prins, J. Reedijk, B. E. Buchanan and J. G. Vos, *Inorg. Chem.*, **1988**, *27*, 2185.

[145] E. Müller, Md. K. Nazeerudin, M. Grätzel, K. Kalyanasundaram and J.-C. Promé, *New J. Chem.*, **1996**, *20*, 759.

[146] G. A. Pearse, Jr., and R. T. Pflaum, *J. Am. Chem. Soc.*, **1959**, *81*, 6505

[147] E. Barnes, *J. Org. Chem.*, **1955**, *22*, 1263

[148] V. G. Adrianov, V. G. Seminikhina and A. V. Eremeev, *Chem. Heterocycl. Comp.*, **1994**, *30*, 475.

[149] W. Zinkiesen, *Chem. Ber.*, **1889**, *22*, 2946.

[150] L. Golic, I. Leban, B. Stanovik and M. Tisler, *Acta Crystallogr., Sect. B*, **1979**, *35*, 2256.

[151] L. Eberson, J. L. Calvert, M. P. Hartshorn and W. T. Robinson, *Acta Chem. Scand.*, **1994**, *48*, 347.

[152] D. Viterbo, R. Calvino and A. Serafino, *J. Chem. Soc., Perkin Trans. 2*, **1980**, 1096.

[153] W. W. Paudler and J. E. Kuder, *J. Org. Chem.*, **1967**, *32*, 2430.

[154] Y.-I. Lin, S. A. Lang, Jr., M. F. Lovell and N. A. Parkinson, *J. Org. Chem.*, **1979**, *44*, 4160.

[155] T. J. Ward and J. C. White, *Eur. Pat. Appl.*, **1989**.

[156] S. Masiero, F. Fini, G. Gottarelli and G. P. Spada, *J. Chem. Res.*, **1998**, *10*, 634, 2736 and 2752..

[157] L. Liete, F. C. da Costa, R. M. Srivastava and A. P. Cavalcanti, *Bull. Soc. Chim. Belg.*, **1989**, *98*, 203.

[158] F. Tiemann and P. Krüger, *Chem. Ber.*, **1884**, *17*, 1685.

[159] Y.-I. Lin, S. A. Lang, Jr., and S. R. Petty, *J. Org. Chem.*, **1980**, *45*, 3750.

[160] A. E. S. Fairfull, J. L. Lowe and D. A. Peak, *J. Chem. Soc.*, **1952**, 742.

[161] A. R. Katritzky, J. Cobo-Domingo, B. Yang and P. J. Steel, *Tetrahedron Asymmetry*, **1999**, *10*, 255.

[162] M. D'Anello, E. Erba, M. L. Gelmi and D. Pocar, *Chem. Ber.*, **1988**, *121*, 67.

[163] For examples see F. Kurzer in *Adv. Heterocycl. Chem.*, **1965**, *5*, 119.

[164] R. I. Meltzer, A. D. Lewis and J. D. King, *J. Am. Chem. Soc.*, **1955**, *77*, 4062.

[165] J. M. Harrowfield, H. Miyamae, B. W. Skelton, A. A. Soudi and A. H. White, *Aust. J. Chem.*, **1996**, *49*, 1157.

[166] G. A. Barclay, R. S. Vagg and E. C. Watton, *Acta Crystallogr., Sect. B*, **1977**, *33*, 3777.

[167] G. A. Barclay, R. S. Vagg and E. C. Watton, *Acta Crystallogr., Sect. B*, **1978**, *34*, 1833.

[168] B. N. Figgis, E. S. Kucharski, S. Mitra, B. W. Skelton and A. H. White, *Aust. J. Chem.*, **1990**, *43*, 1269.

[169] F. H. Case and E. Kroft, *J. Am. Chem. Soc.*, **1959**, *81*, 905.

[170] R. Kitamura, *J. Pharm. Soc. Japan*, **1938**, *58*, 809.

[171] M. W. Cronwyn and T. W. Nakagawa, *J. Am. Chem. Soc.*, **1952**, *74*, 3693.

[172] R. K. Howe and J. E. Franz, *J. Org. Chem.*, **1974**, *39*, 962.

[173] E. Muhlbauer and W. Weiss, *Chem. Abstr.*, **1968**, *68*, 69000w.

[174] C. Moussebois and F. Eloy, *Helv. Chim. Acta*, **1964**, *47*, 838.

[175] F. Eloy, R. Lenaers and C. Moussebois, *Chem. Ind. (London)*, **1961**, 292.

[176] H. W. Roesky, K. Keller and J. W. Bats, *Angew. Chem., Int. Ed. Engl.*, **1983**, *22*, 881.

[177] H. W. Roesky, H. Hofmann, K. Keller, W. Pinkert, P. G. Jones and G. M. Sheldrick, *Chem. Ber.*, **1984**, *117*, 2681.

[178] J. Sundermeyer, H. W. Roesky and N. Noltemeyer, *Angew. Chem., Int. Ed. Engl.*, **1989**, *28*, 609.

[179] J. A. M. Gaurd and P. J. Steel, *Aust. J. Chem.*, **1995**, *48*, 1609.

[180] D. L. Jameson, J. K. Blaho, K. T. Kruger and K. A. Goldsby, **1989**, *28*, 4312.

[181] F. De Sarlo, *J. Chem. Soc., Perkin Trans. 1*, **1974**, 1951.

[182] S. Campagna, G. Denti, G. De Rosa, L. Sabatino, M. Ciano and V. Balzani, *Inorg. Chem.*, **1989**, *28*, 2565.

[183] G. Denti, S. Campagna, L. Sabatino, S. Serroni, M. Ciano and V. Balzani, *Inorg. Chem.*, **1990**, *30*, 4750.

[184] G. Denti, S. Serroni, L. Sabatino, M. Ciano, V. Ricevuto and S. Campagna, *Gazz. Chim. Ital.*, **1991**, *121*, 37.

[185] S. Campagna, G. Denti, L. Sabatino, S. Serroni, M. Ciano and V. Balzani, *Gazz. Chim. Ital.*, **1989**, *119*, 415.

[186] A. Juris, V. Balzani, S. Campagna, G. Denti, S. Serroni, G. Frei and G. Güdel, *Inorg. Chem.*, **1994**, *33*, 1491.

[187] S. D. Ernst and W. Kaim, *Inorg. Chem.*, **1989**, *28*, 1520.

[188] S. D. Ernst, V. Kasack and W. Kaim, *Inorg. Chem.*, **1988**, *27*, 1146.

[189] X. Hua and A. von Zelewsky, *Inorg. Chem.*, **1995**, *37*, 5791.

[190] T. Kunitake, H. Ihara, Y. Okahata, *J. Am. Chem. Soc.*, **1983**, *105*, 6070.

[191] I. G. Phillips and P. J. Steel, *Aust. J. Chem.*, **1998**, *51*, 371.

[192] A. J. Downard, G. E Honey, L. F. Phillips and P. J. Steel, *Inorg. Chem.*, **1991**, *30*, 2259.

[193] V. K. Bel'skii, O. G. Ellert, Z. M. Seifulina, V. M. Novotortsev, V. Sh. Tseveniashvili and A. D. Garnovskii, *Izv. Akad. Nauk SSSR, Ser. Khim.*, **1984**, 1914.

[194] M. Munakata, T. Kuroda-Sowa, M. Maekawa, N. Nakamura, S. Akiyama and S. Kitagawa, *Inorg. Chem.*, **1994**, *33*, 1284.

[195] L. G. Kuz'mina, L. P. Grigor'eva, Yu. T. Struchkov, Z. I. Ezhkova, B. E. Zaitsev, V. V. Davidov and A. K. Molodkin, *Zh. Neorg. Khim.*, **1980,** 25, 2931.

[196] C. E. Stoner, Jr., A. L. Rheingold and T. B. Brill, *Inorg. Chem.*, **1991**, *30*, 360.

[197] W. Kaim, S. Kohlmann, A. J. Lees and M. Z. Zulu, *Anorg. Allg. Chem.*, **1989**, *57*, 97.

[198] M. Munakata, Haiyang He, T. Kuroda-Sowa, M. Maekawa and Y. Suenaga, *J. Chem. Soc., Dalton Trans.*, **1998**, 1499.

[199] See R. M. Patton in A. R. Katritzky and C. W. Rees (Eds.), *Comprehensive Heterocyclic Chemistry*, Pergamon, Oxford, **1991**, *6*, 393 and references therein.

[200] J. V. Burakevich, A. M. Lore and G. P. Volpp, *J. Org. Chem.*, **1971**, *36*, 1.

[201] R. A. Olofson and J. S. Michelman, *J. Org. Chem.*, **1965**, *30*, 1854.

[202] R. H. Wiley and B. J. Wakefield, *J. Org. Chem.*, **1960**, *25*, 546.

[203] G. Ponzio and F. Biglietti, *Gazz. Chim. Ital.*, **1933**, *63*, 159.

[204] M. S. Chang, *J. Org. Chem.*, **1963**, *28*, 3542.

[205] T. Mukaiyama, H. Nambu and M. Okamoto, *J. Org. Chem.*, **1962**, *27*, 3651.

[206] A. Gasco, V. Mortarini, G. Ruá and A. Serafino, *J. Heterocycl. Chem.*, **1973**, *10*, 587.

[207] C. Grundmann, *Chem. Ber.*, **1964**, *97*, 575.

[208] A. J. Boulton, P. Hadjimihalikis, A. R. Katritzky and A. Majid Hamid, *J. Chem. Soc.*, **1969**, 1901.

[209] For examples see L. M. Weinstock and I. Shinkai in A. R. Katritzky and C. W. Rees (Eds.), *Comprehensive Heterocyclic Chemistry*, Pergamon, Oxford, **1991**, *6*, 513.

[210] L. M. Weinstock, P. Davis, B. Handlsman and R. Tull, *J. Am. Chem. Soc.*, **1967**, *32*, 2823.

[211] X.-G. Duan, X.-L. Duan, C. W. Rees and T.-Y. Yue, *J. Heterocycl. Chem.*, **1996**, *33*, 1419.

[212] X.-G. Duan, X.-L. Duan, C. W. Rees and T.-Y. Yue, *J. Chem. Soc., Perkin Trans. 1*, **1997**, 2597.

[213] X.-G. Duan and C. W. Rees, *J. Chem. Soc., Perkin Trans. 1*, **1997**, 3189.

[214] G. R. Newkome and D. L. Koppersmith, *J. Org. Chem.*, **1973**, *38*, 4461.

[215] U. Fritzsche and S. Hunig, *Tetrahedron Lett.*, **1972**, 4831.

[216] L. Brandsma, *Preparative Acetylenic Chemistry*, Elsevier, Amsterdam, 1988.

[217] A. S. Hay, *J. Org. Chem.*, **1962**, *27*, 3320.

[218] W. L. Jolly, and K. D. Maguire, *Inorg. Synth.*, **1967**, *9*, 102.

[219] G. G. Alange, A. J. Banister and B. Bell, *J. Chem. Soc., Dalton Trans.*, **1972**, 2399.

[220] B. F. Abrahams, M. J. Hardie, B. F. Hoskins, R. Robson and E. E. Sutherland, *J. Chem. Soc., Chem. Commun.*, **1994**, 1049.

[221] A. J. Blake, N. R. Champness, A. Khlobystov, D. A. Lemenovskii, W.-S. Li and M. Schröder, *Chem. Commun.*, **1997**, 2027.

[222] K. Swaminthathan, U. C. Sinha, M. B. Kamanth, S. S. Talwar and R. Bohra, *Acta Crystallogr., Sect. C*, **1989**, *45*, 504.

[223] K. A. Hirsh, S. R. Wilson and J. S. Moore, *J. Am. Chem. Soc.*, **1997**, *119*, 10 401.

[224] Dr. O. J. Curnow, personal communication.

[225] G. P. Bean, *J. Org. Chem.*, **1998**, *63*, 2497.

[226] For examples see A. Gasco and A. J. Boulton in *Adv. Heterocycl. Chem.*, **1981**, *29*, 251 and references therein.

[227] F. Eckert, G. Rauhut, A. R. Katritzky and P. J. Steel, *J. Am. Chem. Soc.*, **1999**, *121*, 6700.

[228] For examples see J. V. Greenhill in A. R. Katritzky and C. W. Rees (eds.), *Comprehensive Heterocyclic Chemistry*, Pergamon, Oxford, **1991**, *5*, 305 and references therein.

[229] J. D. Bower, *J. Chem. Soc.*, **1957**, 4510.

[230] K. T. Potts, S. K. Datta and J. L. Marshall, *J. Org. Chem.*, **1979**, *41*, 622.

[231] P. J. Bunyan and J. I. G. Cadogan, *J. Chem. Soc.*, **1963**, 42.

[232] K. T. Potts, U. P. Singh and J. Bhattacharyya, *J. Org. Chem.*, **1968**, *33*, 3766.

[233] H. Ochi, T. Miyasaka, K. Kanada and K. Arakawa, *Bull. Chem. Soc. Jpn.*, **1976**, *49*, 1980.

[234] A. Akahane, H. Katayama, T. Mitsunaga, T. Kato, T. Kinoshita, Y. Kita, T. Kusunoki, T. Terai, K. Yoshida and Y. Shiokawa, *J. Med. Chem.*, **1999**, *42*, 779.

[235] S. Kuroda, A. Akahane, H. Itani, K. Durkin, T. Kinoshita, Y. Tenda and K. Sakane, *Bioorganic Med. Chem. Lett.*, **1999**, *9*, 1979.

[236] J. E. B. Johnson, R. R. Ruminski, *Inorg. Chim. Acta*, **1993**, *208*, 231.

[237] V. W.-W. Yam and K. K.-W. Lo, *J. Chem. Soc., Dalton Trans.*, **1995**, 499.

[238] Y. Fuchs, S. Lofters, T. Dieter, W. Shi, R. Morgan, T. C. Strekas, H. D. Gafney and A. D. Baker, *J. Am. Chem. Soc.*, **1987**, *109*, 2691.

[239] D. P. Rillema, R. W. Callahan and K. B. Marck, *Inorg. Chem.*, **1982**, **21**, 2589.

[240] L. Jacquet and A. Kirsh-De Maesmaker, *J. Chem. Soc., Faraday Trans.*, **1992**, *88*, 2471.

[241] B. J. Hathaway in G. Wilkinson, R. D. Gillard and J. A. McCleverty (Eds.), *Comprehensive Coordination Chemistry*, Pergamon, Oxford **1987**, *5*, 533.

[242] B. T. Patterson and F. R. Keene, *Inorg. Chem.*, **1998**, *37*, 645.

[243] N. C. Fletcher, P. C. Junk, D. A. Reitsma and F. R. Keene, *J. Chem. Soc., Dalton Trans.*, **1998**, 133.

[244] S. D. Ernst and W. Kaim, *Inorg. Chem.*,**1989**, *28*, 1520.

[245] K. Kalyanasundaram and Md. K. Nazeeruddin, *Inorg. Chem.*, **1990**, *29*, 1888.

[246] V. W.-W. Yam, V. W.-M. Lee and K.-K. Cheung, *J. Chem. Soc., Chem. Commun.*, **1994**, 2075.

[247] R. P. Clausen and J. Becher, *Tetrahedron*, **1996**, *52*, 3171.

[248] R. N. Hammer and J. Klienberg, *Inorg. Synth.*, **1953**, **4**, 12.

[249] B. P. Sullivan, D. J. Salmon and T. J. Meyer, *Inorg. Chem.*, **1978**, *17*, 3334.

[250] I. P. Evans, A. Spencer and G. Wilkinson, *J. Chem. Soc., Dalton Trans.*, **1973**, 204.

[251] R. F. Heck, *Palladium Reagents in Organic Synthesis*, Academic Press, London, 1985.

[252] W. Ried and J. Patschorke, *Justus Liebigs Ann. Chem.*, **1956**, 599,44.

[253] G. M. Sheldrick, *Acta Crystallogr., Sect. A*, **1990**, *46*, 467.

[254] G. M. Sheldrick, SHELXL, University of Göttingen.